COPROCESSING OF PYROLYSIS OIL WITH VGO IN FCC UNIT TO PRODUCE LPG AND GASOLINE

Ph.D. THESIS

by

DESAVATH VISWANATHA NAIK

DEPARTMENT OF CHEMICAL ENGINEERING
INDIAN INSTITUTE OF TECHNLOGY ROORKEE
ROORKEE-247 667 (INDIA)
JUNE, 2015

COPROCESSING OF PYROLYSIS OIL WITH VGO IN FCC UNIT TO PRODUCE LPG AND GASOLINE

A THESIS

Submitted in partial fulfilment of the requirements for the award of the degree of

DOCTOR OF PHILOSOPHY

in

CHEMICAL ENGINEERING

by

DESAVATH VISWANATHA NAIK

DEPARTMENT OF CHEMICAL ENGINEERING
INDIAN INSTITUTE OF TECHNLOGY ROORKEE
ROORKEE-247 667 (INDIA)
JUNE, 2015

INDIAN INSTITUTE OF TECHNOLOGY ROORKEE
ROORKEE

CANDIDATE'S DECLARATION

I hereby certify that the work which is being presented in this thesis entitled **"**COPROCESSING OF PYROLYSIS OIL WITH VGO IN FCC UNIT TO PRODUCE LPG AND GASOLINE" in partial fulfillment of the requirement for the award of the Degree of Doctor of Philosophy and submitted in the Department of Chemical Engineering of the Indian Institute of Technology Roorkee is an authentic record of my own work carried out during a period from July, 2011 to June, 2015 under the supervision of Dr. Vimal Kumar, Assistant Professor and Dr. Basheshwar Prasad, Professor, Department of Chemical Engineering, Indian Institute of Technology Roorkee and Dr. Madhukar Onkarnath Garg, Director, CSIR-Indian Institute of Petroleum, Dehradun.

The matter presented in the thesis has not been submitted by me for the award of any other degree of this or any other Institute.

(DESAVATH VISWANATHA NAIK)

This is to certify that the above statement made by the candidate is correct to the best of my (our) knowledge.

(Vimal Kumar)	**(Basheshwar Prasad)**	**(Madhukar Onkarnath Garg)**
Supervisor	**Supervisor**	**Supervisor**

The Ph.D. Viva-Voce Examination of Desavath Viswanatha Naik, Research Scholar, has been held on **14th December, 2015**.

Chairman, SRC **(K.K.Pant)**
External Examiner

This is to certify that the student has made all the corrections in the thesis.

(Vimal Kumar)	**(Basheshwar Prasad)**	**(Madhukar Onkarnath Garg)**	**Head of the**
Supervisor	**Supervisor**	**Supervisor**	**Department**

Dated: 14th December, 2015

ABSTRACT

Lignocellulosic biomass-derived fast pyrolysis oil (FPO) has found applications within the petroleum refinery in recent years. This thesis investigates the possibility of upgrading FPO along with petroleum-derived fraction, vacuum gas oil (VGO), in fluid catalytic cracking (FCC) unit and look into the aspects of fast pyrolysis process integration in refinery context. The expelled *Jatropha curcas seed cake* (JCC) has been chosen as a biomass feedstock which is pyrolyzed in bubbling fluidized bed reactor at 530 °C temperature and atmospheric pressure. The char particles, which are not separable from pyrolysis gases or vapors by cyclone separator, are inherently collected along with FPO in large concentrations from nano-to-micro scale, which are highly dispersible and make FPO highly viscous to semi-solid. The char particles (> 200 nm) are separated by micro filtration (pore size: 0.2 μ) under vacuum line from FPO which helps in stabilization. The char free FPO is highly oxygenated (32 wt.%) and hence it has been hydrodeoxygenated over Pd/Al_2O_3 catalyst in a continuous stirred tank reactor at 300 °C temperature and 80 bar pressure to produce hydrodeoxygenated fast pyrolysis oil (HDO), which contains 10 wt.% of oxygen.

The FPO is blended in proportions of 5, 10, 15, 17, and 20 with vacuum gas oil for catalytic cracking in advanced cracking evaluation (ACE-R) FCC unit. The FCC unit operating parameters like temperature and catalyst-to-oil ratios are optimized based on the higher yields of gasoline on catalytic cracking of pure VGO over equilibrium FCC catalyst. The results of co-processing of FPO with VGO indicated that the yields of gasoline and light cycle oil increased from 29 to 35 wt% and 14.8 to 20.4 wt.%, respectively, whereas the yields of dry gas and LPG decreased from 2.1 to 1.4 wt.% and 38.8 to 23.7 wt%, respectively, for an increase in the blending ratio from 5 to 20%. Moreover, the FCC product distribution pattern at iso-conversion of 66% is compared on co-processing of VGO, VGO with FPO and VGO with HDO. Further, the FPO and HDO are characterized by ^{1}H, ^{13}C, and ^{31}P NMR techniques. From the NMR analysis it is observed that the liquid distillate from the co-processing of FPO with VGO contains more iso-paraffinic CH_3 substructure components, whereas the liquid on co-processing HDO with VGO contains more paraffinic CH_3 substructure. The ^{31}P NMR analysis of crude FPO and

HDO indicated that hydroxyl, carboxylic and methoxy groups are reduced during the hydrodeoxygenation of FPO.

Furthermore, the co-processing studies have been extended to envisage the specific role of nature of aliphatic (acetic acid, acetol and glycolaldehyde) and aromatic (guaiacol) compounds, which helps in understanding the path of fast pyrolysis process integration with refinery units. From the experimental investigations on co-processing of C2-C3 carbonyls and VGO, it is observed that the presence of acetol increased the FCC conversion from 68 to 78 % with an increase in blending ratio. It is due to the increase in the yield of liquefied petroleum gas (LPG) from 21 to 47 wt.% and at the cost of decrease in yield of gasoline from 39 to 23 wt.% followed by light cycle oil (LCO) from 18 to 12 wt.% and heavy cycle oil (HCO) from 11 to 7 wt.%. The yield of LPG increases linearly with an increase in blending ratio. Further, the presence of acetol reduced the coke formation as compared to pure VGO catalytic cracking over FCC equilibrium catalyst at a constant C/O ratio of 5.

While co-processing of glycolaldehyde dimer with vacuum gas oil, the FCC conversion increased from 69 to 75% with an increase in the blending ratio from 5 to 10 %; whereas beyond that the conversion decreased to 65 % for the blending ratio of 20 %. The dry gas and liquefied petroleum gas yield first increased from 1.8 to 2.4 wt.% and 35 to 43 wt.%, respectively with an increase in blending ratio from 5 to 10 %; and on further increase in blending ratio to 20 % the yields of dry gases and LPG decreased to 1.8 and 27 wt.%, respectively. Further, it was observed that the gasoline yield first decreased from 27 to 25 wt.%, and then increased to 32 wt.% with an increase in blending ratio. While the light cycle oil yield first decreased from 17 to 15 wt.% and then increased to 20 wt.%; whereas the yield of heavy cycle oil first decreased from 11 to 9 wt.%, and then increased to 13 wt.% with an increase in blending ratio from 5 to 10 wt.%. The yield of ethylene and propylene also followed the same trend with an increase in blending ratio of glycolaldehyde up to 10 wt.% blending, and there on the yields decreased with further increase in blending ratio. The increase in coke formation is observed beyond the blending ratio of 10% which is due to the increase in poly-aromatics formation. Similar results are found from the poly-aromatics analysis based on nuclear magnetic resonance (NMR) spectroscopy. Furthermore, the blended FCC feedstock and their liquid distillates were structurally characterized by means of average structural parameters like branchiness index, substitution

index, average length of alkyl chains, and fraction of aromaticity per molecule by ^{1}H, and gated decoupled ^{13}C NMR techniques.

Further, an attempt has been made to study the effect of catalyst-to-oil ratio (C/O) on the product distribution for the catalytic cracking of mixture of VGO with guaiacol and acetic acid. The simulated distillation (SIMDIST) based product analysis indicated that the presence of guaiacol increased the product selectivity of gasoline fraction; whereas the presence of acetic acid clearly increased the yield of light olefins, CO and CO_2. The FCC conversion is higher on co-processing guaiacol followed by acetic acid with vacuum gas oil as compared to pure VGO catalytic cracking. An increase in coke and aromatics was observed in the following order: guaiacol +VGO feed > acetic acid +VGO feed > VGO. Higher yields of light olefins, CO and CO_2 are observed while catalytic cracking of acetic acid +VGO feed with equilibrium FCC catalyst, subsequently light olefins have been reduced in case of guaiacol +VGO feed as compared to other feeds. The cracking patterns of liquid distillate have been further supported by FTIR analysis on cracking of acetic acid +VGO and guaiacol+ VGO feeds. It has been found that the carboxylic acid peaks (1650–1720 cm^{-1}) were completely absent which indicated the complete conversion of acetic acid. However, the formation of phenol is observed in the liquid distillate on cracking of guaiacol+VGO feed. Therefore, it is preferable to separate the aromatic oxygenated compounds from pyrolysis oil before co-processing it with vacuum gas oil in refinery FCC unit by keeping in mind the limitations of total aromatics and the benzene percentages in gasoline.

On catalytic cracking of glycerol by varying the temperature from 350 to 550 °C it is observed that a 100% conversion beyond 430°C and a maximum acetaldehyde yield of 53 wt.% is seen at 550 °C. The kinetic parameters were estimated with 4– (VGO, coke, gases and liquid distillate) and 5– (VGO, coke, dry gases, LPG and liquid distillate) lumps kinetic models for catalytic cracking of VGO and VGO with FPO. The experiments for VGO and VGO with FPO cracking have been carried out at different WHSV, varying from 6–24 h^{-1}, a constant reaction temperature (530 ^{O}C) and catalyst–to–oil (C/O) ratio of 5. The deviation between the predicted and experimental products yields, for both 4– and 5– lumps models, is found to be less than 5%.

ACKNOWLEDGEMENTS

I take this opportunity to thank everyone who some or the other way was associated with my research work at Indian Institute of Technology Roorkee and CSIR-Indian Institute of Petroleum, Dehradun. It has been the most exciting and enriching phase of my life. I feel very fortunate and almighty wished to meet my three gurus Dr. Vimal Kumar, Prof. Basheshwar Prasad and Dr. MadhukarOnkarnath Garg who have always inspired me with their research philosophy. Without their guidance and encouragement, this work would not have been possible. Their keen interest and experience helped this research work always on a smooth and steady path.

I would also like to thank Prof. I. M. Mishra, Dr. Neeraj Atheya, Mr. K. K. Singh, and Mr. S. P. Nautiyal for providing me with their unconditional support and useful advices. I also appreciate the help and support provided by my friends and colleagues, especially Babita Behera, Mukesh Kumar Poddar, Rajaram Bal, Om Prakash Khatri, Rajbeer Singh Negi, Piyush Gupta and Ranjan Kumar. During this research, the department has had three heads; Prof. I. D. Mall, Prof. V. K. Agarwal, and Prof. C. Balomazumder and most fortunately they encouraged me by extending every sort of help as and when sought for. The author would like to make a special note of thank to all faculty members of the department of chemical engineering for their continuous co-operation.

Finally, I acknowledge the financial support received from the Council of Scientific & Industrial Research for carrying this work against the In-house project (OLP-321019). At last thanks to the almighty god who has given the author spiritual support and courage to carry out this research work.

(DESAVATH VISWANATHA NAIK)

JUNE, 2015

CONTENTS

CHAPTER 4: CATALYTIC CRACKING OF FAST PYROLYSIS OILS

LIST OF TABLES

LIST OF FIGURES

NOMENCLATURE

LIST OF ABBREVIATIONS

ACE	Advanced cracking evaluation
API	American petroleum institute
BET	Brunauer–Emmett–Teller
BJH	Barrett-Joyner-Halenda
CCR	Conradson carbon residue
C/O	Catalyst-to-oil ratio
CPO	Catalytic pyrolysis oil
DTA	Differential thermal analyzer
DTG	Differential thermogravimetry
E-CAT	Equilibrium FCC catalyst
EDAX	Energy-dispersive X-ray spectroscopy
JCC	*Jatropha curcas seed cake*
ETD	Evehart-Thornley Detector
Feed A	Pure vacuum gas oil
Feed B	Vacuum gas oil + acetic acid
Feed C	Vacuum gas oil + guaiacol
FCC	Fluid catalytic cracking
FBP	Final boiling point
FID	Flame ionization detector
FPO	Heavy fraction of JCC-derived char free fast pyrolysis oil
FTIR	Fourier transform infrared spectroscopy
GA	Glycolaldehyde dimer
HA	Hydroxyl acetone
HCO	Heavy cycle oil
HDO	Hydrodeoxygenated fast pyrolysis oil
HMBC	Heteronuclear multiple-bond correlation
HMQC	Heteronuclear multiple-quantum correlation

H/C	Hydrogen-to-carbon aromatic ratio
IBP	Initial boiling point
IR	Infrared
O/C	Oxygen-to-carbon aromatic ratio
LPG	Liquefied petroleum gas
LCO	Light cycle oil
MAT	Micro activity test
NMR	Nuclear magnetic resonance
RE-Y	Rare earth exchanged Y-Zeolite
RE-USY	Rare earth exchanged ultra stable Y-Zeolite
SEM	Scanning electron microscope
SIMDIST	Simulated distillation
TCD	Thermal conductivity detector
TG	Thermo-gravimetry
TGA	Thermo-gravimetric Analysis
TMDP	2-chloro-4, 4, 5, 5-tetramethyl-1, 3, 2-dioxaphospholane
US-Y	Ultra stable Y-Zeolite
VGO	Vacuum gas oil
WHSV	Weight hourly space velocity
XRD	X-ray diffraction

LIST OF SYMBOLS

ARq	Substituted aromatic carbon
BI	Branchiness Index
^{13}C NMR	Carbon NMR
Cb	Bridgehead aromatic carbon
Ch	Protoned aromatic carbon
Cp	Phenolic Carbon
C_{ali}	Aliphatic carbon
C_{ar}	Aromatic carbon
C_N	Naphthenic carbon
C_{arp}	Protonated aromatic carbon
C_{arBr}	Bridgehead aromatic carbon
C_{arS}	Substituted aromatic carbon
Dp	Mean pore diameters
d-a	Di-aromatics
f_a	Fraction of aromaticity
f_a^s	Fraction of substituted aromatics
^1H NMR	Proton NMR
H_{ar}	Aromatic proton
$H_{m\text{-}ar}$	Mono aromatic proton
$H_{d\text{-}ar}$	Di_aromatic proton
$H_{p\text{-}ar}$	Poly aromatic proton
H_α	H_α to aromatic ring
$H_{\alpha,\ oxy}$	α, oxygenated protons
H_β	H_β to aromatic/in paraffinic CH and CH_2
H_γ	H_γ to aromatic ring/terminal CH_3
H/C_{eff}	Effective hydrogen index based on elemental analysis
$H/C_{eff\text{-}nmr}$	Effective hydrogen index based on NMR
k_d	Catalyst deactivation coefficient
k_i	kinetic constants
m-a	Mono-aromatics

n	Average chain length
^{31}P NMR	Phosphorous NMR
p-a	Poly-aromatics
r_i	Rate of reaction
S	Objective function
SI	Substitution Index
t_c	time-on-stream
P/P_0	Relative pressure
Vp	Total pore volume
W_c	Container weight
W_i	Initial weight
W_f	Final weight
x	Conversion
y_i	Yields

GREEK LETTERS

φ	Deactivation function

CHAPTER 1

INTRODUCTION

1.1 BACKGROUND

The demand of energy due to increase in worldwide population, depletion and concerns of environmental impact with the fossil energy resources forced the nations to take part in the development of alternative energy resources. The worldwide consumption of liquid fuels is bound to increase from 87 to 97 million barrels per day from 2010 to 2020, respectively and it is projected to 115 million barrels per day in 2040 [John et al. 2013]. The proved world oil reserves were estimated to be ~1638 billion barrels as of January 1, 2013 [www.ogj.com]. The fluid catalytic cracking (FCC) process is extensively used for cracking hydrocarbons having high molecular weight into low molecular weight such as petrochemical feedstocks like C3-C4 olefins, liquefied petroleum gas (LPG), gasoline and light cycle oil (blend component of Diesel and Jet fuel). Herein the cracking mechanism follows the carbonium ion theory. The cracking occurs over a catalyst containing hot-fluidized-micro spherical particles of acidic SiO_2-Al_2O_3 with a short contact time. The chief advantages of catalytic cracking are: (i) cost effectiveness when compared to hydrocracking; (ii) enhanced product quality and selectivity over thermal cracking process; (iii) flexibility in processing of various types of feedstocks such as atmospheric gas oil, vacuum gas oil, thermally cracked gas oil, hydro-treated VGO, hydrocracker bottom, coker gas oil, solvent deasphalted oil, reduced crude oil and vacuum residue etc. The FCC process in petroleum refining has evolved over the last 60 years in fulfilling the challenges like cracking heavier and metallic contaminated feeds (with Ni and V), increasing operating flexibility, accommodating environmental legislation, and maximizing reliability.

Routinely, the FCC plants have been operated on either gasoline or middle distillates modes; however the developments in new generation catalysts led to operate in LPG mode. The chief reactions involved in the catalytic cracking are cracking (primary reaction), and many secondary reactions such as isomerisation (double bond and skeletal), dehydrogenation, hydrogen transfer, cyclization, condensation, alkylation and dealkylation. Besides, the non-

condensable gases like methane, ethane and ethylene are also obtained due to the cleavage of terminal bonds of hydrocarbon feedstock. Thus, ultimate composition of catalytic cracking product is a function of relative rates of different competing reactions [Scherzer et al. 1990].

Globally, there are more than 400 FCC units operating in various capacities with fresh feed; wherein the UOP has been participated in the original nameplate design of FCC units from the scale of minimum 2000 bpsd (Montana Refining, Great Falls, USA) to maximum 135,000 bpsd (Reliance Industries, Jam Nagar, India) [Ibsen et al. 2006]. Presently, India and China have emerged as the key players for the growth of refinery FCC capacity. In the period 2005–2010, both countries reached the refinery FCC capacity of 43.0 MMTPA, which is 43.0% of the global refinery FCC capacity in which, India alone is having the refinery FCC capacity of ~18.0 MMTPA to process fresh feed [http://petroleum.nic.in/ refinery.pdf]. It helped in becoming net exporters of gasoline and other light hydrocarbons to the regions like Asia Pacific and the Middle East.

Lignocellulosic biomass has been the potential feedstock for partial fulfillment of primary energy demand and it will increase by 41% between 2012 and 2035 [Dudley et al. 2014]. Various pyrolysis techniques have been developed so far for the conversion of lignocellulosic biomass into biofuels. Fast pyrorlysis technology is considered to be the most promising one for getting higher (50-75%) yields of crude (liquid) fast pyrolysis oil (FPO) as an alternative to crude petroleum. The produced crude FPO as such cannot be used as a liquid fuel due to its lower heating value (15-20 MJ/kg) and the presence of oxygenated compounds that self-react during handling at ambient temperature to form larger molecules [Elliot et al. 1984]. The advantage of FPO is its higher oil density, i.e. ~1200 kg/m^3, as compared to the original biomass (~150 kg/m^3) [Venderbosch et al. 2010b]. The pyrolysis oil obtained either by catalytic or non-catalytic route contains higher oxygen content (~40% with non-catalytic and ~22% with catalytic) in the form of aliphatic and aromatic oxygenates.

The raw FPO is a complex mixture of water, carboxylic acids, hydroxy-aldehydes, hydroxy-ketones, phenolics, guaiacols, catechols, syringols, vanilins, sugars, and levoglucosan [Elliot et al. 1989]. The FPO is immiscible with petroleum-derived fractions as it is highly oxygenated (~40 wt.%), acidic (pH~2-3), thermally and chemically unstable, and hence it cannot be directly utilized for fuel applications. Therefore, the FPO requires further upgrading in order to convert it into usable liquid hydrocarbons. Thereby, a number of upgrading technologies have

been proposed in few last decades, such as thermal treatment [Demirbas et al. 2010], high pressure thermal treatment [Venderbosch et al. 2010a], thermal hydrotreating [Samolada et al. 1998], and catalytic emulsion [Zapata et al. 2012]. Further, the FPO can be upgraded via hydrodeoxygenation at mild operating conditions to get hydrodeoxygenated FPO (HDO). Otherwise, the HDO can be further hydrodeoxygenated in the second stage [Mercader et al. 2010a] or it can be processed partially or co-processed with petroleum fractions in a refinery fluid catalytic cracking process [Graca et al. 2009c] to get a clear liquid hydrocarbons, suitable for fuel applications.

However, among the aforementioned upgrading techniques, catalytic cracking seems to be a good option for effective use of trillion dollars refinery infrastructure as well as integration of fast pyrolysis process with refinery [Jones et al. 2009]. The acidic natured FCC catalyst is also known for deoxygenation (such as dehydration, decarboxylation, and decarbonylation) in addition to conventional FCC reactions [Sadeghbeigi, 2000], due to its very high effectivity. The β-scission reaction is the primary reaction in fluid catalytic cracking, which occurs by breakage of β C-C bond, and various secondary reactions such as alkylation, hydrogenation [Sedran, 1994], isomerization [Mortensen et al., 2011], and condensation [Sedran, 1994; Whitmore, 1934]. Whitmore (1934) reported that the catalytic cracking of hydrocarbons is a chain reaction which follows carbonium ion theory. Adjaye and Bakhshi (1995a) proposed the reaction mechanism for pyrolysis oil catalytic cracking and reported that during pyrolysis oil catalytic cracking over acidic zeolites undesirable products are produced, such as tar and char. Corma et al. (2007) described the reaction mechanism in two categories, former one results in the hydrogen production and the later one leads to the hydrogen consumption. Another simplified reaction mechanism proposed by Fogassy et al. (2010) for deoxygenation reactions of pyrolysis oil is as follows:

$$C_xH_yO_z \rightarrow aC_{x-b-d-e}H_{y-2c}O_{z-2b-c-d} + bCO_2 + cH_2O + dCO + eC$$

Chen et al. (1986) reported that the effective hydrogen index (H/C_{eff}), which is related to the amount of hydrogen available for energy production, and defined as: H/C_{eff} = (H-2O-3N-2S)/C; where H, O, N, S and C are corresponding to the number of moles of hydrogen, oxygen, nitrogen, sulfur and carbon present in the feedstock. For energy production the H/C_{eff} should be

above the inflection point of 1.2, either processing or co-processing the biomass-derived FPO with petroleum-derived VGO or LCO in fluid catalytic cracking unit. Therefore, it is necessary to partially deoxygenate the FPO to reduce the oxygen level in order to improve the H/C_{eff} of pyrolysis oil for better processing in FCC units. This makes the process problematic as the FCC process is originally developed for petroleum fractions. A critical review has been published by Talmadge et al. (2014) on outlook of how to modify the overall chemistry of biomass-derived pyrolysis liquids in order to integrate pyrolysis process with standard petroleum refineries.

The conventional FCC technology is aimed to improve the gasoline yield, however while co-processing the FPO with VGO it is very much essential to look into the product characterization and also the causes of coke formation. Samolada et al. (1998) coprocessed the hydrotreated flash pyrolysis oil (a heavy fraction) with light cycle oil (LCO) for 15:85 blending ratio in a modified MAT fixed bed reactor system (MAT, ASTM D3907-80) over FCC (ReUSY2) catalyst. An increase in coke and gasoline production by 32% and 56%, respectively, was reported while co-processing hydrotreated flash pyrolysis oil (a heavy fraction) with LCO as compared to the pure LCO processing. Fogassy et al. (2010) reported a higher dry gas and coke yields, lower LPG yields, similar yields of gasoline and LCO while co-processing HDO with VGO in 20:80 blending ratio as compared to the processing of pure VGO. They carried out the catalytic cracking reaction in a validated micro-activity test reactor (i.e. a fixed bed quartz reactor) for VGO cracking over equilibrium FCC catalyst. Fogassy et al. (2011) further extended the co-processing of HDO studies with VGO over various types of FCC catalysts in terms of structural parameters of zeolites. It was mentioned that most of the lignin-derived molecules on co-processing of HDO are partially cracked into smaller methoxyphenols over FCC, HY and HZSM-5 catalysts and reported that very few oxygenated molecules are entered into pores of zeolite.

Mercader et al. (2010a) carried out the co-processing of HDO with long-residue in a fluidized bed MAT-5000 reactor over equilibrium FCC catalyst and reported near normal FCC gasoline (44–46 wt.%) and LCO (23–25 wt.%) products without an excessive increase in undesired coke and dry gases, as compared to the base feed. Thegarid et al. (2013) further reported that high levels of oxygen can be allowed in upgraded HDO (up to 28 wt.%) for co-processing in FCC unit without deterioration of the yield structure. These studies were further extended for co-processing of catalytic pyrolysis oil (CPO) with VGO and compared the results

of co-processing of HDO with VGO. An increase in alkyl phenols in addition to increase in coke, olefins, and aromatics were reported, while co-processing of CPO with VGO as compared to HDO with VGO.

With this view preliminary investigations were carried out by Gayubo et al. (2004a, b) and Adjaye et al. (1996), Adjaye and Bakhshi (1995a, b), Sharma and Bakhshi (1993), and Srinivas et al. (2000). It was reported that there was a coke formation during the processing of pyrolysis oil oxygenated compounds over zeolite catalyst in isothermal fixed bed reactor at temperature less than 410 °C, which follows the following order: phenol or aldehyde > acetone or acetic acid > alcohols. Further, it has been mentioned that phenols have low reactivity while high conversions can be achieved with acids, esters, alcohols, aldehydes, and ketones. Graca et al. (2009a, 2009b) studied the transformation of mixtures of methylcyclohexane in a Pyrex fixed bed reactor with small amounts of phenol over an HZSM-5 and HY zeolite for temperature ranging from 350 to 450 °C. It has been reported that by increasing the reaction temperature from 350 to 450 °C, HY zeolite limits the effect of phenol addition on the zeolite activity and stability whereas HZSM-5 does not limit the effect of phenol addition. Graca et al. (2009c and 2011a, b) studied the co-processing of pyrolysis oil model compounds such as acetic acid, phenol, guaiacol and acetol with vacuum gas oil in FCC approach. Besides, Lappas et al., (2009) also studied the effect of FPO representative model compounds on product yields while co-processing them with VGO/LCO.

1.2 MOTIVATION

In spite of several studies on co-processing at laboratory and pilot plant levels, the understanding of presence of type of FPO components on the FCC product distribution remains limited. In addition there is a lack of JCC-derived FPO (indigenous feedstock) scope for co-processing in FCC unit with VGO to get drop in liquid hydrocarbons. The same holds for the understanding on ways to optimizing the process parameters, so as to obtain the limitations on co-processing of raw or hydrodeoxygenated FPO with petroleum-derived fraction i.e., VGO and specific effect of type of FPO compounds on FCC product distribution.

1.3 OBJECTIVES

On overall basis, the objective of the present work is to pursue and describe the studies on co-processing of FPO with VGO in FCC process in an effective way and to find an application as an alternative to fossil based hydrocarbons. These studies will help in broad understanding of the blending limitations of JCC-derived fast pyrolysis oil (FPO) or its hydrodeoxygenated oil (HDO) with VGO before co-processing in a refinery FCC unit. The specific objectives of the present study are as follows:

1) Preparation of biomass-derived feedstocks for co-processing in FCC unit.
   a. Production of FPO from JCC in fluidized bed reactor set up.
   b. To study the effect of operating temperature on hydrodeoxygenation of FPO over Pd/Al_2O_3 catalyst in CSTR.
   c. To perform the characterization of feedstocks and products using ^{1}H, ^{13}C and ^{31}P NMR techniques.
2) Catalytic cracking of FPO and HDO with VGO in FCC unit.
   a. To study the effect of blending ratio of FPO with VGO on FCC unit product distribution.
   b. To perform the catalytic cracking of HDO with VGO at iso-conversion of FPO with VGO and pure VGO.
   c. To perform the characterization of FPOs and their catalytically cracked products using ^{1}H and ^{13}C NMR techniques.
3) Catalytic cracking of pyrolysis oil model compounds and glycerol with VGO in FCC unit.
   a. To optimize the process parameters of catalytic cracking of VGO for gasoline.
   b. To study the effect of aliphatic oxygenates (acetic acid, hydroxy acetone, glycerol & glycolaldehyde) and aromatic oxygenate (2-methoxy phenol) of FPO while co-processing with VGO on FCC product distribution by varying catalyst-to-oil (C/O) and blending ratios.
   c. To perform the characterization of FCC liquid by ^{1}H and ^{13}C NMR, and FTIR techniques.
4) Kinetic modelling for catalytic cracking of VGO and VGO with FPO.

1.4 THESIS ORGANIZATION

The thesis is organized in the following manner:

Chapter 1 introduces the subject matter.

Chapter 2 presents the work of previous researchers in the areas of developments in the fast pyrolysis technologies, challenges ahead of processing FPO in FCC unit. In addition the approaches for the stabilization of FPO are summarized. Finally the scope of integration of fast pyrolysis process with refinery FCC unit is also described.

Chapter 3 deals with the outline of the materials used in the experimental setup, experimental work, synthesis processes description and product analysis using various analytic techniques in detail.

Chapter 4 discusses the catalytic cracking of JCC-derived FPO with VGO in FCC unit. It also discusses the characteristics of feedstock and catalysts used.

Chapter 5 discusses the effect of pyrolysis oil model compounds (acetic acid, guaiacol, acetol, glycolaldehyde) and glycerol addition with VGO on FCC product distribution.

Chapter 6 describes the application of 5–lump kinetic model for estimating kinetic parameters for catalytic cracking of VGO and FPO blended feed with VGO.

Chapter 7 states the overall chapter vise observations, conclusions drawn from the experimental work and possible recommendations for future research.

CHAPTER 2

LITERATURE REVIEW

2.1 GENERAL

Lignocellulosic biomass is considered to be a realistic resource of green energy [Melero et al. 2012], for sustainable development [Eissen et al. 2002] and food security [Moreira et al. 2005, Nogueira et al. 2013a, b]. With this background several thermochemical conversion techniques have been envisaged for the conversion of lignocellulosic biomass into crude pyrolysis oil. Fast pyrolysis has been considered for the production of so called "second generation" biofuels and green chemicals. The production of pyrolysis oils by fast pyrolysis technique at industrial scale has been demonstrated with numerous types of pyrolysis reactor configurations, but nevertheless it has so far not been adopted in commercial practice. The crude FPO is highly oxygenated and unstable; hence it requires further processing by means of deoxygenation in order to convert it into hydrocarbons of fuel range. Thus thermal, catalytic and chemical stabilization techniques have been anticipated for the stabilization of FPO so that the stable liquid can be directly used as fuel or can be easily further upgraded.

This chapter summarizes the various technologies for fast pyrolysis of biomass followed by real challenges, associated with them, for use in refinery FCC as co-processing feedstock. Then, a brief introduction into crude FPO stabilization techniques is given. The investigation leading to the present work wherein the schemes proposed so far for integration of fast pyrolysis process with petroleum refinery was described.

2.2 BIOMASS FAST PYROLYSIS PROCESS DEVELOPMENTS

The typical biomass pyrolysis processes have been classified into the following categories: conventional carbonization, pressurized carbonization, conventional, fast, flash-liquid, flash-gas, vacuum, methano-pyrolysis and hydro-pyrolysis. These typical names have been decided on the basis of their unique characteristics like process environment, operating parameters (i.e., heating rate, residence time, and reaction temperature) and products obtained.

Fast pyrolysis is a process wherein the thermal degradation of organic materials is occurs in the absence of oxygen at atmospheric pressure, 450-600 $^{\circ}$C of temperature, with short hot vapor residence time, typically <3 s. The usual steps involved in the fast pyrolysis process are biomass drying, pyrolysis (reaction) followed by char particle separation and liquid recovery. The produced pyrolysis vapors are further quenched to obtain fast pyrolysis liquid.

The critical challenges involved during the operation of fast pyrolysis are the selection of pyrolysis reactor configuration, rate of heat transfer, controlled reaction temperature and vapor residence time, char/soot particle separation and liquid recovery. Several processes have been proposed based on the type of reactor configurations used and applications. The performance and status of major fast pyrolysis technologies is reported in Table 2.1 and Table 2.2, respectively.

2.2.1 Auger Pyrolyzer

An auger fast pyrolyzer is shown in Figure 2.1a. An auger is used to simultaneously mix and pass on the lignocellulosic biomass continuously by being brought into direct contact with sand or steel shots, which act as a heat carrier. The heat carrier is heated seperately prior to metering into the reactor. The precise control of residence time of biomass particles in the reactor could be possible with this auger technique. The produced volatile vapors and aerosols exit at various ports of the reactor, whereas the char is moved axially along the reactor section and stored in a seperate container along with the heat carrier. This kind of design with mechanical mixing concept could be highly suitable for producing pyrolysis oil in a distributed and decentralized mode of biomass processing scheme. The disadvantages of the auger reactor are: (i) it is very difficult to separate char and heat carrier at the reactor end; (ii) there is chance of more fines formation in the char, and (iii) it requires a heating and circulating system for heat carrier.

The technology so-called Lurgi-Ruhrgas (LR)-mixer reactor earlier in 1950's initiated with a collaboration of Lurgi and Ruhrgas Companies for coal pyrolysis for town gas production [Peters et al. 1963]. Later, the **Karlsruhe Institute of Technology (KIT) has developed** bioliq® process (Biomass to Liquid Karlsruhe) and scaled up to demonstration level of 500 kg/h for the flash pyrolysis pilot plant [Channiwala et al. 2002] using sand as a heat carrier for straw feedstock. Advanced Bio Refinery Inc (ABRI) has developed the commercial units from the scale of 20 kg/day to even 1 t/d and their trials are successful [Hedley et al. 2007].

Table 2.1: Performance of major fast pyrolysis reactors

Reactor	Biomass feedstock	FPO, wt.%	Heat transfer	Residence time, sec	Solids throughput	Inert gas	Particle size, mm	Status
Auger	Pine wood [Ingram et al. 2008]	67	Low	<30	Low	Low	<4	Demonstration
Ablative	Wood [Mohan et al. 2006]	70	High	< 0.1	Low	High	<20	Pilot
Bubbling fluidized bed	Soft wood [Mohan et al. 2006]	75	High	<3	High	High	<3	Commercial
Circulating fluidized bed	Wood [Mohan et al. 2006]	75	High	<1	High	Very high	<2	Commercial
Rotating cone	Palm derived EFB [http://www.btg-btl.com]	70	Very high	<1	Very high	Low	<10	Commercial
	Demonstration: 200-2000 kg/h; Commercial: 2 t/h-20 t/h							

Table 2.2: Status of major fast pyrolysis technologies in 2014 (above 6 tons/day) [Source: Oasmaa et al. 2015]

Technology	**Country**	**Host organization**	**Capacity, TPD***	**Application**	**Status**
Auger	Canada	ABRI-Tech	48	Fuel	Dormant
Ablative	Germany	Pytec	6	Fuel	Dormant
Bubbling bed	Canada	Dynamotive	200	Energy	Dormant
Fluidized bed	Finland	Fortum	240	Fuel	Operational
Circulating bed	Canada	Ensyn	75	Fuel	Operational
Circulating bed	Brazil	Ensyn/Fibria	400	Fuel	In design phase
Circulating bed, catalytic	USA	KiOR	500	Catalytic bio-oil for HDO	Dormant
Rotating cone	Malaysia	Genting	48	Fuel	Operational
Rotating cone	Netherlands	Empyro BV	120	Fuel	Commissioning

*TPD: Tons per day on dry feed basis

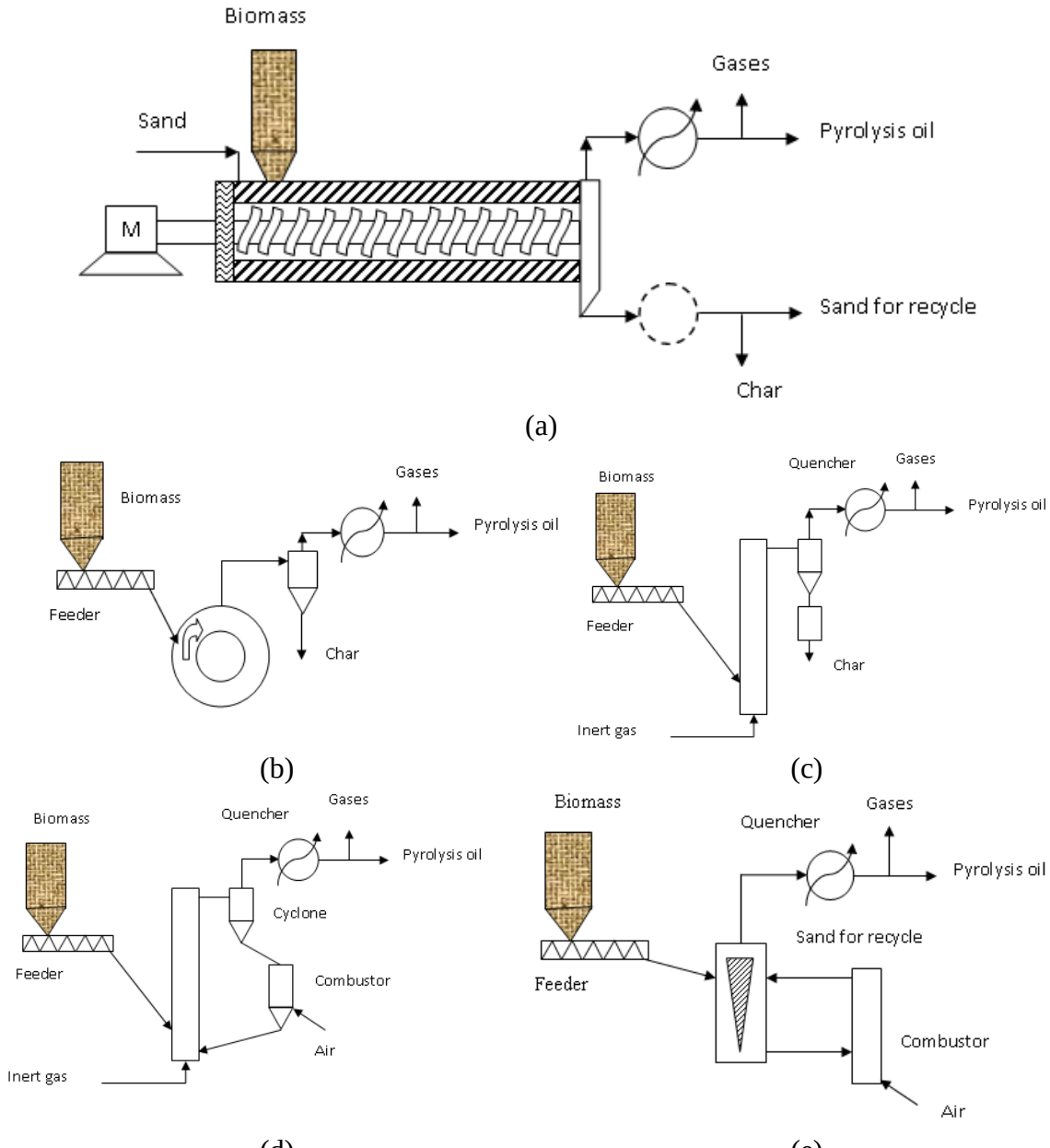

Figure 2.1: Pyrolysis reactor configurations: (a) Auger, (b) Ablative, (c) Bubbling fluidized bed, (d) Circulating fluidized bed and (e) Rotating cone

2.2.2 Ablative Pyrolyzer

The typical ablative fast pyrolyzer is shown in Figure 2.1b. In the ablayive fast pyrolyzer, the higher velocities of carrier gas have been used to centrifuge the lignocellulosic biomass particles on to heated wall of reactor in tangential mode. Here, the rate of pyrolysis is function of pressure, relative velocity of biomass particleand reactor surface temperature. With this design

even the large size biomass particles (up to 20 mm) can get pyrolyzed, whereas a minimum of 2 mm is required for typical fluidized bed designs [Ringer et al. 2006], as the reaction rate is not limited by heat transfer through the biomass particle. The disadvantages of ablative pyrolyzer are: (i) scale up of this process is costlier as it is surface area controlled, and (ii) more wear and erosion problems are encountered as the reactor is mechanically driven. The first pilot scale plant is being operating to produce 4 TPD of FPO since 2005, and it is aimed for the generation of heat and power from biomass [http://www.pytecsite.de/ pytec_eng/]. In Germany, PYTEC Thermochemische Aulagen GmbH, designed, built and operated an ablative pyrolyzer, with a capacity of 15 kg/h. Their typical experience and the promising results obtained so far led them to order for a 48 t/d plant [Meier et al. 2005].

2.2.3 Bubbling Fluidized Bed Pyrolyzer

The typical bubbling fluidized bed fast pyrolyzer (BFB) is shown in Figure 2.1c. BFB pyrolyzer have the advantages of good control of temperature and high heat transfer to biomass particles, and consistently gives high pyrolysis oil yields of biomass. The residence time of biomass particles can be accurately maintained by adjusting the fluidizing gas flow rate in the freeboard zone of the reactor. To achieve the high biomass heating rates, small biomass particle sizes of < 2 mm are required. The particle size and the rate of particle heating are usually the rate limiting parameters. The main difficulty arises during the operation of bubbling fluidized bed fast pyrolyzer is the separation of soot particles from the pyrolysis vapors as cyclone separators can not separate the soot particles less than 2-3 microns, which leads to difficulties in separation of soot with pyrolysis oil. During pyrolysis process, the unseparated pyrolysis char act as a catalyst in cracking vapors, which needs to be separated as quickly as possible.

In the early 1980s, the pioneering work on fundamentals of BFB pyrolyzer was carried out at the University of Waterloo and National Renewable Energy Laboratory (NREL). Based on their experience, a Fast Pyrolysis Process was developed at the University of Waterloo, which led to design of a company so-called Resource Transforms International in Canada [Ringer et al. 2006]. The drawback of BFB fast pyrolyzer is heat transfer to bed at industrial scale of operationdue to the scaleup limitation. The Dynamotive group constructed a 10 t/d fast pyrolysisoil plant in 2000. Based on their experience the group further built a 25 t/d

demonstration plant and also designed and constructed full-scale 100–400 t/d commercial plants, which canbe built in Canada, and other international countries [Vamvuka et al. 2011].

Dynamotive suggested a post fast pyrolysis product called "BioOil Plus" which contains a mixture of 80% BioOil and 20% char, which gives higher energy content than BioOil alone. BioOil Plus is exclusively to be used as an industrial fuel and is targeted as such in boiler and kiln industry. Dynamotive reported that the studies have shown that BioOil Plus is equivalent to natural gas in terms of thermal performance and product quality [http://www.dynamotive.com/industrialfuels/biooilplus].

2.2.4 Circulating Fluidized Bed Pyrolyzer

Circulating fluidized bed (CFB) reactor system has many similar characteristics of bubbling fluidized bed (BFB) reactor.The residence time for the char particle is almost the same as for vapors and gas in CFB and BFB. The typical CFB pyrolyzer is shown in Figure 2.1d. The char obtained from CFB reactor is more attrited due to the higher gas velocities required for the movement of char along with heat carrier from riser to the regenerator/combustor, which can lead to higher char contents in the collected FPO. The main advantage of the CFB fast pyrolyzer is that the large throughputs can be handled even though the hydrodynamics are more complex.

1-2 mm size of biomass particles are required for a CFB fast pyrolyzers, which is very smaller as compared to the particles size used in bubbling beds. The availability of low residence time (0.5-1 sec) in CFB is not sufficient to transport heat to the interior surface of biomass particle. There is a chance of abrasion along the walls of the circulating system due to the complete circulation of sand in the system with higher velocities of carrier gas. Scalability of heat transfer for higher throughputs has to be proven.

Originally the CFB fast pyrolyzer was invented at the University of Western Ontario and is currently commercialized by Ensyn Technologies with a name rapid thermal process (RTP). Currently there are 8 worldwide operational plants: 3 plants at Red Arrow in Wisconsin, one unit at ENEL in Italy, 3 plants at Ensyn in Ottawa, and one plant at VTT in Finland. CRES (Greece) and ENEL (Italy) organizations are also involved in developing CFB based pyrolysis technology in addition to Ensyn Technologies [Graham et al. 1995, Underwood et al. 1992].

2.2.5 Rotating Cone Pyrolyzer

No inert carrier gas is required in rotating cone pyrolysis reactor (RCR). It is a cyclonic reactor wherein both the biomass and hot sand are mixed and transported upwards by the rotation of the cyclone cone over the conical surface. This design gives very high heat transfer rate due to very small distance from the heated surface. The pressures of outgoing materials are slightly above atmospheric levels. The advantages of the reactor are high heating rate and narrower gas phase residence time, which leads to suppression of the coke forming reactions. Figure 2.1e shows a typical rotating cone fast pyrolyzer.

The rotating cone fast pyrolyzer was invented at the University of Twente and further developed by BTG biomass technology group. Originally, in 1989, it was developed using ablative reactor approach by operating it without inert sand. Later on, it was further modified to a sandtransportedbed rotating cone reactor (RCR) [Wagenaar et al. 1994]. It was also reported that using RCR technology a capacity of 5 t/h fast pyrolyzer can be designed with a length/diameter ratio of 1 only [http://www.btg-btl.com]. BTG biomass technology group scaled up Wagenaar's RCR technology to 50 kg/h in 1997. Further in 2005, BTG built a 2 t/h production plant in Malaysia, using Empty Fruit Bunch (EFB) as biomass feedstock.

2.2.6 Vacuum Pyrolyzer

Biomass is moved either by gravity and rotating scrappers through multiple hearths, which carries the biomass into the vacuum chamber [Ringer et al. 2006]. The reactor is operated at reduced pressure (2-20 kPa). The released vapors are quickly condensed and collected as crude pyrolysis oil. This pyrolyzer has a plus point of handling large size biomass particles (up to 20 mm) and lower residence time (<1 sec). Early work on biomass vacuum pyrolyzer was performed by Professor Roy at the Université de Sherbrooke and University of Laval in 1980's. They extended their work to level of erection of demonstration unit (3.5 tpd) in Jonquiere, Canada for the feedstock of bark in 1998. Nevertheless the unit was ceased in 2002 due to the operational limitations of indirect heat transfer with molten salt in the reactor [Brown et al. 2011a]. Indian Institute of Technology, Bombay has the bench scale vaccum pyrolysis setup aimed for conversion of various agricultural and agro-industrial biomasses into crude pyrolysis oil [Raveendran et al. 1995, Das et al. 2003, 2004a, b]. Further, they are working with Ministry of New and Renewable Energy, India to design to demonstrate a 100 kg/d vacuum pyrolysis unit.

2.3 CHALLENGES FOR PYROLYSIS OIL PROCESSING IN FCC

The pyrolysis oil is a mixture of over 300 compounds including carboxylic acids, hydroxyl ketones, hydroxyl aldehydes, lignin-derived monomers and anhydrosugars etc. The typical physical properties of biomass-derived pyrolysis oils are compared with fuel oil in Table 2.3 and different pyrolyzers in Table 2.6. In the present scenario with these physical properties the pyrolysis oil cannot be used in any engine or to upgrading equipment. Therefore, there is a need for stabilization of pyrolysis oil before taking into any upgrading equipment and the same discussed in the section 3. Currently, the available standards for pyrolysis oil are ASTM D7544, which can be specifically applied for direct used in the furnaces and automobile engines.

Table 2.3: Comparison of physical properties of biomass-derived pyrolysis oils with fuel oil (Source: Zacher et al. 2014)

Components	**Pyrolysis oil**	**Petroleum–derived fuel oil**
C, dry (wt.%)	56.0	85.0
H, dry (wt.%)	6.0	11.1
O, dry (wt.%)	38.0	1.0
Water (wt.%)	20–30	0.025
Solid (wt.%)	0.01–0.1	0.0
Ash (wt.%)	0.01–0.2	0.01
Nitrogen (wt.%)	0–0.4	0.0
Sulfur (wt.%)	0–0.05	0.2
Stability	Unstable	Stable
Viscosity @40 ^{o}C	15–35	3.0–7.5
Density @15 ^{o}C	1.10–1.30	0.89
Flash point (^{o}C)	40–110	60
Pour point (^{o}C)	–9 to –36	–15
LHV (MJ/kg)	13–18	40.3
pH	2–3	Neutral
Boling range	Decomposes	140–400 ^{o}C

From the view of maintaining heat balance of the FCC unit and to limit the fresh catalyst consumption within a reasonable level, the feed to the FCC should meet certain specifications with respect to its boiling point, coking tendency, metals content, sulphur content etc. In addition to the above the effective hydrogen index, composition of feedstock also plays an important role for co-processing of FPO with VGO in FCC unit. To meet the aforementioned specifications before feeding FPO into FCC is a real challenge for the development of process in a view of integration of fast pyrolysis process with refinery FCC unit.

Moreover, the quality of biomass-derived FPO is a function of pH, heating value, viscosity, nitrogen, water, ash and char content. The properties (physical, chemical and combustion) of pyrolysis oil changes with change in time. It is reported that over a period six months the viscosity of FPO increases from 1127 to 2283 cP [Tiplady et al. 1991]. A few of the important challenges for meeting the specifications of feed and their significance are given below.

2.3.1 API Gravity

The API (American Petroleum Institute) gravity is tells about the specific gravity at 60 °F by the formula: °API = {141.5-Specific Gravity}-131.5. It is a measure of how petroleum is heavier or lighter in compare to water. The higher value of °API indicates that the feed is more saturated and less aromatic, which helps in easy cracking and the higher yield of gasoline with slightly lower octane.

The °API gravity of feed to the FCC unit is varies from 16 to 48. Therefore, it is very much essential to maintain the °API gravity within the range so that the pyrolysis oil can be easily cracked in FCC for maximization of gasoline yield.

2.3.2 UOP Characterization Factor

UOP or UOP K value is a factor used to measure the paraffinicity of petroleum oils based on its boiling point and specific gravity, which is related by the relation: UOP characterization factor =UOP K= $\{(\text{Cubic average boiling point})^{1/3}/(\text{Specific Gravity})_{60°F}\}$.

The K value of 12.5 would designate a feed is highly paraffinic (saturated); whereas the value of 11.2 would show a more aromatic (unsaturated cyclic). Thus, the pyrolysis oil with K value of 12.5 and above is preferable for processing or co-processing with pyrolysis oil in FCC.

2.3.3 Boiling Range

The boiling range of FCC hydrocarbon feed usually varies from 260 °C (initial boiling point) to 540 °C (final boiling point). While the biomass-derived pyrolysis oil boiling range starts from ambient temperature to even higher temperature of 560 °C as it is contains multi components having lower to higher boiling points.

The presence of heavy components in FCC feed would throw in the formation of undesirable coke. Hence, the heavy components (polynuclear aromatics, organo-metallic and high sulphur compounds) are considered to as coke precursors.

2.3.4 Carbon Residue

Carbon residue gives a measure of the carbon deposition tendencies of FCC feed when heated in a bulb under prescribed conditions. It can be determined by either Conradson or Rams-bottom methods. The petroleum-derived vacuum gas oil containing Conradson carbon residue (CCR), indicative of coke-forming potential, of 0.74 wt.% can be processed through FCC unit[http://petrofed.winwinhosting.net/upload/25-28May10/S_Bose.pdf]. Whereas the residual fluid catalytic cracking (RFCC) process can handle up to CCR of 4.06 wt.%.

Therefore, it is recommended to carry out the hydrotreatment of pyrolysis oils until predetermined level of conversion (<10 wt.% of CCR) is achieved [Ardiyanti et al. 2012]. It is [Oasmaa et al. 1997] reported that the CCR typically ranges from 18to 23 wt.% for pyrolysis oil obtained from hardwood (oak-maple, eucalyptus) and softwood (pine), whereas it varies from17 to18 wt.% for pyrolysis oil from wheat straw.

2.3.5 Metal Content

Specifically, in the refinery FCC unit the presence of metals (Ni, V, Cu and Fe) causes undesirable dehydrogenation reactions resulting in an increase of hydrogen, coke, olefins and lighter hydrocarbons in the cracked products at the expense of LPG or gasoline. Nickel and copper are more effective in promoting these hydrogen producing reactions. Thus, an increase in volume ratio of hydrogen/methane, a measure of the extent of metallic poisoning, or increase of olefinic content of C_3 stream is all indications of contaminations of catalyst. The ratio of H_2/CH_4 from 0.3 to 0.8 is preferred; whereas the value >1.0 specify a significant degree of poisoning. Further, the contamination of a feedstock to FCC like unit is measured by a metal factor (Fm) i.e., Fm= Fe+ V+ 10 (Ni + Cu); where Fe, V, Ni, Cu are the concentration in ppm of iron, vanadium, nickel, and copper. A metal factor of 1.0 is considered as safe and feedstock with metal factor of above 3.0 may result in poisoning the catalyst. The presence of sodium weakens the molecular structure and decreases the hydrothermal stability of catalyst resulting in damage due to sintering at lower temperatures and subsequent loss of surface area.

Thus, the control of ash content before processing of pyrolysis oil in refinery units is very much required to control the side reactions and poisoning of FCC catalyst. In regards to biomass, the inorganic materials especially the potassium and calcium, catalyze biomass decomposition and char-forming reactions [Garcia-Perez et al. 2009].

2.3.6 Nitrogen

Nitrogen acts as a temporary catalyst poison which reduces the catalyst activity by neutralizing the acid sites of cracking catalyst available for promoting reactions. The presence of nitrogen compounds in the FCC feeds is undesirable as the organic nitrogen converts into basic nitrogen compounds (like ammonia, pyridine, quinoline) in FCC riser, which act as a poison by neutralizing the active acid sites of the cracking catalysts, which results in rapid loss of activity [Fu et al. 1985, Scherzer et al. 1986, 1988]. The loss of activity results into changes in product selectivity of FCC. A FCC feed with total nitrogen concentration of <1000 ppm is not detrimental to activity; whereas it detrimental on above 1500 ppm.

In the case of wood-derived pyrolysis oil, the nitrogen content is less than 0.4 wt.% (wet basis) [Oasmaa et al. 2010c]; whereas corn-derived pyrolysis oil is 1% [Elliott et al. 2009], which are highly dependent on type of biomass feedstock. The basic and nonbasic nitrogen species in petroleum also falls in the range of 0.1-0.9% [Abdel-A et al. 2003]; whereas the conventional FCC feedstock, gas oil, contains the nitrogen in the range of 0.1-0.8 wt.% [Scherzer et al. 1987].

2.3.7 Hydrogen Effective Index

Typically, the amount of hydrogen available for energy production is related by the index called effective hydrogen index, which can be defined by the equation [H/C_{eff} = (H-2O-3N-2S)/C] as proposed [Chen et al.1986], where H, O, N, S and C are number of moles of hydrogen, oxygen, nitrogen, sulfur and carbon present in the feedstock. The effective hydrogen index is less than 1 for highly oxygenated compounds, close to 1.5 for triglyceride-based biomass, whereas for hydrocarbons it varies from 2 (liquid alkanes) to 1 (for benzens) [Melero et al. 2012]; while it is 0, 1/3, and 2/3 for glucose, sorbitol, and glycerol, respectively [Corma et al. 2007]. Zhang et al. 2011 reported that onconversion of biomass-derived feedstock's overZSM-5 , the feedstock's

with H/C_{eff} less than 0.15 produce more coke and it is suggested to have a minimum of H/C_{eff} of 1.2 (as an inflection point) to produce optimum aromatics and olefins in refinery set ups.

2.3.8 Composition

It is very difficult to describe the overall composition of pyrolysis oil as it depends on many factors like feed structural composition, type of pyrolysis reactor, pyrolysis operating conditions, liquid collection systems that have been used for condensing vapors, and by the storage stability of FPO. Earlier the typical range of pyrolysis oil composition is reported by Diebold et al. (2005). Further, Brown et al. (2009) also reported the composition of pyrolysis oil obtained from auger pyrolyzer, however, which is out of the range for some compounds as mentioned by Diebold et al. (2005). Branca et al. (2003) compared the pyrolysis oil composition (with the identified 40-43% of compounds) of four major commercial pyrolyzers: bubbling fluidized bed (Dynamotive), rotating cone (BTG), circulating fluidized bed (ENSYN), and vacuum pyrolyzer. However, the recent ASTM D7544-12 covers the specification of pyrolysis liquid biofuel (obtained from biomass) as a fuel for industrial burner; whereas the same is not applicable to home heaters, smallscale boilers and engines applications.

The compounds, identified using GCMS, obtained from fast pyrolysis by various authors are summarized in Table 2.5. From the Table 2.5, it can be seen that a variety of compounds (~175) including acids, alcohols, aldehydes, alkenes, catechols, esters, furans, ketones, phenols, guaiacols, syringols, sugars, and oxygenated compounds are identified using GCMS.

2.3.9 Acid Value

The acidity of FPO is derived mainly from volatile acids (60-70%), which has lowest pKa values as compared to other compounds such as hydoxy acids in sugar (20%), phenolics (5 to10%) and fatty acids (<5%) [Oasmaa et al. 2010b], and these acids, do not react with FPO components at moderate temperature of ≤80 °C. The acidity of FPO causes corrosion in pipelines and process equipment of processing units. Hence, the selection of material for transportation and reactions becomes most vital in order to see the feasibility of integration of fast pyrolysis process with refinery. Table 2.6 shows that pyrolysis oil derived from different types of pyrolyzers, the pH value varies from 2 to 3.

In the case of FCC, the feed stock with high Total Acid Number (TAN) would not affect the stability of FCC catalyst as the large number of acidic compounds decomposes rapidly at FCC riser operating temperature. However, naphthenic acid is highly active at its boiling point and hence it causes severe corrosion in condensation equipments. Thus it is mentioned that the TAN of curde oil fractions >1.5 are believed to be significantly corrosive in the temperature range of 232 to 398 °C [Zeman et al. 2008].

2.3.10 Water

The typical water content and other physic-chemical properties of various pyrolysis oil obtained from different pyrolysis reactors are listed in Table 2.6. Formation of water during the pyrolysis reaction is due to the presence of bound moisture in feed biomass (>10 wt.% leads to phase separation aqueous and oily viscous), and alkali metals especially potassium (which catalyze secondary pyrolysis reaction [Agblevor et al. 1996]. In addition this, the aging reactions (like etherification and esterification between hydroxyl and carbonyl compounds) also take part for the formation of water as a by-product [Lehto et al. 2013]. This cannot be separated from FPO by means of centrifugation [Oasmaa et al. 2010c]. From NREL report [Ringer et al. 2006] it has been observed that even if the bone-dry biomass is subjected to fast pyrolysis, the resulting FPO still contain a minimum of 12 to15 wt.% water.

The high water content in FPO will lead to decrease in the heating value, adiabatic flame temperature and viscosity. Further, the water content (> 30%) will lead to phase separation, leading to non-homogeneous mixture [http://www.btg-btl.com/index.php?r=faq]. The water content of FPO can be analyzed by Karl Fischer volumetric titration technique as per ASTM Standard E 203 [Oasmaa et al. 2010c]. The water content should be low (<0.2 vol.%) in order to prevent shocks and vibrations, resulting from flash vaporization of water droplets in FCC operation. Free water in bulky quantities is dangerous as it can upset the pressure balance of the reactor regenerator system in FCC process. Moreover, the updated list of recommended analysis methods alongwith properties are summarized in Table 2.4 as reported by Oasmaa et al. (2015). In addition to the above mentioned typical challenges of pyrolysis oil properties, the role of proper modeling of biomass decomposition in is very much needed inorder to get high quality of pyrolysis oil [Sadhukhan et al. 2008a, b and 2009].

Table 2.4 Standard test methods for fast pyrolysis oil [Source: Oasmaa et al. 2015]

Property	**Typical range**	**Applicable test methods**
Higher heating value, HHV	14−19 MJ/kg	DIN51900, ASTM D240
Lower heating value, LHV	13−18 MJ/kg	DIN51900, ASTM D240, ASTM D5291 for H
Water	20−30 wt %	ASTM E203
pH	2−3	ASTM E70
TAN	70−100 mg KOH/g	ASTM D664
Kinematic viscosity@40°C	15−40 mm^2/s	EN ISO 3104, ASTM D445
Density at 15 °C	1.11−1.30 kg/dm^3	EN ISO 12185, ASTM D4052
Pour point	−9..-36 °C	EN ISO 3016, ASTM D97
Carbon	50−60 wt % (d.b.)	ASTM D5291
Hydrogen	7−8 wt % (d.b.)	ASTM D5291
Nitrogen	<0.5 wt % (d.b.)	ASTM D5291
Sulfur	<0.05 wt % (d.b.)	EN ISO 20846, ASTM D 5453
Oxygen	35−40 wt % (d.b.)	as difference
Solids	<1 wt %	ASTM D7579
MCR, CCR	17−23 wt %	ASTM D4530, ASTM D189
Ash	<0.3 wt %	EN ISO 6245
Flash point	40−110 °C	EN ISO 2719, ASTM D93B
Sustained combustibility	Does not sustain combustion	EN ISO 9038
Na, K, Ca, Mg	<0.06 wt % (d.b.)	EN ISO 16476
Chlorine	<75 ppm	not specified

2.4 STABILIZATION OF FAST PYROLYSIS OIL

Typically, the stability test of FPO is defined as “the change in viscosity of a sealed sample of FPO for 24 hours at 80 °C”. Further, stable oil also means a FPO which is free from any physical or chemical changes while storage. The process of stabilization can be defined as “the conversion of thermally unstable functionalities into thermally stable corresponding molecules”. Stabilization of FPO can be carried out either by modifying their chemical composition, making it less active or removing its destabilizing components.

Table 2.5: GC-MS identified pyrolysis oil components of various fast pyrolysis reactors and biomasses

	Reactor (*Circulating fluidized bed reactor; #Rotating cone reactor)		**Auger Reactor**				**Bubbling Fluidized Bed Reactor**					**CFB***	**RC#**	
	Feedstock	Typical. wt.%	Pine wood	Pine bark	Oak wood	Oak bark	Beech	Spruce	Iroko	Albizia	Corncob	Soft wood	Hard wood	Soft wood
	Reference	Diebold et al. (2005)		Azad et al. (2011)			http://www.pytec.de/download.php?what56					Wagenaar et al. (1994)		
	Acids													
1	Formic (methanoic)	0.3-9.1										√	√	√
2	Acetic (ethanoic)	0.5-12					√	√	√	√	√	√	√	√
3	Propanoic	0.1-1.8					√	√	√	√	√	√	√	√
4	Hydroxyacetic	0.1-0.9												
5	2-Butenic(crotonic)											√	√	√
6	Butanoic	0.1-0.5												
7	Pentanoic (valeric)	0.1-0.8										√	√	√
8	4-Oxypentanioc	0.1-0.4												
9	Hexanoic (caproic)	0.1-0.3										√	√	√
10	Benzoic	0.2-0.3										√	√	√
11	Heptanoic	0.3												
12	3,4-dimethyl benzoicacid		√	√	√	√								
13	Oleic acid		√	√	√	√								
14	4-Hydroxy-butyric acid											√	√	√
15	glycolic acid											√	√	√
16	2-oxobutanoic acid											√	√	√
17	Lactic acid											√	√	√
18	acrylic acid											√	√	√
19	isobutyric acid											√	√	√
20	methacrylic acid											√	√	√
21	*N*-butyric acid											√	√	√
22	3-hydroxypropanoic acid											√	√	√
23	tiglic acid											√	√	√

24	4-methylpentanoic acid											√	√	√	
25	levulic acid											√	√	√	
	Alcohols														
26	Methanol	0.4-2.4										√	√	√	
27	Ethanol	0.6-1.4										√	√	√	
28	2-Propene-1-ol											√	√	√	
29	Ethylene glycol	0.7-2.0													
30	But-2-en-1-ol											√	√	√	
31	dihydroconiferyl alcohol						√								
32	isomer of coniferyl alcohol						√	√	√						
33	isomer of sinapyl alcohol					√			√						
	Aldehydes														
34	Formaldehyde	0.1-3.3										√	√	√	
35	Acetaldehyde	0.1-8.5										√	√	√	
36	2-Propenal (acrolein)	0.6-0.9													
37	2-Methyl-2-butenal	0.1-0.5													
38	Pentanal	0.5													
39	Ethanedial	0.9-4.6													
40	3-hydroxypropionaldehyde					√	√	√	√	√					
41	Propanal					√	√	√	√	√					
42	furaldehyde, 2-					√	√	√	√	√		√	√	√	
43	furaldehyde, 3-									√					
44	furaldehyde, 5-methyl-2-						√	√	√	√		√	√	√	
45	furaldehyde, 5-(hydroxymethyl)-, 2-						√								
46	benzaldehyde, 4-hydroxy-									√		√	√	√	
47	benzaldehyde, hydroxy-					√	√	√	√	√					
48	phenylacetaldehyde, 4-hydroxy-3-methoxy-(homovanillin)					√	√	√	√						
49	Vanillin		√	√	√	√	√	√	√	√	√	√	√	√	
50	Acetovanilline		√	√	√	√									
51	coniferylaldehyde					√	√	√	√	√		√	√	√	
52	sinapaldehyde (trans)					√		√	√						

53	propionaldehyde											√	√	√
54	glyoxal											√	√	√
	Esters													
55	Methyl formate	0.1-0.9												
56	Butyrolactone	0.1-0.9												
57	Valerolactone	0.2												
58	Angelicalactone	0.1-1.2												
	Ketones													
59	Acetone	2.8										√	√	√
60	2-Butenone													
61	2-Butanone (MEK)	0.3-0.9										√	√	√
62	2-Cyclopentenone								√		√			
63	2,3 Pentenedione	0.2-0.4												
64	3Me2cyclopenten2ol1one	0.1-0.6												
65	2-Et-cyclopentanone	0.2-0.3												
66	Dimethylcyclopentanone	0.3												
67	Trimethylcyclopentenone	0.1-0.5												
68	Trimethylcyclopentanone	0.2-0.4												
69	2-methyl-2-cyclopenten-1-one		√	√	√	√	√	√	√	√	√	√	√	√
70	3-methyl-2-cyclopenten-1-one		√	√	√	√	√	√	√	√	√	√	√	√
71	3-Hydroxy-cyclohexanone													
72	1-hydroxy-2-butanone,						√	√	√	√	√	√	√	√
73	3-acetoin hydroxy-2-butanone						√	√	√					
74	acetyloxy-2-propanone						√	√	√	√	√			
75	2,3-dimethyl-2- cyclopentene-1-one						√	√	√	√	√			
76	2-hydroxy-1-methyl-1-cyclopentene-3-one						√	√	√	√	√			
77	γ-butyrolactone						√	√	√	√	√			
78	2-hydroxy- γ-butyrolactone						√	√	√	√	√			
79	3-hydroxy-5,6-dihydro-, (4H)-pyran-4-one						√	√	√	√	√			
80	2-hydroxymethyl-5-hydroxy-2,3-dihydro-, (4H)-pyran-4-one						√	√	√	√	√			

81	Guaiacyl acetone						√	√	√	√	√			
82	2-ethyl-3-hydroxy-2-cyclopentene-1-one											√	√	√
83	2-hydroxy-2-cyclopentene-1-one						√	√	√	√	√	√	√	√
84	acetoxyacetone											√	√	√
	Phenols													
85	Phenol	0.1-3.8	√	√	√	√	√	√	√	√	√	√	√	√
86	2-Methyl phenol	0.1-0.6	√	√	√	√	√	√	√	√	√	√	√	√
87	3-Methyl phenol	0.1-0.4	√	√	√	√	√	√	√	√	√	√	√	√
88	4-Methyl phenol	0.1-0.5					√	√	√	√	√	√	√	√
89	2,3 Dimethyl phenol	0.1-0.5	√			√								
90	2,4 Dimethyl phenol	0.1-0.3	√	√	√	√	√	√	√	√	√	√	√	√
91	2,5 Dimethyl phenol	0.2-0.4										√	√	√
92	2,6 Dimethyl phenol	0.1-0.4			√	√								
93	2-Ethylphenol	0.1-1.3										√	√	√
94	3-Ethylphenol		√	√	√	√								
95	2,4,6 TriMe phenol	0.3												
96	1,2 DiOH benzene	0.1-0.7												
97	1,3 DiOH benzene	0.1-0.3												
98	1,4 DiOH benzene	0.1-1.9												
99	4-Methoxy catechol	0.6												
100	1,2,3 Tri-OH-benzene	0.6												
101	4-Ethyl-phenol								√	√	√			
102	Ethyl-methyl phenol										√			
103	4-vinyl phenol								√	√	√			
104	2-methyl-4-propylphenol											√	√	√
	Guaiacols													
105	2-Methoxy phenol	0.1-1.1	√	√	√	√	√	√	√	√	√	√	√	√
106	4-Methyl guaiacol	0.1-1.9	√	√	√	√	√	√	√	√	√	√	√	√
107	Ethyl guaiacol	0.1-0.6												
108	Eugenol (4-allyl guaiacol)	0.1-2.3	√	√	√	√	√	√	√	√	√	√	√	√
109	Isoeugenol	0.1-7.2	√	√	√	√	√	√	√	√	√			

110	4-Propylguaiacol	0.1-0.4					√	√	√	√	√	√	√	√
111	Acetoguiacone	0.8					√	√	√	√	√			
112	Propioguiacone	0.8						√						
113	4-Ethyl guaiacol		√	√	√	√	√	√	√	√	√	√	√	√
114	4-vinyl guaiacol						√	√	√	√	√	√	√	√
115	4-acetonguaiacol											√	√	√
	Furans													
116	Furan	0.1-0.3												
117	2-Methyl furan	0.1-0.2												
118	2-Furanone	0.1-1.1					√	√	√	√	√	√	√	√
119	Furfural	0.1-1.1	√	√	√	√								
120	3-Methyl-2(3h)furanone	0.1												
121	Furfural alcohol	0.1-5.2										√	√	√
122	Furoic acid	0.4												
123	5-Methylfurfural	0.1-0.6	√	√	√	√								
124	5-OH-methyl-2-furfural	0.3-2.2			√	√						√	√	√
125	2-furnanmethanol		√	√	√	√								
126	2,5-Dimethoxy-tetrahydrofuran (cis)						√					√	√	√
127	4-Methyl-5H-furan-2-one						√	√	√	√	√			
128	3-methyl-5H-furan-2-one						√	√	√	√				
129	2,5-Dimethoxy-tetrahydrofuran (trans)											√	√	√
130	2-acetylfuran											√	√	√
131	5-Methyl-5H-furan-2-one						√	√	√	√	√			
	Syringols													
132	2,6-DiOMe phenol	0.7-4.8					√		√	√	√	√	√	√
133	Methyl syringol	0.1-0.3												
134	4-Ethyl syringol	0.2					√		√	√	√			
135	Propyl syringol	0.1-1.5												
136	Syringaldehyde	0.1-1.5					√		√	√	√	√	√	√
137	4-Propenylsyringol	0.1-0.3												
138	4-OH-3,5-diOMe phenyl ethanone	0.1-0.3												

139	syringol, 4-methyl-							√		√	√	√	√	√	√
140	syringol, 4-vinyl-							√		√	√	√			
141	syringol, 4-allyl-							√		√	√	√			
142	syringol, 4-propyl-							√		√	√				
143	syringol, 4-(1-propenyl)-, cis							√		√	√	√	√	√	√
144	syringol, 4-(1-propenyl)-, trans							√		√	√	√	√	√	√
145	homosyringaldehyde							√		√	√				
146	acetosyringone							√		√	√	√	√	√	√
147	propiosyringone							√			√	√			
148	syringylacetone							√		√	√	√			
	Sugars														
149	Levoglucosan	0.4-1.4	√	√	√	√	√	√	√	√	√				
150	Glucose	0.4-1.3													
151	Fructose	0.7-2.9													
152	D-xylose	0.1-1.4													
153	D-Arabinose	0.1													
154	Cellobiosan	0.6-3.2													
155	1,6 Anhydroglucofuranose	3.1													
156	anhydro-β-D-arabinofuranose, 1,5-														√
157	anhydro-β-D-xylofuranose, 1,5-										√				√
158	dianhydro-α-D-glucopyranose, 1,4:3,6-										√	√	√	√	√
	Oxygenates														
159	Hydroxyacetaldehyde	0.9-13						√	√	√	√	√	√	√	√
160	Acetol (hydroxyacetone)	0.7-7.4						√	√	√	√	√	√	√	√
161	Acetal	0.1-0.2													
162	Acetyloxy-2-propanone	0.8													
163	2-OH-3-Me-2-cyclopentene-1-one	0.1-0.5													
164	Methyl cyclopentenolone	0.1-0.9													
165	1-Acetyloxy-2-propanone	0.1													
166	2-Methyl-3-hydroxy-2-pyrone	0.2-0.4													
167	2-Methoxy-4-methylanisole	0.1-0.4													

168	4-OH-3-methoxybenzaldehyde	0.1-1.1													
169	Maltol												√	√	√
	Catechols														
170	1,2-benzenediol		√	√	√	√							√	√	√
171	4-methyl catechol		√	√	√	√									
172	3-methyl catechol		√	√	√	√									
173	4-ethyl-1,3-benzenediol (4-ethylresorcinol)		√	√	√	√									
174	methyl-benzenediol,							√	√	√	√				
	Aromatics														
175	Benzene						√	√	√	√	√				
176	Toulene						√	√	√	√	√				
177	Naphthalene					√									
178	hydroquinone (benzene, 1,4-dihydroxy-)						√		√	√	√		√	√	√
	Alekenes														
179	3-methyl-1,2-cyclopentadiene		√	√	√	√									

Table 2.6: Pyrolysis oil properties from various fast pyrolysis reactors

Reactor	**Feedstock**	**Water, wt.%**	**pH**	**Density, g/cc**	**Viscosity**	**HHV, MJ/kg**	**C, wt.%**	**H, wt.%**	**N, wt.%**	**O, wt.%**	**Ash, wt.%**	**Reference**
Auger	Pine wood	16.0	3.1	1.19	60.9 cSt @50 ^{o}C	18.7	52.6	7.53	0.09	39.5	0.2	Ingram et al. (2008)
	Oak wood	22.5	3.1	1.2	41.6 cSt @50 ^{o}C	21.9	47.2	4.51	0.12	48.0	0.18	Ingram et al. (2008)
	Pine bark	19.8	3.2	1.17	70 cP @80 ^{o}C	19.0	54.0	6.97	0.37	38.2	0.43	Ingram et al. (2008)
	Oak bark	22.0	3.2	1.2	131cP @80 ^{o}C	18.3	45.5	6.05	0.32	47.8	0.08	Ingram et al. (2008)
Ablative	Oak wood	16.1	2.9	1.29	159 cP @25 ^{o}C		46.3	6.8	0.1	46.8	0.05	Mohan et al. (2006)
BFB	Beech	22.2	2.5	--	15.2 cSt @40 ^{o}C	16.9	41.4	7.1	0.2	51.2	--	Azeez et al. (2010)
	Spruce	22.0	2.8	--	14.8 cSt @40 ^{o}C	17.2	42.3	7.2	0.2	50.3	--	Azeez et al. (2010)
	Iroko	32.3	2.9	--	--	15.9	38.2	7.5	0.3	54.0	--	Azeez et al. (2010)
	Soft wood	21.1	--	--	10 cSt @40 ^{o}C	---	44.7	7.2	0.1	48.1	--	Branca et al. (2006)
	Miscanthus	31.6	--	--	--	22.5	51.8	6.0	1.6	40.6	--	Heo et al. (2010)
	Bagasse	20.8	2.6	1.2	57.0 cSt @20 ^{o}C	15.4	--	--	0.7	--	<0.02	Oasmaa et al. (2005)
	Albizia	25.1	2.9	--	57.1 cSt @40 ^{o}C	17.4	41.9	7.4	0.6	50.1	--	Azeez et al. (2010)
	Corn cob	32.2	3.0	--	6.7 cSt @40 ^{o}C	15.8	38.1	8.0	0.7	53.2	--	Azeez et al. (2010)
	Rice husk	28.0	3.2	1.14	13.2 cSt @40 ^{o}C	16.5	39.92	8.15	0.61		0.25	Quiang et al. (2008)
CFB	Maple oak	26.0		1.19	107 cSt @25 ^{o}C	21.0	55.1	6.7	0.15	38.0	0.14	Mohan et al. (2006)
	Hard wood	20.3		--	210 cSt @40 ^{o}C	--	47.2	6.9	0.1	45.6	--	Luo et al. (2004)
RCR	Fir wood	14.0	2.7	1.22	10 cP @70 ^{o}C	22.2	58.1	6.6	0.5	38.4	<0.05	Mohan et al. (2006)
	Beech wood	22.0	2.5	--	450 cP @40 ^{o}C	20.9	55.1	7.2	2.0	35.1	--	Mohan et al. (2006)
	Soft wood	30.4	--	--	30 cSt @40 ^{o}C	--	37.1	7.6	0.1	55.1	--	Luo et al. (2004)

2.4.1 Modification of Chemical Composition

The chemical composition of FPO could be modified by changing the reaction mechanism of biomass in the pyrolyzer set up. The reaction mechanism in gas phase can be altered either by using catalysts i.e., catalytic pyrolysis approach or changing the process modifications or process parameters. In other way the composition may varied in liquid phase by catalytic hydrogenation techniques.

2.4.1.1 In process (gas phase) approaches

2.4.1.1.1 *Catalytic pyrolysis*

In catalytic pyrolysis approach, the catalyst composition plays an important role for the staibilization of pyrolysis oil compounds in pyrolysis vapors by optimizing the reactions like cracking, decarbonylation, decarboxylation, hydrocracking and hydrodeoxygenation, which leads to balance the activities of inorganic compounds present in biomass. In particular, the catalytic pyrolysis of biomass may carry out in three ways. Dickerson et al. (2013) reviewed various catalysts developments in his catalytic fast pyrolysis review article.

A. *Catalyst-mixing method*

The first one is catalyst-mixing method, where the catalyst is used instead of fluidizing or heating medium i.e., sand to catalytically crack the biomass in the pyrolysis reactor itself. During catalytic pyrolysis all carbonyl compounds are deoxygenated to aromatic compounds in the presence of HZSM-5 catalyst [Gopakumar et al. 2011, Samolada et al. 2000]. Gopakumar et al. (2011) mentioned that up to 41% of aromatics yield was observed in the products with biomass-to-catalyst ratio of 1:9 using HZSM-5 as a catalyst. It indicates that catalyst-mixing method is better option for the production of aromatics. Moreover, Carlson et al. (2008) revealed that the highest yield of aromatics (containing motor octane number of ~111) could be obtained at a nominal temperature of 600 °C from the catalytic fast pyrolysis of cellulosic compounds in a batch pyrolysis reactor (Pyroprobe 2000).

B. *Catalyst-bed method*

Another type of catalytic pyrolysis is the catalyst-bed method, where the catalyst used as a bed in the separate cracking fixed bed reactor which is located next to the pyrolyzer for catalytic cracking of pyrolysis vapors. In this scenario, an integrated fast pyrolysis followed by pyrolysis vapors cracking (in a second catalytic cracking reactor), proposed by National Renewable Energy Laboratory [Diebold et al. 1987, 1988], where the pyrolysis vapors are converted into aromatic and olefin hydrocarbons. On using commercial Mobil MCSG-2 as a catalyst in the second reactor for upgrading of wood-derived pyrolysis vapors, they could able to achieve ~12% of hydrocarbons yield. However, on using modified zeolite as a catalyst for upgrading of aspen wood-derived pyrolysis vapors resulted to hydrocarbons yields of 14 and 16 wt.% at 500 and 600 °C temperatures, respectively, with excessive coke formation [French et al. 2010]. Whereas the use of MCM-41and Ru/MCM-41 catalysts resulted to increase the hydrogen-to-carbon atomic ratio of 1.61 and 1.94 respectively as compare to non-catalytic pyrolysis (1.54) of waste tires [Dung et al. 2009].

Besides, Adam et al. (2006) used the same technique for upgrading different biomass, such as spruce wood and miscanthus-derived fast pyrolysis vapors, in a fixed bed reactor over various mesoporous catalystsincluding a commercial FCC catalyst. There it is stated that the increase of hydrocarbon and phenol yields in the organic phase; whereas the decrease of carbonyl and acid yield are observed.

Lu et al. (2010b) employed variety of six nano catalysts with metal oxides of Mg, Ca, Ti, Fe, Ni and Zn for the catalytic cracking of pyrolysis vapors, released from fast pyrolysis of poplar wood using analytical pyrolysis-gas chromatography/mass spectrometry (Py-GC/MS). It was reported that calcium oxide reduce the concentration of phenols, anhydrosugars and acids significantly, whereas it increased the concentration of cyclopentanones and hydrocarbons. Their results indicated that the use of CaO catalyst considerably decreased the yield of anhydrosugars (levoglucosan) from 9.5 to 1.8 wt.%. Levoglucosan is identified as the major primary product of pure cellulose pyrolysis using micropyrolyzer and fluidized bed pyrolyzer by Patwardhan et al. (2011) with yields of 58.8 and 42.0 respectively. Lu et al. (2010a) reported that the use of Pd/CeTiO2 (Rutile) catalyst is very effective for upgrading of pyrolysis vapors (obtained from poplar wood pyrolysis) by means of converting the lignin-derived oligomers to monomeric phenolic compounds (with yield of 37.2%), while the yield was 25.6% in the case of non-

catalytic route. The results of Mihalcik et al. (2011) also indicated that the yields of levoglucosan reduced below the level of 0.031% and 0.026% with HZSM-5 and H-beta series catalysts while upgrading the pyrolysis vapors of biomass (oak, corn cob, corn stover and switch grass) and its components (cellulose, hemicelluloses, lignin and ETEK lignin) using Py/GCMS.

C. *Cocatalytic pyrolysis*

Another type of doing catalytic pyrolysis is the way of cocatalytic pyrolysis with hydrogen donor solvent. It can be carried out in two ways. The first one may called as pre-mixing technique, where alcohol is fed into the preheated inert gas, before pyrolyzer, where it is being vaporized and moved to pyrolyzer. By carrying out the similar kind of work with cellulose and methanol for cocatalytic pyrolysis, the overall reaction chemistry was described by Carlson et al. (2010, 2011). The synergistic effect on cocatalytic pyrolysis of pine wood with alcohol shows the promising results for aromatic yield of products [Zhang et al. 2012].

In the second one is post-mixing technique, where alcohol is fed after the pyrolyzer along with pyrolysis gas. In this regard, Horne et al. (1995) studied the co-processing of pyrolysis vapors with hydrogen donor solvent i.e. methanol over a fixed bed reactor containing HZSM-5 catalyst at 500 ^{o}C temperature. They reported that the addition of methanol favored the dehydration reaction in comparison to de-carbonylation and de-carboxylation reactions thereby increased the overall hydrocarbon liquid products. The similar kind of findings can be seen from Chen et al. (1988), as 23% of hydrocarbon yield on co-processing of wood pyrolysis vapors with methanol in compare to 3.2% on catalytic (HZSM-5) pyrolysis. These techniques can be applied to increase the H/C_{eff} ratio of pyrolysis oil from around 0.3 to above the inflection point of 1.2 before co-processing in a refinery FCC equipment.

2.4.1.1.2 *Operational parameters*

The quality and quantity of FPO is also a function of operating parameters like pressure, heating rate, pyrolysis temperature, condenser temperature, residence time and feedstock allied properties, like water content, ash content, particle size and composition. The effect of pyrolysis temperature on FPO quality with pine wood as a biomass feedstock was reported by Westerhof et al. (2010). It was reported that with increase in pyrolysis temperature gas yield increases constantly whereas the yield of char noticebly decreases. The pyrolysis oil yield is relatively

constant for the temperature range of 450- 530 °C, as well as the elemental composition (C, H, and O) of the pyrolysis oil. It was also reported that with increasing in pyrolysis temperature: (a) the average molecular size increases, (b) the content of water insolubles in the pyrolysis oil increases. This may be due to increasing the rate of volatilization of the lignin fraction of wood. However, at the higher pyrolysis temperatures ranging from 530-580 °C, the enhanced vapor cracking led to decrease in viscosity and the water insoluble compounds.

Blackadder et al. (1985) worked on pyrolysis of wood, lignin, and cellulose in a pressurized thermobalance. It was found out that at a particular temperature, the residue of char increases with an increase in pressure. Higher pressure leads to increase in the residence time of the volatiles in the reaction zone, which increased the yield of light gases and decreased the formation of tar and pyrolysis oil due to cracking reactions.

Heating rate is also a function of the biomass particle size and the type of pyrolyzer configuration used. With increase in biomass particle size the rate of thermal diffusion within a particle decreases and henceled to lower the heating rate. Residence time is vital factor to control primary reaction of fast pyrolysis of biomass; increase in residence time leads to occurring secondary reactions. It is very much agreed that the moisture, ash and volatile contents of biomass vary depending on their type and particle size. Wang et al. (2005) reported that the water content of the liquid product increases with increase in the particle size from 3 to 12 mm.

Moreover, the presence of inorganic compounds leads to further cracking pyrolysis vapors to gaseous products. From the above it appears to be the selection of process parameters plays a decisive role while controlling the FPO quantity as well as quality. Hence, it is very much essential to modify the process flow diagrams and designs of various equipments (such as pyrolyzer and quencher) in order control FPO's quality and quantity.

2.4.1.2 Post process (liquid phase) approaches

2.4.1.2.1 *Transfer hydrogenation*

Transfer hydrogenation technique wherein the inclusion of catalytic hydrogen from hydrogen donor (a non-gaseous source) takes place. This method can be applied for stabilization of FPO, wherein it is operated without using high pressure and high purity of hydrogen gas. On using this method with various hydrogen donors (ammonium formate, hydrazine dihydrochloride, and isopropanol) over various carbon supported catalysts by Pacific Northwest

National Laboratory (PNNL) group, while with the use of triethylsilane and palladium on carbon support catalyst decreases the viscosity. It is pointed out that on using this technique a minimum oxygen reduction and no phase separation of water can be seen; however, the pyrolysis oil is enough stable to viscosity changes to allow storage and transportation [Elliott et al. 2012a].

2.4.1.2.2 *Hydrothermal treatment*

Hydrothermal treatment route is in similar to hydrothermal liquefaction wherein no hydrogen is required. It this treatment most of functional reactive groups are reduced, thus stabilizing the FPO for long time storage or further processing. The extensive work in this way was carried out by the consortium of BIOCOUP within the limited range of temperature from 200 to 350 °C. The consortium was proposed a bio-refinery concept in a view of co-processing FPO in conventional petroleum refinery, which is shown in Figure 2.6. It was revealed that a quantifiable deoxygenation take place which results to increase in molecular weight, viscosity, and phase separation (heavy oil phase and aqueous/water phase) of oil. However, a maximum allowable severity for this method was reported to be LHSV of 4 and reaction temperature of 100 °C, which is allowed for homogeneous product recovery [Elliott et al. 2012a]. Further, they concluded that the hydrothermally treated FPOs are not much stable than the original one while processing them in fixed bed catalytic reactor for further converting into hydrocarbon fuels.

2.4.1.2.3 *Thermal treatment*

Bertero et al. (2011) approached for another option i.e. thermal treatment (TT) for pyrolysis oil stabilization. On thermal treatment of pine sawdust-derived pyrolysis oil (with 48% oxygen), about 40% of the oxygen was removed; while a decrease in phenolic compounds by 30 to 50% is also observed. Further, there is a improvement in physic-chemical properties i.e., a decrease in the CCR from 4.8 to 1.5 wt.%, and the increase in H/C_{eff} by 30% was observed. Based on their results, they proposed the process scheme (Figure 2.7) for valorization of pyrolysis oil through co-processing in FCC unit with the inclusion of thermal conditioning set up in their process scheme. Besides, Huber et al. (2006 and 2007) also reported that the co-processing of pyrolysis oil in standard refinery processes is an attractive option to upgrade pyrolysis oil as a standard feedstock.

2.4.1.2.4 *High pressure thermal treatment*

High pressure thermal treatment (HPTT) process was developed by BTG and University of Twente to reduce the oxygen and water content of FPO. The experimental results showed that HPTT treated FPO contain low concentrations of oxygen and water with higher heatingvalue (28.4 MJ/kg). The undesirable formation of high molecular weight components was also detected in HPTT treated FPO. In HPTT, FPO's were subjected to temperatures above 250 °C and pressures above 100 bar to impart the water in the liquid phase and avoid relentless charring [Mercader et al. 2010a]. The oxygen content of such oils reduces from 40 to 25 wt.% in the organic phase of the HPTT product (both on dry basis). They also reported that the heating value of the organic phase increases from 16 to 26 MJ/kg. However, Mercader et al. (2010c) reported that the HPTT treated FPO proved to be immiscible with long residue (a heavy fraction of refinery stream) and could not be processed in the microactivity unit due to its high coking tendency (MCRT of 45.1 wt.% on dry basis). Therefore it was suggested to further process the HPTT oil via hydrodeoxygenation. In HPTT approach, the possible reactions causing the formation of gas were referred as decarboxylation, decarbonylation, yielding carbon monoxide, carbon dioxide, and dehydration reaction (by condensation reactions or polymerization).

2.4.1.2.5 *Thermal hydrotreating*

Initially, Veba Combi-Cracking (VCC) process is a slurry phase hydrogenation process for upgrading petroleum residues [Graeser et al., 1983; Wenzel et al. 1992.] into distillates. This process may be applied to process refinery residues, bitumen, and coal [http://www.kbr.com/Technologies/Refining/Veba-Combi-Cracking/Process/Default.aspx].

Samolada et al. (1998) tried to explore the thermal hydrotreatment process, a modified VEBA Combi Cracking Process, as the stabilization step for the deoxygenation of eucalyptus flash pyrolysis liquid obtained from the Union Fenosa Pilot Plant Unit (Spain). Their results indicate that the deoxygenation rate was 80% of the feed.

2.4.1.2.6 *Catalytic emulsion*

Zapata et al. (2012) proposed the catalytic emulsion system in order to convert the biomass-derived oxygenates into fuel-range condensation products (C_8-C_{13}) by the use of simultaneous emulsion stabilization and condensation followed by hydrodeoxygenation

reactions. Their use of nanohybrid (supported on MgO) catalyst has shown promising results (i.e. total carbon balance is more than 90%) for aldol condensation reaction for the case studies like (i) furfurol and acetone and (ii) synthetic pyrolysis oil. The added advantage of this route is hydrodeoxygenation can be done at lower pressures as compare to conventional pyrolysis upgrading (hydrogenation) route.

2.4.1.2.7 *Catalytic hydrogenation*

Stabilization of FPO may also be carried out by hydrogen addition processes (hydroprocessing) with higher processing cost of hydrogen. Hydroprocessing of pyrolysis oils is different from processing of hydrocarbons due to the involvement of saturation of olefinic groups (C=C bonds) and the addition of hydrogen to carbonyl groups (C=O bonds) to form alcohols ('mild hydrogenation'). Elliott et al. (2007, 2012b) reviewed the historical developments in hydroprocessing of pyrolysis oils. These reactions may be classified into (i) mild hydrotreating, (ii) mild hydrodeoxygenation, and (iii) two-stage hydrodeoxygenation [Venderbosch et al. 2011]. The main differences between these reactions are temperature and the weight hourly space velocity (WHSV in kg.oil/h.kg.catalyst).

The stabilization of FPO by catalytic hydrotreatment route using various heterogeneous noble-metal catalysts (Ru/C, Ru/TiO_2, Ru/Al_2O_3, Pt/C, and Pd/C), in a two-stage hydrodeoxygenation method, was carried out by Wildschut et al. (2009). They reported that the Ru/C is a better catalyst as compared to the sulphided NiMo/Al2O3 and CoMo/Al2O3, with respect to oil yield (60 wt.%) and deoxygenation level (90 wt.%). It was observed that the stabilized FPO was less acidic and have less water content as compared to the original FPO with the HHV of about 40 MJ/kg, which is about twice the value of pyrolysis oil. Based on Van Krevelen diagrams, they reported that the two-stage hydrodeoxygenation approach gives much higher deoxygenation rates as compared to the mild hydrotreating and hydrodeoxygenation approaches. In the first stage, to avoid excessive coking, the FPO is hydrotreated below 280 °C. In the next stage, the actual deoxygenation reaction was carried out at higher temperatures (350-450 °C). In the similar manner Jones et al. (2009) proposed the design case for catalytic upgrading of pyrolysis oil into hydrocarbon fuel by adopting two-step hydrotreating pathway, which is shown in Figure 2.8.

Churin et al. (1989) concluded that if the FPO is to be hydrotreated independently, due to the polymerization of the pyrolysis oxygenates which are able to produce free radicals. After hydrodeoxygenation it leads to formation of high water which again deactivates the catalysts. Arbogast et al. (2008) recommended that the reduction of oxygen duringHDO should be ≈7%, which is very much required to avoid the hydrogenation of aromatic compoundss while reducing hydrogen consumption. They also proposed various blending approaches for pyrolysis oil in the standard refinery. However, from the work of French et al. (2011) on mild hydrotreating of pyrolysis oil, it is observed that the upgraded or stabilized organic pyrolysis oil with 7% oxygen content has a carboxylic acid number (CAN) varies from 20 to 33. The acceptable limit of total acid number (TAN) in the feedstock for modern petroleum refineries is as high as 2. Therefore it is suggested that a further decrease of oxygen content to less than 5% and higher blending ratio of 10/1 (petroleum-derived to bio-derived) is required for co-processing. Grange et al. (1996) described a two-stages processing approach for the stability of pyrolysis oils. They mentioned that a low temperature hydrotreatment in the first stage enables stabilization by reducing the groups of olefin, carbonyl and carboxylic. Further, in the second step hydrotreatment aims at hydrodeoxygenation of phenols and hydrocracking of larger molecules. It is also reported that the reactivity of phenol is higher than the olefin, carbonyl and carboxylic groups.

Further, Elliott et al. (1996) mentioned that the hydrotreated product contains 10-15 wt.% of oxygen and the density around 1.0, which tend to form mix with water as by-product. Therefore, it is very difficult to separate water from hydrotreated product. It is also reported that the hydrogen consumption is very high, approx. 779 liters/liters of pyrolysis oil for NREL pyrolysis oil [Elliott et al. 1996]. Baldauf et al. (1994) also recommended the refining of pyrolysis oil over hydrotreating process. It was mentioned that based on the properties of the hydrotreated pyrolysis oil, it should be fractionated in the distillation column, the resulted fractions could be blended in various refinery cuts and be sent for downstream processing.

The same concept was supported by French et al. (2011) and it is suggested that a two-stage process involving low severity (low pressure and temperature) stabilization followed by high severity (high pressure and temperature) hydrotreating with inter stage elimination of aqueous phase from the pyrolysis oil. This would help in limiting the issues of corrosion and reducing the overall hydrogen consumption. Furthermore, Stournas et al. (1990) described that

non-oxygenated compounds produced at higher severity would be an excellent gasoline feedstock.

The other option is to coprocess the pyrolysis oil after upgrading through hydrotreating and hydrodeoxygenation steps. In addition to several pretreatment options for pyrolysis oil co-processing in refinery, Meloro et al. (2012) proposed the scheme for integration of pyrolysis process with conventional petroleum refinery, as shown in Figure 2.10. It is indicated that with this scheme the obtained product hydrogen effective index would be in the range of 1 to 2. If the process is successful, this would be better option for the effective utilization of petroleum infrastructure for bio-fuels industries.

Details of HDO catalysts:

A hydrotreating catalyst should comprise a hydrogenating component on a catalyst carrier that is inert at the reaction conditions. Inert catalyst carrier is necessary to not to dissolve and decaying under the HDO reaction conditions in order to avoid metal leaching or weakening of the catalyst pellets for instance due to the amount of water present in the feed. Further, the catalyst support or carrier comprises solid substances with high porosity and able to withstand the temperature, pressure and the environment encountered in a specific HDO conditions, i.e. the presence of relatively large amounts of water in the feed. The preferable shape should be in the form of balls, rings or otherwise shaped extrudates, which may serve as a support for the active elements in the catalyst. The active metals can be chosen for the hydrotreating of pyrolysis oil as Nickel (Ni), Chromium (Cr), Molybdenum (Mo), and Tungsten (W), Cobalt (Co), Platinum (Pt), Palladium (Pd), Rhodium (Rh), Ruthenium (Ru), Iridium (Ir), Osmium (Os), Copper (Cu), iron (Fe), Zinc (Zn), Gallium (Ga), Indium (In) and Vanadium (V) in elementary form, alloys, but not limited to Rh-Co-, Ni- and Ni-Cu, preferably in the form of oxides, sulfides or other metal-organic compounds.

The carrier typically may comprise a refractory oxide or their mixtures preferably alumina, titania, ceria, zirconia. Otherwise, it may consist of an inert component such as carbon or silicon carbide or carbon. Carriers that were found inert under the conditions are ZrO_2, CeO_2, CeO_2 and their mixtures as CeO_2-ZrO_2, silicon carbide and carbon. If a catalyst comprising sulphided CoMo, NiMo or NiW is used, the catalyst may be sulphided in-situ or ex-situ. In the case of in-situ sulphiding, a sulphur source, usually hydrogen sulphide or a hydrogen sulphide

precursor, is typically supplied to the catalyst during operation of the process. The carrier may further comprise a zeolitic compound. Any acidic zeolitic compound having sufficient stability at the reaction conditions to limit catalyst decay may suitably be used.

2.4.2 Separation of Destabilizing Compounds

2.4.2.1 In process (gas phase) approaches

2.4.2.1.1 *Hot gas filtration*

A gas cleaning is very common problem in biomass pyrolysis processes like gasification as well as fast pyrolysis. Conventionally, the unconverted part of biomass i.e., char particles can be separated via cyclone next to the pyrolyzer (where fluidized bed used as reactor). However, the char particles of less than 2-3 µm cannot be separated through even series of cyclone separators. Because of char contains a considerable amount of inorganic compounds, are known to be active in the cracking of the pyrolysis vapors into gases and as a result the pyrolysis oil yield will decrease. Therefore, the char particles have to be separated as quickly as possible from pyrolysis of vapors/gas. Hence, the fast pyrolysis reactor outlet vapor phase temperature is maintained at around 400 °C to avoid the secondary cracking reactions of pyrolysis oil vapors, and the char particle are being separated at that temperature. Various type of filters (e.g. high temperature bag houses, ceramic candle filters, and moving bed granular filters) are available for the cleaning of char particles from pyrolysis vapors which are not able to separate using cyclone separators.

The coupling pressure pulse (CPP) cleaning technique is based on ceramic filter candles with integrated individual safety filters system, which was developed in cooperation between the Karlsruhe Research Centre and Pall Schumacher. A prototype hot gas filter with CPP cleaning was built up as a part of the pyrolysis pilot plant "PYDRA" at the Karlsruhe Research Centre [http://www.netl.doe.gov/publications/proceedings/02/.../2.04paper.pdf]. NREL is also working for the development of proper hot gas filtration technology which can be used along with their vortex fast pyrolyzer [Diebold et al. 1995]. They reported that the viscosity of the as-produced oils met the requirements of fuel oils and the yields of wet organic condensates were progressively increased from 36–49% by weight of dry organic oil yield. Much of the work has been hampered by the absence of real-time instrumentation to measure filtration efficiency. However, as per Pattiya et al. (2012) study the water content of Cassava Rhizome and Stalk-

derived pyrolysis oils with the hot vapor filter unit was higher than that without the hot filter unit in the bubbling fluidized bed pyrolyzer system. It was explained that this may be due to the secondary reactions taking place in the hot vapor filter, which leads to production of water and many gases. The concept of use of hot filter leads to decrease oil conversion by 5–6 wt.% was supported by Chen et al. (2011), Kang et al. (2006), and Jung et al. (2008). In this regard, a new technique was developed by the Thermal Engineering group of the University of Twente for separation of char particles and aerosols from gases. In this patented technology (US Patent US5073177) the reactor and the oil-vapor cleaning unit are in-built in one cyclonic reactor with a rotating particle separator. The advantages of the integrated system are: (i) a compact system; (ii) solids-free oil; (iii) less contaminant in the oil; (iv) lower viscosity; and (v) lower costs [Brem et al. 2007].

2.4.2.1.2 *Selective fractionation*

Pyrolysis vapors, non-condensable gases and aerosols are to be separated at the end of fast pyrolysis reactor in conventional approach. In doing so a quencher or condenser followed by electrostatic precipitator (ESP) are being used to separate 1 to 2 fractions of liquid fractions and aerosols. However, the Iowa state university developed a fractionating condenser train wherein the system collects the FPO in five unique fractions like carbohydrate-rich (anhydrosugars), lignin-rich, and an aqueous solution of aldehydes and ketones [Brown et al. 2011b].

2.4.2.2 Post process (liquid phase) approaches

During protracted storage, the FPO becomes unstable due to oxidation (lead to polymerization) or thermal degradation (lead to loss of volatile components), which helps to change in physical properties and chemical composition. FPO's should retain their initial physical properties before going to any further upgrading techniques. Initially, researchers tried to add alcohols after pyrolysis to increase the stability and heating value of FPO [Moens et al. 2009, Oasmaa et al. 2004, Diebold et al. 1997]; hence the decrease in viscosity is seen. Esterification route also improves the quality of pyrolysis oil in terms of decreasing the viscosity, water content and free-acid content; with this an increase in heating value (by 50%) and stability are observed [Zhang et al. 2006, Peng et al. 2008, Xiong et al. 2009].

2.4.2.2.1 *Micro filtration*

Liquid filtration is another option to separate the char/soot particles from pyrolysis oil, but it seems to be very difficult due to the nature of char and pyrolysis lignin. The filtration of pyrolysis oil removes only fines of char particles, which results into high-ash sludge as a by-product. The drawback of liquid filtration is that it does not remove char particles of smaller size and inorganics, which are already solubilized by the acidic solution of pyrolysis oil. Javaid et al. (2010) employed a technique of microfiltration using tubular ceramic membranes having a nominal pore sizes 0.5 and 0.8 μm . They reported the removal of the major quantity of char particles (up to 1 micron) in overall ash content of the pyrolysis oil. Recently, the ASTMD-7579 standard has been developed for the separation of solid particles from pyrolysis oil by the technique of filtration in a methanol solution.

2.4.2.2.2 *Selective fractionation*

Radlein et al. (1999) stated that pyrolysis oil can be separated into aqueous and organic fractions by the inclusion of water. Mercader et al. (2011) also referred aqueous fraction as AFWA (aqueous fraction water addition) and left over oily fractionwas referred as OFWA (oil fraction water addition) and powderlike fraction was referred as pyrolytic lignin. For hydrodeoxygenation the quality of AFWA-derived HDO oil is high in terms of H/C, micro carbon residue (MCR) and molecular weight distribution (MWD), at the cost of high hydrogen consumption. This huge consumption of hydrogen is for the production of low value gas like methane. Therefore they suggested further to separate the light components (e.g. acids) of AFWA to reduce the consumption of hydrogen and use the light components for the production of chemicals/hydrogen. The OFWA-derived oil can be sent to co-processing route. In this way the overall recovery of carbon in the HDO oil was ≈35 wt.%, while it was 78 wt.% for the processing of whole pyrolysis oil. In a similar way VTT [Oasmaa et al. 2003] developed a solvent fractionation scheme in order to characterize the pyrolysis oil, in which water-to-oil ratio was 10:1, however in case of AFWA and OFWA separation techniques it was 1:2. Further, UOP LCC patent [Marker et al. 2008] states that OFWA's hydrotreatement followed by hydrocracking results into the production of 30 wt.% gasoline.

2.5 CO-PROCESSING OF PYROLYSIS OIL IN REFINERY UNIT

Bulushev et al. (2011) mentioned the following negative aspects of hydrodeoxygenation: (i) high pressure requirement (70–200 bar), (ii) catalyst deactivation, (iii) loss of carbon content (20–30%) of the biomass to the gas phase. Huber et al. (2006) mentioned that the cost of hydrogen generation from biomass is \$1.1–2.0 kg^{-1} which is modestly higher than the market cost of hydrogen of \$0.7–1.4 kg^{-1}. These drawbacks put researchers to further work on effectively removal of oxygen content of pyrolysis oil instead of going for proven hydrodeoxygenation approach.

2.5.1 Fluid Catalytic Cracking

Catalytic cracking has many advantages over thermal cracking in terms of offering more stable products, giving high octane gasoline (~93) and operation of FCC unit at less severe conditions. In FCC, the fluidized catalyst bed, which has the properties of liquid, is formed by carefully controlling the size of catalyst particle and velocity of fluidizing gas passing through it. The finely powdered FCC catalyst is lifted into the riser by incoming oil which instantly cracked and vaporizes upon direct contact with hot catalyst. After the reaction is completed, the hot catalyst along with the coke formed during reaction is transferred into a regenerator zone. In the regenerator, the coke formed during the cracking reaction is burned off with air and thereby provide heat for cracking reactions. The change of heavy feedstock into lighter products is represented by a percent conversion which is defined as the "percentage of gas oil cracked to un-stabilized gasoline and lighter products". A weight % conversion can also be defined as the fraction of components boiling below 216 °C along with coke. A high severity mode of FCC unit operation will yield more LPG and gasoline; whereas a lower severity mode will produce more of middle distillates [Das et al. 2001, Mandal et al. 2011, Dinda et al. 2014]. The feed stocks rich in aromatics are difficult to crack and on cracking, it makes more coke.

The catalytic cracking in refinery fluid catalytic cracking (FCC) unit is another method of deoxygenation of pyrolysis oil. In the catalytic cracking approach, the oxygen content of pyrolysis oil could be removed in the form of water, CO, and CO_2 as per the following reaction scheme [Fogassay et al. 2010]:

$$C_xH_yO_z \rightarrow aC_{x-b-d-e}H_{y-2c}O_{z-2b-c-d} + bCO_2 + cH_2O + dCO + eC$$

Further, there is a possibility of upgrading the pretreated pyrolysis oils (pure or blended with VGO/LCO) in FCC unit to produce transportable fuels. FCC is the major secondary process of petroleum refinery due to its flexibility in terms of catalyst and operating conditions as per product demand. Huber et al. (2007) extended the reaction pathway of cracking of hydrocarbons over fluid catalytic cracking catalyst to the cracking of oxygenated hydrocarbons by adding dehydration reaction along with cracking, hydrogenproducing and consuming reactions and C-C bond formation reactions for pretreated pyrolysis oil cracking over an acid catalyst.

The conversion of non-conventional feedstock in fluid catalytic cracking unit is complicated because of their crackability, catalyst type and testing conditions. Oasmaa et al. (2010a) also mentioned that the variations in properties of pyrolysis oil (containing both aliphatic and aromatic oxygenates) and FCC feed (a typical aliphatic) would pose a real challenge for co-processing of pyrolysis oil in refinery FCC unit. The crackability pattern of FCC feedstock is described by either aromaticity (H/C ratio) or the CCR content of the feedstock. Generally, oxygen rich aromatic feed stocks are highly polar and characterized by high carbon residues.

2.5.1.1 Processing of pyrolysis oil model compounds

Gayubo et al. (2004a, 2004b, and 2005) ascertained the order of reactivity and reaction pathways of model pyrolysis oil compounds, such as 1- and 2-propanol, 1- and 2-butanol, acetic acid, acetone, acetaldehyde, phenol and 2-methoxy phenol over an acid zeolite (HZSM-5) catalyst in isothermal fixed bed reactor at different temperatures ranging from 200 to 450 ^{o}C. According to them the order of coke content produced is as follows: aldehyde> acetone or acetic acid> alcohols. Their results indicate that deoxygenation is favored by decarboxylation and decarbonylation at around 400 ^{o}C temperature and deoxygenation is favored by dehydration at around 250 ^{o}C temperatures on catalytic transformations of acetone and acetic acid. Alcohols has higher reactivity over acid zeolite catalysts leads to formation of light olefins (~200 ^{o}C) then to higher olefins (at 250 ^{o}C) followed by considerable amount of C_{5+} paraffins and smaller amount of aromatics at temperatures above 400 ^{o}C. Acetone was less reactive as compares to alcohols; however, they also produced C_{5+} paraffins and aromatics (more than obtained from alcohols). The reactivity of acetic acid was very low up to the temperature of 400 ^{o}C; whereas due to autocatalytic effect the acetic acid was converted into acetone at a temperature more than 400 ^{o}C. Once the acetone is formed from acetic acid, it follows similar path of acetone on catalytic

transformations. The phenol has low reactivity to produce hydrocarbons over an acid HZSM-5 zeolite catalyst they produce small amount of light olefins and thermal coke. Aldehyde also has the lower reactivity over HZSM-5 catalyst and resulted higher amount of thermal coke.

Therefore, the recommended presence of aldehydes in pyrolysis oil is 3.6 wt.% excluding water, which is attained by [Aguado et al. 2000]. Besides Gayabu et al. (2004a, 2004b, and 2005) studies, Adjaye et al. (1995a, 1995b, and 1996), Sharma et al. (1993), and Srinivas et al. (2000) also tested zeolite catalysts, such as ZSM5, HY, H-mordenite, silicalite, and silica alumina, for upgradation of wood-derived fastpyrolysis oils in a temperature range of 290 to410 ^{o}C. It was mentioned that the similar kind of reactivities of pyrolysis oil components. It was mentioned that ethers and phenols have low reactivity while high conversions can be achieved with acids, esters, alcohols, aldehydes, and ketones. Their study also revealed that catalyst deactivation by coke formation is particularly important with aldehydes and phenols.

Graca et al. (2009a, 2009b) studied the transformation of mixtures of methylcyclohexane with small amounts of phenol over an HZSM-5 and HY zeolite for temperature ranging from 350 to 450 ^{0}C in a Pyrex fixed bed reactor. It was reported that by increasing the reaction temperature from 350 to 450 ^{0}C, HY zeolite allows limiting the effect of phenol addition on the zeolite activity and stability, whereas HZSM-5 does not allow limiting the effect of phenol addition. The impact of phenol addition on the naphthenes (methylcyclohexane) and alkanes (n-heptane) transformations over the HMFI zeolite was studied by Graca et al. (2011b) in Pyrex fixed bed reactor.

2.5.1.2 Co-processing of pyrolysis oil model compounds with VGO

Graca et al. (2009c) carried out the catalytic cracking of mixtures of gasoil and FPO representative model compounds (acetic acid, hydroxyacetone and phenol) in a labscale unit using an E-CAT and a mixture of E-CAT and ZSM-5 additive. It has been reported that the co-processing of oxygenated compounds with vacuum gas oil results into (i) increase of gasoline, gaseous products (CO, CO_2, fuel gas, LPG); (ii) decrease of coke yield except for phenol; (iii) decrease of hydrogen yield (in the order of hydroxyacetone>acetic acid>phenol) in the product and it is confirmed by increase in C_{2-4} olefins/C_{2-4} parrafins ratio. Further it was concluded that these oxygenated compounds can be processed in a FCC unit up to 10 wt.%. However, the presence of phenol might be critical due to the benzene content specification in the gasoline

(max. 1 vol.%). The typical product distribution pattern on catalytic cracking of pyrolysis oil model representative compounds with vacuum gas oil is shown in Table 2.7. The catalytic cracking of pyrolysis oil model compounds using zeolite catalyst resulted into the decrease of hydrogen yield for two carbon-oxygenate (e.g. acetic acid) and three carbon-oxygenates (e.g. hydroxyacetone). It has been reported that the hydrogen is consumed during the de-oxygenation reactions like decarbonylation and decarboxylation. These observations indicates to further focus on catalytic fast pyrolysis reactions instead of conventional fast pyrolysis reaction to get the product having lower carbon number based oxygenates, which can be easily converted into products in similar to FCC distillates without changing much the existing FCC infrastructure.

2.5.1.3 Co-processing of pyrolysis oil and HDO with VGO

Fogassy et al. (2010) explored the co-processing studies of catalytically hydrotreated pyrolysis oil over Ru/C catalyst in a FCC unit. A mixture of HDO with VGO in a ratio of 80:20 was processed in a fixed bed reactor under simulating FCC conditions and compared the results with the processing of pure VGO. They observed that during co-processing major part of the oxygen is removed in the form of carbon dioxide and water by means of decarboxylation and dehydration reactions. Cracking of this particular 80:20 mixture produces higher dry gas and coke yields, lower LPG yield while gasoline and light cycle oil yields were comparable to those of the cracking of VGO. Their results indicate that C-C bond cleavage takes place before decarboxylation and decarbonylation reactions while cracking HDO as it contains unsaturated hydrocarbons; whereas Osmont et al. (2007) mention that C-O bond breaking reactions proceeds faster than carbon-to-carbon (C-C) bond cleavage for saturated hydrocarbons. It is also emphasized that hydrogen-consuming reactions dominate by water formation and hydrogenation reactions besides some hydrogen-elimination reactions which leads to favor higher yields aromatics (continuation of reaction such leads to coke formation) in the products while cracking VGO/HDO oil. They mentioned that the decrease of LPG may be due to the well known fact that HDO oil containing more aromatics, which are difficult crack than aliphatic rich-petroleum feedstock. Similarly, Ng et al. (2006) also mentioned that the aromatic rich feedstock side chains could be detached and fragmented using acid catalysts but the cracking of refractory aromatic rings needs the presence of hydrogen at higher pressure.

Table 2.7: Status of catalytic cracking of pyrolysis oil over equilibrium FCC catalyst

Product yields @ Iso-conversion of 63.0 wt.%					
Feed/Products	VGO	VGO + Guaiacol	VGO + Acetic acid	VGO + Hydroxyacetone	VGO + Phenol
Reference	Graca et al. 2011a			Graca et al. 2009c	
Fuel gas	2.7	3.3	3.7	3.0	2.5
Carbon monoxide	--	0.05	0.47	0.07	0.04
Carbon dioxide	0.25	0.33	0.54	0.35	0.17
LPG	12.5	13.8	15.7	14.0	13.2
Gasoline	36.0	36.2	33.4	35.9	38.1
LCO	19.7	18.8	18.9	20.0	18.6
DO	17.3	17.3	17.7	16.8	18.0
Coke	11.8	9.5	9.4	9.6	8.6

Samolada et al. (1998) performed the catalytic cracking experiments on heavy fraction of hydrotreated pyrolysis oil (80% deoxygenated) in a modified microactivity test fixed bed reactor system (MAT, ASTM D3907-80), with the light clarified oil (LCO) in a ratio of 15:85 by wt.%. They results indicate that both saturated naphthenes (from 3.8 to 4.2%) and aromatics (from 50.5 to 53.8%) were increased on using $ReUSY_2$ catalyst. Lappas et al. (2009) extended the work of Samolada et al. (1998) and carried out the experiments with thermally hydrotreated heavy FPO fraction as cofeed with conventional vacuum gas oil (VGO) in the Chemical Process and Energy Resources Institute (CPERI) FCC small-scale pilot plant unit. In order to avoid the problem of plugging of the nozzle of FCC unit with such feed, the upgraded oil was diluted in light cycle oil (LCO) in a portion 15/75 by wt.% and the mixture was blended with a conventional FCC feed (VGO). Their experimental result showed that the VGO/upgraded FPO cofeed produces about 1 wt.% more gasoline, 0.5 wt.% more coke, and more LCO as compared to the VGO feed expected. Their PONA analysis of liquid product also indicated more aromatics and less olefins and paraffins in compare to pure vacuum gas oil cracking. It was suggested that the option of cofeeding petroleum VGO with upgraded oil is technically viable for FCC unit running with good quality feedstock.

Mercader et al. (2010a) mentioned that high levels of oxygen can be allowed in upgraded HDO oil (≈28 wt.%) for co-processing in FCC unit without deterioration of the yield structure. It was also mentioned that the co-processing of HDO oils (20 wt.%) with a long residue, a promising yields of FCC gasoline yield (44–46 wt.%) and light cycle oil yield (23–25 wt.%)

were obtained ithout an increase of undesired coke and dry gas, as compared to the base feed only [Mercader et al. 2010a]. The typical product properties of upgraded or HDO are shown in Table 2.8. Further, product yields at constant 60% conversion relative to feed alone of 20% HDO oil + Long Residue (wt.%) at 520 °C reported by Hogendoorn et al. (2011) with the variation of dexoygenation quantity is shown in Table 2.9. Also, FCC product yields on co-feeding of pyrolysis oils with VGO/LCO at batch or pilot levels carried out by various organizations (Fjare et al., 2013 and Zacher et al. 2014), and is shown inTable 2.10.

Table 2.8: Status of upgraded or hydrodeoxygenated pyrolysis oil

Author	**Feed-stock**	**Reactor**	**Catalyst**	**T, °C**	**P, bar**	**Time, h**	**Product properties**				**MCRT, wt.%**
							C, wt.%	**H, wt.%**	**$(H/C)_{eff}$**	**O, wt.%**	
Mercader et al. (2010b)	Forest residue	CSTR	Ru/C	340	290	4.0	74.4	10.0	1.30	15.6	5.33
Naik et al. (2015)	JCC	CSTR	Pd/Al_2O_3	300	80	4.0	76.18	8.8	1.68	10.0	8.0

T – Temperature, P - Pressure

Table 2.9: Product yields at constant 60 % conversion relative to feed alone of 20 % HDO oil + Long Residue (wt %) at 520 °C (Hogendoorn et al., 2011)

Product yield	Long Residue only	Upgraded pyrolysis oils				
Dry oxygen content (wt %)	0	28.0	24.2	22.6	15.5	16.9
Cat/Oil ratio	3.1	4.3	3.4	3.4	3.7	3.8
LPG yield	8.5	11.0	10.1	10.2	9.3	9.6
Gasoline yield	44.1%	43.7	44.7	46.0	45.3	44.7
Coke yield	5.9%	7.8	7.1	5.51	5.7	6.0
LCO yield	25.2%	23.1	23.8	23.9	24.8	25.0

Table 2.10: FCC product yields on co-feeding of pyrolysis oils with VGO/LCO at batch or pilot levels (Fjare et al., 2013 and Zacher et al. 2014)

Organization	**CPERI**				**IRCELYON**		**TWENTE**			**GRACE**		**ALBEMARLE**	
Year	1998		2009		2010-11		2010-11			2013		2013	
Reactor	MAT		Pilot.		MAT		MAT			Pilot.		ACE	
Co-feed	LCO	LCO	LCO/VGO		VGO		Long residue			VGO		VGO	
HDO oil, wt%	0	15	0	2	0	20	0	20	100	0	3 (raw)	0	20 (raw)
FCC conversion,%			57-74	63-73	75	75	60	60	60	81.6	81.7	69.1	69.1
Temp., °C	550	550	520	520	500	500	520	520	520	521	521	535	535
C/O	2-6	2-6			1-6	1-6	3.1	3-4	12-20	9.9	9.8	4.8	2.5
C1-C2, wt%					1.5	2	1.5	1.9-2.5	6-11	3.2	3.0	2.2	2.3
LPG					24	20	8.5	9-11	10-12	8.5	8.1		
Gasoline (<221 °C)	17-22	20-25	38-46	42-47	46	44	44	44-45	22-36	49.1	47.5	48.9	44.1
LCO (221-370 °C)			17-22	18-21	20	20	25.2	23-25	11-19	14.1	14.2	19.0	17.2
HCO (>370 °C)					4	3	14.8	12-13	7-8	4.4	4.2	11.2	10.5
Coke, wt%	2-3	3-5	2-5.5	3.7-5.7	3.2	4.6	5.9	5.5-7.8	22-38	6.4	7.1	3.5	4.0

2.5.1.4 Co-processing of catalytic pyrolysis oil with VGO

Thegarid et al. (2013) performed the co-processing studies of catalytic pyrolysis oil (obtained from commercial lignocellulosic biomass i.e.Lignocel HBS 150–500 originated from beech wood) with vacuum gas oil in a fixed bed quartz reactor with FCC catalyst in a ratio of 10:90. Their results indicate that higher yields of coke, dry gas and gasoline; lower yields of hydrogen, LPG, LCO and bottoms were obtained as compare to pure vacuum gas oil processing. Further, their observations are: (i) the presence of more oxygen (27 wt.%) in CPO resulted to hydrogen consumption reactions via water formation; (ii) the presence of alkyl phenols already in the CPO and narrow pore size limitation of ZSM-5 catalyst lead to significant amount of alkyl phenols in the gasoline fraction; (iii) the aromatic-rich gasoline fraction lead to less reactive for further cracking and thereby decreases LPG yield; (iv) their ^{31}PNMR data also shows that all oxygenated compounds (except the phenolic fraction) has converted. It is also mentioned that the overall yield of organic oil is 30% as compare to 24% on co-processing of HDO oil with VGO.

From the report of DOE awarded project [Marker et al. 2005] on "Opportunities for bio-renewable in oil refineries" it was stated that the FPOs appeared to increase the rate of cracking of VGO and shift the product pattern towards the increase of light hydrocarbons and decrease of LCO and clarified slurry oil (CSO) which is an economically attractive outcome. It was also mentioned that the high levels of coke formation with 20% blend os notacceptable for most of the refinery FCC units. It was suggested that the co-processing of 5% blends might be possible and further testing of 5% blends of FPO with vacuum gas oil would be required to determine the viability of this approach.

The VTT technical research centre of Finland is coordinating an integrated project with 17 partners, with the acronym of BIOCOUP, to coprocess upgraded bio-liquids in conventional refinery units and to selectively separate value-added chemicals under a European project supported within the Sixth Framework Programme for Research and Technology. To achieve above objective, the Consortium has developed the concept on bio-refinery, as shown in Figure 2.3. They have presented several initial conclusions based on the work at the 15th European Biomass Conference and Exhibition [Gutierrez et al. 2007]. It has been reported that in a lab scale simulated FCC reactor, the co-processing of hydrocarbons and oxygenates model compounds resulted into (i) decrease in hydrocarbon conversion, (ii) increase in coke production,

(iii) changes in product distribution, and (iv) catalyst deactivation. Further, following conclusions were also made:

i. the co-processing of upgraded fast pyrolysisoils in FCC units requires the development of better and more robust catalysts, and
ii. the better understanding of the catalyst structure and reaction kinetics is needed.

2.6 SCHEMES ENVISAGED FOR THE INTEGRATION OF FAST PYROLYSIS WITH REFINERY FCC

From the above section of literature it is clear that the FPO can't be processed directly or coprocessed with fossil hydrocarbons in order to convert into fuel range hydrocarbons. However, the stabilized or upgraded FPO can be coprocessed with fossil hydrocarbons in refinery units after overcoming the challenges as discussed in the section 2.3. The option of co-processing of biomass-derived fractions with petroleum-derived fraction is relatively inexpensive and also helps in increase of profitability of present low margins of petroleum refineries [Hew et al. 2010, Alhajri et al. 2014]. A list of petroleum refinery units like fluid catalytic cracking, hydrotreating, hydrocracking and steam reforming units can be utilized for the specific applications by approaching the specific pathways.

In this scenario, several options have been pointed out by various research groups for the effective use of a refinery infrastructure for upgrading of biomass-derived FPO into liquid hydrocarbons, chemicals and materials. Moreover, this kind of option is more viable in countries like India, wherein the demand of petroleum-derived fraction is extremely high. It also helps the refineries with a safe and secured domestic feedstock source. With this scenario, it has been tried to put some of the schemes for integration of fast pyrolysis process with petroleum refinery in and another approaches in the following sections from 2.6.1 to 2.6.7.

2.6.1 Biorefinery and Refinery Integration

Zacher et al. (2014) proposed a way for the conversion of biomass into companionable petroleum –derived hydrocarbons by the pyrolysis and HDO route, as shown in Figure 2.2. The pathway has been divided into a series of stages, wherein the scope of insertion into the hydrocarbon economy has been considered. The stages of FPO upgrading have been classified into the FPO purification by physical and chemical modifications, heteroatom removal by mild

hydro treating, cracking into small hydrocarbons, and separations into various products by various unit operations as shown in Figure 2.2.

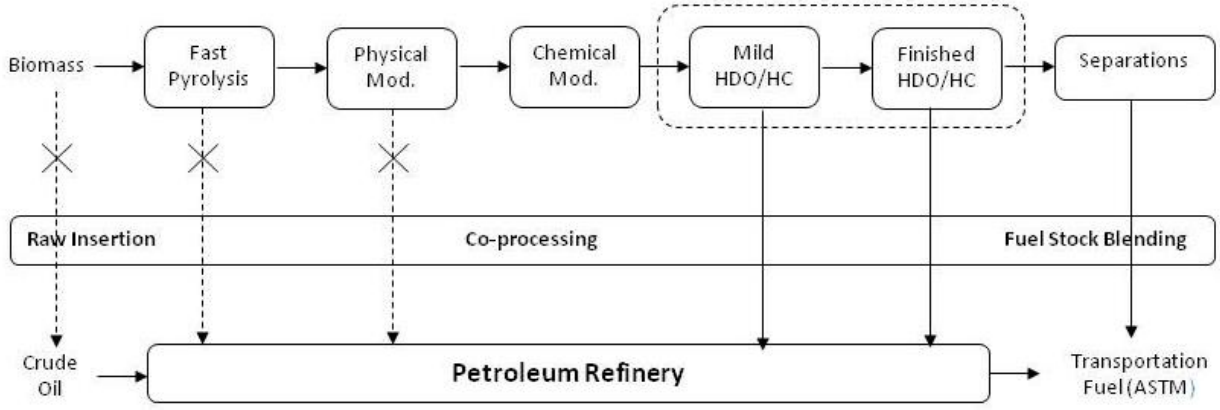

Figure 2.2: Biorefinery and refinery integration [Zacher et al. 2014]

This kind of pathway is very much essential in order to produce fuel range hydrocarbons. The refinery infrastructure of hydro treating or hydrocracking processes can be utilized as a part of biorefinery unit. Otherwise, the well treated FPO (after purification and hetero atom removal) can be utilized in the refinery units wherever it is suited. As Zacher et al. (2014) mentioned that it is an integrative approach in which the mild hydrotreated FPO with compatible petroleum intermediate streams [Holmgren et al. 2008] or direct blending of processed biofuels and petroleum products.

2.6.2 BIOCOUP Consortium Concept for Overall Biorefinery

The European Community has funded an integrated project named "BIOCOUP" in the year 2006 for a period of five years. Venderbosch et al. (2010a) proposed a different pathway against overall biorefinery concept for the conversion biomass residues into conventional energy, fuels and chemicals. Their pathway is follows the different thermochemical conversion i.e. hydrothermal liquefaction followed by separation of various fractions like hydrocarbon-rich pyrolysis oil, lignin-rich pyrolysis oil, derivatives of holocelluloses and process residues, as shown in Figure 2.3. In which they have emphasized to use the hydrocarbon-rich pyrolysis oil with petroleum-derived fraction for co-processing in conventional petroleum refinery processes.

In the course of project, the consortium has been worked on various upgrading processes of pyrolysis oil. Among them, the route of hydrodeoxygenation quoted as very much suitable for decreasing the oxygen concentration and acidity of raw pyrolysis oil before co-processing in refinery processes. Further, they suggested that the 20% of HDO oil can be coprocessed with VGO with slight decrease in the yield of gasoline and the presence of more unsaturated compounds and oxygenates [Way et al. 2011]. However, the impact of such co-processing on fuel range hydrocarbons is remains limited answer in the literature.

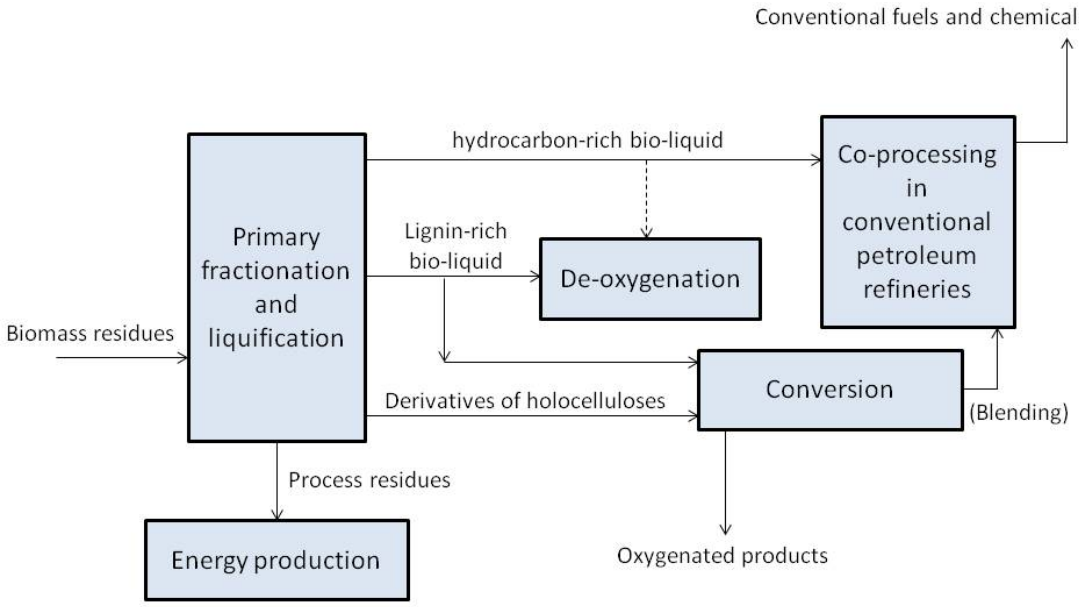

Figure 2.3: BIOCOUP consortium's overall Bio-refinery concept

2.6.3 Biomass Feedstocks Processing in Refinery

Melero et al. (2012) proposed a pathway for the conversion of biomass feedstock's such as sugar rich, starch rich and lignocellulosic biomasses into biofuels using standard petroleum refinery processes, as shown in Figure 2.4. This pathway has been critically described on the basis of feedstock's effective hydrogen index, energy density, and specific chemistry involved in the conversion or upgrading processes. It has been mentioned that the catalytic cracking (FCC process) is more specific than thermal cracking (delayed coking or visbreaking units). This is due to the advantages of operating FCC process without hydrogen. However, thermal cracking

processes are non-selective due to the presence of heavy oxygen in pyrolysis oils which leads to severe coking on thermal treatment.

Another major refinery process which can be effectively utilized for the processing of biomass-derived feedstocks is hydro treating. The hydrotreating processes aimed for higher selectivity towards the liquid fraction (diesel) by minimizing the lighter hydrocarbons, gases and coke as compared to the catalytic cracking units. Originally, the process has been used for the removal of sulfur by hydrodesulfurization, nitrogen by hydrodenitrogenation, metals by hydrodemetalation and oxygen by hydrodeoxygenation from the heavy gas oil feedstock. Herein, the process can be used for the mild hydrotreating of pyrolysis oil or triglycerides. Further, it was emphasized to produce the hydrogen required for hydrotreating processe from aqueous phase reforming (APR) process from sugar rich biomass feedstock, which helps in reducing the cost of overall biorefinery integration with petroleum refinery and to produce more energy-dense products. Besides, the numerous challenges (like thermal stability, high concentration of water, oxygen and metals of FPO, Graca et al. (2009c) mentioned that upto 10 wt.% of oxygenated compounds can be possibly fed to a FCC unit while co-processing with VGO. To make it possible, Melero et al. (2012) proposed several pretreatment options for co-processing pyrolysis oil with VGO in FCC process, as shown in Figure 2.5.

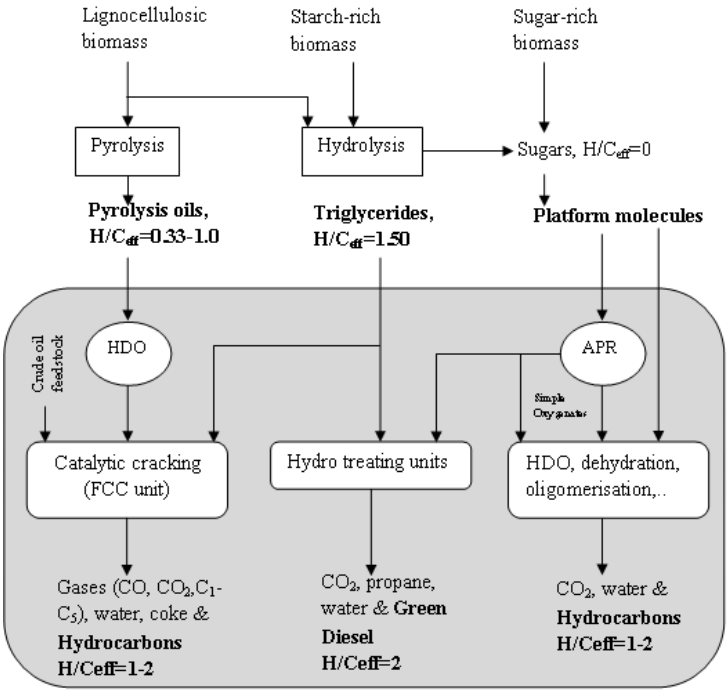

Figure 2.4: Integration of biomass-derived feedstocks in conventional refinery processes

2.6.4 A Stand-Alone Refinery for Fast Pyrolysis-Hydrotreating-Hydrocracking Process

Jones et al. (2009) proposed a design case for the conversion of hybrid poplar into gasoline and diesel and its block diagram is shown in Figure 2.6 in terms of stand-alone refinery for fast pyrolysis-hydrotreating-hydrocracking approach. This approach has tried to use the refinery's hydrocracker unit for the upgrading of pyrolysis oil into drop-in liquid hydrocarbons like gasoline and diesel by avoiding the challenges (like the presence of oxygen and a high intensity of aromatic content in diesel cut of hydrotreated pyrolysis oil, which mismatches the specifications of fossil-derived diesel fuels) on using hydrotreating process. Hence, it is said to be use the hydrotreatment process for getting stable pyrolysis oil and then further crack its heavy stable pyrolysis oil into drop-in diesel fuel in a hydrocracker, which can be a more viable option in terms better economy.

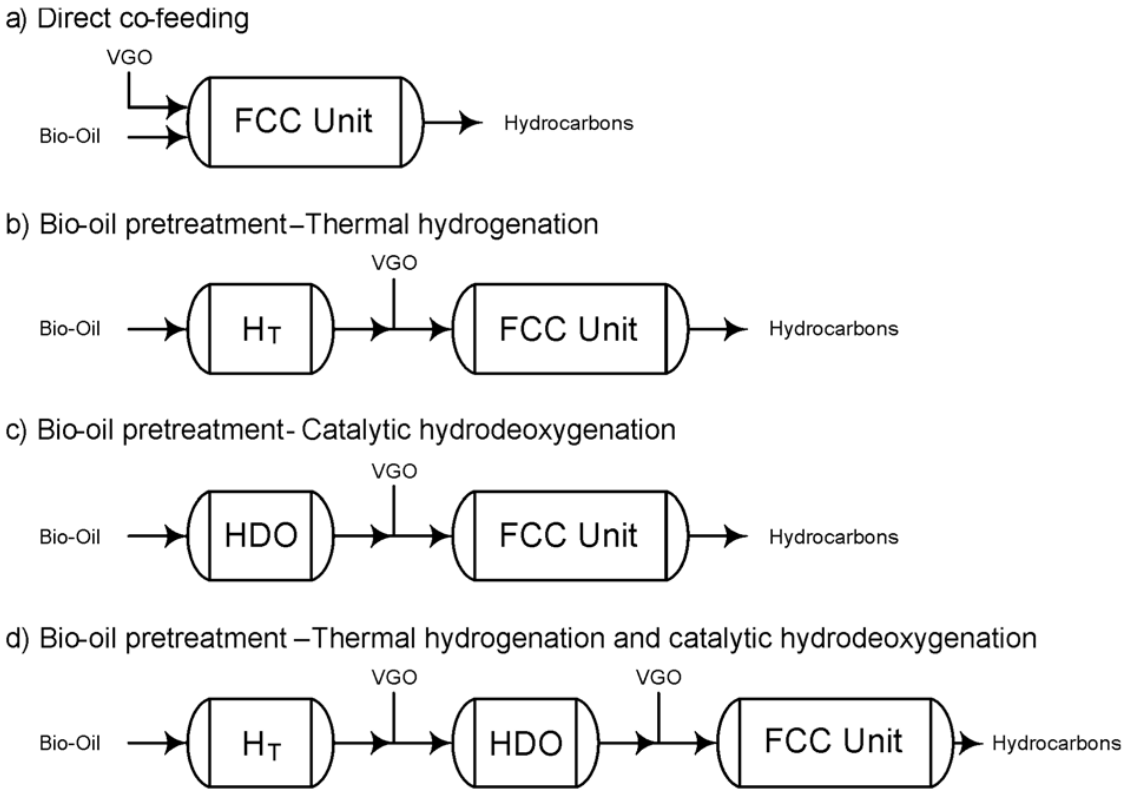

Figure 2.5: Pretreatment options for co-processing of pyrolysis oil with VGO in FCC process [Source: Melero et al. 2012]

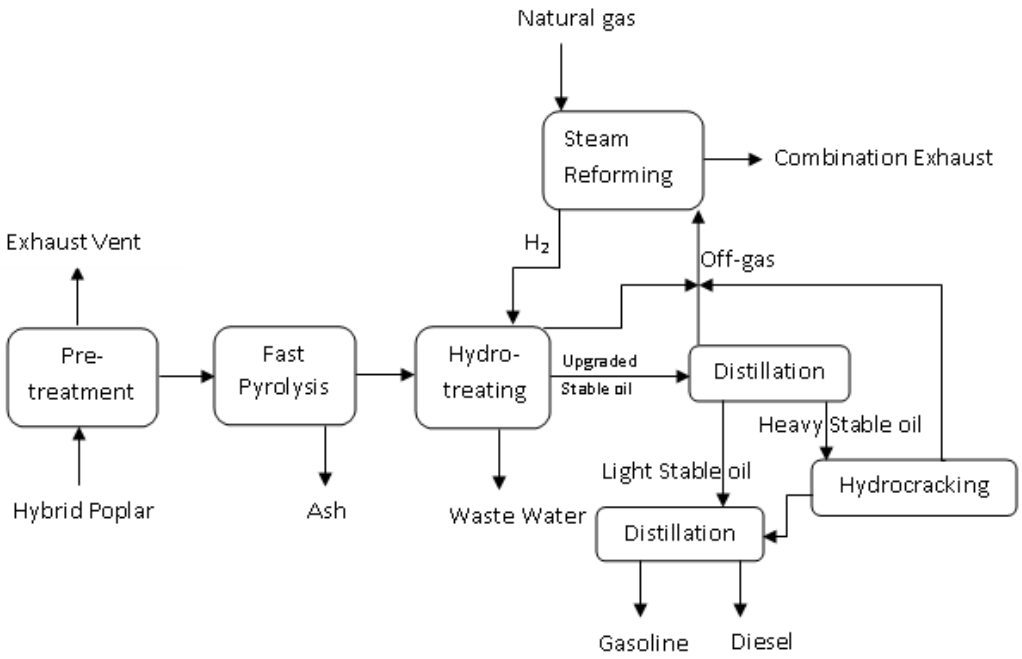

Figure 2.6: A design case stand-alone refinery for fast pyrolysis-hydrotreating-hydrocracking process to produce hydrocarbons [Source: Jones et al. 2009]

Based on their process economics analysis it has been suggested that the production of transport fuels range hydrocarbons from biomass via the pyrolysis route is potentially economically attractive. Further, it is said to be the cost becomes even more economical if the integration of conversion and upgrading processes are brought together under one roof with an existing refinery to take the advantage of infrastructure.

The catalytic steam reforming is one of the techniques which can utilize the refinery equipment. It is very well understood that the pyrolysis oil contains both aqueous and organic fractions. The aqueous fraction can be effectively utilized for the production of hydrogen by processing in very well established steam reforming unit. The added advantage of this technique is that the resulted hydrogen can be utilized for the hydrodeoxygenation of FPO and as a result the whole process can be integrated. The promising results on hydrogen production from steam reforming of pyrolysis oil model compounds were reported in the literature [Mohanty et al. 2012, Goyal et al. 2013, Pant et al. 2013].

2.6.5 Multi-Stage Biomass Torrefaction with Cascading Catalytic Upgrading

The complex nature and multi composition of pyrolysis oil leads to difficulties in direct processing in refinery processes. Anh et al. (2014) proposed a different kind of biorefinery

integration with thermochemical conversion of biomass route i.e torrefaction, as shown in Figure 2.7. The motive of scheme is to collect the pyrolysis vapors on torrefaction of biomass by condensation in the form of oil at three different pyrolysis temperature zones. The first zone temperatures varies in between 220 and 315 °C wherein the pyrolysis oil fraction is enriched with light oxygenates and water. The second zone temperatures would be from 315 to 400 °C in which the oil fraction contains cellulose-derived compounds; whereas the third zone is from 400 °C in which the oil fraction contains lignin-derived compounds. Then it has proposed several chemical synthesis techniques like ketonization, aldol condensation, and alkylation etc. for converting zone-1 and zone-2 fractions into C8-C13 oxygenates and C10-C13 phenolics, as shown in Figure 2.7. Further, it has been emphasized to use the refinery process units like hydro treating, hydrodesulphurization, and fluid catalytic cracking unit for final upgrading into fuel range hydrocarbons.

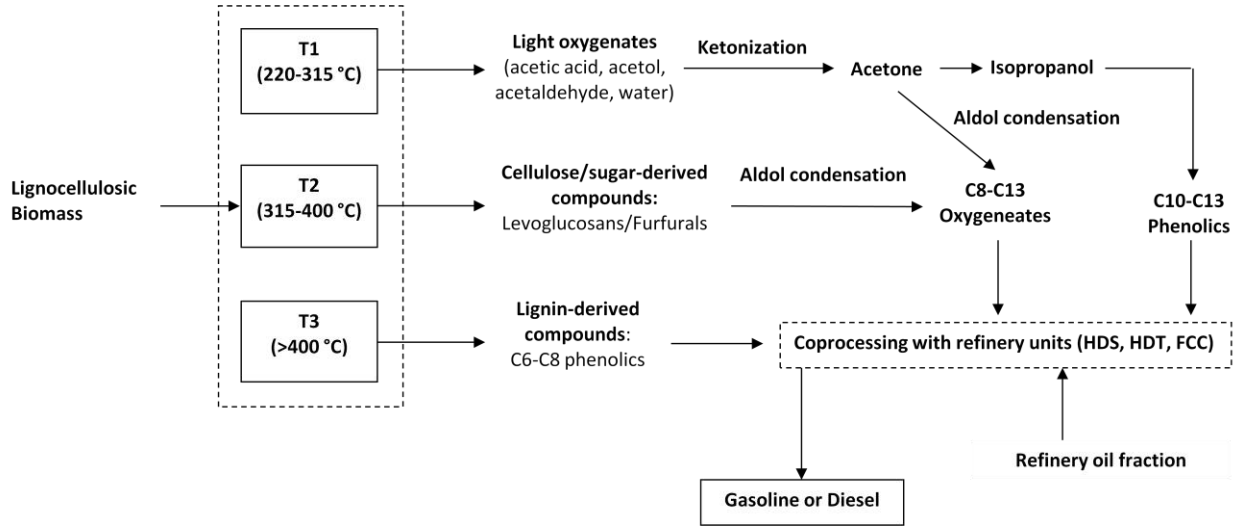

Figure 2.7 Integration of multi-stage biomass torrefaction with catalytic upgrading (Source: Anh et al., 2014)

2.6.6 Synergistic Fast Hydropyrolysis Process Integration

Venkatakrishnan et al. (2014 and 2015) proposed synergistic process integration with gasification, reforming and combustion. This pathway works against the traditional catalytic hydrodeoxygenation in which the loss of carbon is seen due to poor thermal stability while hydrotreating and thus it is aimed for "no carbon left behind" during biomass pyrolysis and further upgrading. This scheme takes the advantage of left over carbon by synergistic utilization

of CO, CO_2, C_1–C_3 hydrocarbons and char by means of incorporating a combination of heat assisted gasification and reforming processes, as shown in Figure 2.8. This process could be customized for the production of hydrogen and the same can be utilized for fast-hydropyrolysis as well as conversion of the syngas stream to fuel range hydrocarbons through a Fischer–Tropsch (FT) process, and conversion to methanol or dimethyl ether. It also helps in improving overall carbon and energy efficiency of an integrated biorefinery process. The process also has a scope for combustion of non-carbon dioxide components for obtaining process heat and getting the acceptable limit of CO_2 emissions of the process. Further, this kind of process integration also helps in effective utilization of petroleum refineries reforming unit in producing the hydrogen. In their H_2Bioil process, they could able achieve carbon recovery as C_1–C_{8+} hydrocarbons is ~73% (C_{4+} ~55%) from cellulose and ~54% (C_{4+} ~32%) from poplar [Venkatakrishnan et al. 2015].

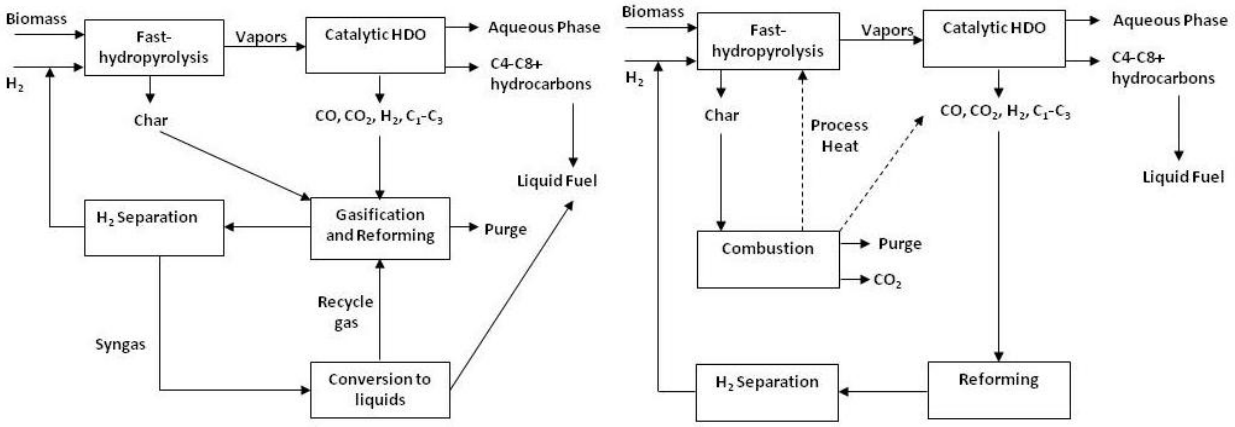

Figure 2.8 Synergistic process integrations of fast-hydropyrolysis and HDO along with gasification and reforming (left side scheme), combustion and reforming (right side scheme)

2.6.7 Kior Process: Fluid Catalytic Cracking of Oxygenates

The KIOR group proposed a scheme for fluid catalytic cracking of biomass-derived oxygenates like glycerol and pyrolysis oil with VGO in traditional refinery FCC unit at various levels [Cantu et al. 2012]. The first option is to feed the biomass separately into the riser reactor bottom from where the pyrolysis vapors and char particles move towards the cyclone separator. From where the char and FCC catalyst particles are separated and moves into regeneration reactor wherein the char and the deposited coke on FCC catalyst are combusted with air to produce process heat. In alternative to first option, the three other options have been encouraged

to coprocess the biomass along with VGO either just before VGO feeding or along with VGO or just after VGO feeding. In the similar the synergistic effects of co-processing of petroleum vacuum residue with plastics, coal and biomass by thermogravitric studies have beed reported in the literature [Ahmaruzzaman et al. 2005, 2007a, b, c, 2008 and 2013].

2.6.8 Petrobras-NREL approach

Recently, Petrobras-NREL CRADA is decided to produce 200 gallons of raw pyrolysis oil for co-processing in FCC (200 Kg/h) of Petrobras demonstration refinery SIX facility in collaboration with ENSYN group. This project has been funded by the governments of US and Brazil. Their scheme on petroleum refinery integration for testing of pyrolysis oil at demonstration level is shown belowwith Figure 2.9.

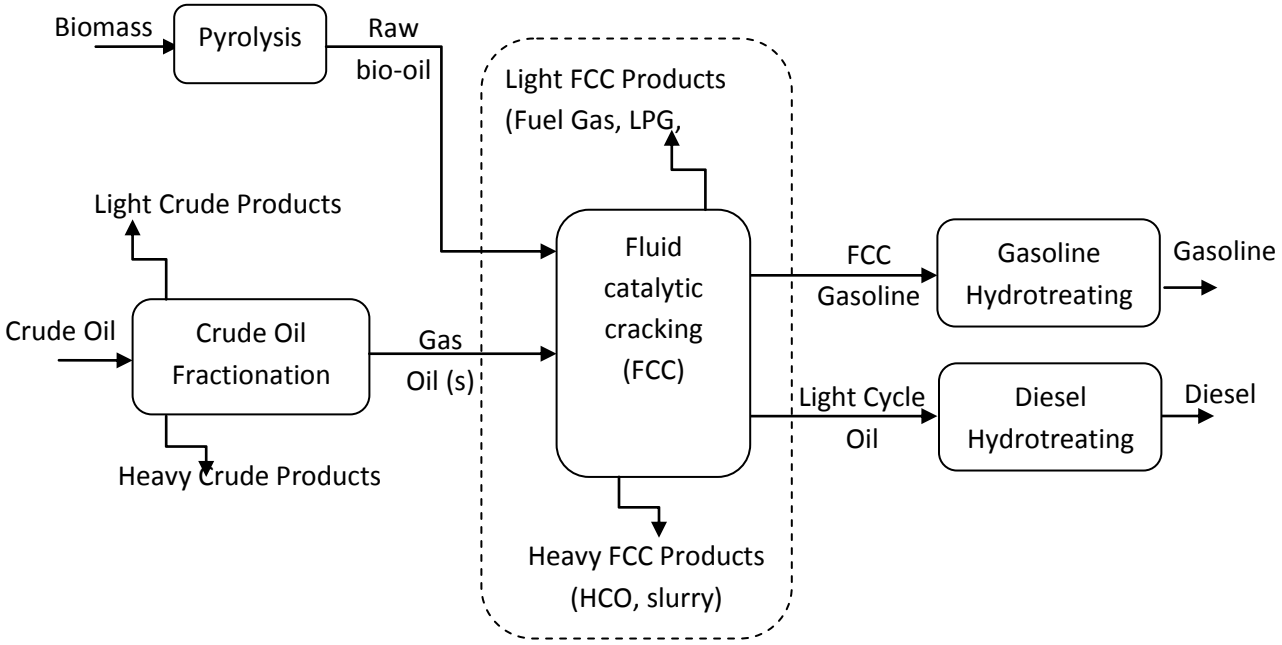

Figure 2.9 Conventional petroleum refinery integration of bio-oil tested in demo scale

2.7 SUMMARY

A detailed literature on the fast pyrolysis of biomass and their co-processing with various approaches has been discussed in this chapter. It has been observed that the reactor configurations such as fluidized bed (bubbling and circulating) and rotating cone are the best option for larger production rates and higher yields (70-75 wt %) of FPO. In process fast

pyrolysisoil stabilization techniques such as process modifications, soot removal, catalytic upgrading of pyrolysis vapors etc. needs attention to further improve the fast pyrolysis-oil yield and composition. The fast pyrolysisoil is a complex mixture of aldehydes, alcohols, and acids together with more complex carbohydrate- and lignin derived oligomeric materials. Two stage hydrogenation step for hydro-deoxygenation has been the best option to upgrade the fast pyrolysisoil by decreasing the oxygen content from 30-40 wt.% to acceptable limit of refinery FCC unit. Thus, upgraded fast pyrolysis-oil can be easily processed in an existing petroleum refinery unit like fluid catalytic cracking unit along with vacuum gas oil/clarified oil to convert it into liquefied petroleum gas and gasoline range products. Beside FCC unit, steam reforming is also one of the proven refinery technologies of refinery to produce the hydrogen. Subsequently the resulted hydrogen can be utilized for hydrogenation of fast pyrolysis-oil. Further, fast pyrolysis units have potential to integrate with refinery units e.g., fluid catalytic cracking unit, steam reforming unit and hydrodesulfurization unit. Also it is possible to upgrade fast pyrolysis-oil within refinery HDS unit with the similar operating conditions and the catalyst.

From the detailed literature study carried out it was found that the quantity and quality of FPO is a function of type of reactor, heating rate, particle size and amount of minerals. The FPO produced on thermochemical conversion is highly unstable due to its chemical composition. In order to aim for co-processing of FPO with VGO in FCC, one needs to be very careful on keeping the blending feed within the limits or specifications of FCC feed. The challenges ahead for co-processing of FPO in FCC are the boiling range (<550 °C), UOP K value (>12.5), API° gravity (16-48), CCR (<4), metal factor (<3), H/C_{eff} (>1.2), nitrogen content (<0.8%), acid value (TAN<1.5), water (<0.2 vol.%), and chemical composition. The FPO can be upgraded or stabilized either by modifying composition (in gas or liquid phase approaches) or separating the de-stabilizing compounds (in gas or liquid phase approaches). In deciding the best pathway several schemes have been proposed and discussed. From the literature it seems that the HDO method is better for stabilization of FPO to further process it with VGO in FCC. The HDO approach has been applied to stabilize FPO by Fogassy et al. (2010) and Samolada et al. (1998) and hence it is decided to process upgraded FPO with VGO in FCC unit.

CHAPTER 3

MATERIALS AND METHODS

3.1 GENERAL

In this chapter, the physicochemical and structural analyses of various feedstocks used in the present work have been discussed. The instruments (like gas chromatography, ^{1}H, ^{13}C and ^{31}P NMR, FTIR and IR analyzers), equipment (pyrolysis reactor system, hydrodeoxygenating autoclave reactor, fluid catalytic cracking unit) and methodologies used for the analysis of feedstocks and products have been discussed in the following sections.

3.2 MATERIALS

3.2.1 Jatropha curcas seed cake

The cake was obtained from M/s Bhoot Oil Mills, Jodhpur, Rajastan, India. The expelled *Jatropha curcas seed cake* (JCC) was milled to small size and then sieved to give fractions of particular size using mesh. The average particle size of ~1.4 mm was used as a biomass feedstock for pyrolysis experiments.

3.2.2 Vacuum gas oil

The commercially available petroleum-derived oil fraction, i.e. vacuum gas oil (VGO), from an Indian refinery was used for the co–processing studies. In general, the vacuum gas oil is obtained by distillation of crude oil with the boiling range of 350 to 550 °C. Basically, it is a mixture of homogeneous hydrocarbon compounds, containing carbon and hydrogen, and heterogeneous hydrocarbon compounds, containing sulphur (i.e. hydrogen sulphide and methyl mercaptan), and nitrogen (i.e andole and carbazole) as well as a very small amounts of non-hydrocarbon metallic compounds (such as iron, copper, nickel, zink and vanadium).

The boiling range distribution was determined by ASTM D-2887 method in SIMDIST analyzer. The carbon residue of VGO was determined by ASTM D-4530-93, which is the amount left out after evaporation and pyrolysis of VGO at 550 °C temperature for a period of

four hours. The left out sample was removed, cooled and weighed. The carbon residue of pyrolysis oils were estimated by weight difference.

The asphaltene content of VGO was determined by the following method: about 10 g of the sample was taken in a conical flask and refluxed with n-heptane. The heptane insoluble portion of the VGO was then extracted with toluene. After 30 minutes toluene extraction, the toluene soluble portion was evaporated in an evaporating dish. The residue remaining is the asphaltene contents, which was determined by weight difference.

3.2.3 Chemicals

The pyrolysis oil model compounds like acetic acid (99%, Sigma-Aldrich Chemical), hydroxyacetone (assay 90%, Sigma-Aldrich Chemical), glycolaldehyde (Sigma-Aldrich Chemical), and guaiacol (98%, Tokyo Chemicals Industry Co. Ltd) were used as a co-processing feedstock with VGO. The glycerol (98%, Sigma-Aldrich Chemical), was also used as one of the co-processing feedstock in catalytic cracking studies.

3.2.4 Equilibrium FCC catalyst

The catalyst used in advanced cracking evaluation (ACE-R) FCC unit was also an industrially available equilibrium fluid catalytic cracking (FCC) catalyst, referred as E-CAT. The equilibrium FCC catalyst contains synthetic faujacite zeolite (Y, RE-Y, USY or RE-USY), silica-alumina matrix, clay (e.g. Kaolin clay) with binder and special additives (like NO_x reduction additives, gasoline sulfur reduction additives, CO combustion promoters, ZSM-5 as an additive for the production of light olefins). In addition to these components, E-CAT could contain also so-called metal traps for the elimination of poisoning of acid centers by V and Ni from feed.

The ASTM D-1977-03 method has been applied to find out the nickel and vanadium of equilibrium catalysts. The silica content was determined by alkaline flux fusion method, wherein the flux is a mixture of 90% dilithium tetraborate ($Li_2B_4O_7$) and 10% lithium fluoride (LiF).

The specific surface area (S_{BET}) of E-CAT was measured by nitrogen adsorption-desorption isotherms at a temperature of –196 °C on a Micromeretics ASAP 2010 system. Before the measurement, the samples were degassed at a temperature of 120 °C for a period of 3 hours and then increased the temperature to 350 °C and maintained the same for 4 hours under

vacuum. The total pore volumes (Vp) of catalyst sample were found out at a relative pressure (P/P_0) of 0.995. The mean pore diameters (Dp) of sample were calculated with the Barrett-Joyner-Halenda (BJH) equation using corresponding deposition branches of the isotherms.

3.2.5 HDO catalyst

Palladium (99.9%, Sigma-Aldrich Chemicals) and γ-alumina Al_2O_3 (97%, Sigma-Aldrich Chemicals) were chosen as an active and support materials for the preparation of hydrodeoxygenating catalyst. Mesoporous alumina was prepared using the literature method [Ray et al. 2007]. The Pd was loaded over alumina by incipient wetness impregnation method. In a typical preparation method, 1.0 g of Palladium (II) nitrate dihydrate was dissolved in 30 ml of water, and 20 ml of ethanol. Subsequently, 20 g of γ-alumina (Al_2O_3) (Surface area = 243 m^2 g^{-1}) was added. The mixture was stirred constantly at 80 °C for 5 hours to dry the sample. The dried sample was further dried at 120 °C for overnight in an oven. Finally, the Pd metal loaded on alumina was calcined at 500 $^{\circ}$C in a furnace for 8 h to prepare Pd/Al_2O_3 catalyst (2% Pd on alumina).

3.3 EXPERIMENTAL SETUP

3.3.1 Biomass Pyrolysis Unit

The continuous electrically heated fluidized bed reactor with the volume of 34.95 liter was used as a pyrolysis reactor. The reactor is typically divided into three sections as the bottom section (Shell= 125 N.B. pipe; Height above diffuser plate = 1200 mm; Internal diameter = 122.26 mm), conical section (top diameter = 250 N.B. pipe; bottom diameter = 125 N.B. pipe; straight height= 100 mm) and top section (shell diameter = 250 N.B. pipe; length = 400 mm; end cover = dished end). The design temperature of reactor is 750 °C and pressure 12 bars (g); while the material of construction is SS316. The sand, with average particle size of 284 microns, was used as a fluidizing media, and was used for the pyrolysis of JCC. The nitrogen gas was used as a fluidizing gas and was preheated up to 400 °C temperature using an electric furnace before sending it into fluidized bed reactor which was operated at ~530 °C temperature and atmospheric pressure.

The JCC with average particle size of ~1.4 mm fed into the fluidized bed reactor by screw feeder system in continuous mode at a feed rate of 300 g h^{-1}. The feed biomass directly

gets contacted with fluidizing media (sand) and fluidizing gas (nitrogen) at the bottom zone of the reactor. The biomass particles were cracked or pyrolyzed in the reactor. The resulted pyrolysis vapors and non-crackable portion, called as char, followed the fluidizing gas came out from the top of the reactor followed by cyclone and series of condensers. The residence time of pyrolysis vapors was maintained as 2.9 sec by adjusting the flow rate of fluidizing gas. The gas velocity of pyrolysis plant was 1.09 m/s. The pyrolysis reactor temperature was decided to be 530 °C on the basis of maximum pyrolysis oil yield obtained. The part of char was separated by a cyclone separator located next to the fluidized bed reactor; whereas pyrolysis vapors were condensed and separated as crude pyrolysis oil in a series of condensers-collectors; the non-condensable gases were vented off to atmosphere. The schematic diagram and experimental setup of fast pyrolysis unit are shown in Figure 3.1a and 3.1b, respectively.

3.3.2 Advanced Cracking Evaluation (ACE-R) FCC Unit

The fluid catalytic cracking is the most widely used secondary conversion process in the petroleum refineries, operated mainly in gasoline mode. Catalytic cracking is a process in which the large molecular weight hydrocarbons cracked down into small molecular weight hydrocarbons over hot fluid catalytic cracking catalyst. In this way, heavy oils can be converted into lighter hydrocarbons, such as dry gas, liquefied petroleum gas, gasoline and light cycle oil. Here, the catalytic cracking experiments were carried out using an advanced cracking evaluation (ACE^{TM}) unit supplied by M/s Kayser Technologies Inc., USA. It is a laboratory scale system for studying the fluid catalytic cracking process in batch mode. The schematic diagram and experimental setup of ACE research unit are shown in Figure 3.2a and Figure 3.2b, respectively.

The ACE-R unit was equipped with an automated fixed-fluidized bed reactor, which is widely accepted in the petroleum refinery for fluid catalytic cracking (FCC) catalyst evaluation studies. Commercial FCC unit operate with continuous feed and catalyst circulation through several reactors or vessels which comprise the fluid catalytic cracking unit. Here, the model R represents a tubular reactor (containing batch of fluidized bed particles) operated in a cyclic to simulate the reactors (riser, stripper and regenerator) of FCC unit. The feedstock, VGO, and gases (nitrogen and air) were sequentially supplied during the defined steps of cracking cycle. The steps of the cracking cycle are as follows:

(i) Injection of vacuum gas oil over the FCC catalyst, which simulates the riser reactor

(ii) Catalyst stripping, which simulates the catalyst stripper,

(iii) Catalyst regeneration with air at elevated temperature, which simulates the regenerator.

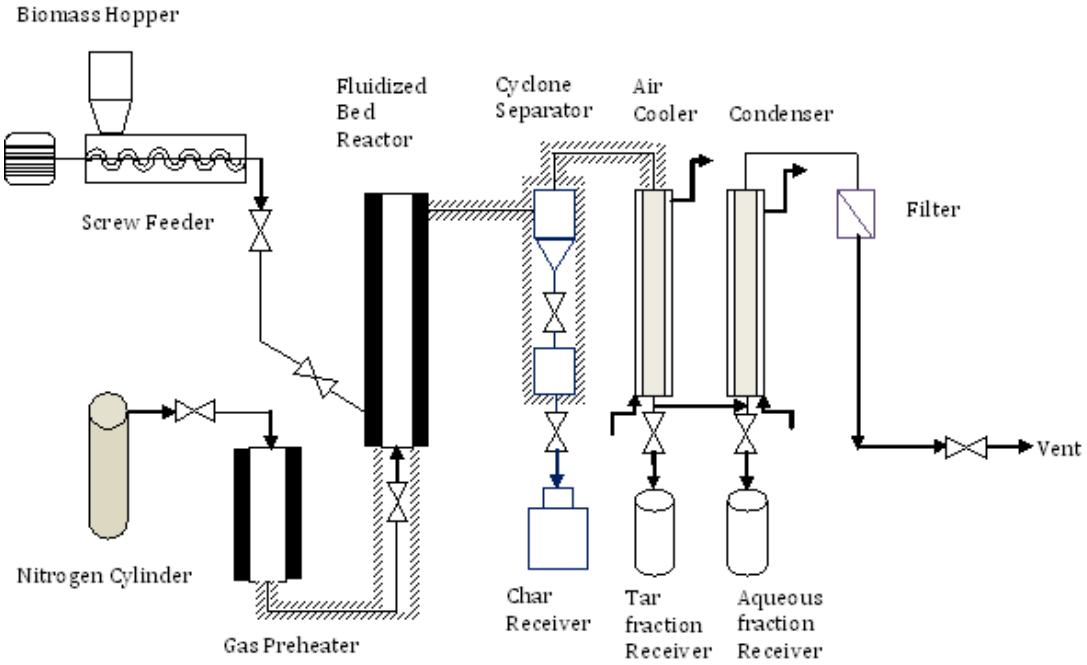

Figure 3.1a: Schematic diagram of fluidized bed pyrolyzer

Figure 3.1b: Experimental setup of fluidized bed pyrolyzer

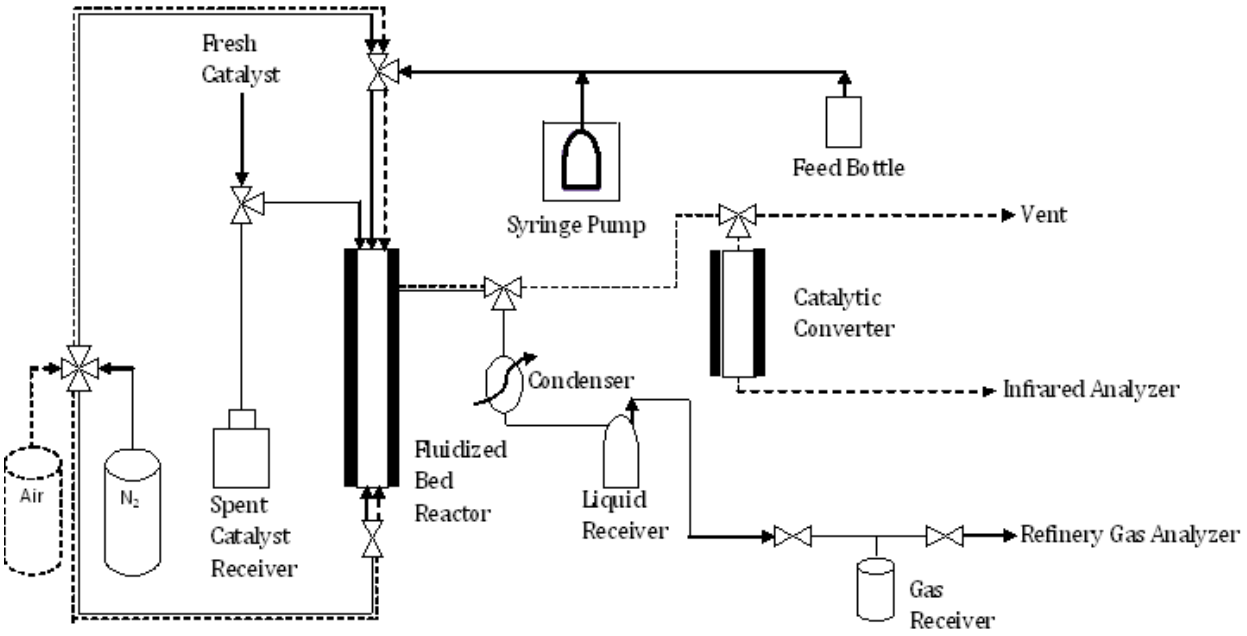

Figure 3.2a: Schematic diagram of advanced cracking evaluation (ACE-R) FCC unit

Figure 3.2b: Experimental setup of advanced cracking evaluation (ACE-R) FCC unit

The main parts of the FCC unit are syringe, syringe heater, syringe pump, furnace, 316 stainless steel fixed-fluidized bed reactor, liquid recovery system, gas collection system, weighing balances, and analytical instruments, such as gas chromatography and infrared

analyzer. The temperature of the reactor was maintained as high as 750 °C, while the system was in regeneration mode. A syringe of 2.5 ml was used for VGO addition and it was fitted with a multiport, high-pressure three way solenoid valve to allow nitrogen gas and VGO entry to the riser reactor through a common feed line. The electric heating tape was used to heat the syringe to ~100 °C temperature. The maximum capacity of syringe pump is 3 g/min of VGO. The feed rate of syringe pump was adjusted to 1.2 g/min. The top feed injector involves two pieces of stainless steel tubing, 1/16 inch feed tube inside a 1/8 inch fluidization line.

The catalyst-to-oil ratios (3, 5, 7 and 9) were maintained by adjusting the injection times of feedstock. The typical range of catalyst-to-oil ratio in FCC operation varies from 3 to 12, as in the present work the C/O ratio was varied from 3 to 9. In the present study the C/O ratio was varied by varying time on-stream (t) at feed rate (1.2 g/min), hence constant weight hourly space velocity (WHSV). In other words, C/O ratio can be defined as per the following equation:

$$\mathrm{C/O} = 3600/(\mathrm{WHSV} \times \mathrm{t}) \qquad (3.1)$$

The reactor was heated up to the set point of cracking temperature before adding catalyst. A known amount of catalyst (preferably 9 g) was placed into the reactor through catalyst addition line near the top of the reactor, and the system was closed to perform the cracking run. After cracking of feedstock the catalyst was stripped off by nitrogen several times, i.e. for a period of 7 times of injection time. During the catalytic cracking and stripping, the liquid product was collected in a glass receiver, maintained at –10 °C temperature, which is located at the end of the reactor exit. Meanwhile, the gaseous products were collected in a gas receiver by water displacement. After cracking and stripping steps the reactor was operated in regeneration mode, where the coke deposited on the catalyst surface during the cracking reaction was burnt off with air at a temperature of 700 °C. The flue gases generated during regeneration process were sent to the catalytic converter/furnace packed with cuprous oxide, where carbon monoxide was converted into carbon dioxide at 540 °C temperature. The step of regeneration process/mode was continued till the amount of carbon dioxide formation becomes nil in the flue gases. The reactor effluent gases were measured on on-line mode and the same values were used to estimate the coke or the amount of carbon deposited on E-CAT during cracking.

3.3.3 Continuous Stirred Tank Reactor (CSTR)

A 100 ml stainless steel, high pressure stirred tank reactor (M/s Autoclave Engineers, USA) with bolted closure, floor stand and magnetic drive assembly was used to partially hydrodeoxygenate the heavy fraction of FPO in batch mode. Various accessories like PID temperature controller, rupture disk, pressure gauge, cooling water lines, pressure safety valve, and pressure transmitter were included to control of the temperature, pressure, and safety of operation. The schematic diagram and experimental setup for high pressure stirred tank reactor are shown in Figures 3.3a and Figure 3.3b, respectively. The design temperature of reactor is 750 °C and pressure is 250 bars.

Before starting the reaction, the reactor was purged with hydrogen gas for a period of 5 min, and then it was pressurized up to 80 bar pressure. A constant speed of stirrer was maintained at 700 rpm. The reactor temperature was raised to 300 $^{\circ}$C from ambient with heating rate of 5 $^{\circ}$C min^{-1}. As a result an increase in reactor pressure was observed from 80 to 120 bars. The same temperature was maintained for a period of 4 h. The reactor was then cooled down to ambient temperature. The liquid products were collected and analyzed separately using NMR spectroscopy.

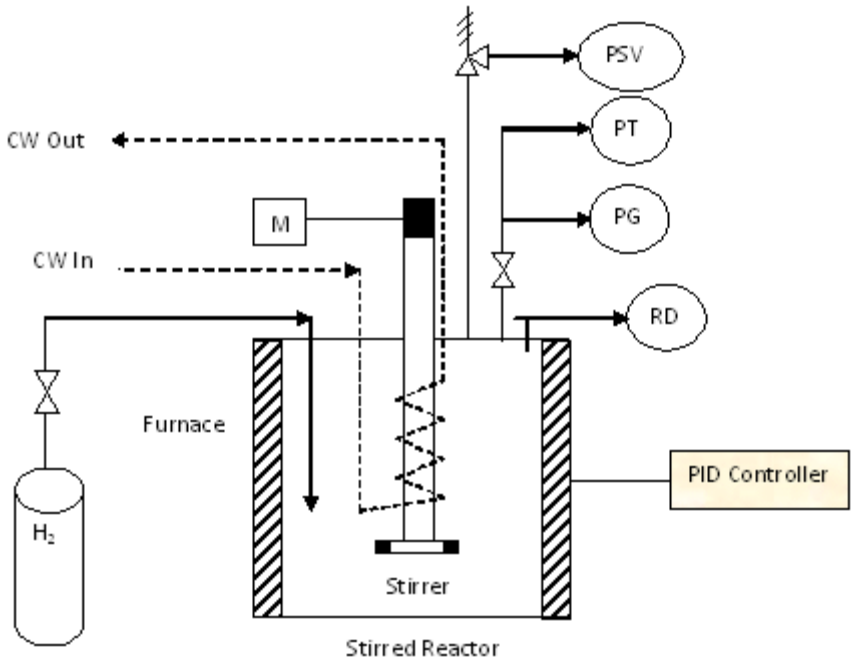

Figure 3.3a: Schematic diagram of CSTR set up

Figure 3.3b: Experimental setup of CSTR

3.4 ANALYTICAL METHODS

3.4.1 Structure and Composition of Biomass

Scanning Electron Micrographs (SEM) were obtained using a FEI Quanta 200 FE-SEM operating at 20–25 kV, using tungsten filament doped with lanthanum hexaboride (LaB6) as a X-ray source fitted with a secondary electron detector i.e. Evehart-Thornley Detector (ETD). The samples were dispersed on a carbon coated adhesive followed by vapor-deposition with gold before analysis.

The patterns of powder X-ray diffraction were noted on a Bruker D8 advanced X-ray diffractometer (fitted with a Lynx eye high-speed strip detector) using Cu Ka radiation (λ = 0.15432 nm), which was operated at 30 mA and40 kV. For data collection from 0.5 ° to 5° of 2θa continuous mode was used at a scanning speed of 2°/min.

The TG experiments were carried out in a Perkin-Elmer Thermogravimetric/Differential Thermal Analyzer (TG/DTA) using a Pyris Diamond TG-DTA instrument under nitrogen flow (99.99%) of 100 ml/min for the temperature ranging from 50 °C to 1000 °C at a heating rate of 10 °C/min. The TG apparatus gives the continuous measurement of sample weight as a function of temperature.

For the determination of moisture content of biomass, the sample (500 g) was taken in an air tight jar from the bulk storage. The empty container was dried for 30 min at 105±1°C in an oven, and cooled in a desiccator to achieve room temperature. The sample container was weighed to the nearest 0.02 g and recorded as container weight; W_c. 50 g of the sample was taken in that container and then weighed to the nearest 0.01 g, and recorded as initial weight W_i. The container with sample was placed in an oven for 16 h at 103 ± 1 °C. Then it was removed from the oven and cooled in the desiccators to the room temperature and weighed immediately to the nearest 0.01 g. This procedure was repeated till the final weight (W_f) of the container becomes constant. The moisture content was calculated by weight difference.

For the determination of the volatile matter, 1 g of the dried sample was taken from the container in a platinum crucible and heated to 950 ± 20 °C for 7 min, and the crucible was removed, cooled, and weighed till it get constant and accounted as final weight W_f. The percent moisture in the analysis sample was calculated as follows:

$$\text{Volatile matter of the sample, wt.\%} = \{[W_f - W_i]/[W_i - W_c]\} \times 100 \qquad (3.2)$$

where W_i is the initial weight (sample + container), W_c is the container weight and W_f is the final weight.

Ash content of JCC was obtained by Thermogravimetry ASTM D-482/IP 4 method. The silica crucible was heated at 700 °C for 10 min and cooled to room temperature for taking the initial weight. 5 g of the sample was taken in this dish and burned thoroughly. After complete burning, the dish was placed in 700 °C muffle furnace for 30 min. The ash content was calculated by weight difference.

The calorific value was obtained in a bomb calorimeter (Parr-6300 model) by using ASTM-3308 method. 1.0 g sample was placed in a calorimeter, and ignited in the presence of

oxygen. The heat of combustion was calculated for the estimation of calorific value of biomass and char.

3.4.2 SIMDIST Analysis

The liquid sample obtained from catalytic cracking of various feedstocks were analyzed by chromatographic simulated procedure, described by ASTM D-2887 method, with an Agilent 6890 gas chromatograph, using a HP-1 methyl silicon column and a flame ionization detector. As in petroleum refinery practice, the product distribution was quantified by their boiling point range: dry gas (H_2 and C_1-C_2 hydrocarbons), LPG (C_3-C_4 hydrocarbons), gasoline (IBP–216 °C), LCO (216–370 °C), heavy cycle oil i.e. HCO (> 370 °C) and coke, respectively. The FCC conversion was estimated using the equation (3.3) as follows:

$$\text{FCC Conversion}, \% = 100 - (\text{LCO wt.}\% + \text{HCO wt.}\%) \quad (3.3)$$

3.4.3 NMR Analyses

3.4.3.1 ^{1}H and ^{13}C NMR analysis

^{1}H and ^{13}C NMR spectra of FCC liquid distillates, produced from co-processing of FPO or HDO oil with VGO, were recorded on a Bruker Avance III NMR spectrometer equipped with BBFO probe resonating at the frequency of 500.13 and 125.7 MHz, for ^{1}H and ^{13}C, respectively. The conventional ^{1}H spectra were recorded using 5% w/v sample solutions in $CDCl_3$ containing 0.03% tetra methylsilane (TMS, 98% Merck) with a sweep width of 6 kHz, 16 number of scans, 13.4-μs π/2 proton pulse and 2-s relaxation delay. The ^{13}C NMR spectra of the sample were recorded using 30% (w/v) in $CDCl_3$ solutions. Quantitative ^{13}C spectra were acquired using the NOE suppressed, inverse gated proton decoupled technique (Waltz-16), with a sweep width of 19 kHz. 8k numbers of scans were collected using a 5-s relaxation delay. All the ^{13}C spectra were processed with 1.0 Hz line broadening prior to FT.

All the ^{1}H and ^{13}C NMR spectra were referenced to tetra methylsilane at 0 ppm. Before starting the analysis, the spectra obtained were corrected for phase and baseline and then each of them was separated into different regions that corresponded to different types of protons and carbons according to their position in the molecule. Later, each spectrum was integrated thrice and averaged within the indicated regions. The chemical shift assignments are shown in Table

3.1. The chemical shift regions of ^{13}C NMR spectrum have been divided into aliphatic carbons (0-50 ppm), oxygenated alcoholic carbons (50-110 ppm), aromatic carbons (110-150 ppm) and carboxylic (150-200 ppm) carbons; whereas the ^{1}H NMR spectrum to aromatic hydrogen (9-6 ppm), aliphatic hydrogen (0-5 ppm), olefinic (5-6 ppm) and oxygeneted hydrogen (3.5-5 ppm). Furthermore, the aliphatic proton region has been subdivided into Hα (2-3 ppm), Hβ (1-2 ppm), Hγ regions (0.5-1 ppm); whereas the aromatic region to mono aromatics (m-a; 6-7.2 ppm), diaromatic (d-a; 7.2-8.00 ppm) and polyaromatic proton regions (p-a; 8-10 ppm). The aliphatic proton corresponds to the methyl and methylene groups.

The details of average structural parameters have been calculated from ^{13}C NMR and ^{1}H NMR data and defined as follows:

n=Average chain length= $C_{parafinic}/C_{CH3,}$

$C_{parafinic=}$ $I_{14.1}+I_{22.7}+I_{29.7}+I_{30.1}+I_{32.0}$

f_a=Fraction of aromatics= $C_{ar}/C_{ar}+C_{oxy}+C_{ali}$

C_h=Normalized percentage of protonated aromatic carbon

C_b= Normalized percentage of bridgehead aromatic carbon

Ar_q= Normalized percentage of substituted quaternary aromatic carbon

Ch+Cb+Arq=1

f_a^s= fraction of substituted aromatic carbons $=Ar_q/Ar$

BI=Branchiness index= H_γ/H_β

m-a= Percentage of mono-aromatic protons

d-a=Percentage of di-aromatic protons

p-a= Percentage of poly-aromatic protons

3.4.3.2 ^{31}P NMR analysis

For ^{31}P NMR analysis, the solvents used with the bio-oil sample are usually a mixture of anhydrous pyridine and deuterated chloroform (1.6: 1.0, v/v) containing a relaxation agent (i.e., chromium (III) acetylacetonate) and an internal standard. 20 mg of FPO was dissolved in pyridine $CDCl_3$ solvent of 0.5 ml. TMDP reagent (0.05–0.10 ml) was added, stirred and transferred into a 5 mm NMR tube for ^{31}P NMR recording. Quantitative ^{31}P NMR spectra were recorded with a long pulse delay of 10s using a 90^0 ^{31}P pulse. 128 number of transients were

recorded in inverse gated decoupling mode on a Bruker Avance III 500 MHz spectrometer at room temperature. Chemical shifts are typically calibrated with respect to the phosphitylation product of TMDP with water, which gives a sharp and stable signal at 132.2 ppm in pyridine–$CDCl_3$ solvent.

3.4.3.3 DEPT/QUAT NMR

The liquid sample obtained on catalytic cracking of pure glycerol was characterized by a set of NMR experiments (like ^{1}H, ^{13}C, DEPT-45, 90 and135, Quat) and two dimensional hetero-nuclear correlation techniques (like ^{1}H-^{13}C HMQC, ^{1}H-^{13}C HMBC). These techniques were used to have a detailed understanding about the structural connectivity between groups. The DEPT experiments were carried out at pulse angles of $3\pi/2$, using pulse sequences as reported by Bandall and Pegg [Doddrell et al. 1982]. In these experiments $\pi/2$ pulse width used for ^{1}H and ^{13}C were 13.4 and 9.9 µs, respectively. J_{CH} values were set to 145 Hz, an intermediate value between aliphatic, aromatic and oxygenated carbons for DEPT experiments. The relaxation delays are 2 for DEPT experiments, respectively. 2K numbers of transients were acquired for DEPT experiments and 4K number scans were acquired for QUAT spectra. The variation of different CHn magnetization with pulse angle is shown in Figure 3.4.

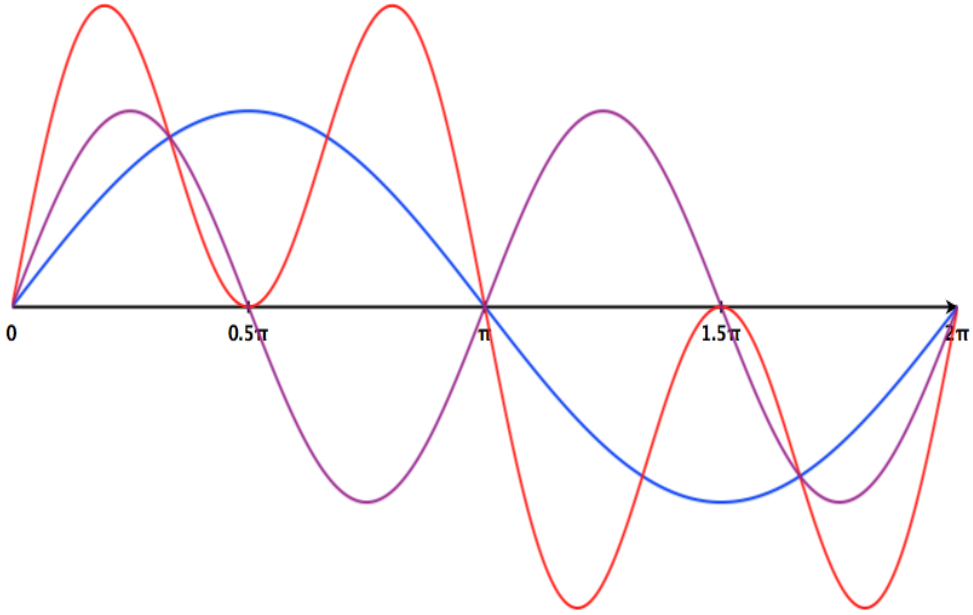

Figure 3.4: Evolution of CHn (n=1-3) magnetization with respect to pulse angle red: CH_2, blue: CH, Purple CH_3 carbon resonances

All the five spectra were linearly combined to generate CH_n (n=0-3) sub-spectra. The modified equation suggested by Netzel's for hydrocarbon fractions [Netzel et al. 1987] was used to generate sub-spectra, instead of using the conventional Bandall equation [Doddrell et al. 1982]. The equations for sub spectra generation are given below:

$$\theta_{CH} = \left[\theta_{90} - a\theta_{CH_2}\right] - x[\theta_{45} + y\theta_{135}] \quad (3.4)$$

$$\theta_{CH_2} = \theta_{45} - y\theta_{135} \quad (3.5)$$

$$\theta_{CH_3} = [\theta_{45} + y\theta_{135}] - z\left[\theta_{90} - a\theta_{CH_2}\right] \quad (3.6)$$

$$\theta_C = \theta_{QUAT} - b\theta_{CH_2} \quad (3.7)$$

In equations (3.4)–(3.7) 'θ' represents the integrated area of the peak descripted in the DEPT spectra; *x, y, z* are the original Bandall valueS of 0.0, 0.7 and 1.0 with best spectra with corrected phase.

3.4.3.4 Two-dimensional NMR spectroscopy

3.4.3.4.1 *Correlation spectroscopy (^1H-^1H COSY)*

^1H–^1H COSY experiments were carried out at room temperature for all samples (10% solution in $CDCl_3$ with TMS). 64 scans using 2k data points and 262 transients were acquired F2 and F1 dimensions, respectively. For resolution enhancement, 1k × 1k data matrix and QSINE window function with SSB = 0 in both dimensions were used for processing all the spectra. The phase mode in F2 and magnitude mode in F1 were applied for line broadening of 0.3 Hz.

3.4.3.4.2 *Heteronuclear multiple-quantum correlation (^1H–^{13}C)*

Heteronuclear multiple-quantum correlation (HMQC) experiment utilizes one-bond couplings. HMQC spectroscopy determines which proton of a molecule is bonded to which ^{13}C nuclei. It also suppresses the signals of those protons which are not attached to ^{13}C. The gradient HMQC spectrum was collected on same spectrometer with a 13.40 µs 90° ^1H pulse and a 9.90 µs 90° ^{13}C pulse, 0.17s acquisition time (with 13C GARP decoupling), 2K points, an 6 kHz spectral window in *f*2, a 125 kHz spectral window in *f*1, 1.5-s relaxation delay, 32 transients were averaged for each of the 512 complex FID's. The data were processed using a shifted sine bell weighting and zero filled before Fourier Transformation.

3.4.3.4.3 *Heteronuclear multiple-bond correlation ($^{1}H–^{13}C$)*

Heteronuclear multiple-bond correlation (HMBC) spectroscopy is a modified version of HMQC suitable for determining long-range $^{1}H–^{13}C$ connectivity. It is used for the determination of structure as well as ^{1}H and ^{13}C assignments of molecules. HMBC differs from HMQC and HSQC, where multiple-bond couplings over two or three bonds (J = 2–15 Hz) are utilized. In this approach one-bond cross-peaks are suppressed.

The gradient HMBC spectrum was collected on the same spectrometer with a 13.40 µs 90° ^{1}H pulse, and a 9.90 µs 90° 13C pulse, 0.17 s acquisition time, 2K points, a 6 kHz spectral window in *f*2, a 125 kHz spectral window in *f*1, 1.5 s relaxation delay heteronuclear multiple-bond coupling) 32 transients were averaged for each of the 512 complex FID's. The data were processed using shifted sine bell weighting and zero filling.

Table 3.1: Assignment of various proton and carbon resonances

Type of Proton/Carbon [Altgelt et al. 1994, Petrakis et al. 1987]	**Symbols**	**Chemical Shift Range (ppm)**
Aromatic proton	H_{ar}	6–9
Mono aromatic proton	$H_{m\text{-}ar}$	6–7.25
Di_aromatic proton	$H_{d\text{-}ar}$	7.25–9
Poly aromatic proton	$H_{p\text{-}ar}$	7.25–9
H_{α} to aromatic ring	H_{α}	2.05–4.5
α, oxygenated protons	$H_{\alpha,\ oxy}$	2.05–4.5
H_{β} to aromatic/in paraffinic CH and CH_2	H_{β}	1.1–2.05
H_{γ} to aromatic ring/terminal CH_3	H_{γ}	0.4–1.1
Aliphatic carbon	C_{ali}	5–10
Aromatic carbon	C_{ar}	100–160
Naphthenic carbon	C_{N}	25–60
Protonated aromatic carbon	C_{arp}	100–130
Bridgehead aromatic carbon	C_{arBr}	124–133
Substituted aromatic carbon	C_{arS}	133–160

3.4.4 FTIR Analysis

Fourier transform infrared spectroscopy (FTIR) develops the electromagnetic radiation where the energy is adequate to excite vibrational states of chemical bonds. These chemical bonds have a dipole moment that can transform over a time absorb infrared radiation in a quantized process, in which a particular bond will give rise to only absorptions that match their respective stretching or bending modes of vibration. FTIR is a powerful characterization tool to have direct information about the functional groups of FCC feedstock and liquid products. Hence, functional groups analysis of liquid samples was carried out using Fourier Transform Infrared Spectroscopy (Nicolet 8700 - Thermo Fisher Scientific FTIR spectrometer) with the sample powder diluted in 1% potassium bromide (KBr). The FTIR spectrum in the range of 400-4000 cm^{-1} was measured with a resolution of 4 cm^{-1}. The type of FTIR absorption peaks in relation their wave number is shown in Table 3.2.

Table 3.2: FTIR absorption peaks

Wave number, cm^{-1}	**Band**
3500-3550 (s)	O-H stretch, phenol
3010-3100 (s)	C-H stretch, aromatic/alkene
2850-2860 (m)	C-H stretch, alkanes
2920-2930 (s)	C-H stretch, alkanes
1710 (s)	C=O stretch, carboxylic acid
1460 (m)	C-H bend, alkanes
1600-1630 (s)	C=C stretch, aromatic/conjugated alkene
1370-1380 (w)	C-H rock, alkanes
1030-1060 (s)	C-O stretch
910-960 (w)	=C-H bend, alkenes/aromatics

3.4.5 Infrared Analysis

The IR analyzer (Servomex 1440 gas analyzer) was used to analyze the coke deposited on the FCC catalyst by burning with air in regeneration mode and the resulted total carbon dioxide was quantified by a CO_2 analyzer based on the adsorption of infrared light that is capable of measuring the concentrations of CO_2 analyzed.

3.4.6 Gas Chromatography Analysis

The product gases were analyzed with a Varian CP-3800 gas chromatograph (Refinery Gas Analyzer) equipped with three detectors, a flame ionization detector (FID) and two thermal conductivity detectors. FID has been used for the analysis of hydrocarbons; whereas TCD for the analysis of hydrogen and nitrogen gases. Temperature program has been used to make sure the adequate separation of compounds in as short duration as possible. The details of columns and temperatures used for the analysis are shown in Table 3.3.

Table 3.3: Details of refinery gas analyzer column

Detector	Columns used	Temperature, °C
Front TCD	Haysep Q (CP 1305)	Detector = 175
	Molecular Sieve 5A (CP 1306)	Filament = 200
Middle TCD	Haysep N (CP 1307)	Detector = 175
	Haysep Q (CP 1308)	Filament = 200
	Molecular Sieve 13X (CP 1309)	
FID	CPSIL 5CB (CP 1310)	Detector = 175
	Al2O3 MAPD (CP 7433)	
	Deactivated Fused Silica (CP 735732)	
Injector temperature, °C = 150 °C		

CHAPTER 4

CATALYTIC CRACKING OF JCC–DERIVED PYROLYSIS OILS

4.1 GENERAL

The fast pyrolysis of JCC–derived feedstock and the co-processing of FPO (FPO) with vacuum gas oil (VGO) have been carried out in the experimental setup described in the previous chapter. In this chapter, the production of FPO from JCC followed by pretreatment of FPO (char removal and deoxygenation of FPO) and co-processing of FPO with VGO and HDO. Further the characterization of FPO and HDO by NMR techniques have been discussed. The characterization of the catalyst used in hydrodeoxygenation and co-processing in FCC unit has also been discussed.

4.2 PRETREATMENT OF FAST PYROLYSIS OIL

4.2.1 Separation of Char Particles

The JCC-derived FPO obtained from fluidized bed pyrolysis reactor was found to have large concentration of char particles (nano-to-micro scale), which are highly dispersible and makes the pyrolysis oil highly viscous to semi-solid. The separation of these char particles is very important, in order to utilize the pyrolysis oil as a fuel. In this context, initially, the semi-solid pyrolysis oil was diluted with ethanol and then bigger size particles (>200 nm) were separated by membrane filtration (pore size: 0.2 μ) under vacuum. Subsequently, the filtrate containing large amount of small particles, was centrifuged at 8000 rpm for 20 minutes. The centrifuge force at high rpm forces the char nanoparticles at the bottom of the tubes. As a result, the filtrate component was separated into two portions; upper liquid phase containing blend of pyrolysis oil and ethanol, and the deposited char particles at the bottom of the centrifuge tubes. The ethanol present in the residual pyrolysis oil was then recovered by vacuum distillation. As a result, the viscosity of pyrolysis oil had come down drastically and become a more thin liquid with very good flow property, compared to earlier semi-solid like phase. The char-free FPO i.e

FPO-derived tar fraction is used for further co-processing studies. The scheme for separating char particles are shown in Figure 4.1.

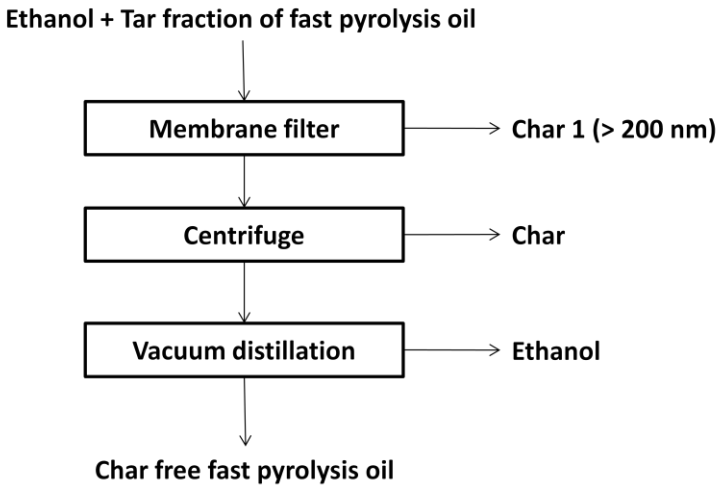

Figure 4.1: Char particles separation scheme for FPO

4.2.2 Hydrodeoxygenation of Fast Pyrolysis Oil

4.2.2.1 Product profile

The FPO was stabilized by mild hydrodeoxygenation over palladium catalyst. The partially hydrodeoxygenated FPO, which is suitable for co-processing in petroleum refinery fluid catalytic cracking unit, was produced in a fast pyrolysis unit (section 3.3.1). A known amount (2 wt.%) of palladium on alumina catalyst was used in a 100 ml batch high pressure stirred tank reactor to hydrogenate the heavy fraction of FPO.

In the second step of pretreatment of FPO, a hydrodeoxygenation method has been applied to reduce the oxygen content of FPO. The obtained FPO, containing 32 wt.% of oxygen, was subjected to hydrodeoxygenation with Pd/Al_2O_3 catalyst in a batch stirred reactor at 80 bar pressure. The increase of reactor pressure from 80 to 105 and 120 bars was observed with an increase in temperature from ambient to 250 and 300 $^{\circ}$C, respectively. The gas analysis indicated that the bound oxygen was removed in the form of carbon dioxide by decarboxylation reaction, which is higher in yield, i.e. 45 and 51 wt.%, at 250 and 300 $^{\circ}$C temperatures, respectively, in gas analysis. The respective CHNO analysis of feed JCC, FPO, and HDO are shown in Table 4.1.

Table 4.1: Elemental analysis of JCC, FPO and HDO oils

Sample name	C, wt.%	H, wt.%	N, wt.%	O, wt.%	S, wt.%	H/C	O/C
JCC	45.50	6.70	2.43	45.33	0.04	1.767	0.747
FPO	56.50	7.10	4.308	32.0	0.092	1.507	0.424
HDO oil at 250 °C	64.98	8.0	4.91	22.0	0.11	1.500	0.257
HDO oil at 300 °C	76.18	8.8	4.91	10.0	0.11	1.404	0.099

From the elemental analysis (Table 4.1), it was found that the amount of oxygen content was reduced from 32 to 22 and 10 wt.% for 250 and 300 °C temperatures, respectively. If the oxygen contents could not be removed, the deep or high deoxygenation levels of >95% is needed to match the specifications of pyrolysis oil with standard crude oil in terms of carbon-hydrogen ratio, oxygen content and density [Samolada et al. 1998]. The Van krevelen diagram is a realistic and handy way to compare the elemental composition of biomass-derived pyrolysis products with conventional crude petroleum oils, which also helps in gaining insights of various reactions taking place [Van Krevelen et al. 1950]. The Van krevelen diagram was originally developed for the process and structural study of coal. The Van krevelen diagram for dry H/C and O/C ratios of the FPO and HDO is shown in Figure 4.2.

It was observed that the O/C atomic ratio of HDO drastically decreased to 0.257 and 0.099, respectively, as compared to FPO (0.424); whereas a relatively minor change and declination in H/C ratio at 250 °C and 300 °C temperature, respectively, was observed. A similar kind of trend was observed by Mercader et al. (2011). The lower values of O/C ratio might be due to thermal polymerisation reactions with the concomitant formation of water, which is not a good measure for catalytic activity [Ardiyanti et al. 2013].

The carbon residue is defined as "a measure of the carbonaceous material left in a fuel after all the volatile components have been vaporized in the absence of air", which may be expressed as Conradson Carbon Residue (CCR) or Micro Carbon Residue (MCR). From the present study, the CCR analysis (Table 4.2), the carbon residue was found to be higher (~16 wt.%) in FPO; whereas it decreased to about 8 wt.% on hydrodeoxygenation at 300 °C temperature. The CCR value was found to be 3.88 wt.% (for the blending feedstock of HDO: VGO ratio of 5:95) which was slightly higher than VGO (CCR value was 3.64 wt.%) used.

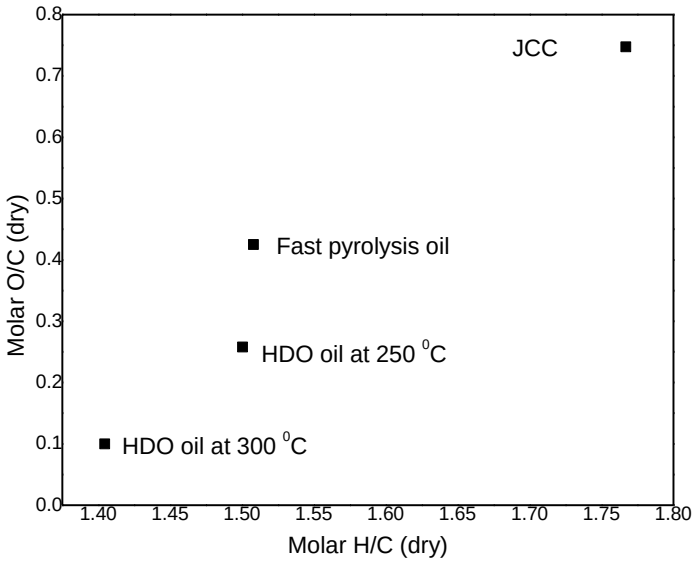

Figure 4.2: Van Krevelen diagram for dry H/C and O/C molar ratios of the FPO and HDO oils

Table 4.2: Physicochemical characterization and SIMDIST analysis of feedstock

Feedstock	**Blending ratio**	**Density at 15 °C, g cc^{-1}**	**CCR, wt.%**	**H/C$_{eff}$**	**Boiling point, °C**						
Mass recovery, wt.%					IBP	10%	30%	50%	70%	90%	FBP
VGO	100	0.919	3.64	1.725	350	369	400	441	489	550	550
FPO	100	1.18	16.26	--	36	162	259	328	357	445	592
VGO:FPO	95:5	0.932	4.27	1.65	36	359	393	435	482	545	592
	90:10	0.945	4.90	1.59	36	348	386	430	476	539	592
	85:15	0.958	5.53	1.53	36	337	379	424	469	534	592
	80:20	0.971	6.16	1.47	36	327	372	418	462	529	592
HDO	100	1.04	8.6	--	36	159	270	344	405	499	597
VGO:HDO	95:5	0.925	3.88	1.68	36	358	394	436	485	548	597

4.2.2.2 NMR characterization of fast pyrolysis oils

^{31}P NMR has been employed for characterizing hydroxyls by phosphitylation with a phosphorous reagent followed by quantitative ^{31}P analysis [Pu et al. 2011]. The oxygenates in the FPO are problematic components aroused from the cracking of ligno-cellulosic components of biomass, and imposed complexity in ^{1}H NMR analysis, and takes long time for ^{13}C measurement

due to long relaxation time of C-O groups. ^{31}P derivatization is a preferred method for fast analysis of oxy-component in pyrolysis oil. Thus, oxygenates like aliphatic and aromatic alcohols, and acids were derivatized using 2-chloro-4, 4, 5, 5-tetramethyl-1, 3, 2-dioxaphospholane (TMDP) and quantified from ^{31}P spectra. The reaction scheme for phosphorous derivatization is shown in Figure 4.3.

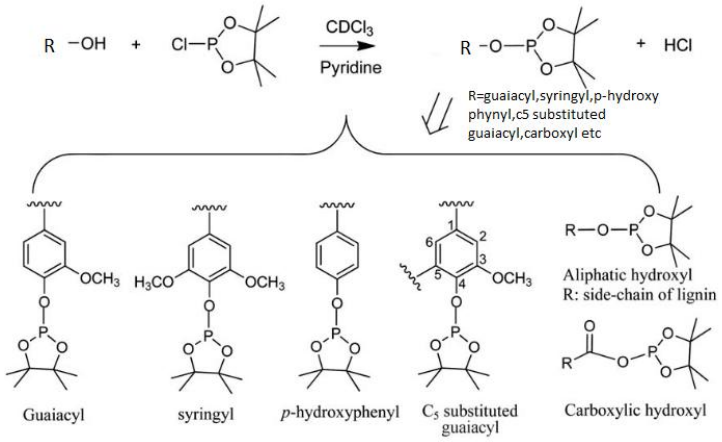

Figure 4.3: Reaction scheme for derivatized ^{31}P NMR

TMDP reacts with hydroxyl groups in the presence of a base such as pyridine to form phoshitylated product, with the base to capture the liberated HCl and drive the exothermic reaction to complete conversion. All the oxy-components were derivatized and the typical chemical shift assignments with integration region for different hydroxyl groups are shown in Table 4.3.

^{31}P NMR spectra of derivatized FPO and HDO (at 250 and 300 °C) are shown in Figure 4.4a,b,c. The chemical shifts were referenced with respective to the endo-N-hydroxy-5-norbornene-2,3-dicarboximide, internal standard NHND, at (152 ppm). Carboxylic acids corresponding to chemical shift region of 133-136 ppm were found to be absent in FPO, as shown in Figure 4.4a. The above result is also evidenced from ^{13}C NMR (Figure 4.5) results showing absence of carboxylic carbon peaks. It was further observed from the spectra that the aliphatic alcohols corresponding to chemical shift regions of 145.07 to 150.02 ppm were absent in FPO and HDO (300 $^{\circ}C$). It indicated the reduction in hydroxyl groups due to process conditions and the process was efficient for hydrodeoxygenation.

Table 4.3: ^{31}P NMR Chemical shift regions in pyrolysis oil after derivatization with 2-chloro-4, 4, 5, 5-tetramethyl-1, 3, 2-dioxaphospholane (TMDP)

S. No.	Functional group	Integration region, ppm	
		Ben et al. (2012)	Present study
1	Aliphatic OH	150.0 to 145.5	150.02 to 145.07
2	C5 substituted β-5	144.7 to 142.8	145.07 to 140.42
3	Guaiacyl phenolic OH	140.0 to 139.0	140.42 to 138.2
4	p-hydroxy-phenyl OH	138.2 to 137.3	138.2 to 136.96

The FPO contains a major guaiacyl phenolic, and p-hydroxy phenyl phenolics. Although from the Figure 4.4b it can be seen that the signals due to phenols and syringyl alcohols corresponding to region 142-144 ppm are present in HDO oil (obtained at 250 °C); whereas Figure 4.4c shows that the components are completely removed in HDO (obtained at 300 °C). Moreover, strong signals due to guaiacol, catechol and p-hydroxy phenyl groups were completely removed in HDO (obtained at 300 °C). On the basis of ^{31}P NMR analysis, it was found that hydroxyl and mono lignol groups were eliminated during hydrodeoxygenation. Thus, the HDO obtained at 300 °C can be used along with VGO as a co-processing feedstock for processing in a refinery FCC unit. Therefore, the HDO obtained, at 300 °C temperature, was used for further co-processing studies. Generally, the oxygen was removed from FPO on deoxygenation over Pd/Al_2O_3 in three ways dehydration, decarboxylation and decarbonylation. In the present work, it was observed that the oxygen was removed from FPO as CO, CO_2 and water. The gas yield on HDO of FPO was 26.1% (which contains 2 mol.% of CO and 49 mol.% of CO_2). The water content of HDO was found to be 1.6%.

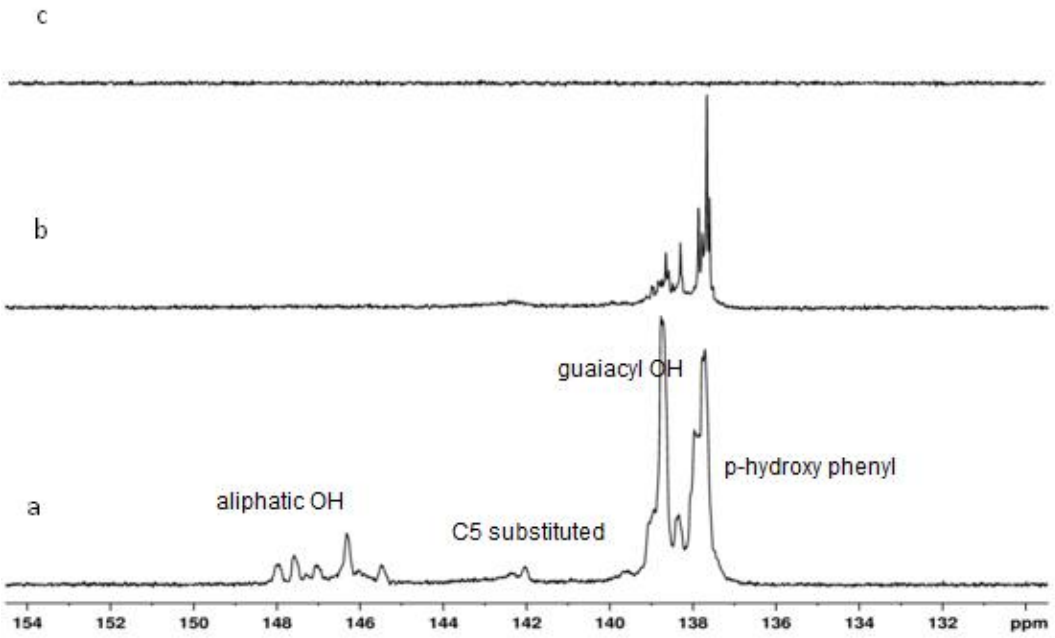

Figure 4.4: Quantitative ^{31}P NMR of (a) FPO; (b) HDO oil at 250 °C, and (c) HDO oil at 300 °C

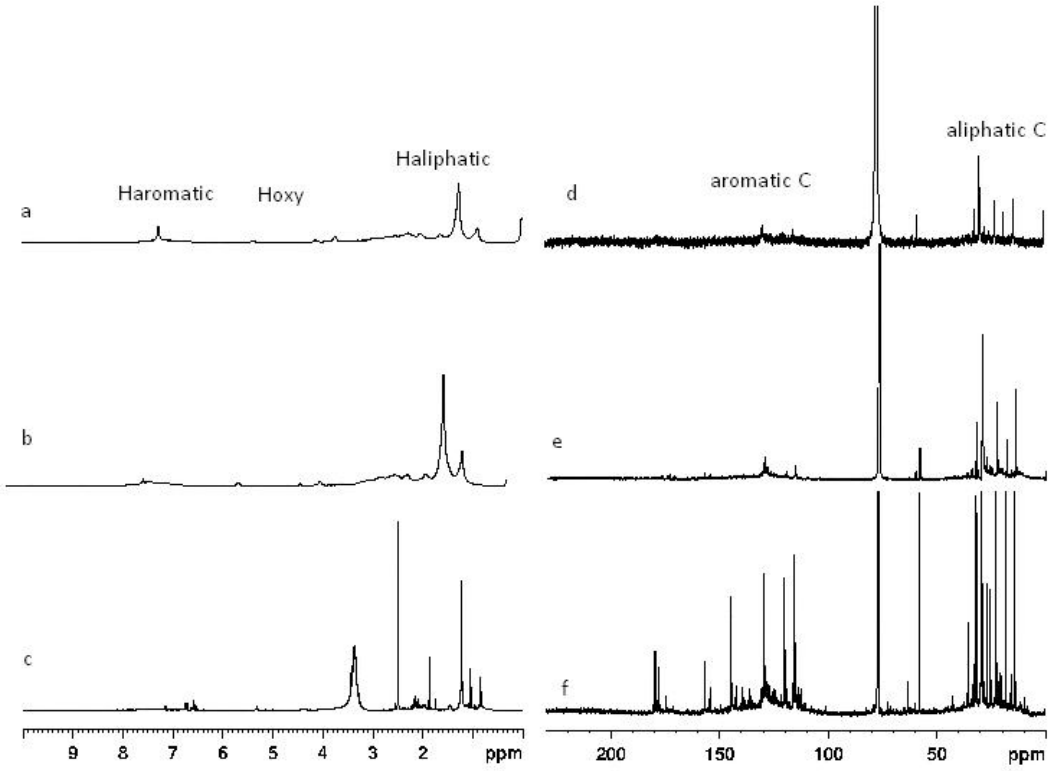

Figure 4.5: (a) ^{1}H NMR of HDO oil at 300 °C; (b) ^{1}H NMR of HDO oil at 250 °C; (c) ^{1}H NMR of FPO; (d) ^{13}C NMR of HDO oil at 300 °C; (e) ^{13}C NMR of HDO oil at 250 °C; and (f) ^{13}C NMR of FPO at 530 °C and C/O=5

4.3 CATALYTIC CRACKING OF VACUUM GAS OIL

The understanding of catalytic cracking process in fluidized bed riser over FCC catalyst is very complicated due to the fact that the change in one parameter will lead to change in one or several parameters [Stratiev et al. 2007]. Typically, most of the world petroleum refinery fluid catalytic cracking (FCC) risers are operated in the range of 480–570 °C temperature, catalyst-to-oil ratios in the range of 3-12. Thus, the preliminary studies were carried out to study the effect of reactor temperature and C/O ratio on FCC product yields at constant WHSV (weight hourly specific velocity) of 8 h^{-1}.

4.3.1 Effect of Temperature

The FCC product quality as well as quantity in terms of yield is highly dependent on riser temperature. The VGO was catalytically cracked in advanced cracking evaluation FCC unit over equilibrium FCC catalyst. Initially, series of experiments were performed by keeping the varying reactor temperature from 510 to 570 °C and constant catalyst-to-oil ratio of 5 and weight hourly space velocity of 8 h^{-1}. From Table 4.4, the increase in FCC conversion and coke formation were observed with an increase in reactor temperature from 510 to 570 °C. The increase in FCC conversion may be due to the increase in dry gas yield from 1 to 6 wt.% and LPG yield from 13 to 20 wt.%. Whereas the gasoline yield was found to be more at 530 °C temperature and thereon the decrease in gasoline was observed which is due to the over-cracking. Hence, the reactor temperature was chosen as 530 °C in the present experimental studies. While the product yields of LCO and HCO were decreased with an increase in temperature. The higher yield of gasoline from catalytic cracking of VGO may be due to the following mechanisms: (i) maximizing the primary cracking reaction, which produces an unsaturated gasoline, (ii) controlling the secondary reactions like (ii-a) over-cracking to gases, and (ii-b) oligomerization or cyclo-addition of its unsaturated compounds to coke or dehydrogenated products [Decroocq, 1984]. However, the secondary hydrogen transfer reactions play an important role in net increase of gasoline yield by the saturation of the gasoline range olefins before they catalytically crack further into LPG range olefins [Niccum, 2013].

Table 4.4: Effect of temperature on VGO catalytic cracking product yields at constant C/O (5) and WHSV (8 h^{-1})

Temp. °C	Dry gas, wt.%	LPG, wt.%	Gasoline, wt.%	LCO, wt.%	HCO, wt.%	Coke, wt.%	Conversion, wt.%
510	1.17	13.21	43.34	20.47	14.97	4.96	62.68
530	1.79	15.5	44.02	19.84	12.4	5.58	66.89
550	4.22	17.46	41.94	18.98	10.22	6.12	69.74
570	6.40	20.12	40.31	17.5	8.17	6.48	73.32

4.3.2 Effect of Catalyst-to-oil Ratio

In a process of optimizing process parameters for the higher yield of gasoline on catalytic cracking of VGO over equilibrium FCC catalysts in ACE-R FCC unit, the catalyst-to-oil (C/O) ratio was varied from 3 to 9. The experiments on C/O ratio variation were carried out by keeping the constant reactor temperature of 530 °C and WHSV of 8 h^{-1}. The increase in FCC conversion from 61 to 72 wt.% was observed with an increase in C/O ratio (Table 4.5). Herein, the increase in conversion was due to increase in the yields of dry gas, LPG and gasoline; whereas the yields of LCO and HCO were decreased with increase in C/O ratio. The yield of coke formation was linear with C/O ratio. From the results, the maximum gasoline (IBP-216 °C) yield was found to be at C/O ratio of 5.0. Therefore, it was decided to operate the FCC unit at C/O ratio of 5.0 for better yield of gasoline.

Moreover, it was found that the yield of gasoline first increases then attains a maximum, and finally decreases; the yields of gases keep on increasing with an increase in C/O ratio. It may be due to the consecutive reaction which can be seen while catalytic cracking of vacuum gas oil over zeolite catalyst in a fluidized bed reactor [Mohammed et al. 2010]. The primary cracking of VGO produces an unsaturated hydrocarbon, which further undergoes through secondary reaction either by over-cracking to gases or oligomerization and cyclization of unsaturated hydrocarbons into dehydrogenated product like coke [Decroocq et al. 1984]. However, it was believed that the formation of coke takes place within the first 50 milli seconds [Hollander et al. 1999]. Besides, relative rates of reactions like cracking, hydrogen transfer, cyclisation, and dealkylation decides the rate of formation of aromatics [Corma et al. 2001], which helps in formation of coke. The increase in C/O ratio beyond 5 may lead into the cracking of gasoline range hydrocarbons into LPG range hydrocarbons. The FCC could be operated with higher C/O ratios if the aim of the product is LPG range hydrocarbons which are basic feedstock in petrochemical industry.

Table 4.5: Effect of catalyst-to-oil ratio on VGO catalytic cracking product yields at constant temperature of 530 °C

C/O ratio	Dry gas, wt.%	LPG, wt.%	Gasoline, wt.%	LCO, wt.%	HCO, wt.%	Coke, wt.%	Conversion, wt.%
3	1.56	14.50	40.60	24.94	13.34	4.64	61.31
5	1.79	15.50	44.02	19.84	12.40	5.58	66.90
7	2.10	19.04	40.12	18.36	11.22	7.48	68.75
9	2.34	23.43	38.34	14.91	10.65	8.52	72.63

4.4 CATALYTIC CRACKING OF FPO/HDO WITH VGO

The catalytic cracking studies on co-processing of FPO with VGO were carried out in an advanced cracking evaluation (ACE-R) FCC unit at the optimum operating conditions. The maximum yield of gasoline was found to be 44 wt.% at C/O ratio of 5 and 530 °C temperature with the FCC conversion of ~66% [Naik et al. 2014a]. The similar kind of optimized process parameters were used for further co-processing reactions of VGO with FPO or HDO.

Initially, the blending ratio of FPO with VGO was varied at 5, 10, 15, 17, and 20% in order to see its effect and optimize the same for getting the similar FCC conversion. The FCC conversion of different feeds and their product yields of dry gas, LPG, gasoline, LCO, HCO, and coke are shown in Table 4.6. The mass balance obtained was more than 98%. From Table 4.6 it can be seen that the conversion decreases from 75 to 64 % with an increase of blending ratio of FPO from 5 to 20%. The decrease in conversion was due to the decrease in yield of dry gases and LPG from 2.1 to 1.4 and 38 to 23 wt.%, respectively. Whereas, the yields of gasoline, LCO and HCO increased from 29 to 35 wt.%, 14 to 20 wt.%, and 8 to 14 wt.%, respectively, with an increase in blending ratio of the FPO with VGO from 5:95 to 20:80.

However, the results on co-processing at a lower blending ratio (5:95) indicated higher conversion (~around 9 wt.%) as compared to the direct catalytic cracking of pure VGO at constant C/O ratio and temperature. It was due to higher yield (38 wt.%) of LPG fraction as compared to 15 wt.% in case of pure VGO catalytic cracking. The increase in the LPG yield was at the cost of gasoline, as it appeared from its yield i.e 29 wt.%; whereas the gasoline yield was 44 wt.% on pure VGO catalytic cracking at similar conditions. Further, there was also a decrease in LCO and HCO yield by 5 and 4 wt.%, respectively.

Table 4.6: A selectivity data for VGO: FPO, VGO: HDO and VGO at different blending ratios at 530 °C and C/O of 5

Feedstock	**VGO:FPO**				**VGO:HDO**	**VGO**	**VGO:FPO**
Blending ratio	95:5	90:10	85:15	80:20	95:5	100	83:17
FCC conversion	75.68	74.69	69.35	64.39	66.96	66.89	66.08
Yield, wt.%							
Dry gas	2.182	2.05	1.43	1.41	1.507	1.798	1.42
LPG	38.876	35.70	28.69	23.77	28.78	15.5	25.44
Gasoline	29.038	31.14	35.11	35.04	32.50	44.02	35.08
LCO	14.885	15.43	17.99	20.49	18.98	19.84	19.11
HCO	8.054	8.48	10.67	14.08	13.27	12.4	12.31
Coke	5.48	5.21	4.23	4.16	4.17	5.58	4.14

However, with an increase in blending ratio from 5:95 to 10:90, there was decrease in the LPG yield by ~3 wt.%; increase in gasoline yield by ~2 wt.%; increase in LCO yield by ~1 wt.%; whereas slight increase of HCO yield by ~0.5% was observed. Clearly these results indicated that the FPO could be coprocessed with VGO at lower blending ratios of 5:95 and 10:90 for LPG production at the cost of gasoline followed by LCO and HCO range hydrocarbons. Furthermore, with an increase in blending ratio from 10:90 to 15:85, similar (as 10:90 blending studies) trends of LPG (decreases by 7 wt.%), gasoline (increases by 4 wt.%), LCO (increases by 2.5 wt.%), HCO (increases by 2 wt.%) yields were observed.

Moreover, with an increase in blending ratio FPO: VGO to 17% the FCC conversion of ~66% was observed. At this particular blending ratio, the dry gas, gasoline, and coke yields were decreased by 0.4, 9, and 1.4 wt.%, respectively; whereas the LPG yield was increased by ~10 wt.% and the yields of LCO and HCO were found to be almost constant.

The similar trend of product yields were observed with an increase in blending ratio from 17:83 to 20:80. In general perspective the C5+ liquid hydrocarbons increases with an increase in H/C_{eff}. Similar observations were made in the present study, the C5+ hydrocarbons increased with an increase in H/C_{eff}. From the above results, it can be concluded that in addition to H/C_{eff} the type of oxygenated molecules present in FPO also plays a major role in the distribution of FCC product profile. However, the increase in the yield of gasoline with an increase in blending ratio of FPO with VGO was observed even with the decrease in H/C_{eff}. This may be due to the

presence of lignin monomers present in the FPO, which is further discussed with the help of NMR analysis in the following section.

The coke yield for all blending ratios was within the limits and was lower as compared to pure VGO processing. The previous studies on co-processing of aliphatic oxygenates like acetic acid, hydroxyacetone and glycolaldehyde with VGO with similar conditions also indicated the coke yield within the limits except on co-processing of lignin-derived monomer (guaiacol) with VGO [Naik et al. 2014a,b]. The water formation was also observed on co-processing of FPO with VGO; however their yield is not shown.

Furthermore, an attempt has been made to coprocess the HDO, obtained on hydrodeoxygenation of FPO at 300 °C temperature and 80 bar pressure, with VGO in a blending ratio of 5:95 in an ACE-R unit. As shown in Table 4.6, the conversion was found to be 66.96%, which is approximately equivalent to the conversion obtained on catalytic cracking pure VGO or co-processing of FPO with VGO at the similar operating parameters. It can be seen that the highest conversion is possible with co-processing of HDO with VGO as compared to pure VGO catalytic cracking and co-processing of FPO with VGO. The increase in conversion was due to the increase in the yields of LPG and gasoline. Whereas the yield of dry gas was lower for the case of FPO: VGO co-processing as compared to HDO: VGO co-processing and VGO direct catalytic cracking, which may be due to the direct relation of effective hydrogen index. The increase in the effective hydrogen index from 1.65 to 1.68 on addition HDO instead of FPO resulted in an increase in the yield of C5+ liquid hydrocarbons. However, the yields of LCO and HCO observed were similar for all cases.

Fogassay et al. (2010) reported that the hydrogen-consuming reactions play an important role in HDO oxygenates cracking over solid acid catalysts. It was reported that the hydrogen yield produced from the catalytic cracking of HDO with VGO (20:80) was lower than that of the cracking of pure VGO due to the hydrogen synergetic reaction.

4.5 ^{1}H AND ^{13}C NMR CHARACTERIZATION

The average structural parameters of FCC product liquid distillates were studied by NMR. The chemical shift region of ^{1}H spectrum has been subdivided into aromatic hydrogen (9-6 ppm), aliphatic hydrogen (0-5 ppm), olefinic (5-6 ppm) and oxygeneted hydrogen (3.5-5 ppm), as shown in Figure 4.6a-e. The aliphatic proton region has been further subdivided into Hα (2-3

ppm), Hβ (1-2 ppm), Hγ regions (0.5-1 ppm). Further, the aromatic region has been divided into mono aromatics (m-a; 6-7.2 ppm), diaromatic (d-a; 7.2-8.0 ppm) and polyaromatic proton regions (p-a; 8-10 ppm). The ^{13}C NMR spectrum has been divided into different integration domains as aliphatic (0-50 ppm), oxygenated alcoholic (50-110 ppm), aromatic (110-150 ppm) and carboxylic (150-200 ppm) carbons, as shown in Figure 4.7a-e.

Figures 4.6a-e and Figure 4.7a-e represents ^{1}H NMR and ^{13}C NMR spectra of the blended VGO. From the normalized integrals of the signals, a series of average structural parameters like average chain length (n), fraction of carbon aromaticity (f_a), percentage of proton aromatic carbon (Ch), bridgehead aromatic carbon (Cb), substituted aromatic carbon (ARq), branchiness Index (BI), fraction of substituted aromatics (f_a^s, percentage of mono-aromatics (m-a), di-aromatics (d-a), and poly-aromatics (p-a) protons have been derived and are listed in Table 4.11. The results can only be considered approximate, since they present an over-simplified picture of very complex mixtures containing a wide range of components; however the method described has the advantage that the few spectra can be obtained on crude material without preliminary treatment.

The recording of NMR data generated twice and processed thrice for each and averaged. Since phosphorous is sensitive like proton, the spectra were recorded in inverse gated decoupled mode for quantification having NOE (nuclear overhauser effect) suppressed during acquisition. Thus, the standard deviation of detection limit falls in the range ±0.5%. Elemental analysis report for detection of oxygen is always based on difference method and the generated data have different principle than NMR, indicating presence of oxygenated compounds (which includes interior oxygen). Only alcohol and acids can be derivative by the above TMDP process. Etherial aldehydic, ketonic and ester compounds could not be detected by ^{31}P NMR. This is because the molecule should have acidic hydrogen that reacts with chlorine of TMDP produces HCl that get neutralized by pyridine.

In the present FPO samples the alcoholic peaks contributing to 145-150 ppm as shown in ^{31}P NMR was corroborated by cellulosic peak 60-110 ppm region and 140-160 ppm region as shown in ^{13}C spectra before derivatization with TMDP. Again, beside these peaks, signals from ester carbon contributing to 170-185 ppm in ^{13}C NMR spectra are observed with strong OCH_3 peak at 58-60 ppm. In HDO, the ester and ether carbon intact were found in the region 170–185 ppm and 58 and 60 ppm.

Table 4.7 shows the average structural parameters of VGO, and blended VGO and their products. The average alkyl chain length of VGO is 18 while in the products the average chain length varies from 3-6. The fraction of carbon aromaticity varies from 0.13 in VGO to the range of 0.13-0.14 in FPO blended VGO and to 0.15 in HDO. In products, the aromaticity varied from 0.47 to 0.55. From Table 4.7, it can be seen that f_a increases with an increase in FPO while co–processing with VGO.

This indicated that the incomplete cracking of lignin-derived monomers, which are present in FPO; whereas, the co-processing of HDO (obtained at 300 °C) with VGO resulted into a product with a similar f_a of ~0.47, which indicated that the lignin-derived monomers were cracked with hydrodeoxygenation of FPO. This was also confirmed from the yield of gasoline on co-processing of HDO with VGO, which was higher while co–processing of FPO with VGO.

Table 4.7: NMR derived average structural parameters of feedstock's and their liquid distillates (*) at constant 530 °C and C/O of 5

Feedstock	Blending Ratio	n	fa	Ch	Cb	ARq	BI	fa^s	m-a	d-a	p-a
VGO	100	18	0.13	4.90	1.36	5.70	0.35	0.44	2.33	1.6	0.55
VGO*		6	0.48	37.27	3.19	7.32	--	0.15	9.2	7.63	2.15
FPO:VGO	5:95		0.13								
FPO:VGO*		3	0.55	43.5	3.3	7.8	0.47	0.14	10.56	8.66	2.47
FPO:VGO	10:90		0.13								
FPO:VGO*		3	0.54	44.2	3.1	6.4	0.53	0.12	10.00	8.51	2.58
FPO:VGO	15:85		0.14								
FPO:VGO*		3	0.52	41.7	3.0	6.8	0.47	0.13	10.46	6.84	1.05
FPO:VGO	20:80		0.14								
FPO:VGO*		3	0.49	39.5	2.9	6.7	0.6	0.14	10.05	5.26	0.19
HDO: VGO	5:95		0.15								
HDO:VGO*		3	0.47	37.2	3.0	6.3	0.53	0.13	9.67	5.51	0.79

Again the total CH_3 carbon content remains same and the amount of long end chain CH_3 was lower in the case of co-processing of FPO (at 5:95 ratio) as compared to the co-processing of HDO (at 5:95 ratio). The finding is also reflected from higher value of BI in oil (at 5:95). This indicated that the product of HDO co-processing with VGO contain more iso-paraffinic CH_3 substructure and the product of FPO co-processing with VGO contains more paraffinic CH_3 substructure. Further, the fraction of substituted aromatics fa^s showed the fraction of aromatics substituted per molecule. In feeds the H/C_{eff} was found to varying from 1.47 to 1.725.

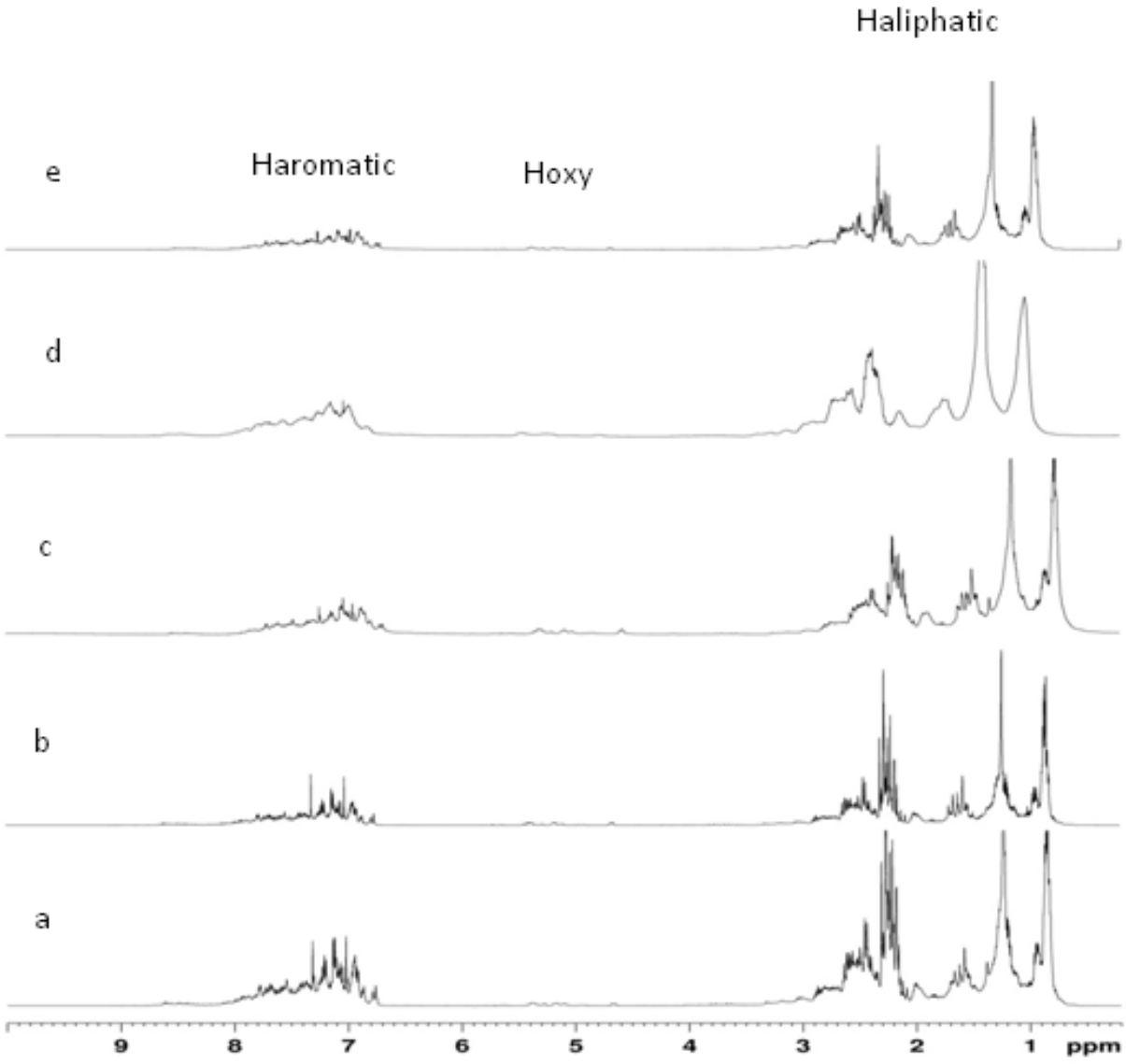

Figure 4.6: ^{1}H NMR of FCC liquid distillates on co-processing of FPO with VGO in a blending ratio of (a) 5:95; (b) 10:90; (c) 15:85; (d) 20:80 and (e) co-processing of HDO oil with VGO for a blending ratio of 5:95 at 530 °C and C/O of 5.

The aromatic protons varying from 15.5 to 21.69, with higher di-aromatic and poly aromatic protons in products of blending ratio with 5:95 and 10:90. This indicated that the product of HDO co-processing with VGO contain more paraffinic CH_3 substructure and the product of FPO co-processing with VGO contains more iso-paraffinic CH_3 substructure. Further, the normalized average percentage of protonated aromatic carbons varies from 37.2 to 44.2,

bridgehead aromatic carbons varies from 2.9 to 3.3, substituted aromatics varies from 6.3 to 7.8. The branchiness index showed the percentage of branching within the alkyl side chains. The more the BI, more is the branched side chains to aromatics. It can also be seen from the Table 4.7 that the side chains are more branched in the blending ratio of 20:80.

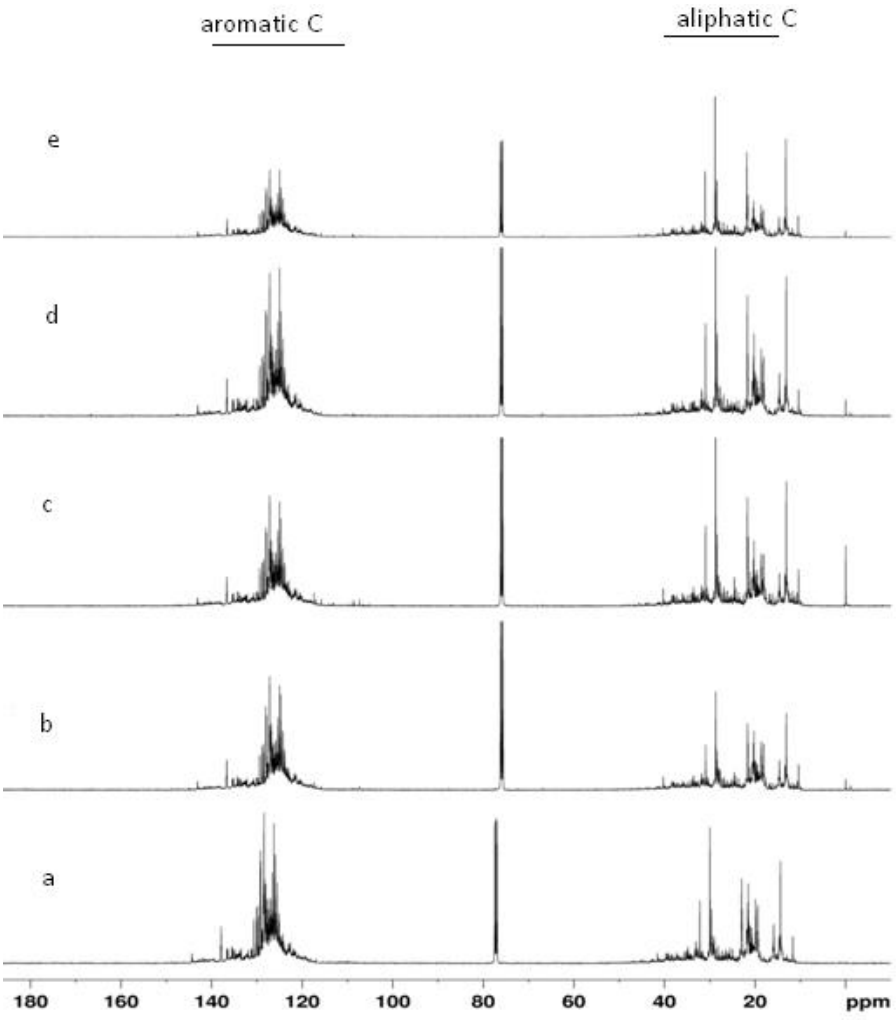

Figure 4.7: ^{13}C NMR of FCC liquid distillates on co-processing of FPO with VGO in a blending ratio of (a) 5:95; (b) 10:90; (c) 15:85; (d) 20:80 and (e) co-processing of HDO oil with VGO for a blending ratio of 5:95 at 530 °C and C/O of 5

4.6 JCC AND ITS FAST PYROLYSIS CHAR CHARACTERIZATION

4.6.1 Thermogravimetric Analysis

Figure 4.8 shows the TG-DTG of pure JCC in nitrogen atmosphere at a constant heating rate of 10 ^{o}C min^{-1}. A Thermogravimetric study revealed that three stages of weight loss are involved during JCC decomposition. The first, second and third stages occur in the temperature range of 110 to 200 ºC with a peak at 120 ºC, 200 to 400 ºC with a peak at 305 ºC; and 400 to 740ºC with a peak at 480 ºC, respectively. The first stage is representative of moisture, i.e. release of physically adsorbed water, the decomposition of holocellulose occur in the second stage and the third stage is corresponding to the decomposition of lignin [Gronli et al. 1999]. However, the decomposition of lignin starts much earlier to the major decomposition peak observed at 480 °C. The rate of weight loss is clearly related to the pyrolysis final temperature: higher the final temperature, greater the weight loss. This may be due to the fact that at high temperatures, the pyrolysis proceeds faster. It was observed that the 90% of holocellulose content present in the JCC is completely converted into bio-vapor and gases below 400 ºC, the remaining part is converted after 400 ºC temperature.

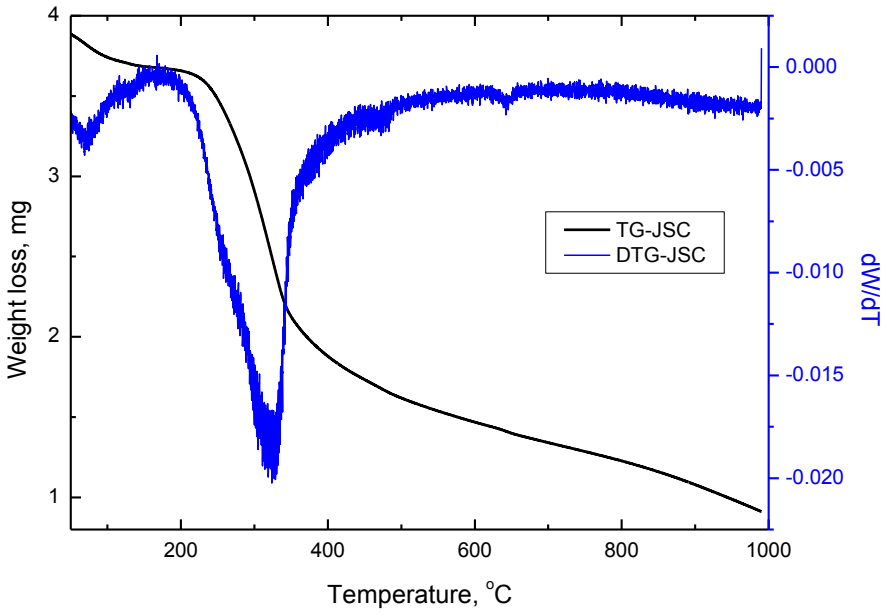

Figure 4.8: TG/DTG of JCC in N_2 environment at 10 ^{o}C min^{-1}

Figure 4.9 shows that the TG-DTG of char in nitrogen atmosphere at a constant heating rate of 10 ^{o}C min^{-1}. The additional 45% reduction in weight was found during the heating of char sample from ambient temperature to 1000 ^{o}C. Here, the first stage of weight loss occurs in the temperature range of 60-90 ºC with a peak (T_{max}) at 70 ºC, second stage of weight loss occurs in the temperature range of 630–690 ºC with a peak at 670 ºC; and the third stage range of weight loss from 750 to 990 ºC with a peak at 940 ºC. The first stage is representative of moisture i.e. release of physically adsorbed water and the second & third stages are corresponding to the decomposition of lignin in the form of CO_2 and CO [Guerrero et al. 2008]. The derivatives (CO_2 and CO) of lignin confirm the presence of oxygen functional groups in char. Typically of the various oxygen functional group decomposes in to a specific product; such as CO_2 from carboxyl and lactones groups and CO from carbonyl phenols, quinones and pyrones and ether-type oxygen [Arenillas et al. 2004, Figueiredo et al.1999, Tremblay et al. 1978]. The detailed functional groups analysis was carried out using FTIR spectroscopy and is discussed in the following sections.

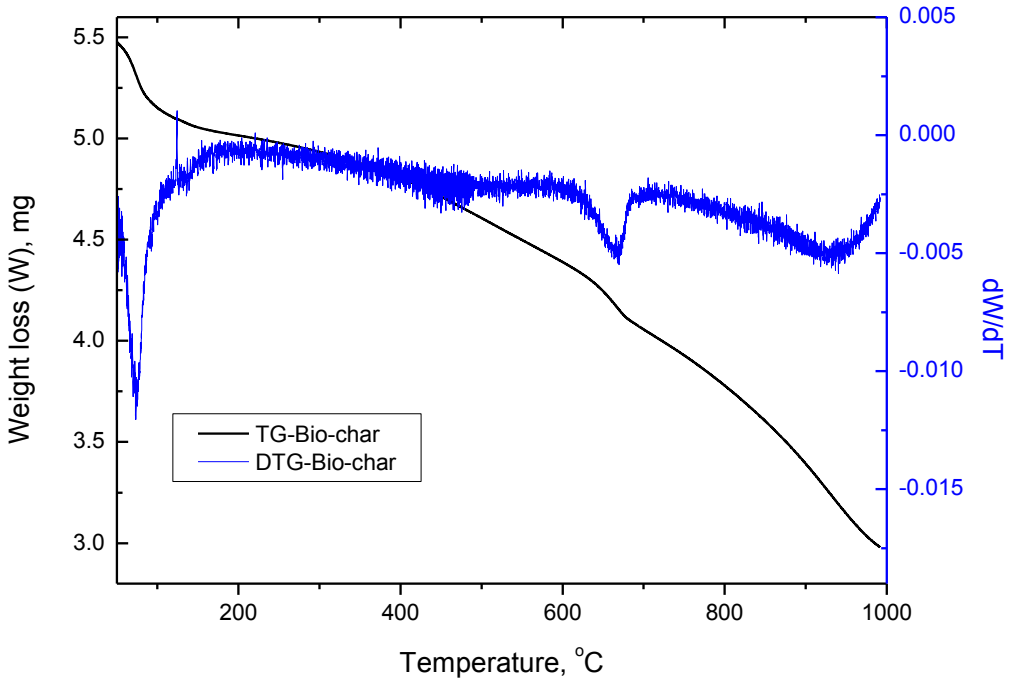

Figure 4.9: TG/DTG of JCC-derived fast pyrolysis char in N_2 environment at 10 ^{o}C min^{-1}

4.6.2 FTIR Analysis

The FTIR spectra of JCC and char are shown in Figure 4.10. For JCC, the band at 3420 cm^{-1} represent the stretching vibration of –OH hydroxyl groups of phenol. The methylene group was detected by –CH stretching at a wave number of 2929 cm^{-1}. The aldehyde group of –O–CH_3 was found around 2845 cm^{-1}. Band at 1647 cm^{-1} indicated C–O stretching of carboxyl or carbonyl groups [Efremova et al. 2008]. The bands at 1452, 1419, 1403 and 1378 cm^{-1} were assigned mainly to CH_2 units in biopolymers [Chen et al. 2005]. The peak at 1154 cm^{-1} is assigned to C-O stretching vibration of ester bonds. The band due to aliphatic C-O-C and alcohol -OH (1154-1030 cm^{-1}) represents oxygenated functional groups of cellulose [Bustin et al. 1999]. The peak at 1544 cm^{-1} represents the C=C ring stretching vibration of lignin. The band at 1272 cm^{-1} was assigned to the aromatic CO and phenolic -OH stretching [Chun et al. 2004]. Methyl or amine groups were shown by a peak around 1381 cm^{-1}.

The band from 1200 to 1000 cm^{-1} is the fingerprint of syringyl units. Aldehyde and derivatives of benzene were detected by peaks at 897 and 775 cm^{-1}[Efremova et al. 2008]. The FTIR spectrum of char showed an increasing drift in the baseline at high wave numbers, which is an indication of an increase in the carbonaceous component content of chars [Sharma et al., 2000]. All these bands experience different changes after the fast pyrolysis reaction, which can be clearly seen in fast pyrolysis char. The absorbance peaks in the range of 1740 and 1100 indicated the presence of hemicelluloses components, which became weak and broadened due to the structural collapse of the holocellulose. The band intensities were dramatically decreased at 3420 cm^{-1} (-OH) and 1154-1030 cm^{-1} (C-O). The intensity of the absorbance of -OH hydroxyl decreased due to the decrease in hydrogen bonded -OH stretching after fast pyrolysis of JCC. It may due to loss of phenolic or alcoholic groups since the oxygen/carbon (O/C) ratio of the bio-char also decreased.

The same was confirmed from the SEM-EDAX analysis. The broad band at 3340-3570 cm^{-1} and 3230-3310 cm^{-1} are generally assigned to hydrogen bonded OH groups in intramolecular and intermolecular cellulose, respectively. The symmetric CH_3 stretch of the O–CH_3 group in JCC and its intensity got decreased after fast pyrolysis. It indicated that the CH_3 groups have been removed from the substituted aromatic rings after fast pyrolysis. The loss of ether groups leads to a more ordered carbon structure. The presence of peaks at 1510, 1425 and

1270 cm^{-1} in the JCC clearly showed that the carbon frame work of lignin components are present in the cake and the same is absent in the JCC, due to the amorphous nature of lignin.

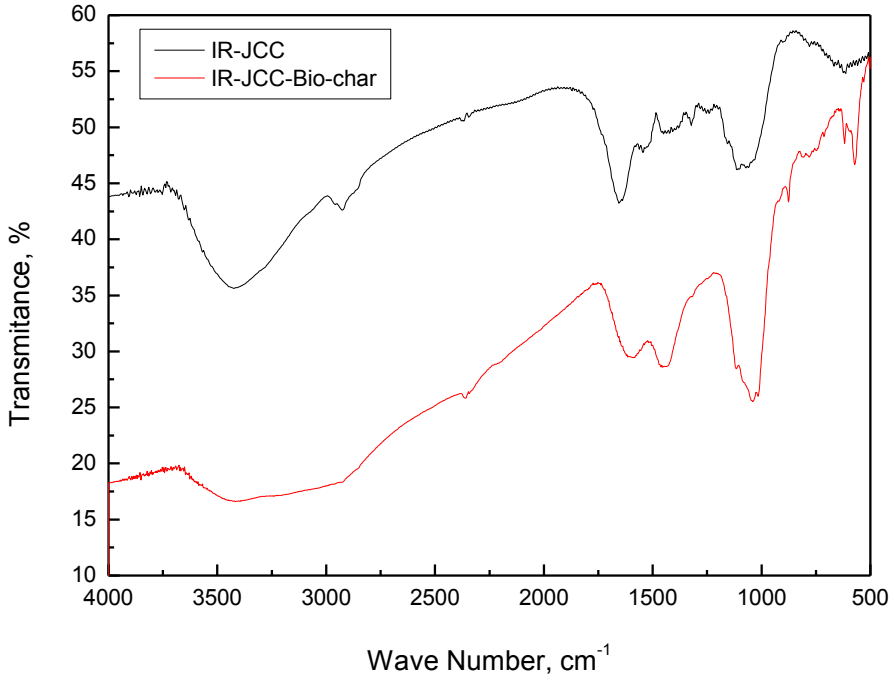

Figure 4.10: FT-IR of JCC and JCC-derived fast pyrolysis char

4.6.3 SEM Analysis

The morphology of JCC and JCC-derived fast pyrolysis char was investigated using SEM analysis and presented in Figure 4.11a, b and Figure 4.11c, d, respectively. It can be seen that surface of JCC char is smooth as well as cracked and pitted morphology and the presence of macro pores (varies from 1.82 to 4.28 µm) on the surface leads to develop an elementary pore network. The shape of the particles varies and many long fibrous particles were observed. The average diameter of macro pore size was greater than 50 nm according to IUPAC (International Union of Pure and Applied Chemistry).

The typical observations were: various sizes of round holes were found in the smooth areas which suggests a melt formation and volatile gas release during fast pyrolysis; precipitation of potassium, magnesium, phosphorous and sulfur was also observed along with the carbonaceous deposits; large number of vesicles presence was observed along the surface of fast pyrolysis char. Even though the well developed porous structure was seen in the various

resolutions of the cake images, the decomposition of biomass components was not uniform as the bigger particles break apart into several particles sequentially during the condensation and decomposition reaction of components. The elemental analysis or chemical characterization of fast pyrolysis char is shown in Table 4.8. It can be seen that the carbonaceous content of fast pyrolysis char is 88.03 wt % and the same was also confirmed by EDAX analysis, while that of JCC is 68.11 wt%. The amount of oxygen content in fast pyrolysis char is (11.07 wt%) less as compared to JCC (30.58 wt%).

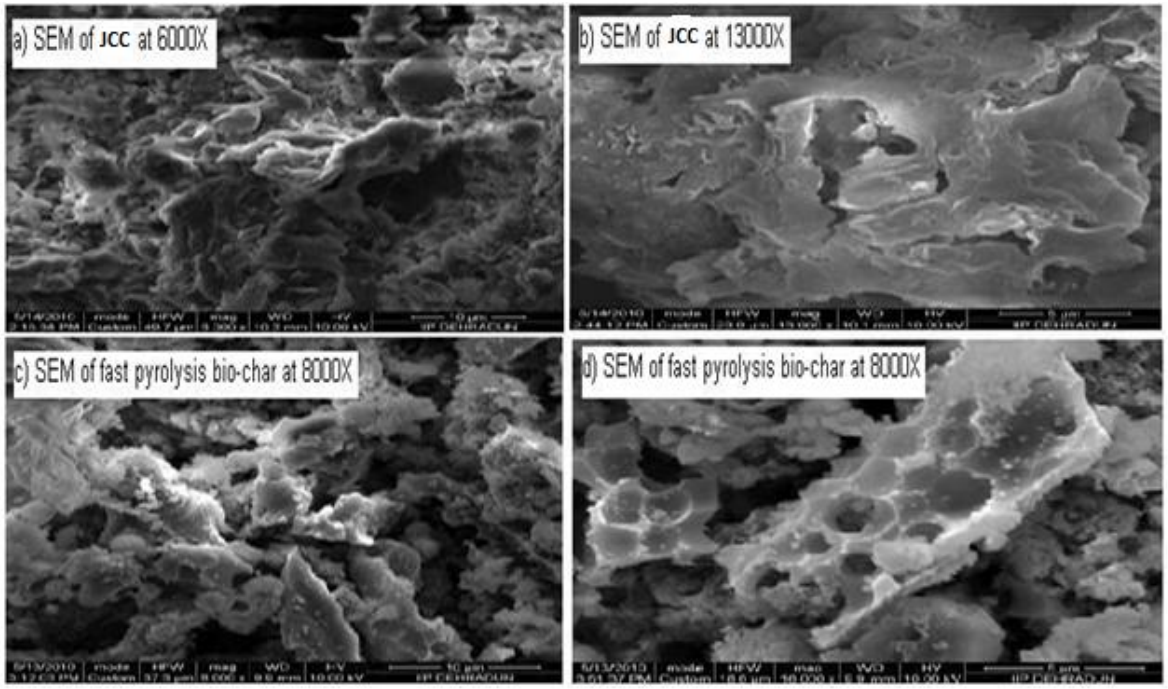

Figure 4.11: SEM of JCC (a & b) and JCC-derived fast pyrolysis char (c & d)

4.6.4 XRD Analysis

The image of JCC and fast pyrolysis char X-ray diffractograms (XRD) are displayed in Figure 4.12. The X-ray diffraction pattern of JCC have a wide halo in the 2θ range from 5 to 16°, which is characteristics of multi component carbon-containing materials [Fu et al. 2009]. The two bands were observed at 2θ ≈22.5 ° and 44 °, which correspond to the diffuse graphite (002) and (100) bands, respectively in bio-char. Further, it can be seen a broad peak centered at 2θ≈ 28 ° in the X-ray difractogram of bio-char, which showed the presence of silica. The peaks at 15, 17 and 22.7 ° are derived from cellulose one [Borosiac et al. 2005]. Furtehr, XRD of the alumina support confirms that the alumina is crystalline in nature and most of it has γ-alumina phase.

After 2 wt% Pd loading the intensity of the alumina peaks reduced. This is because Pd was highly dispersed on alumina and subsequently it reduces the crystallinity of alumina.

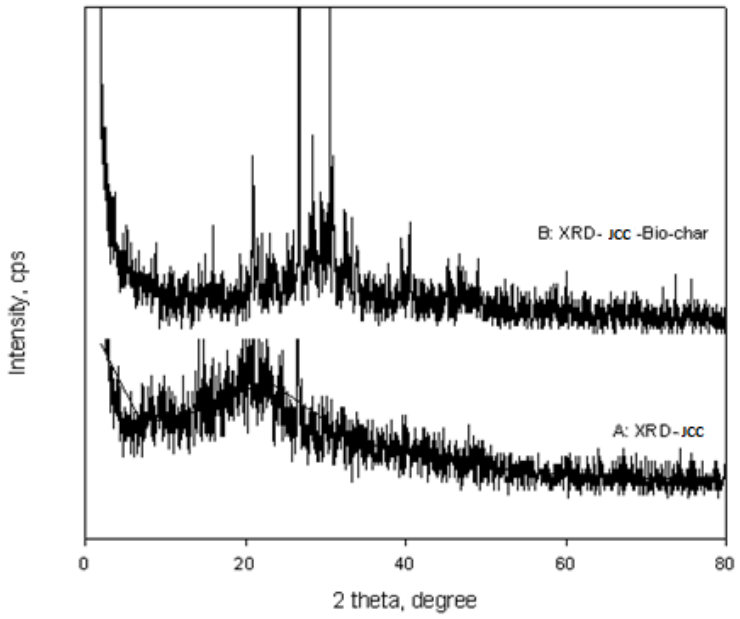

Figure 4.12: XRD of JCC and JCC-derived fast pyrolysis char

Table 4.8: Ultimate and structural composition analysis of JCC and JCC-derived fast pyrolysis char

Ultimate analysis, wt.% (Dry basis)			**Structural analysis, wt.% (Dry & Extractive)**	
	JCC	**FP Char**		
Carbon	45.50	88.20	Holocellulose	45.55
Hydrogen	6.70	04.10	Total lignin	16.16
Nitrogen	2.47	01.50	Ash	9.42
Oxygen (by difference)	45.33	06.20	Pentosan	7.70
Calorific value, MJ/kg	17.00	30.00	Moisture	7.20

4.6.5 CHNO Analysis

The ultimate and structural analysis of JCC feedstock is shown Table 4.8. From the Table 4.8 it can be seen that the carbon content of JCC-derived pyrolysis char is very high, 88 wt.%, as compared to the JCC biomass feedstock, which is 45 wt.% on dry basis.

The ash content of JCC is about 9% on weight basis from trace metal analysis and as a result some of the trace metals were also seen in the pyrolysis char and pyrolysis oil fractions. The trace metal analysis of JCC feedstock and JCC-derived pyrolysis products like fast pyrolysis char, pyrolysis oil including aqueous fraction and heavy fraction are shown in Table 4.9. It can be seen that the fast pyrolisys char have higher content of trace metals as compared to the liquid fractions.

4.6.6 Vacuum Gas Oil and E-CAT Analysis

The vacuum gas oil, a petroleum-derived oil fraction, was used for the present work of co-processing studies and its characteristics are given in Table 4.10. The boiling range of VGO is 350-550 ^{o}C. Table 4.10 also shows the trace metal contents in the VGO. The physicochemical characteristics of E–CAT are listed in Table 4.11. The surface area of the catalysts used was ~171 m^2 g^{-1}.

4.7 HDO CATALYST CHARACTERIZATION

4.7.1 HDO Catalyst Characterization

The typical nitrogen adsorption-desorption isotherm is shown in Figure 4.13. N_2 adsorption-desorption peaks shows type IV isotherms, and the presence of hysteresis loop confirms the mesoporosity of the alumina materials. The pore diameter of mesoporous alumina obtained was around 5 nm.

The SEM monograms of the mesoporous alumina (upper) and Pd supported mesoporous alumina (lower) are shown in the Figure 4.14a, b. From the monograms it can be seen that the morphology of the catalysts is similar before and after Pd loading. The typical XRD patterns of the mesoporous alumina (red colour) and Pd supported on mesoporous alumina (black) are shown in Figure 4.15. The peaks at the 2θ values of 12.2, 27.8, 36.9 and 49.4 correspond to the Pd (II) oxide species present in the Pd-supported mesoporous alumina catalyst.

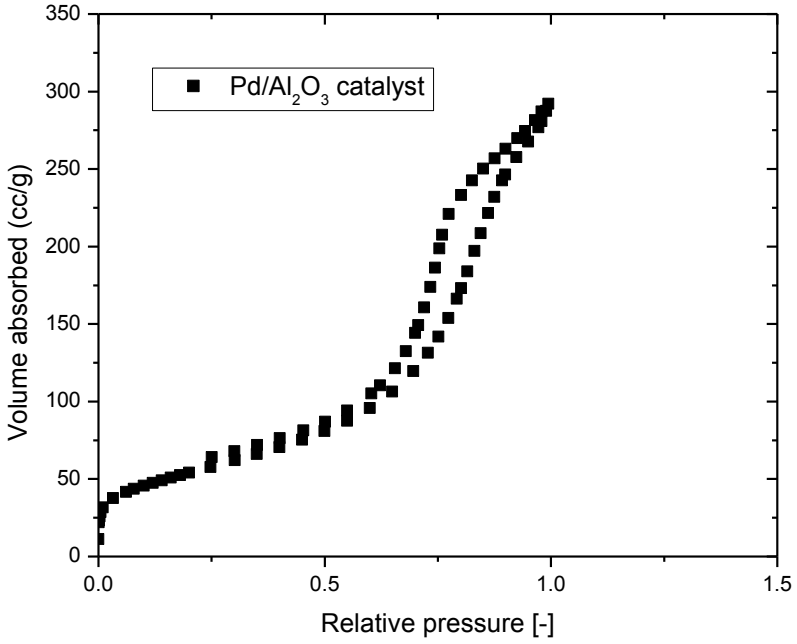

Figure 4.13: Nitrogen adsorption-desorption isotherm of Pd/Al_2O_3

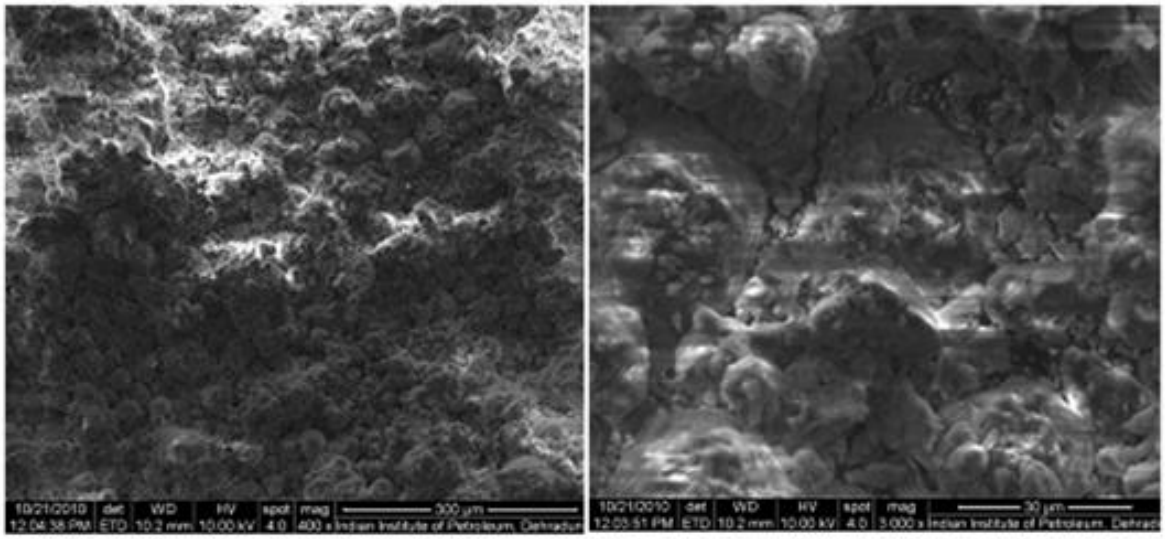

a b

Figure 4.14: The SEM monograms of (a) mesoporous alumina and (b) Pd supported mesoporous alumina

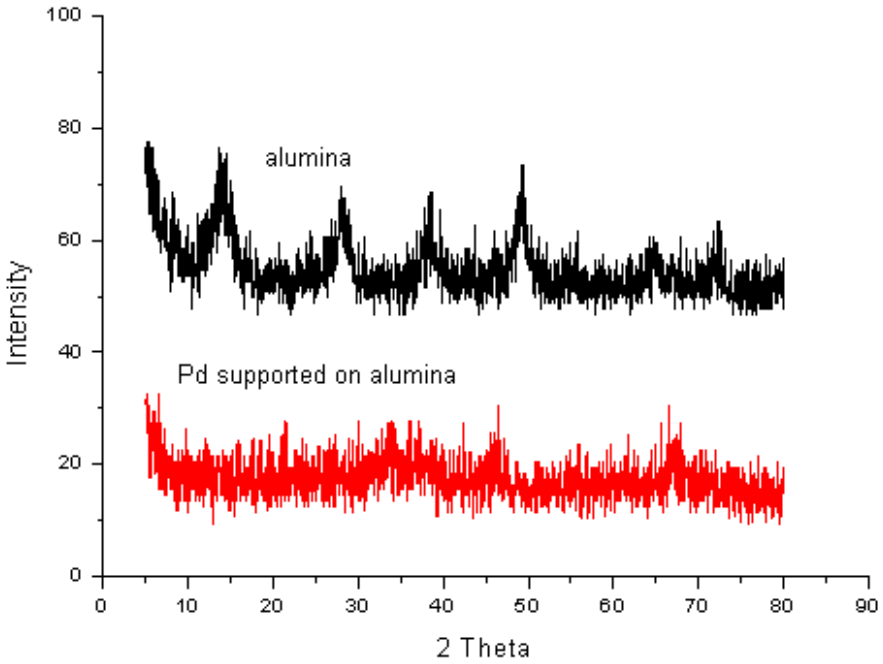

Figure 4.15: The XRD patterns of the mesoporous alumina (black colour) and Pd supported on mesoporous alumina (red colour)

Table 4.9: Trace metal analysis of JCC and its fast pyrolysis products

Elements (mg/l)/Sample	**JCC**	**FPO-Aqueous fraction**	**FPO-Heavy fraction**	**FP Char**
Co	2	6	1	1
Fe	111	343	62	1813
Ni	2	15	13	40
Cu	5	38	7	57
Zn	34	112	24	170
K	13517	62	46	85273
Ca	5852	1029	522	30279
Mg	5275	907	326	22196
Na	334	143	134	1940
P	7037	838	40	43362
Pb	21	7	1	8
Mn	33	11	4	172
Cr	5	9	5	69
Mo	10	9	7	38
Cd	4	3	4	5
V	7	7	8	13

Table 4.10: Characterization of vacuum gas oil

Properties	**Vacuum gas oil**
Density at15^{o}C, g cc^{-1}	0.919
Kinematic viscosity at 100 ^{o}C, cSt	10.83
API gravity	22.39
Basic N UOP269, ppm	540
Total N_2, wt.%	0.106
Total S, wt.%	0.19
CCR, wt.%	3.64
Asphaltene content, wt.%	2.01
Wax content, wt.%	19.2
IBP	350 ^{o}C
10%	369 ^{o}C
30%	400 ^{o}C
50%	441 ^{o}C
70%	489 ^{o}C
90%	550 ^{o}C
FBP	550 ^{o}C
Iron, ppm	134.7
Vanadium, ppm	1.1
Nickel, ppm	4.0
Copper, ppm	0.43
Zink, ppm	3.15

Table 4.11: Physico-chemical characteristics of E-CAT

Properties	**E-CAT**
SiO_2 (wt.%)	39.05
Al_2O_3 (wt.%)	20.8
Na_2O (wt.%)	0.3124
Ni (ppm)	762
V (ppm)	57
Fe (ppm)	4182
Cu (ppm)	459
Surface area (m^2/g)	171

CHAPTER 5

CATALYTIC CRACKING OF PYROLYSIS OIL MODEL COMPOUNDS

5.1 GENERAL

In the present work, the pyrolysis oil representative model compounds, such as acetic acid, guaiacol, hydroxyacetone and glycolaldehyde, were chosen for co-processing studies. In this chapter, a first attempt has been made to study the effect of catalyst-to-oil (C/O) ratio on co-processing of mixture of vacuum gas oil with guaiacol (aromatic oxygenate) and acetic acid (aliphatic oxygenate). Secondly, the effect of pyrolysis oil representative C2−C3 carbonyls (e.g., hydroxyacetone or acetol and glycolaldehyde) upon co-processing with VGO in an FCC advanced cracking evaluation unit by varying blending ratio from 5% to 20% was studied. The liquid product (FCC distillate) was characterized by spectroscopic techniques like NMR and FTIR. The average structural parameters like branchiness index, substitution index, average length of alkyl chains, and fraction of aromaticity per molecule were reported using the NMR characterization. Further, results were compared with pure VGO catalytic cracking by varying C/O ratios. The co-processing studies have been carried out based on the optimized process parameters for maximizing gasoline yield on catalytic cracking of pure VGO. Further the catalytic cracking of pure glycerol and co-processing glycerol with VGO has been discussed.

5.2 CATALYTIC CRACKING OF VGO WITH ACETIC ACID AND GUAIACOL

5.2.1 Product Profile

The degree of conversion is an important parameter controlling the product quality determined by the contact time, directly related to the catalyst-to-oil ratio (C/O) in refinery fluid catalytic cracking process. Figure 5.1a shows the conversion for the Feeds (A: vacuum gas oil; B: VGO+ acetic acid; C: VGO+ guaiacol) as a function of catalyst-to-oil ratio. The typical values of *x*, *y* and *z* in Scheme 5.1 for Feeds A, B and C, respectively, are mentioned in terms of effective hydrogen index (H/C_{eff}), based on both elemental analysis and NMR analysis, as shown

in Table 5.1. It was found that the effective hydrogen index of all three feedstocks is above inflection point (i.e. $H/C_{eff} = 1.2$), which can be processed for energy production in fluid catalytic cracking unit as per Chen et al. (1986). The Scheme 5.1 is as follows:

$$C_xH_yO_z \longrightarrow a\,C_{x-b-d-e}\,H_{y-2c}\,O_{z-2b-c-d} + b\,CO_2 + c\,H_2O + d\,CO + e\,C$$

Scheme 1

It can be seen from Figure 5.1a that the conversion increases with increase in C/O ratio for all three feeds. Figure 5.1a also shows that the higher conversion is obtained on processing Feed C in comparison with Feeds A and B at all C/O ratios. The possibilities of resulting higher conversion for the case of Feed C are either unconverted guaiacol or converted guaiacol into phenol or methanol are supposed to fall in the boiling range of gasoline (which is accounted in conversion). Similarly, the yield of dry gas and LPG (Figure 5.1b-c) is lower for Feed C and higher for Feed A. From Figure 5.1e-f it can be seen that there is no further increase in LCO or HCO conversion with the addition of acetic acid or guaiacol. Figure 5.1g shows coke formation is higher in case of guaiacol followed by acetic acid addition and lower for pure VGO catalytic cracking at all C/O ratios which is also in good agreement with the work of Graca et al. (2009c, 2011a).

The amount of coke deposition on catalyst is related with time on-stream, which is also related to C/O ratio. The C/O ratio was varied by varying time on-stream (*t*) at feed rate (1.2 g/min), hence constant weight hourly space velocity (WHSV). In other way C/O ratio can be defined as per the following equation: C/O =3600/ (WHSV × t). The increase of C/O ratio means increasing the amount of catalyst in the fixed fluidized bed reactor. Hence, the number of active sites of catalyst for the catalytic cracking secondary reactions also increases and it results into increase in the conversion of vacuum gas oil as well as coke formation. It was observed that the conversion increased in all three cases of feedstocks with an increase in C/O ratio. Similarly, the coke deposition also increased with an increase in C/O ratio or a decrease in time on-stream. As proposed in Scheme 5.2 of guaiacol transformation with gas oil over E-CAT the presence of phenol is observed in the liquid distillate of NMR spectra and thereby the yield of liquid naphtha increased by 3–4%.

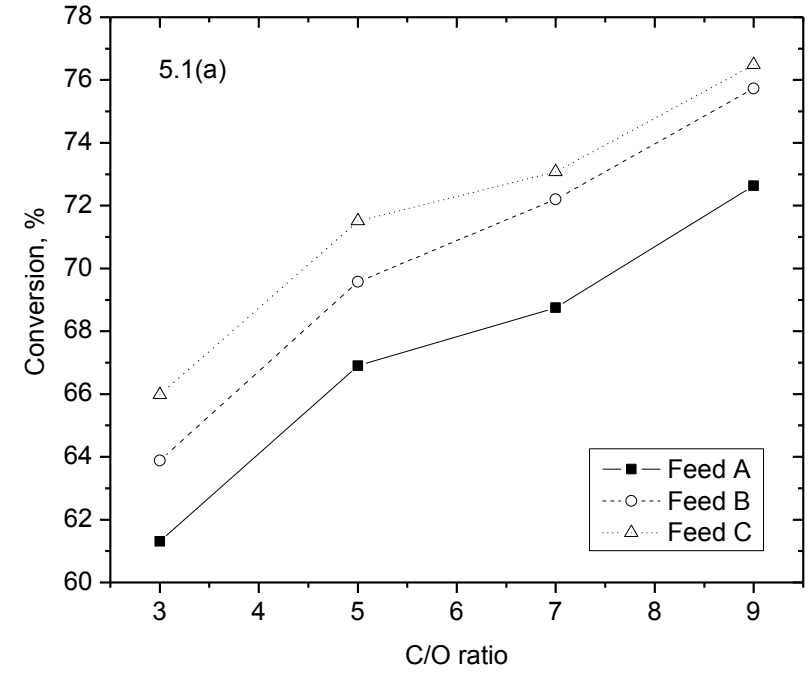

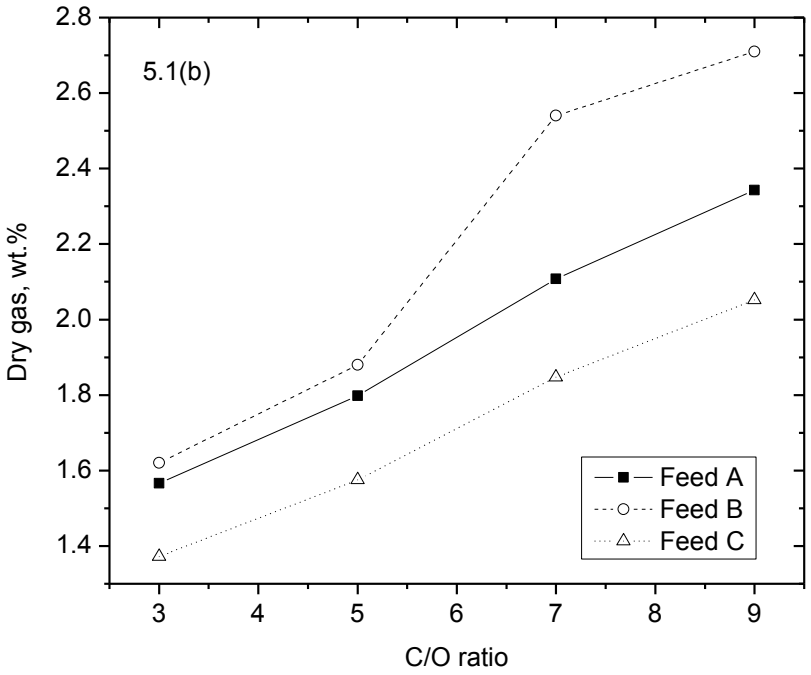

Figure 5.1a-b: Effect of C/O ratio on (a) conversion, (b) dry gas on catalytic cracking of Feed A (VGO), B (VGO+Acetic acid) and C (VGO+Guaiacol) at 530 °C and C/O ratio of 5

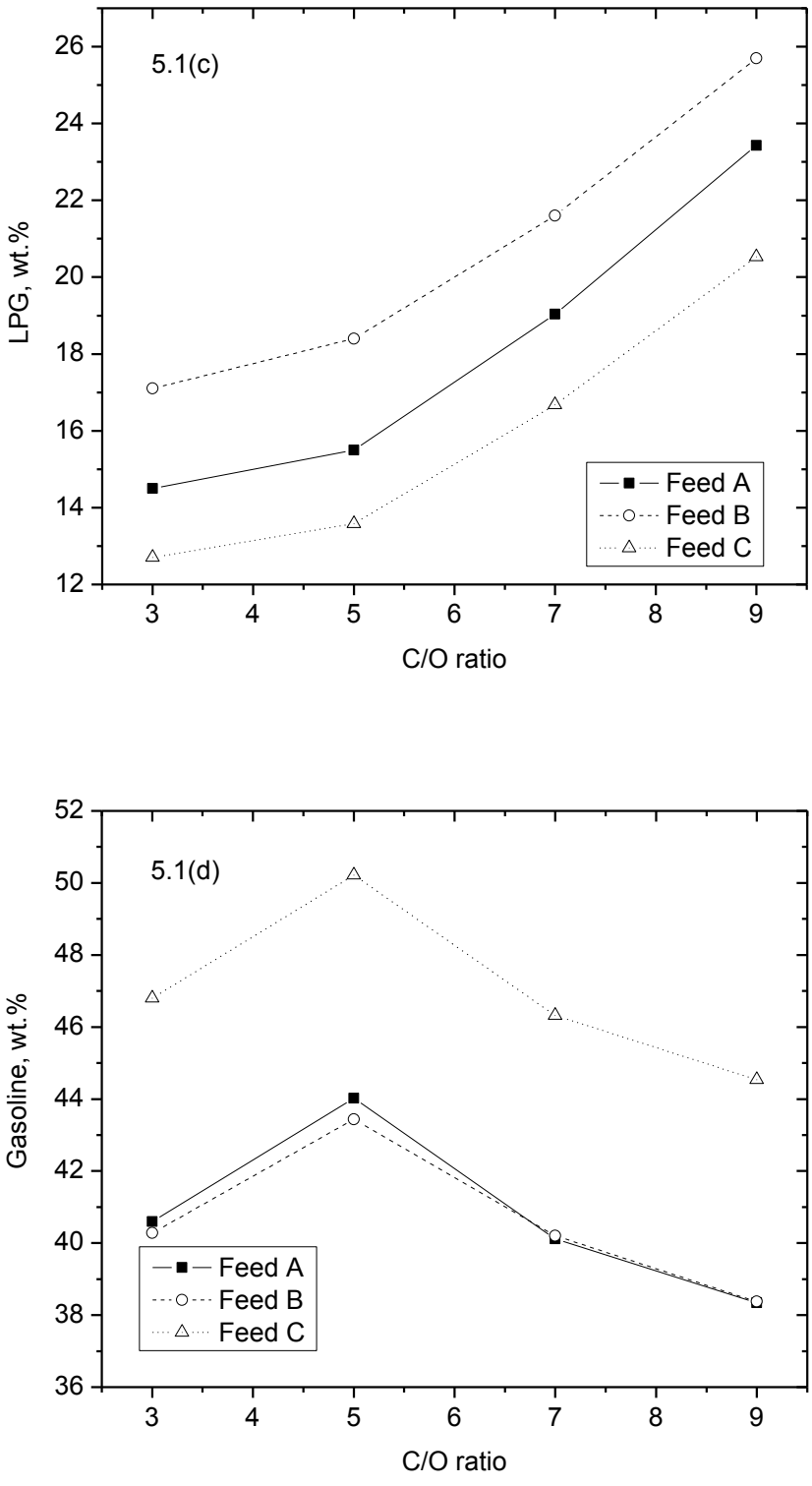

Figure 5.1c-d: Effect of C/O ratio on (c) LPG, (d) Gasoline on catalytic cracking of Feed A (VGO), B (VGO+Acetic acid) and C (VGO+Guaiacol) at 530 °C and C/O ratio of 5

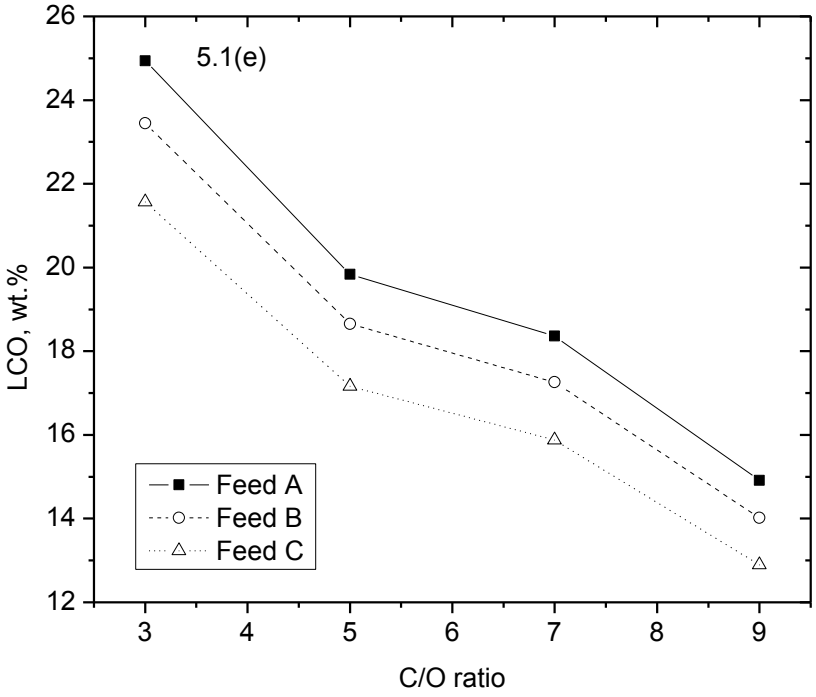

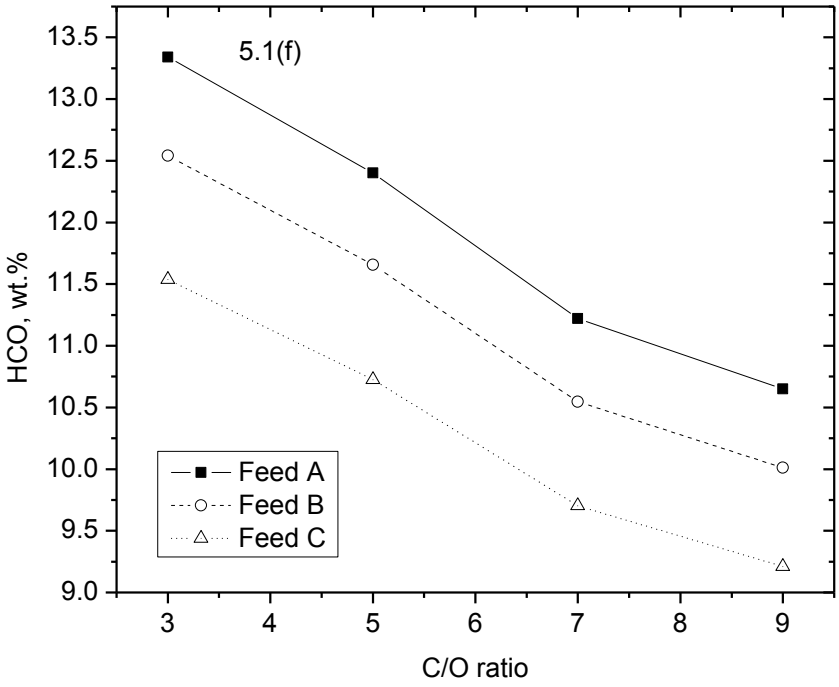

Figure 5.1e-f: Effect of C/O ratio on (e) LCO, (f) HCO on catalytic cracking of Feed A (VGO), B (VGO+Acetic acid) and C (VGO+Guaiacol) at 530 °C and C/O ratio of 5

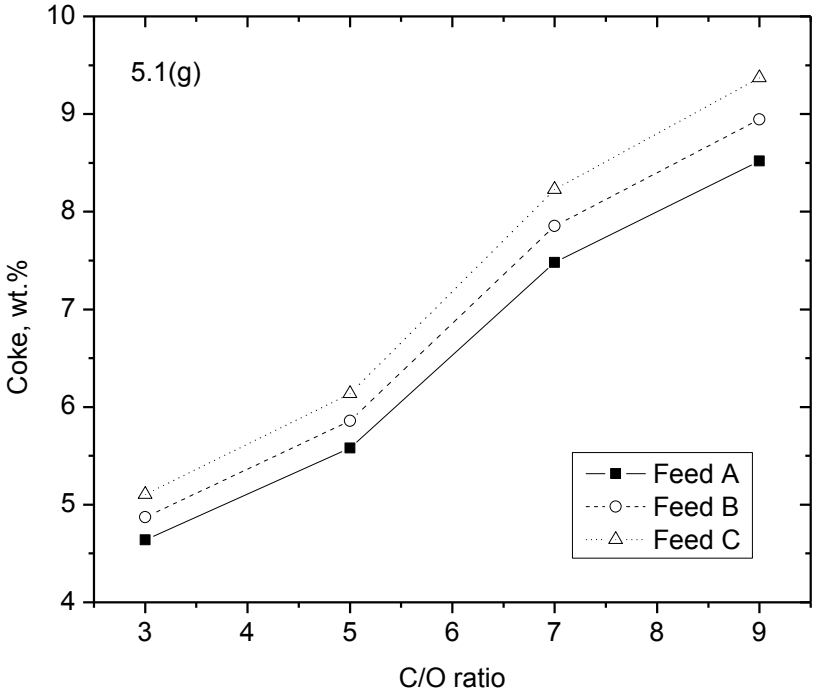

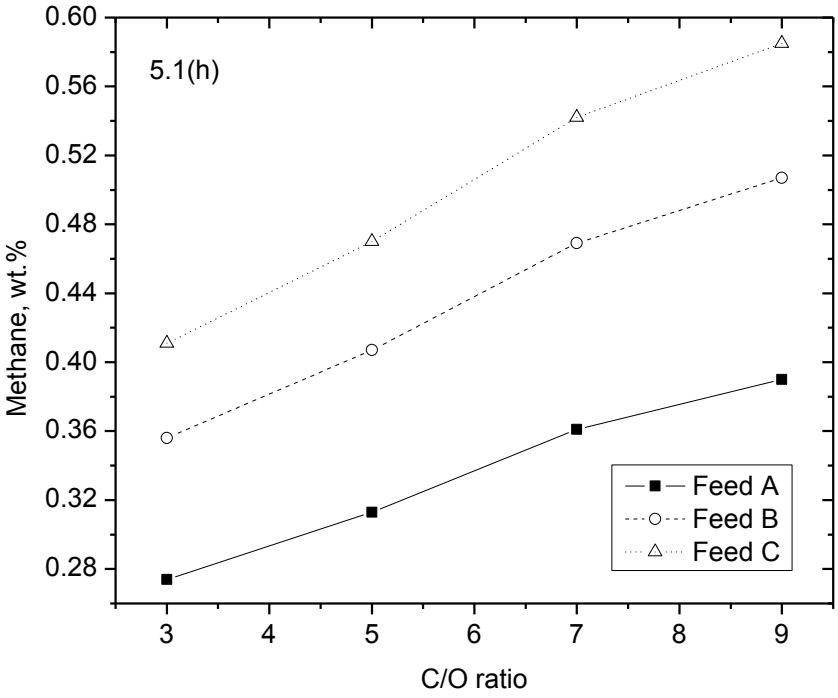

Figure 5.1g-h: Effect of C/O ratio on (g) Coke, (h) Methane on catalytic cracking of Feed A (VGO), B (VGO+Acetic acid) and C (VGO+Guaiacol) at 530 °C and C/O ratio of 5

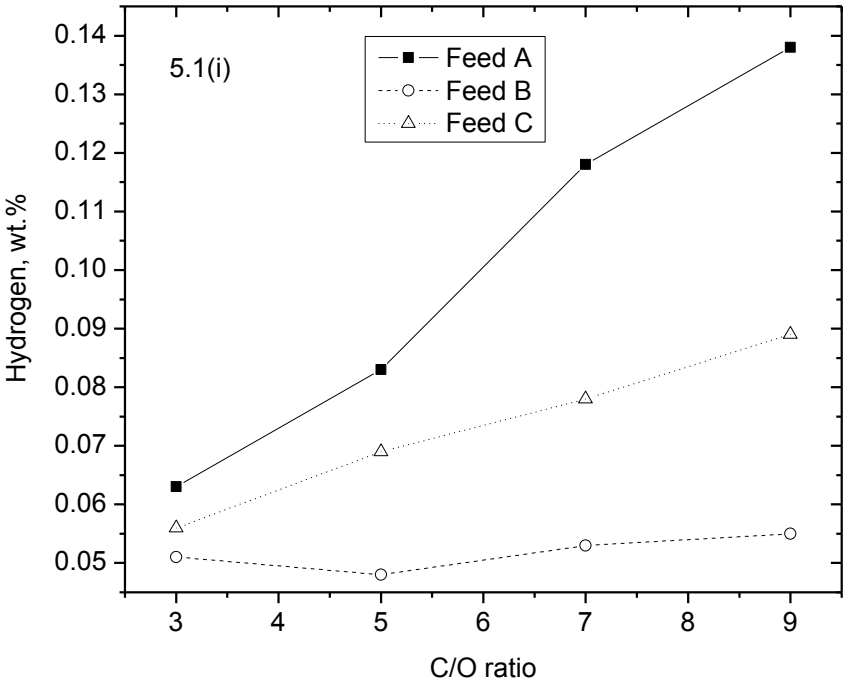

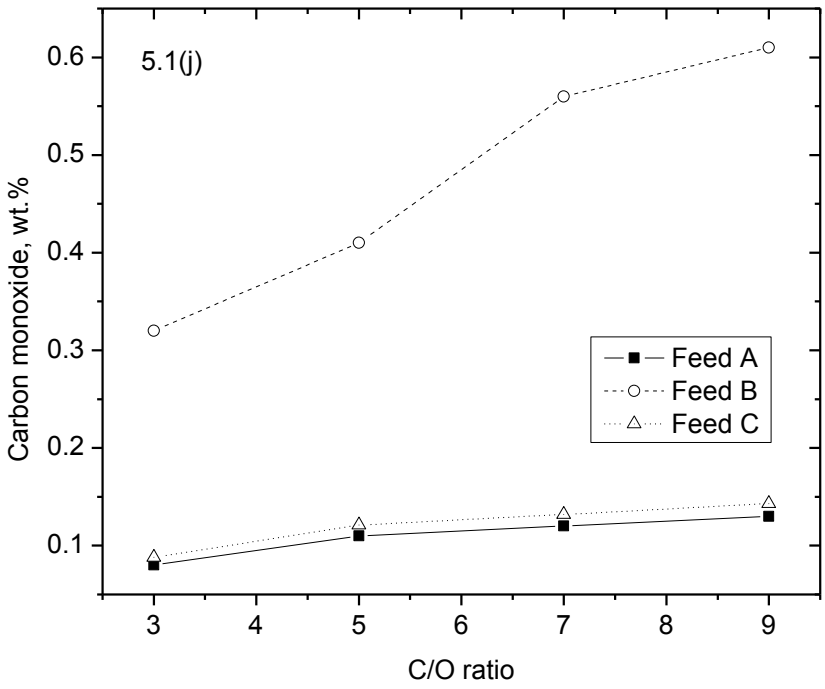

Figure 5.1i-j: Effect of C/O ratio on (i) Hydrogen, (j) CO_2 on catalytic cracking of Feed A (VGO), B (VGO+Acetic acid) and C (VGO+Guaiacol) at 530 °C and C/O ratio of 5

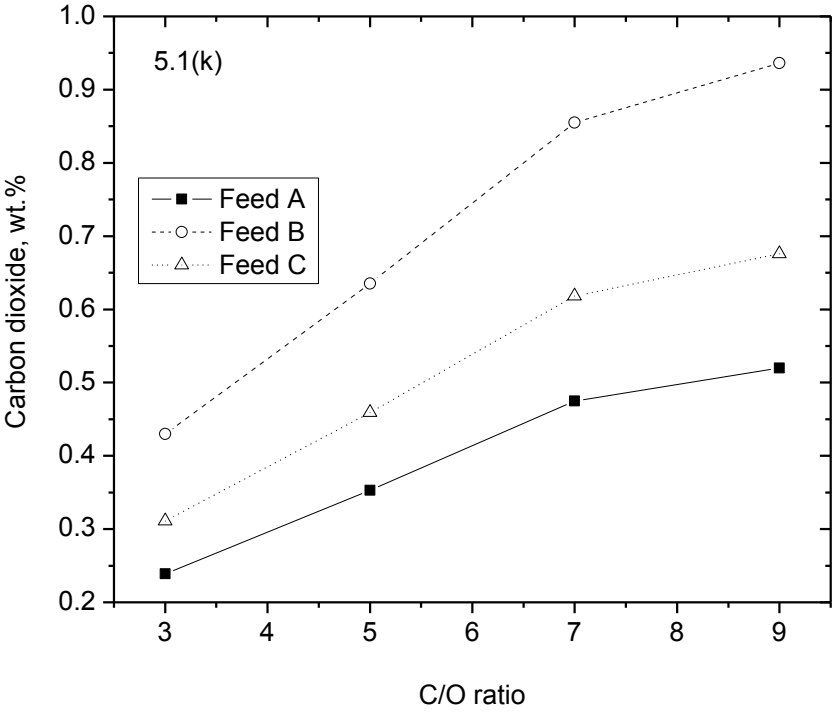

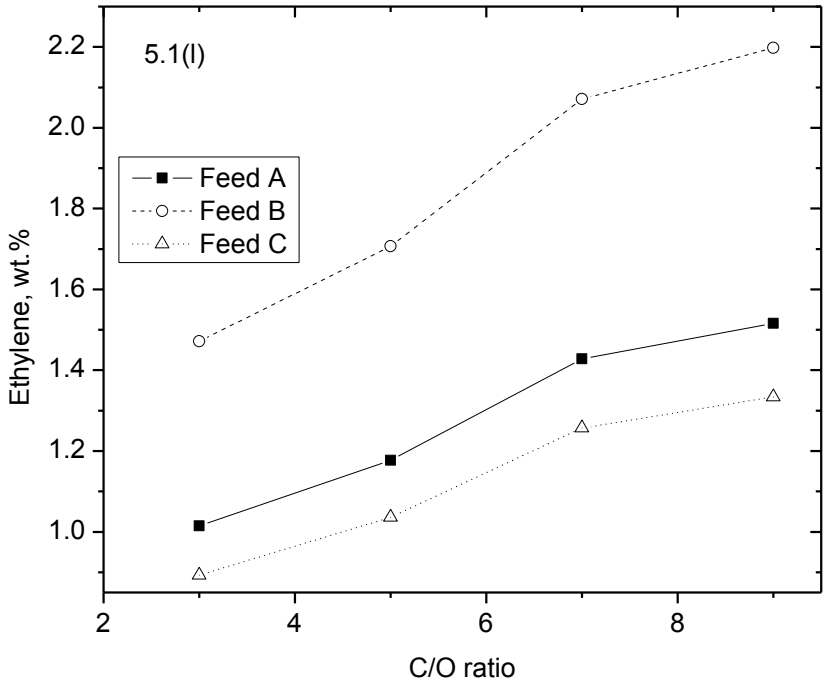

Figure 5.1k-l: Effect of C/O ratio on (k) CO, (l) Ethylene on catalytic cracking of Feed A (VGO), B (VGO+Acetic acid) and C (VGO+Guaiacol) at 530 °C and C/O ratio of 5

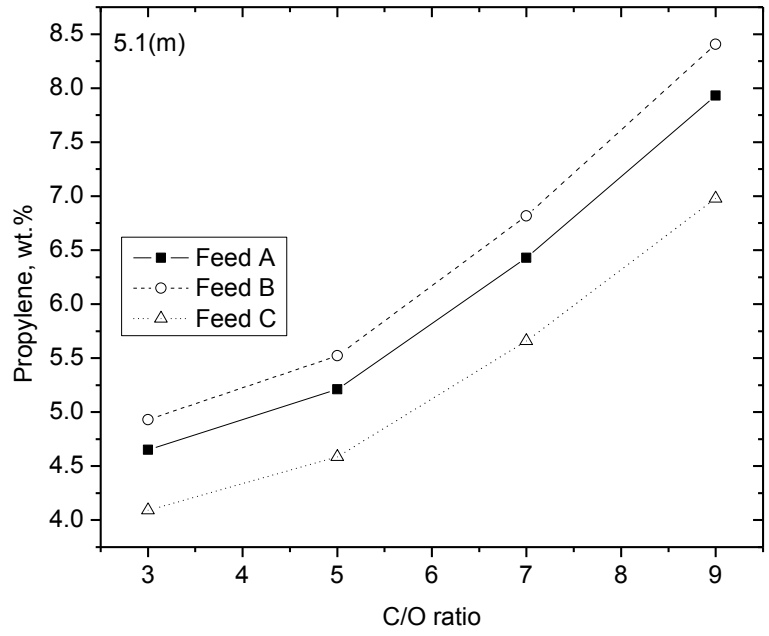

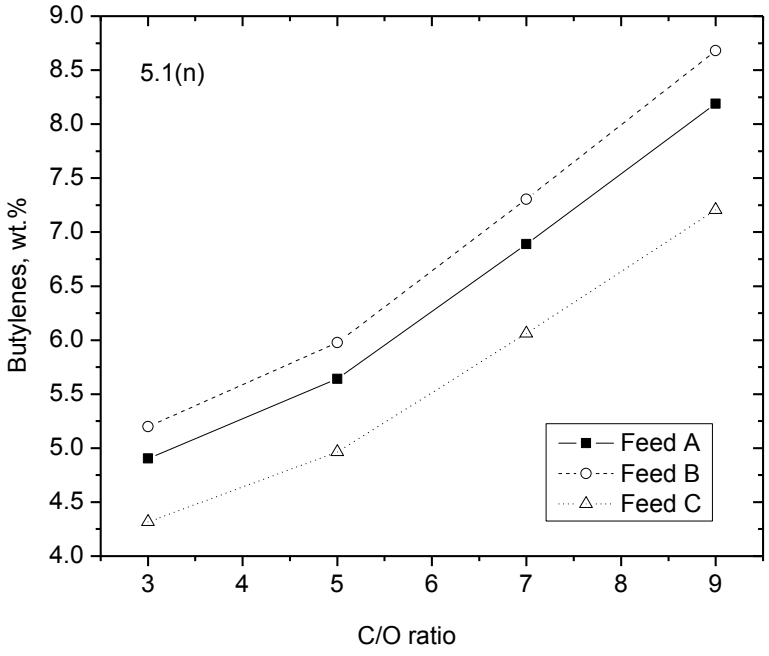

Figure 5.1m-n: Effect of C/O ratio on (m) Propylene, (n) Butylene on catalytic cracking of Feed A (VGO), B (VGO+Acetic acid) and C (VGO+Guaiacol) at 530 °C and C/O ratio of 5

Table 5.1: NMR derived average structural parameters of feed and distillates on co-processing of acetic acid and guaiacol with VGO at 530 °C and C/O ratio of 5

C/O	n	fa	Ch	Cb	ARq	Cp	BI	SI	H/C_{eff}	$H/C_{eff\text{-}nmr}$
Feed A (VGO)	18	0.13	4.90	1.36	5.70	--	0.35	0.47	1.725	1.45
3	8	0.45	32.3	3.80	9.26	--	--	--	--	--
5	6	0.48	37.27	3.19	7.32	--	--	--	--	--
7	5	0.50	40.02	3.24	7.07	--	--	--	--	--
9	5	0.52	41.40	3.30	7.21	--	--	--	--	--
Feed B (VGO+ Acetic acid)	19	0.11	4.00	1.00	2.32	--	0.38	0.55	1.70	1.40
3	7	0.44	38.7	1.99	3.53	--	--	--	--	--
5	8	0.51	39.97	3.23	7.37	--	--	--	--	--
7	8	0.52	43.07	3.45	5.36	--	--	--	--	--
9	5	0.56	47.07	3.32	4.75	--	--	--	--	--
Feed C (VGO+ Guaiacol)	19	0.23	18.1	1.20	4.23	0.00	0.32	0.33	1.65	1.33
3	5	0.49	41.00	3.00	5.81	0.12	--	--	--	--
5	4	0.55	44.34	3.22	4.20	3.13	--	--	--	--
7	6	0.57	42.70	4.18	5.75	4.50	--	--	--	--
9	6	0.62	50.50	3.59	6.40	n.d	--	--	--	--

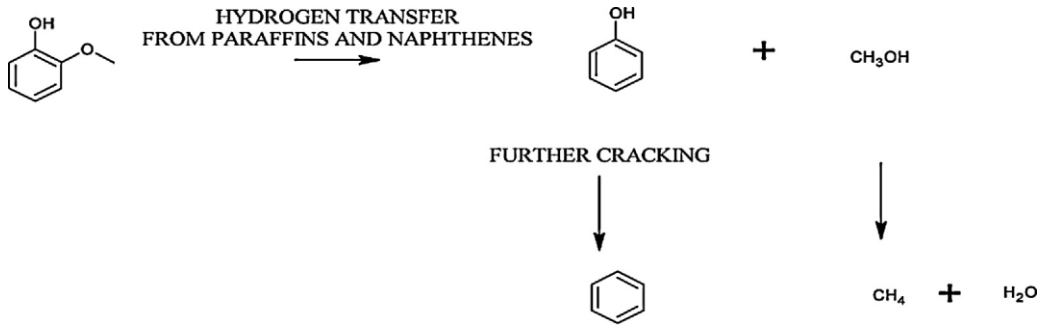

Scheme 5.2: Probable mechanism for cracking of guaiacol with VGO

The aromaticity for the case of Feed C is higher as compared to other Feed A and B, which indicated that the severe aromatization taking place on adding oxygenates, subsequently it helps to further increase coke formation. Further, it was observed that the coke formation process was inhibited to some extent due to water formation while catalytic cracking, which is also in agreement with the results of Yingxian et al. (2008), i.e. steam dilution in 2-methyl pentane catalytic cracking on USHY zeolite. Their analysis indicated that steam dilution reduces the coke formation by increasing the rate of desorption of coke precursors like di-ions and cyclic-ions and inhibiting them to undergo further reactions like dehydrogenation and cyclization to produce aromatics.

From Figure 5.1i it can be seen that the yield of hydrogen is higher in the case of Feed A followed by Feed B and Feed C. It seems that the hydrogen obtained from dehydrogenation of hydrocarbons present in vacuum gas oil is being consumed for the bimolecular hydrogen transfer reaction. In hydrogen transfer reactions one of the reactant is olefin, which further reacts with olefin or naphthenes and converts to paraffins and aromatics (Venuto et al., 1966; Weekman, 1969).

Further hydrogen transfer from aromatics, coupled with condensation and polymerization reactions, can lead to the formation of coke (Magee and Mitchell, 1993). As a result lower olefins (Figure 5.1l–n) and higher aromatics and coke are seen in the case of Feed C. From Figure 5.1i–k it can be seen that the yield of CO and CO_2 is higher in the case of Feed B as compared to other feeds which indicated that the catalytic cracking also favors decarbonylation as well as decarboxylation of acetic acid. Water formation was also observed during the co–processing of both Feed B and Feed C in ppm level. To check the stability of the catalyst the

experiments, on fluid catalytic cracking ACE-R unit, were carried in a sequence of reactions, i.e. catalytic cracking followed by stripping (with nitrogen gas) and regeneration (with air).

The regenerated catalyst was used for three times in a series to carry out the same set of experiments with Feed C at C/O ratio of 5. It was found that the similar yields of FCC products were observed within the range of ±2% error. From the analysis of product slate it can be said that the catalyst was stable even for three series runs at the above mentioned operating conditions.

In the present work, to consider the repeatability of the experiments, each experiment was carried out three times and the average value was considered for final analysis. The precision was maintained within ±2%. The reproducibility of experiments was checked for Feed C (guaiacol+ VGO) three times at C/O ratio 5, which is shown in Table 5.2. From Table 5.2 it can be seen that the results are within the range of 0.5 to 2%.

Table 5.2: Reproducibility of Feed C (VGO+Guaiacol) product profile with regenerated catalyst at 530 °C and C/O=5

Feedstock	C/O	Dry gas, wt.%	LPG, wt.%	Gasoline, wt.%	LCO, wt.%	HCO, wt.%	Coke, wt.%	Conversion, wt.%
Feed C	5.00	1.575	13.578	50.220	17.16	10.72	6.14	71.511
(VGO+Guaiacol)	5.00	1.580	13.120	49.560	17.12	10.86	6.12	70.380
	5.00	1.526	13.190	50.920	17.58	10.34	6.21	71.846

5.2.2 NMR Characterization

In order to obtain the detailed structural profile of the mixtures of petroleum fractions, several spectroscopic and analytical techniques have been used [Lee and Glavincevski et al. 1999; Clutter et al. 1972; Yang et al. 2003; Satou et al. 1991; Guillen et al. 1998; Cantor et al. 1978; Williams et al. 1958; Brown and Ladner et al. 1960; Behera et al. 2007, 2008]. Particularly, the structural skeleton of several petroleum fractions have been determined using ^{1}H (proton) and ^{13}C (carbon) nuclear magnetic resonance (NMR) techniques [Lee and Glavincevski et al. 1999; Clutter et al. 1972; Yang et al. 2003; Satou et al. 1991; Guillen et al. 1998; Cantor et al. 1978; Williams et al. 1958; Brown and Ladner et al. 1960; Behera et al. 2008]. However, neither the NMR spectra nor other spectroscopic techniques are able to provide enough information to completely describe the individual components of a hydrocarbon mixture.

Although there are much more precise and accurate techniques are available to describe complex mixtures of hydrocarbons. However the new techniques are more complicated and difficult to apply. The complexities in the new techniques and the necessity to characterize the hydrocarbon fractions, Behera et al. (2008) proposed a new concept of "average structure". In the proposed concept the average structures are developed based on the combined information from NMR, elemental analysis, and molecular weight. In this approach a soluble fraction is characterized in a particular solvent using average structural parameters, which later can be used to delineate the possible average chemical structures. Williams et al. (1958) and Brown and Ladner (1960) were the first who reported the structural distribution of hydrocarbon fractions by ^{1}H NMR. They reported a set of structural parameters of heavy oil fractions, such as aromaticity, degree of substitution, branchiness index, and aromatic condensation index. Clutter et al. (1972) further improved the "average structure" approach by introducing ^{13}C NMR analysis in the analysis of their results.

The NMR spectra of Feeds A–C and their distillates at various C/O ratios are shown in Figure 5.2 to 5.4. The spectra of feeds were quite different from their respective distillates both qualitatively and quantitatively. The chemical shift region of ^{1}H spectrum was broadly divided into three regions [Behera et al. 2007; Yingxian et al. 2008] aromatic hydrogens (9–6 ppm), aliphatic hydrogens (0–4.5 ppm) and olefinic hydrogens (4.5–6 ppm). The aliphatic proton region was further subdivided into H_{α} (2–4.5 ppm), H_{β} (1–2 ppm), H_{γ} (0.5–1 ppm). The ^{13}C NMR spectrum has been divided into different integration domains as aliphatic carbons (0–50 ppm), aromatic carbons (110–150 ppm) and oxygenated as alcoholic carbons (50–110 ppm) and carboxylic (150–200) carbons. The NMR spectra of Feed B (Figure 5.3a) show the presence of acetic acid peak corresponding to 2.0 ppm in ^{1}H and 20.7 and 175.4 ppm for CH_3 and COOH in ^{13}C spectra, respectively.

In the Feed-B derived liquid distillates the peak at the same chemical shift was found to be absent that indicated the active participation of acetic acid during catalytic cracking. Similarly, ^{13}C NMR spectrum of Feed C (Figure 5.4a) shows the peaks at 55.86, 11.92, 115.2, 120.2, 121.43, and 146.86 for methoxy and aromatic carbons due to the presence of guaiacol. In all the Feed C-derived distillates, the signal due to guiacol was found to be absent. The average structural parameters of FCC Feed A, the hybrid FCC Feeds B and C and the product liquid distillates are derived from NMR data, and are shown in Table 5.1.

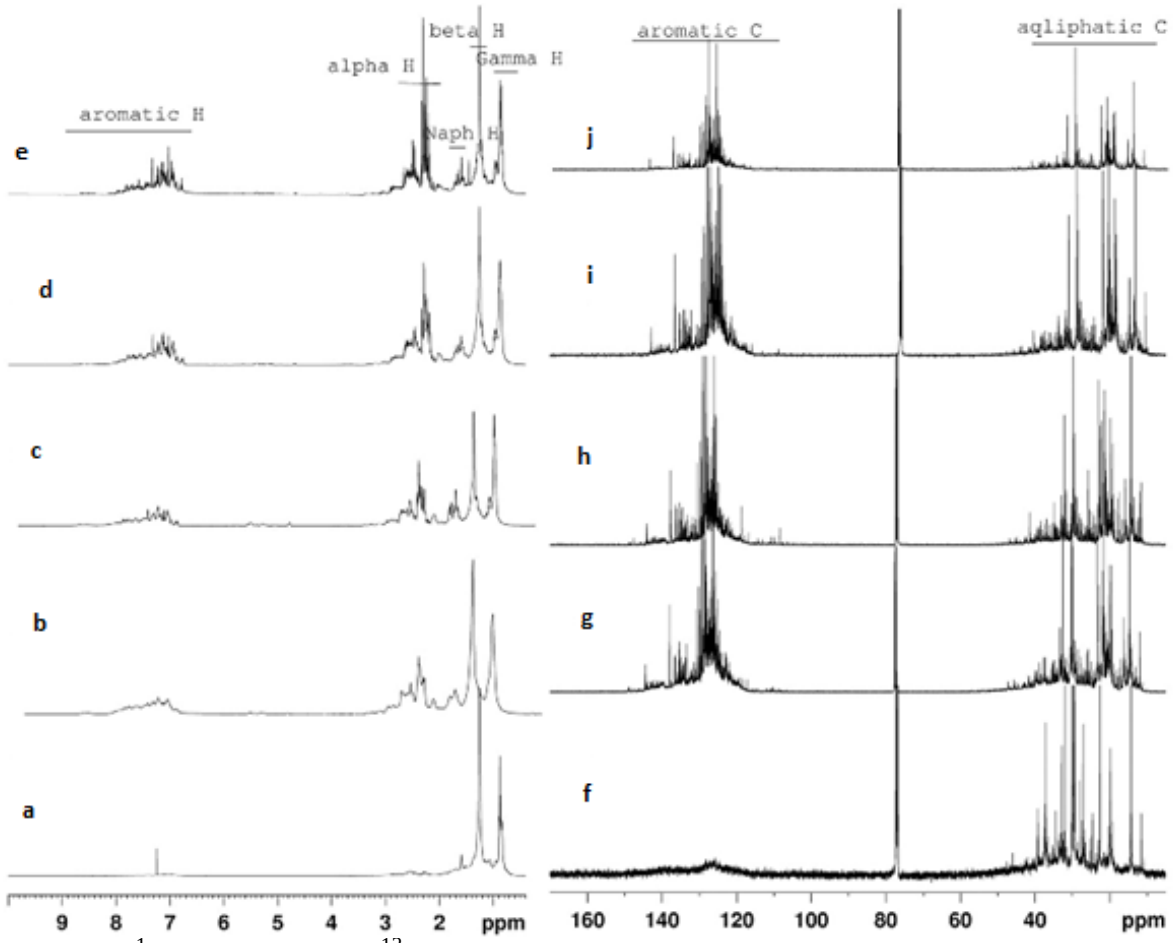

Figure 5.2: ^{1}H NMR (a-e) and ^{13}C NMR (f-j) spectra of Feed A (VGO) and their distillates on catalytic cracking at 530 °C and C/O=5

The results were averaged over the feed and their distillates, to represent a simplified picture of complex hydrocarbon mixtures containing a wide range of components. However, the abovementioned approach has the advantage that only few NMR experiments give maximum idea about the average nature of the crude material and distillates without any treatment. The normalized relative distribution shows the Feed A contains 13.4 and 86.6% of aliphatic and aromatic carbons. The distillates showed higher aromaticity, which indicated the cracking of feedstock. Again aromaticity increases with higher C/O ratio implying more active site participation of catalysts and increase in aromaticity of distillates.

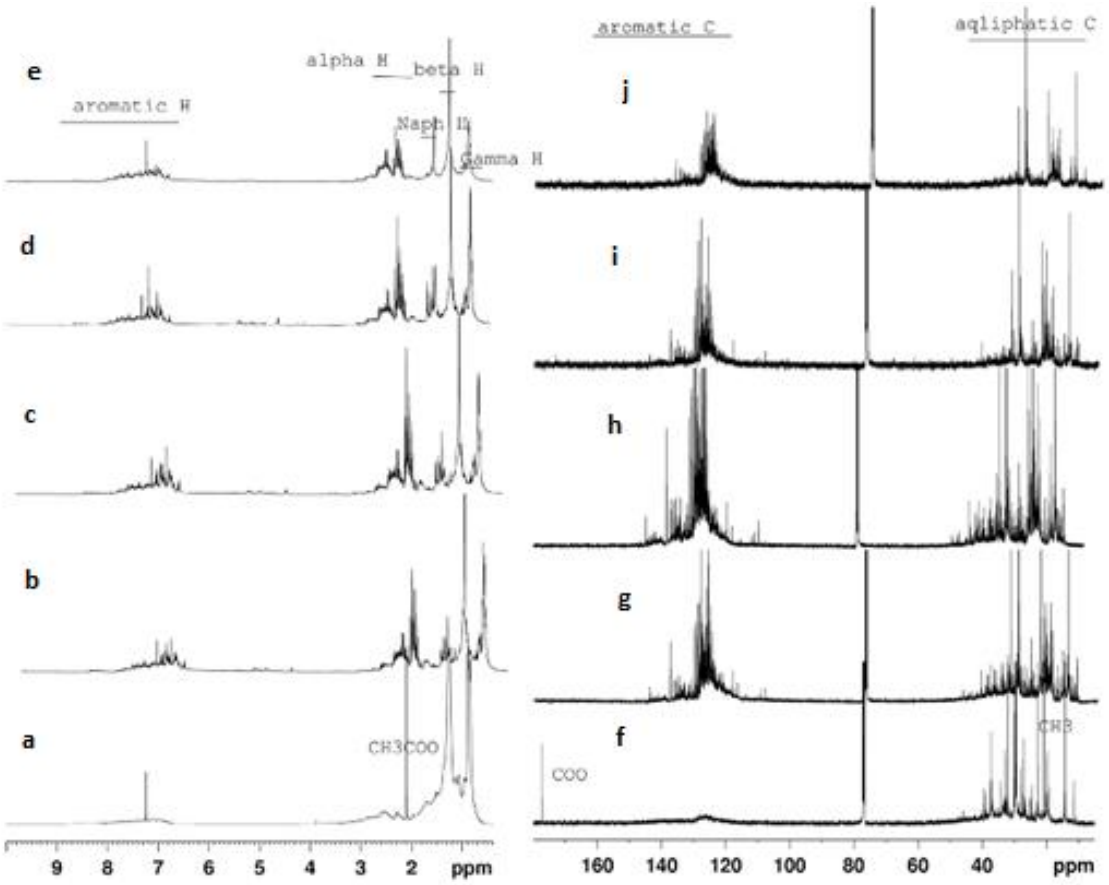

Figure 5.3: ^{1}H NMR (a-e) and ^{13}C NMR (f-j) spectra of Feed B (VGO+Acetic acid) and their distillates on catalytic cracking at 530 °C and C/O=5

In Feed C distillates the phenolic carbon signal was observed at 156 ppm in ^{13}C spectra of all distillates while the same signal was absent in Feed C, which suggested that phenol is a probable compound from the cracking of guaiacol and evidenced by ^{13}C NMR of the liquid distillates. Similarly, the phenolic carbon (Cp) was not observed in other distillates and in feeds. The ranges of substituted (ARq) carbons not followed any regular trend with C/O ratio. The H/C_{eff} was found to fall in the range of FCC feed for effective cracking.

In principle higher branchiness index (BI), which correlates naphthenes and iso-paraffins, of feedstock was inclined to more catalytic cracking. The increase of BI from 0.35 to 0.38 was observed on adding acetic acid. Simultaneously it helped to increase the conversion from Feed A to Feed B at all C/O ratios. In other case, the decrease in BI from 0.35 to 0.32 was observed on adding guaiacol as it contain aromatics, even then the conversion was higher for Feed C than Feed A as the converted product also falls in the boiling range of naphtha.

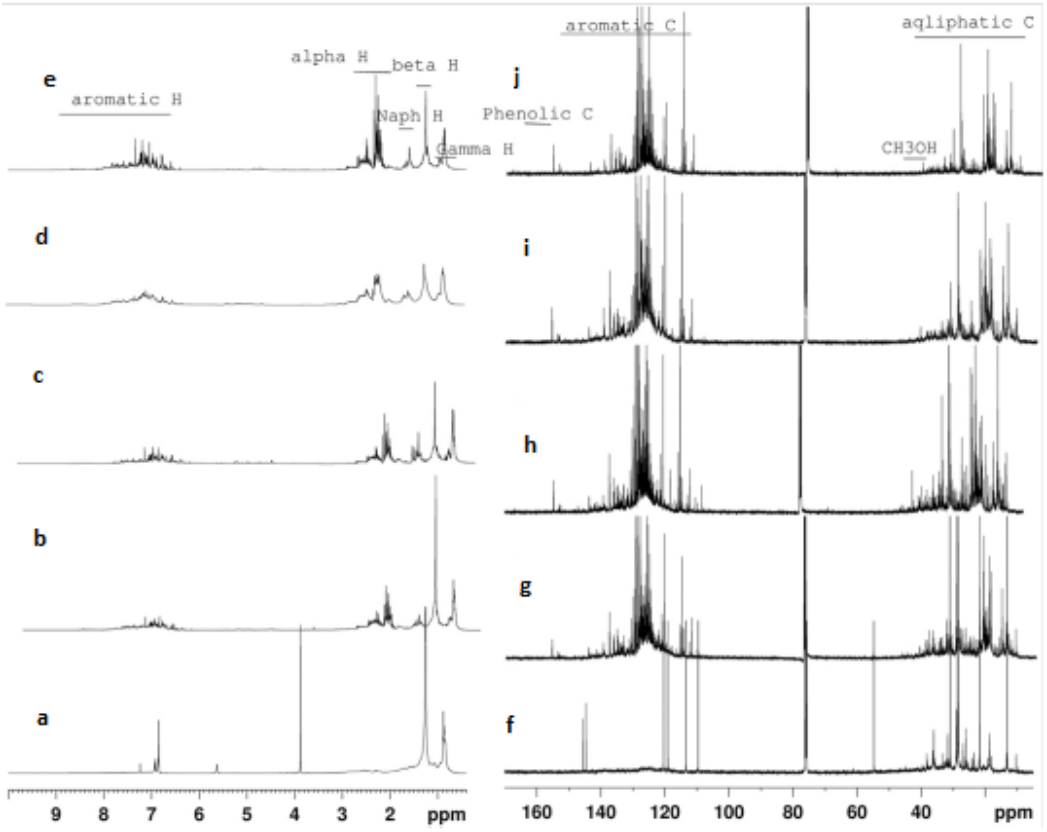

Figure 5.4: ^{1}H NMR (a-e) and ^{13}C NMR (f-j) spectra of Feed C (VGO+Guaiacol) and their distillates on catalytic cracking at 530 °C and C/O=5

It is well reported that the cracking of small polycyclic aromatics under FCC conditions is very difficult. The reason may be due to the type one reason of resonance stabilization of the shared electrons in the ring, which makes it a very poor Lewis base as compared to olefins [Dupain et al. 2003]. The other reason is even if the benzene like aromatic is activated, the beta-scission would be difficult because theremaining pi-electrons restrict the weakening of beta C-C bond. Nevertheless, there is possibility of further bigger aromatics formation by self-alkylation reactions of mono-alkyl aromatics with side chain [Dewachtere et al. 1999] or dealkylation of alkylated aromatics on cracking of aromatic rich feeds.

5.2.3 FTIR Characterization

The FTIR absorption peaks of Feeds A (VGO), B (VGO+ Acetic acid) and C (VGO+ Guaiacol) and their product distillates A, B and C are reported in Table 5.3 and their spectra are shown in Figure 5.5A–C. Wang et al. (2007) indicated that the O-H stretching vibrations

between 3300 cm^{-1} and 3600 cm^{-1} is due to the presence of phenol and alcohols. The peak of phenol functional group was identified in the Feed C as well as in their distillates. It indicated that the equilibrium FCC catalyst was not able to crack the total aromatic oxygenated hydrocarbon of pyrolysis oil. The symmetrical and asymmetrical C-H stretching vibrations between 2800 cm^{-1} and 3000 cm^{-1} of aliphatic CH_3 and CH_2 groups, in addition with C-H deformation vibrations between 1390 cm^{-1} and 1475 cm^{-1} indicated the presence of alkane [Ozbay et al. 2001; Boucher et al. 2000], and bending vibrations of CH_3 is located at 1375 ± 15 cm^{-1}[Putun et al. 1999; Gomez-serrano et al. 1996]. In the similar manner peaks observed at 2920, 2860, 1460 and 1380 cm^{-1} indicated the presence of alkane in all three feeds and product FCC distillates.

The peak of C=O stretching vibration at 1710 cm^{-1} gave the clear indication of carboxylic acid (acetic acid) in case of Feed B; whereas the similar peak was not observed in case of their distillate, which means that the total carboxylic acid was converted into some other form of product. In other words, it indicates that the equilibrium FCC catalyst was able to crack the aliphatic oxygenate like acetic acid. The bands between 1575 cm^{-1} and 1675 cm^{-1} indicated the presence of C=C stretching vibrations, and hence the presence of alkenes and aromatics [Wang et al., 2007]. In the similar manner peak observed at 1600 cm^{-1} indicated the presence of alkene and aromatics in all three feeds and product FCC distillates as the feed contains vacuum gas oil in major ratio.

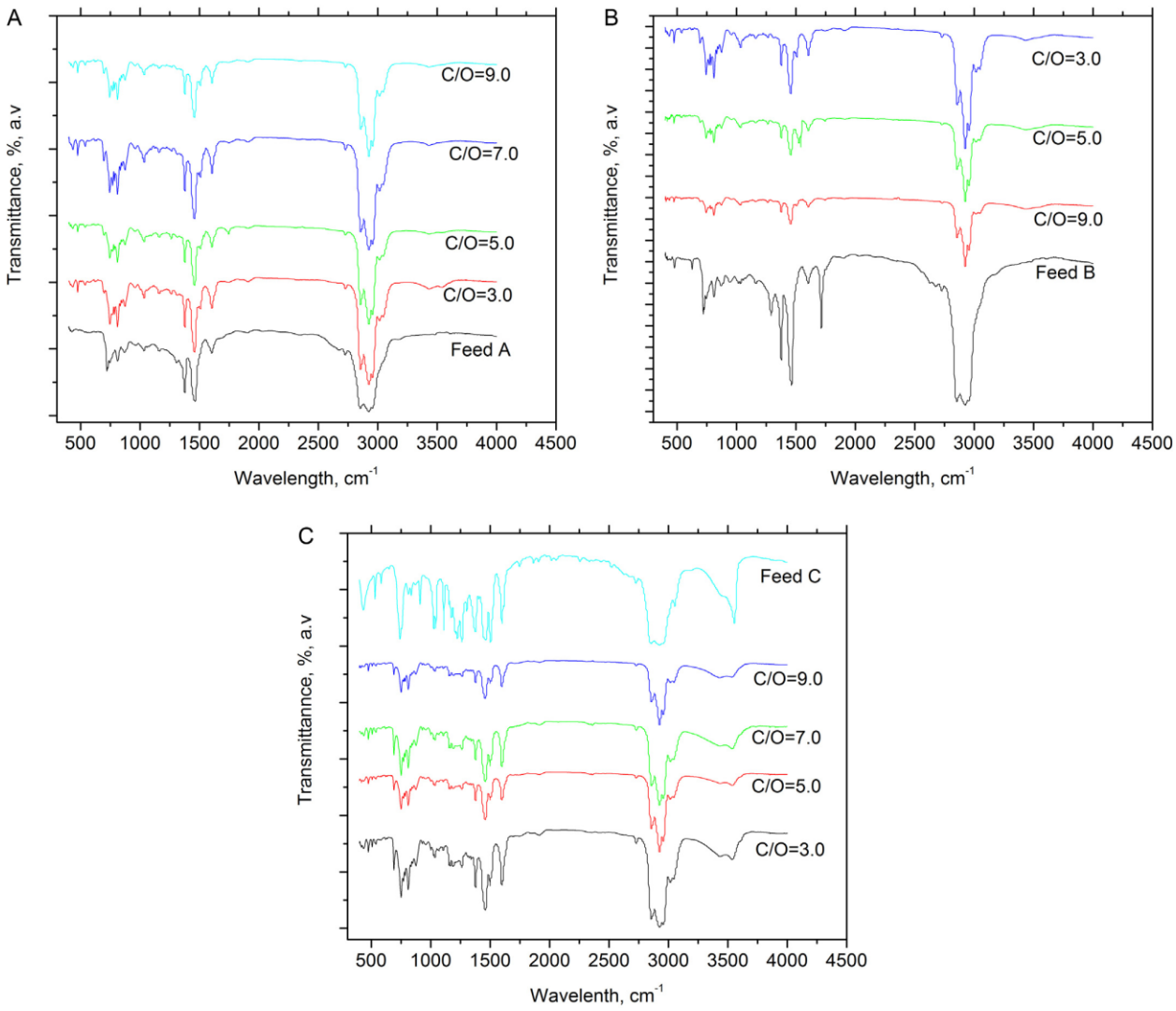

Figure 5.5A-C: (A) FTIR Spectra of Feed A (VGO) and their distillates at various C/O ratios; (B) FTIR Spectra of Feed B (VGO+Acetic acid) and their distillates at various C/O ratios; (C) FTIR Spectra of Feed C (VGO+Guaiacol) and their distillates at various C/O ratios on catalytic cracking at 530 °C and C/O=5

Table 5.3: FTIR absorption peaks of feed and FCC distillates on co-processing of acetic acid and guaiacol with VGO at 530 °C and C/O=5

Wave number, cm^{-1}	**Band**	**Feed A**	**Feed B**	**Feed C**	**Distillate A**	**Distillate B**	**Distillate C**
3500-3550 (s)	O-H stretch, phenol	×	×	√	×	×	√
3010-3100 (s)	C-H stretch, aromatic/alkene	√	√	√	√	√	√
2850-2860 (m)	C-H stretch, alkanes	√	√	√	√	√	√
2920-2930 (s)	C-H stretch, alkanes	√	√	√	√	√	√
1710 (s)	C=O stretch, carboxylic acid	×	√	×	×	×	×
1460 (m)	C-H bend, alkanes	√	√	√	√	√	√
1600-1630 (s)	C=C stretch, aromatic/conjugated alkene	√	√	√	√	√	√
1370-1380 (w)	C-H rock, alkanes	√	√	√	√	√	√
1030-1060 (s)	C-O stretch	√	√	√	√	√	√
910-960 (w)	=C-H bend, alkenes/aromatics	√	√	√	√	√	√

5.3 CATALYTIC CRACKING OF VGO WITH ACETOL AND GLYCOLALDEHYDE

5.3.1 Product Profile

The co-processing of a pyrolysis oil model compound (i.e. hydroxyacetone $C_3H_6O_2$), with petroleum-derived VGO was carried out at different blending ratio, which was varied from 5 to 20%. Figure 5.6 shows the conversion of VGO and yields of dry gas, LPG, gasoline, LCO, HCO, coke, propylene, C3 paraffin/olefin ratio and CO_2 when the blending ratio were varied. The conversion of VGO with hydroxyacetone for different blending ratio is shown in Figure 5.6a. Figure 5.6a shows that the presence of acetol increased the conversion from 68 to 78% as the blending ratio increased. It may be due to the increase in the yield of liquefied petroleum gas from 21 to 47 wt. % (Figure 5.6c), which is at the cost of a decrease in yield of gasoline (Figure 5.6d) from 39 to 23 wt. %, followed by a decrease in light cycle oil (Figure 5.6e) from 18 to 12 wt. % and a decrease in heavy cycle oil (Figure 5.6f) from 11 to 7 wt. %.

From our previous study, it was found that, upon the catalytic cracking of VGO at a C/O ratio of 5 and a temperature of 530 °C, the yield of gasoline was found to be 44%, which is considered to be optimum; whereas the presence of acetol with VGO results in a decrease in hydrogen content of the feed and, thus, the gasoline yield and conversion across the FCC unit further decreased. The decrease in gasoline yield may be due to decrease in hydrogen content of feedstock on adding acetol with VGO in FCC unit, and is considered as over-cracking of gasoline. Figure 5.6c shows that the yield of LPG increases linearly as the blending ratio increases. However, the increase in olefins may not be due to only the overcracking of gasoline, but it was also due to low hydrogen transfer reactions. A higher paraffin-to-olefin ratio is an indicator of secondary hydrogen transfer reactions.

Figure 5.6h shows that, as the acetol blending ratio increased, the C3 paraffin-to-olefin ratio decreased from 0.28 to 0.16. It indicated that the amount of secondary hydrogen transfer reactions was reduced, which led to a decrease in the gasoline yield and an increase in propylene yield (Figure 5.6i), which was also confirmed from the coke yield analysis. From Figure 5.6g, it can be seen that the presence of acetol reduced the coke formation, as compared to the pure VGO catalytic cracking over an FCC equilibrium catalyst at a constant C/O ratio of 5.

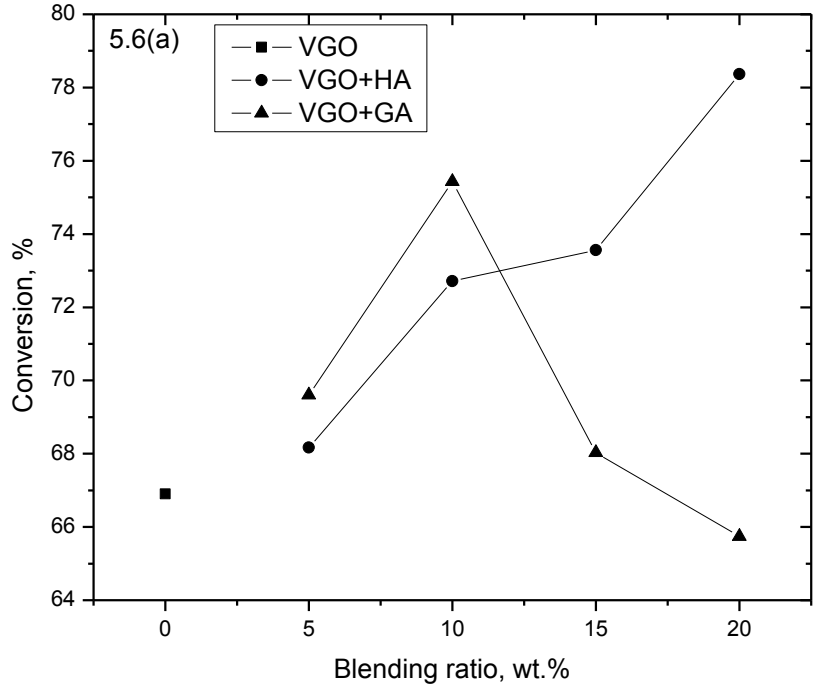

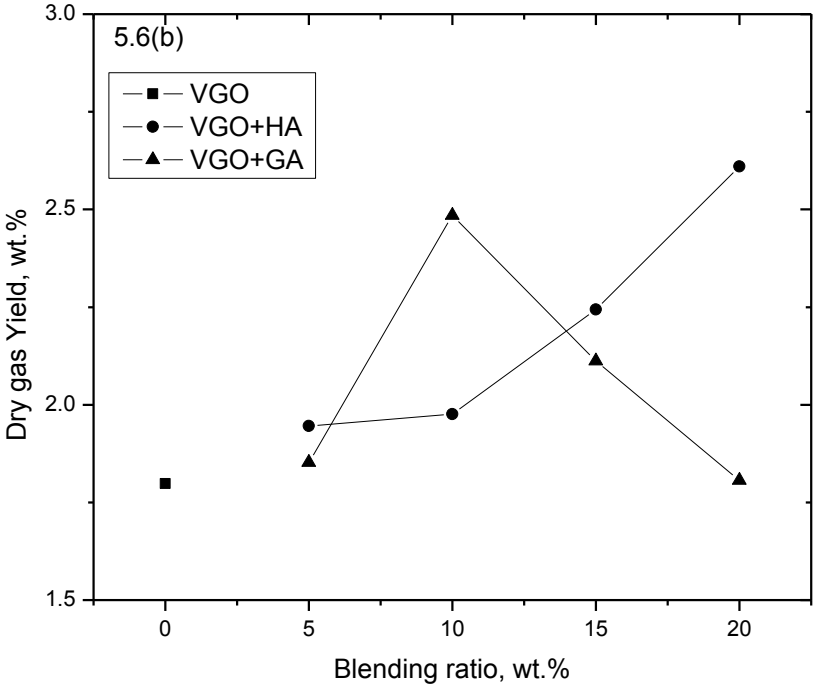

Figure 5.6a-b: Effect of blending ratio on (a) FCC conversion, (b) dry gas yield while catalytic cracking of C2-C3 carbonyls at 530 °C and C/O ratio of 5

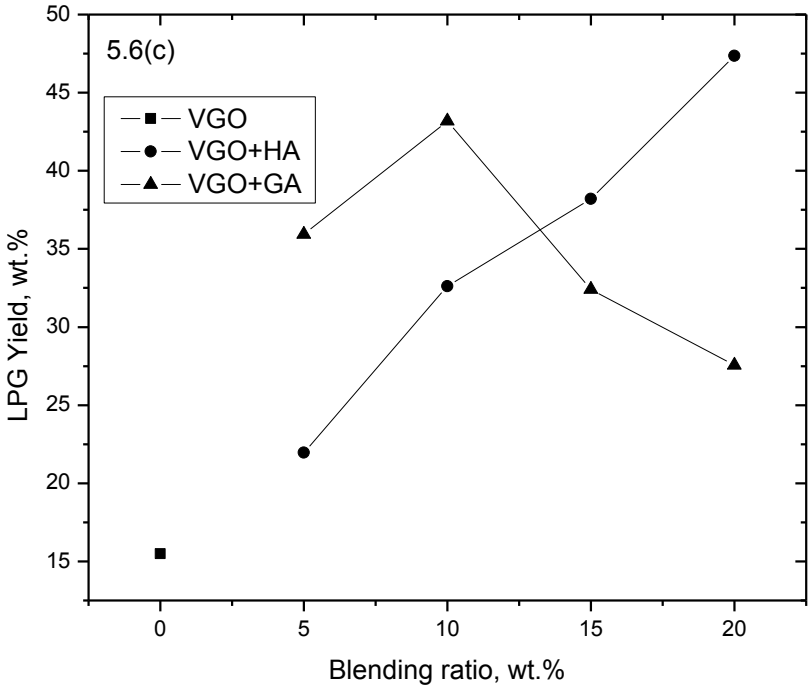

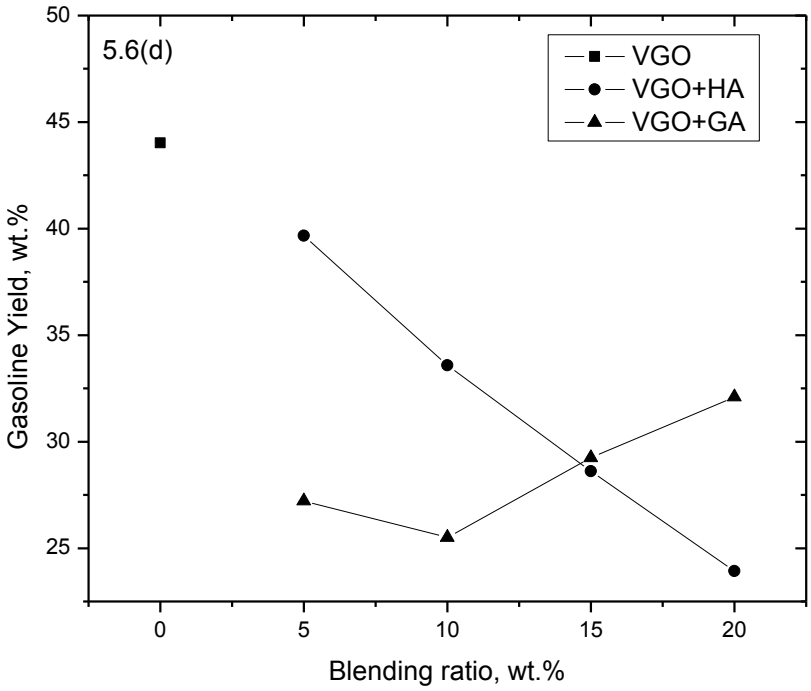

Figure 5.6c-d: Effect of blending ratio on (c) LPG, (d) Gasoline yield while catalytic cracking of C2-C3 carbonyls at 530 °C and C/O ratio of 5

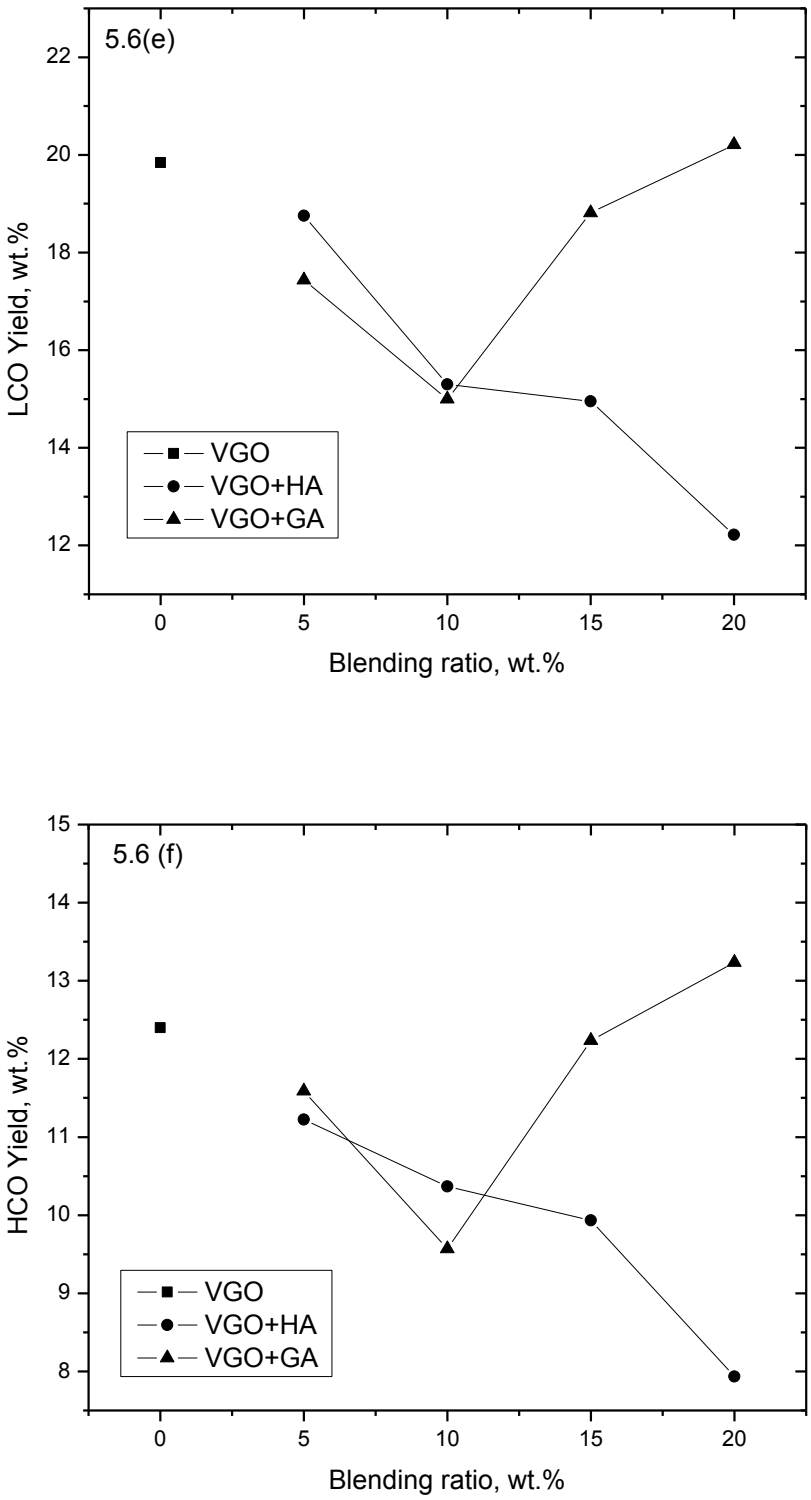

Figure 5.6e-f: Effect of blending ratio on (e) LCO, (f) HCO yield while catalytic cracking of C2-C3 carbonyls at 530 °C and C/O ratio of 5

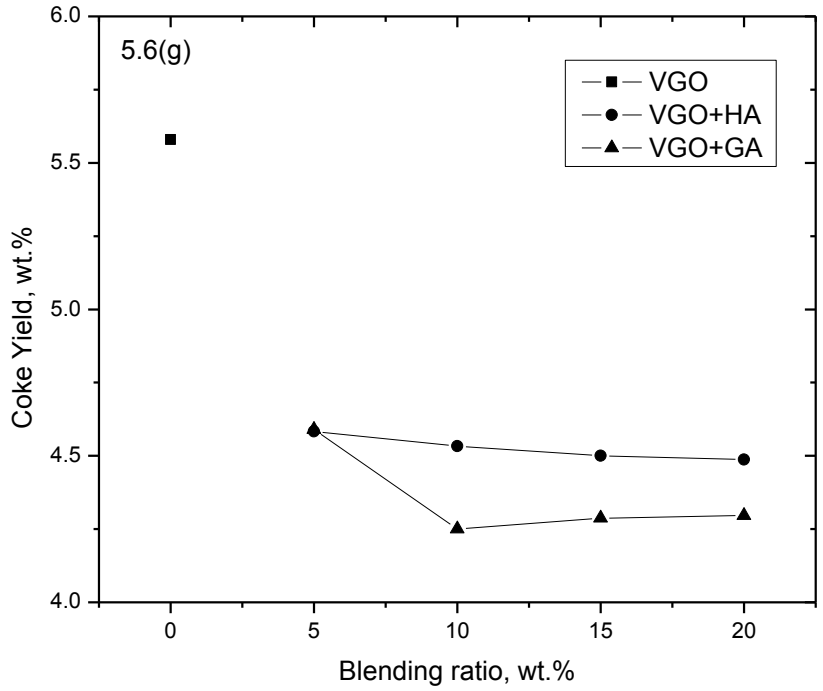

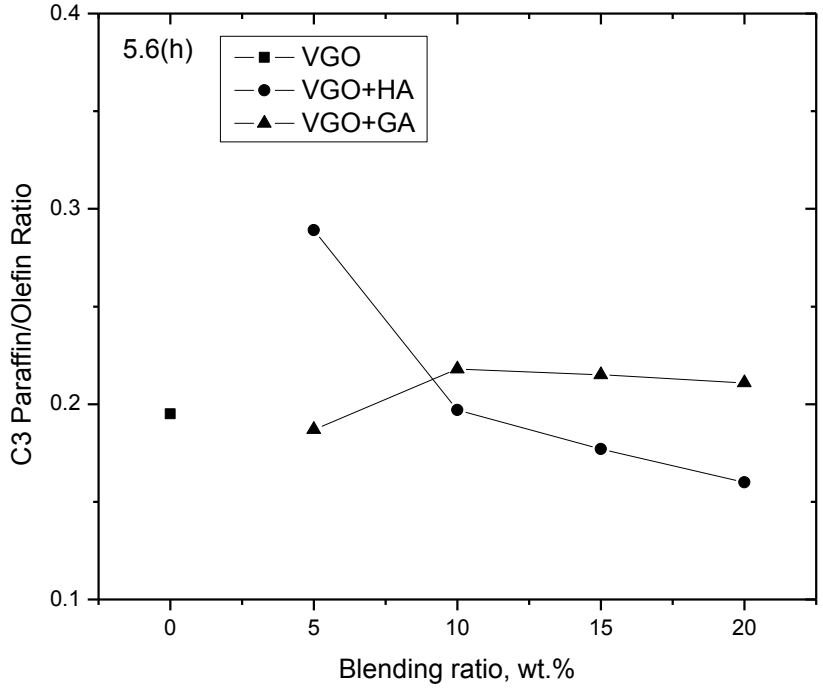

Figure 5.6g-h: Effect of blending ratio on (g) Coke yield, (h) C3 paraffin/olefin ratio while catalytic cracking of C2-C3 carbonyls at 530 °C and C/O ratio of 5

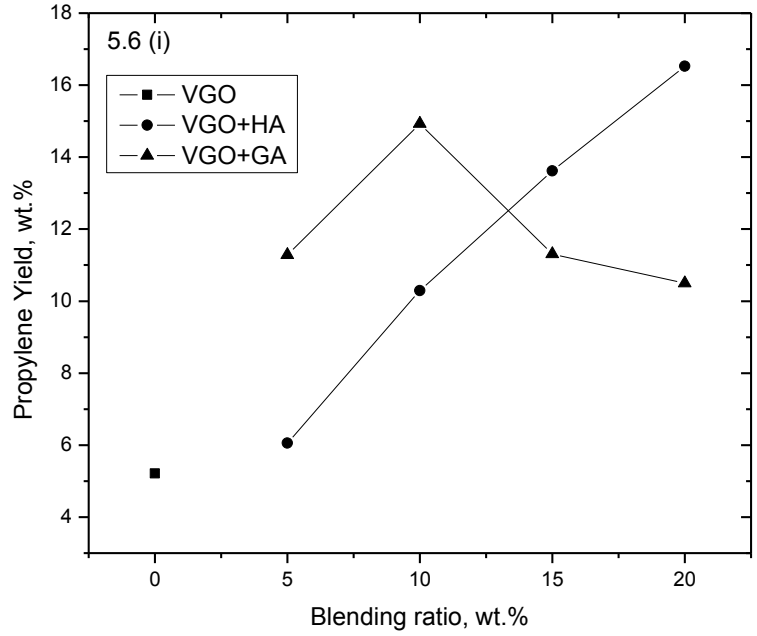

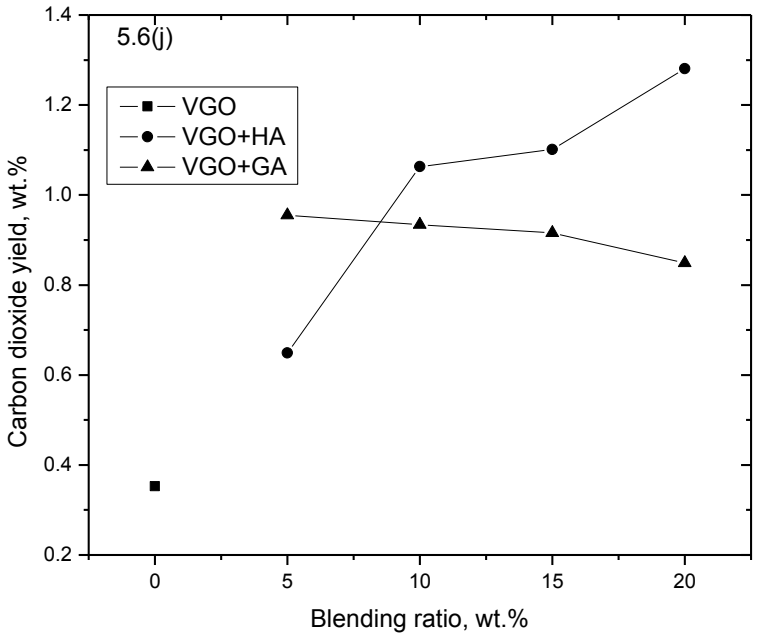

Figure 5.6i-j: Effect of blending ratio on (i) Propylene, (j) CO_2 yield while catalytic cracking of C2-C3 carbonyls at 530 °C and C/O ratio of 5

Table 5.4: NMR derived average structural parameters of liquid samples on co-processing of acetol and glycoldehyde with VGO at 530 °C and C/O=5

	C/O	**Blending ratio**	**n**	**f_a**	**Ch**	**Cb**	**ARq**	**BI**	**SI**	**H/C_{eff}**	**m-a**	**d-a**	**p-a**
VGO	--	100	18	0.13	4.90	1.36	5.70	0.35	0.47	1.725	2.33	1.6	0.55
	5	100	6	0.48	37.27	3.19	7.32	--	--	--			
HA:VGO	--	5:95		0.14						1.67			
	5	5:95	3	0.54	45.09	3.57	5.51	0.51	10.20	--	14.63	6.57	--
	--	10:90		0.14				--	--	1.62			
	5	10:90	3	0.48	36.94	3.81	7.14	0.5	15.19	--	10.75	5.81	0.11
	--	15:85		0.14					--	1.57			
	5	15:85	3	0.46	37.79	3.41	5.02	0.5	10.91	--	10.59	5.81	0.25
	--	20:80		0.15				--		1.51			
	5	20:80	3	0.49	40.36	2.14	6.94	0.48	14.16	--	9.89	6.83	0.81
GA:VGO	--	5:95		0.12						1.64			
	5	5:95	3	0.54	43.28	3.34	7.21	0.51	13.60	--	9.8	8.05	1.95
	--	10:90		0.11						1.55			
	5	10:90	3	0.49	40.41	3.73	4.46	0.56	9.10	--	13.3	6.26	0.59
	--	15:85		0.11						1.46			
	5	15:85	3	0.51	40.86	3.71	6.73	0.52	13.19	--	10.42	7.63	1.49
	--	20:80		0.12						1.38			
	5	20:80	3	0.50	39.51	3.35	7.27	0.56	14.54	--	8.16	8.13	3.15

Furthermore, it was observed that the coke formation decreased as the amount of acetol increased, in VGO, during catalytic cracking; whereas in case of catalytic cracking of raw pyrolysis oil over FCC catalyst results in heavy coking. Furthermore, it was also observed that the yield of carbon dioxide (Figure 5.6j) increases as the blending ratio increased, which was clearly indicated the decarboxylation reaction. In addition, for the purpose of reproducibility and regeneration studies, the regenerated catalyst was used three times in a series to carry out the same set of experiments with both feeds at a C/O ratio of 5 and a blending ratio of 5. The yields of FCC products were observed within the range of ±2% error.

The conversion and yields of various FCC products on the co-processing of glycolaldehyde dimer with VGO in an ACE unit by varying the blending ratio from 5 to 20% are shown in Figure 5.6a–j. It can be seen from Figure 5.6e that the light cycle oil yield first decreased from 17 to 15 wt. % and then increased to 20 wt. %; whereas the yield of heavy cycle oil (Figure 5.6f) first decreased from 11 to 9 wt. %, and then increased to 13 wt. % when increasing the blending ratio from 5 to 10%. The yield of ethylene and propylene also followed the same trend: yields increased as the blending ratio of glycolaldehyde increased up to 10% blending, and beyond that value, the yields decreased with further increase in blending ratio. The change in the product profiles during the catalytic cracking of VGO with more than 10% glycolaldehyde may be due the fact that the glycolaldehyde, which is an acetaldehyde, has low reactivity to hydrocarbons and can be attributed mainly to oligomerization products with noticeable coke formation.

The present findings are in good agreement with the work of Gayubo et al. (2004a). Gayubo et al. (2004a) carried out the catalytic cracking of acetaldehyde up to 450 °C temperature over HZSM5 catalyst in an isothermal fixed bed reactor and reported that, as the blending increases beyond 10%, there is an increase in liquid hydrocarbons, which may be due to the formation of oligomerized products. Figure 5.6g shows that the coke yield decreased from 4.5 to 4.25 wt % as the blending ratio increased from 5 to 10%; thereafter, it increased to 4.29 wt. % for higher blending ratio (20 wt. %). The increase of coke formation may be due to the increase in polyaromatics formation beyond a blending ratio of 10%. Similar results were found from nuclear magnetic resonance (NMR) spectroscopy analysis. The polyaromatics formation initially decreased from 1.95 to 0.59; thereafter, it increased to 3.15 as the blending ratio increased. NMR analysis indicated that the amounts of monoaromatics and diaromatics first increased as the

blending ratio increased from 5 to 10% and then decreased upon further increasing the blending ratio up to 20%.

5.3.2 NMR Characterization

Figures 5.7a−d show ^{1}H spectra and Figures 5.7e−h show ^{13}C NMR spectra of liquid samples obtained from catalytic cracking of hydroxyacetone with VGO. Although the spectra look similar, however their quantitative information derived varied. Analysis of NMR results showed that the fraction of aromaticity (f_a) decreased from 0.54 to 0.46 when the blending ratio of hydroxyacetone increased from 5% to 15%, while an increase in f_a was observed at a blending ratio of 20%. Here, f_a was the ratio of aromatic carbons to total carbons, expressed as a percentage. The substitution index was calculated from the ratio of substituted aromatic carbon to total aromatic carbons, which indicated that the aromatics upon blending of 10% of acetol were heavily substituted, followed by 20%, 15%, and 5% of acetol.

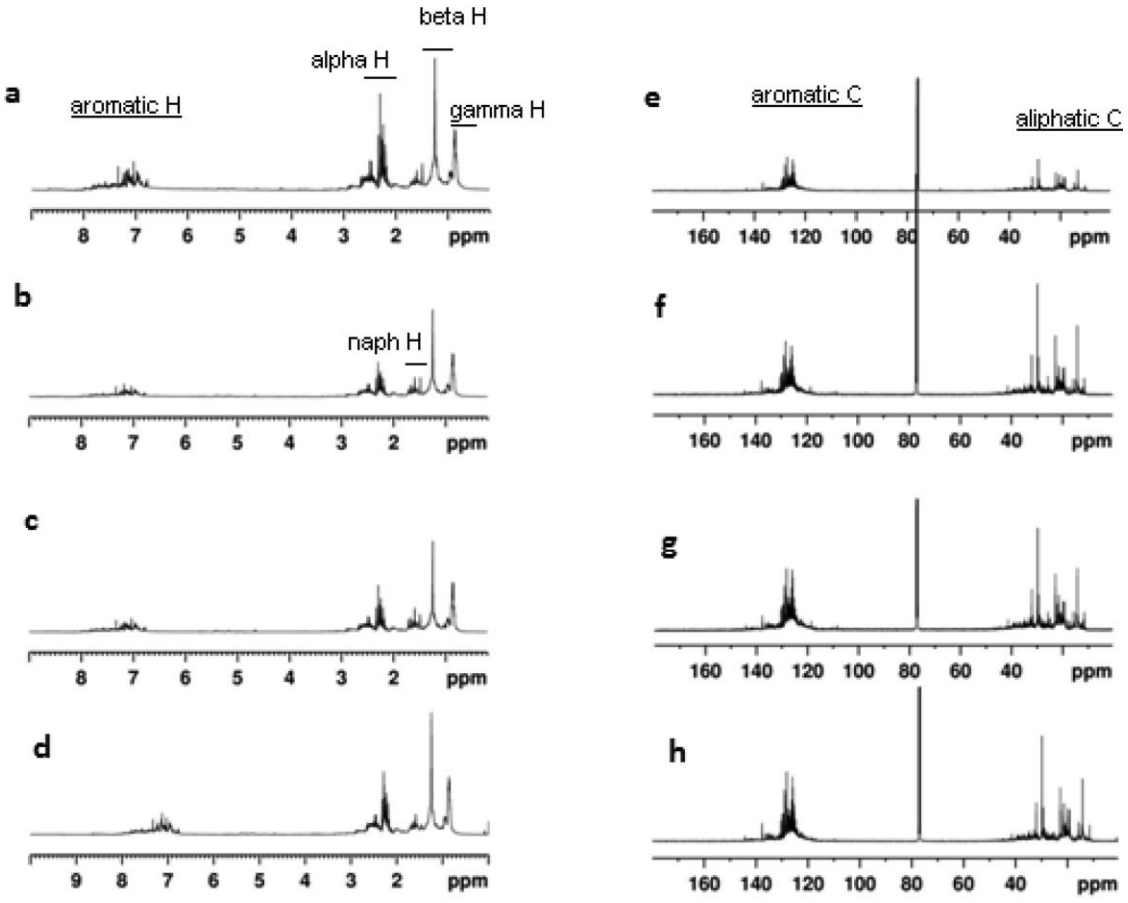

Figure 5.7: (a-d) ^{1}H NMR spectra and (e-h) ^{13}C NMR spectra of liquid samples obtained from catalytic cracking of VGO with hydroxyacetone at 530 °C and C/O=5

The branchiness index (BI) showed a decrease in the branching of alkyl chains with blending. The condensation index was derived from the ratio of bridgehead aromatics to the total protonated aromatic carbons, and it was observed that the aromatics from 20% blending were least condensed. The NMR spectroscopy analysis indicated that monoaromatics decreased from 14.63 to 9.89 while the polyaromatics increased from 0.1 to 0.81 when the blending ratio of acetol increased from 5 to 20% with VGO. Although the blending component in both cases containing oxygenates, the product showed the absence of oxygenated protons and carbons, which indicated that the oxygen is removed in the form of a gaseous fraction. It can be seen from Figure 5.7 that there is no sharp peak for oxygenated proton in the chemical shift region of 3.5−6 ppm and carbon in the chemical shift region of 60−110 ppm and >160 ppm, respectively.

Hence, it was concluded that the liquid products upon catalytic cracking of VGO with acetol and glycolaldehyde are free from oxygenates and the quality of the FCC distillate is same as that of the conventional one, which matches the gasoline RON/MON and diesel cetane index. Figures 5.8a−d and 5.8e−h show the ^{1}H NMR and ^{13}C NMR spectra of liquid samples, respectively, obtained from the catalytic cracking of the glycolaldehyde dimer with VGO. In this case, the spectra obtained were similar to those in the case of acetol with VGO. However, their quantitative information derived was different. From the NMR analysis, it was observed that the aromaticity is higher at a lower blending ratio of 5%. The substitution index, which indicates the degree of substitution to aromatics, was lower for a blending ratio of 10%. The branchiness index was higher for 10% and 20% blended distillates, followed by 15% and 5% blended cracked distillate. The condensation index shows that the 10% and 15% derived liquids are equally condensed, which suggest similar nature of aromatics. Based on other results in collaboration with NMR product analysis, the 10% blended glycoldehyde can be considered as optimum. The average chain length of alkyl chain in the distillate was found to be 3. The higher percentage of monoaromatic protons can be self-explanation for a lower substitution index, as well as a low percentage of substituted aromatic carbon with highly branched alkyl chain, with 10% glycolaldehyde loading. The NMR derived average structural parameters of liquid samples obtained on co-processing of acetol and glycoldehyde with VGO are shown in Table 5.4.

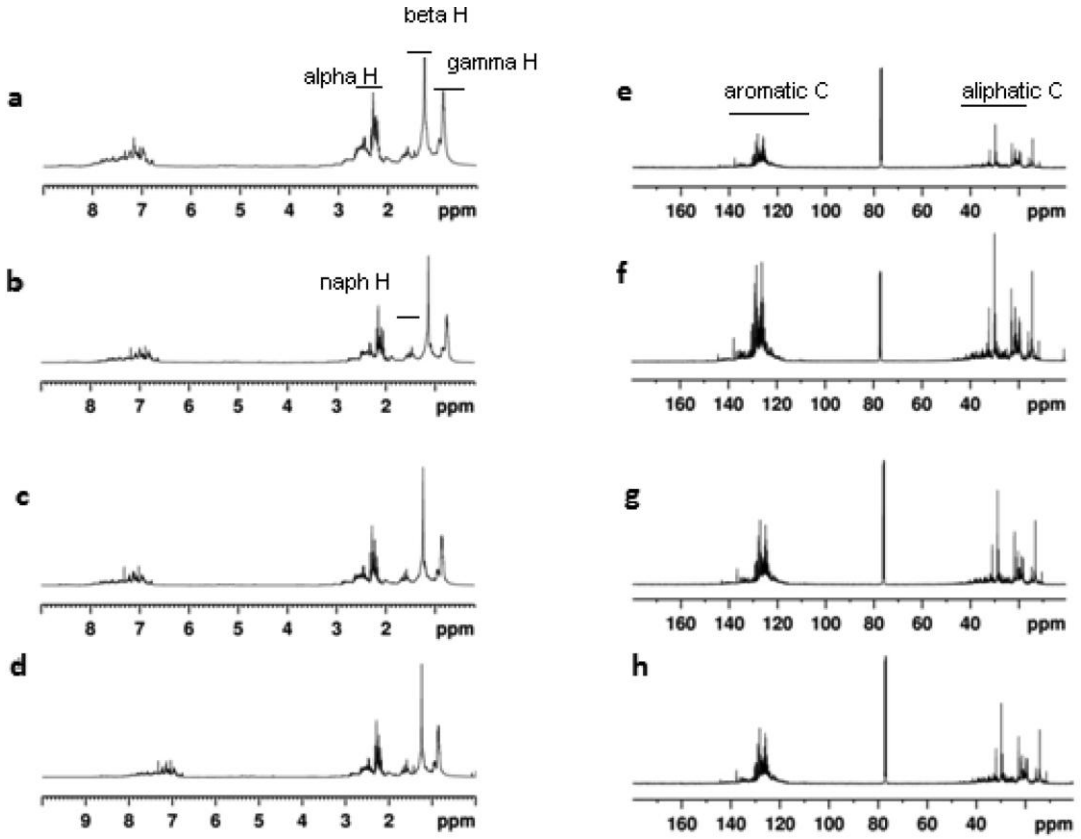

Figure 5.8: (a-d) ^{1}H NMR spectra and (e-h) ^{13}C NMR spectra of liquid samples obtained from catalytic cracking of VGO with glycolaldehyde dimer at 530 °C and C/O=5

5.4 PROPOSED SCHEME FOR PROCESSING OF FPO IN REFINERY UNITS

Based on the present results (Naik et al. 2014a,b) for the co-processing of pyrolysis oil model compounds (such as acetic acid, 2-methoxy phenol, hydroxyacetone, and glycoldehyde dimer) with VGO in an FCC unit, it has been observed that the aliphatic oxygenates are easily crackable in the FCC process at lower blending ratios, whereas the aromatic hydrocarbons are not easily cracked. Therefore, it is proposed to first separate the aliphatic and aromatic oxygenates from the pyrolysis oil, either by solvent extraction or other techniques. Accordingly, an approach for the processing of pyrolysis oil in refinery units is proposed in Figure 5.9. This type of approach may help petroleum refineries to integrate it with fast pyrolysis process to increase the yield of LPG and also the valuable and most demanded petrochemical feedstock (i.e., propylene).

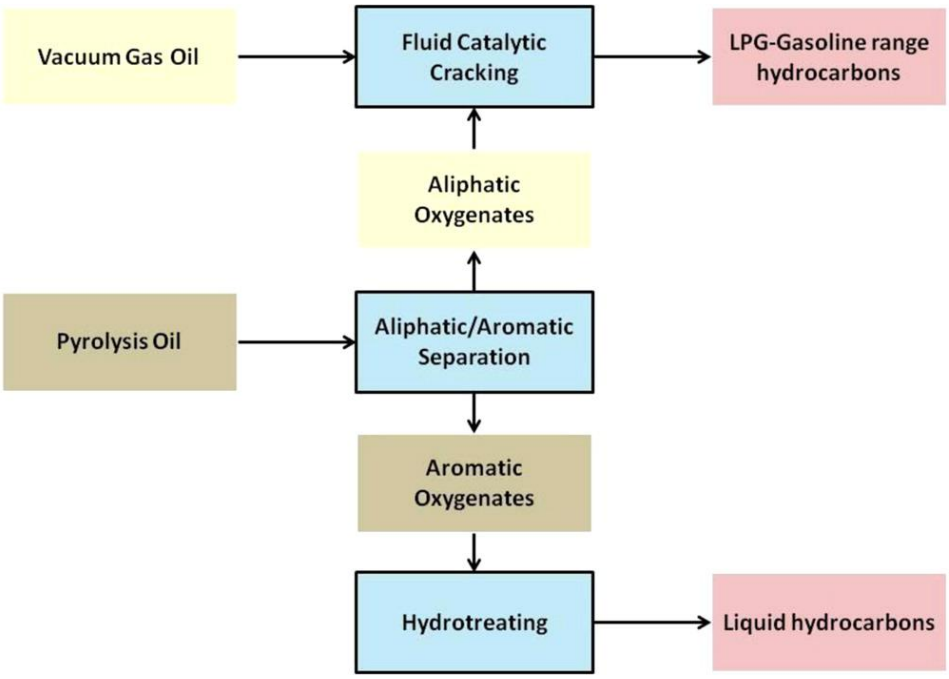

Figure 5.9: Proposed approach for co-processing of FPO in refinery FCC unit

5.5 CATALYTIC CRACKING OF GLYCEROL

It is well understood that the addition of biomass-derived oxygenated hydrocarbon in catalytic cracking follows the pathway of series of reactions like dehydration, hydrogen producing and consuming reactions, and aromatic formation reactions [Corma et al. 2008]. In the present work, the co-processing of glycerol with vacuum gas oil (VGO) was carried out in the fluid catalytic cracking (FCC) unit. Glycerol is a byproduct during the formation of biodiesel, which is a first generation biofuel, from vegetable oils. The results for pure glycerol cracking and the co–processing of glycerol with VGO are discussed in terms of product distribution and characterization using NMR in the following sections. Further the aim of cracking of pure glycerol was to convert the biomass–derived glycerol into possible fine chemicals (such as acetaldehyde, acrolein etc.). The glycerol conversion was carried out by operating conventional fluid catalytic cracking process in a block operation mode at various temperatures and at constant catalyst-to-oil ratio. The gas and liquid products were analyzed with gas chromatography and nuclear magnetic spectroscopy.

5.5.1 Co-processing of VGO with Glycerol

5.5.1.1 Product profile

The product profiles on co-processing of glycerol with vacuum gas oil over equilibrium fluid catalytic cracking catalyst at different blending ratio are shown in Table 5.5. The conversion was calculated as per standard refinery practice as the sum of coke, gases including dry and liquefied petroleum gas, and gasoline. The decrease in conversion was mainly due to the complete cracking of glycerol (B.P. of 290 °C) on co-processing with VGO.

The complete conversion of glycerol is possible beyond the temperature of 470 °C, which can also be seen from our previous study [Naik et al. 2014c]. From Table 5.5, it can be seen that the FCC conversion is about (~66%) for catalytic cracking of pure vacuum gas oil at C/O ratio of and 530 °C temperature. While the conversion increased from 68 to 69.8 wt.% with an increase in blending ratio of glycerol from 5 to 15%. It was due to the increase in the yield of coke and LPG from 6.1 to 8.4 wt.% and 17.8 to 19.4 wt.%, respectively, with an increase in blending ratio of glycerol. Most of the aromatics formed were found in the boiling range of gasoline hydrocarbons. While the yield of light cycle oil decreased slightly from 19.1 to 18.1 wt.%. However, the yield of heavy cycle oil (Figure 5.9f) decreased from 12 to 11.3 wt.% with an increase in blending ratio. It was observed that the coke yield increased from 6.1 to 8.46 wt.% with an increase of blending ratio (Table 5.5); however it was lower for direct cracking of VGO. However, the yield of coke was higher (~9 wt.%) for catalytic cracking of pure glycerol. These results indicated that the increase of coke formation may be due to either dehydrogenation or condensation of polynuclear aromatics/olefins.

It was observed that the presence of glycerol with VGO, while co-processing in FCC unit, follows the reaction pathways of Corma et al. (2008). Further, it was found that the activity of equilibrium FCC catalyst was towards the formation gas, coke and aromatics. It can also be mentioned that the aromatics formation increased with an increase blending ratio or a decrease in conversion and the pattern of the result followed the similar path of Corma et al. (2007).

Table 5.5: Product profile on co-processing of VGO: Glycerol at different blending ratio at 470 °C temperature and C/O ratio of 5

Feedstock	**VGO: Glycerol**			
Blending ratio	100:0	95:05	90:10	85:15
FCC conversion	66.9	68.05	68.54	69.87
Product Yields (wt.%)				
Dry gas	1.79	2.2	2.27	2.52
LPG	15.50	17.8	18.68	19.48
Gasoline	44.02	41.94	40.32	39.43
LCO	19.84	19.19	18.76	18.15
HCO	12.4	12.08	11.61	11.31
Coke	5.58	6.11	7.27	8.44

5.5.1.2 NMR Characterization

The average structural information was derived from the integral of NMR spectra to the structural specificity of the carbon and hydrogen type distribution with associated chemical shift regions. The chemical shift regions of ^{13}C NMR spectrum has been divided into aliphatic carbons (0-50 ppm), oxygenated alcoholic carbons (50-110 ppm), aromatic carbons (110-150 ppm) and carboxylic (150-200 ppm) carbons; whereas the ^{1}H NMR spectrum to aromatic hydrogen (9-6 ppm), aliphatic hydrogen (0-5 ppm), olefinic (5-6 ppm) and oxygeneted hydrogen (3.5-5 ppm). Furthermore, the aliphatic proton region has been subdivided into Hα (2-3 ppm), Hβ (1-2 ppm), Hγ regions (0.5-1 ppm); whereas the aromatic region to mono aromatics (m-a; 6-7.2 ppm), diaromatic (d-a; 7.2-8.0 ppm) and polyaromatic proton regions (p-a; 8-10 ppm). The aliphatic proton corresponds to the methyl and methylene groups.

Figures 5.10a-f represents ^{1}H NMR and ^{13}C NMR spectra of vacuum gas oil blended with glycerol at different ratios. The results were averaged to represent a simplified picture of complex hydrocarbon mixture containing a wide range of components. The fraction of aromaticity (f_a) is defined as the percentage of aromatic to the total carbons. It was observed that the value of f_a increased from 0.48 to 0.53 with an increase in blending ratio from 5 to 15 wt.%. Mono-aromatics decreased from 12.7 to 7.7; whereas di-aromatics and poly-aromatics increased from 6.8 to 8.7 and 0.3 to 3.8, respectively, with an increase in blending ratio. However, the

mono, di and poly-aromactics were found to be low on catalytic cracking of pure glycerol at the same temperature and catalyst-to-oil ratio, as shown in Table 5.6.

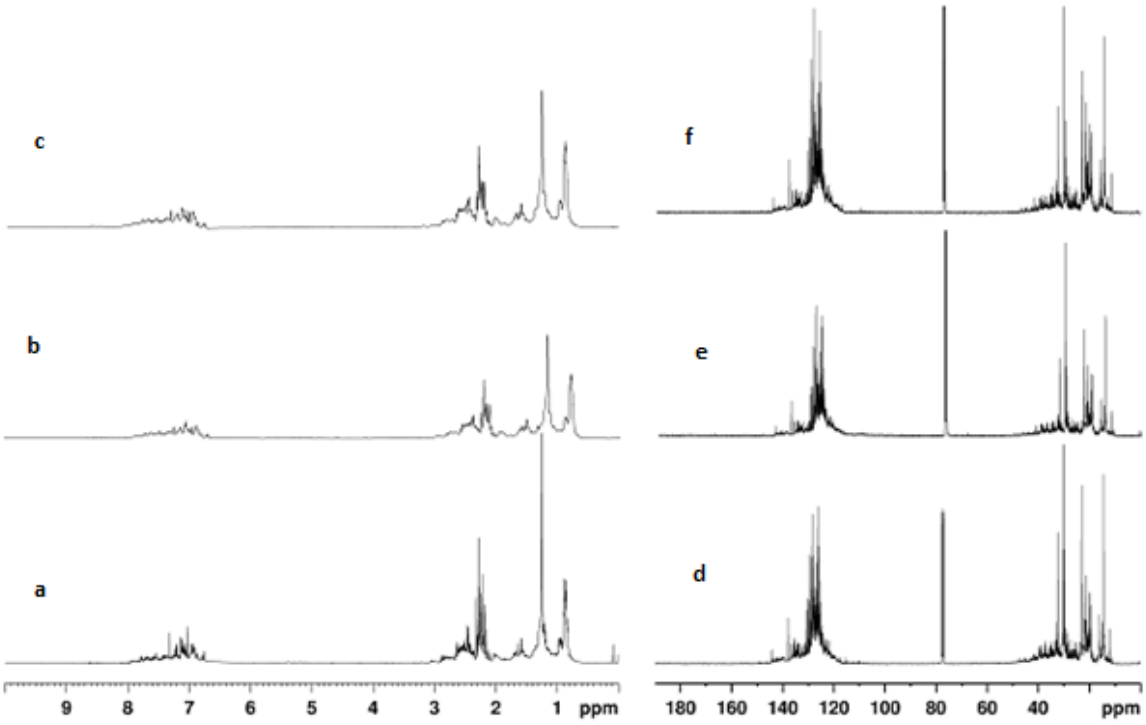

Figure 5.10: (a-c) ^{1}H NMR spectra and (d-f) ^{13}C NMR spectra of liquid products obtained from catalytic cracking of VGO with glycerol

Table 5.6: NMR analysis of feed and product on catalytic cracking of glycerol with VGO at various blending ratio at 470 °C temperature and C/O ratio of 5

Glycerol: VGO	**Feed**			**Product**		
	5%	10%	15%	5%	10%	15%
NMR parameters						
f_a	0.138	0.143	0.149	0.486	0.526	0.535
p_{ar}	1.4	1.48	1.41	0.31	1.82	3.82
d_{ar}	1.91	2.06	2.2	6.82	7.17	8.76
m_{ar}	0.28	0.29	0.25	12.7	10.4	7.79
H_{ar}	0.23	0.42	0.24	19.83	19.39	20.37
H_{ol}	8.44	8.79	8.65	0.32	0.35	0.54
H_{alpha}	12.69	13.5	13.06	28.49	28.88	29.7
H_{naph}	52.36	51.71	52.07	10.79	10.81	10.37
H_{beta}	22.66	21.7	22.07	24.03	22.7	22.38
H_{gamma}	96.15	95.7	95.85	16.5	17.8	16.57

5.5.2 Catalytic Cracking of Glycerol

5.5.2.1 Product profile

The conversion of biomass-derived glycerol over equilibrium FCC catalyst was 100 w/w% for the temperatures ranging from 470-550 °C in FCC unit. However, at lower temperatures, i.e. 350 and 390 °C, unconverted glycerol was found, therefore, the conversion decreased at lower temperatures. The coke yield increased from 7.7 to 10.4 wt.% with a decrease in temperature from 550 to 350 °C. The different products formed during the fluid catalytic cracking of biomass–derived glycerol were analyzed using gas chromatographic and are shown in Table 5.7. Acetaldehyde, acrolein, 1, 2-propanediol, and unconverted glycerol were observed in the liquid products, while carbon dioxide, methane, ethane, ethylene, propane and propylene were found in the gas products. It was observed that the acetaldehyde yield increases from 18 to 53 wt.% with an increase in temperature from 350 to 550 °C.

Table 5.7 Effect of temperature on product yields of catalytic cracking of glycerol at 470 °C temperature and C/O ratio of 5

Temp. °C	Glycerol Conversion, %	Coke Yield, wt.%	Yield, wt.% (GC identified)			
			Acetaldehyde	Acrolein	1,2-propanediol	Glycerol
350	94.3	10.4	18.88	3.24	4.35	5.7
390	98.3	9.8	22.38	6.44	3.64	1.7
430	100	9.2	29.36	7.61	2.31	<1
470	100	8.6	50.49	5.09	nd	<1
510	100	8.2	52.32	4.07	nd	<1
550	100	7.7	53.33	3.14	nd	<1

At higher temperatures, 100% glycerol conversion and more than 53% of acetaldehyde yield was achieved by operating a fluid catalytic cracking process in block operation mode; whereas the maximum acrolein yield was observed at lower temperature, i.e. 430 °C. It was observed that the yield of acetaldehyded increased with an increase in temperature at catalyst-to-oil ratio of 5; whereas maximum yield of acrolein, i.e. 7.6%, was obtained at lower temperature, i.e. 430 °C. The present experimental results were in good agreement with the experimental findings of Corma et al. (2008). The carbon dioxide yield also increased from 4.2 to 7.7 wt.% with an increase in temperature, which indicated that equilibrium FCC catalyst is also effective

for dehydration as well as decarboxylation reactions in addition to cracking. Further the increasing trend of ethylene (from 0.17 to 1.5 wt.%) and propylene (from 0.59 to 2.9 wt.%) yields were observed with an increase in temperature.

5.5.2.2 2D-NMR Characterization

The yield of acrolein was analyzed using both gas chromatography and NMR spectroscopy, and the results were found in good agreement at higher temperatures (Figure 5.11). Acetaldehyde and acrolein were identified from $^{1}D–^{1}H$, ^{13}C, $^{1}H–^{1}H$ COSY, $^{1}H–^{13}C$ HMQC and $^{1}H–^{13}C$ HMBC NMR, and quantified from quantitative NMR. Figure 5.12 shows the qualitative analysis of acetaldehyde and acrolein. Figure 5.11 shows the acrolien yields analyzed using both gas chromatography as well as 2D NMR spectroscopy. It can be seen from Figure 5.11 that at lower temperature, i.e. at 470 °C, the deviation in between both the analyses was approximately 40%. However, at higher temperature, i.e. 510 and 550 °C, the deviation in the yield from both the analysis was within ±10%. From the findings of the present work, it can be concluded that the existing refinery FCC process can be effectively utilized for the production of acetaldehyde from glycerol using commercial equilibrium FCC catalyst at the cost of higher coke deposition. However, the catalyst deactivation due to coke deposition could be sorted out by regenerating catalyst in a regenerator.

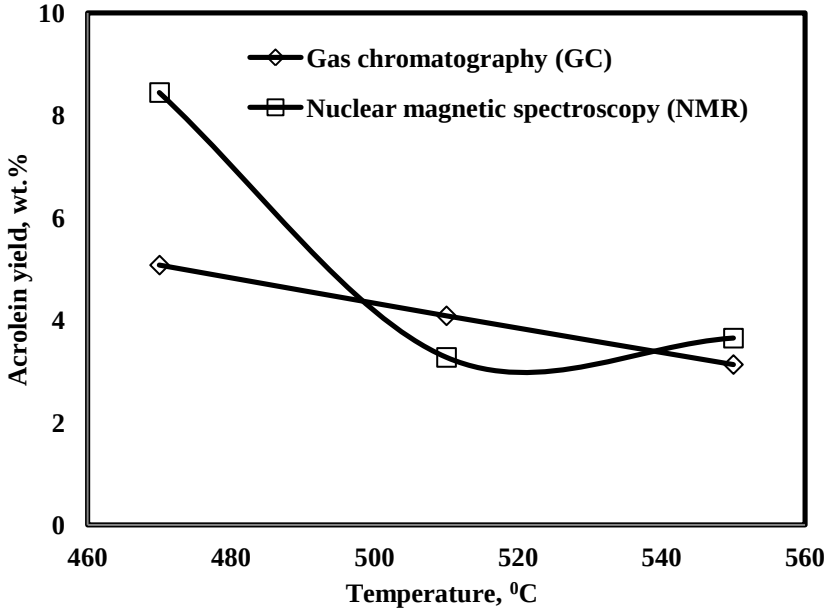

Figure 5.11 Comparison of acrolein yield (from GC and 2D-NMR) on catalytic cracking of glycerol at 470 °C temperature and C/O ratio of 5

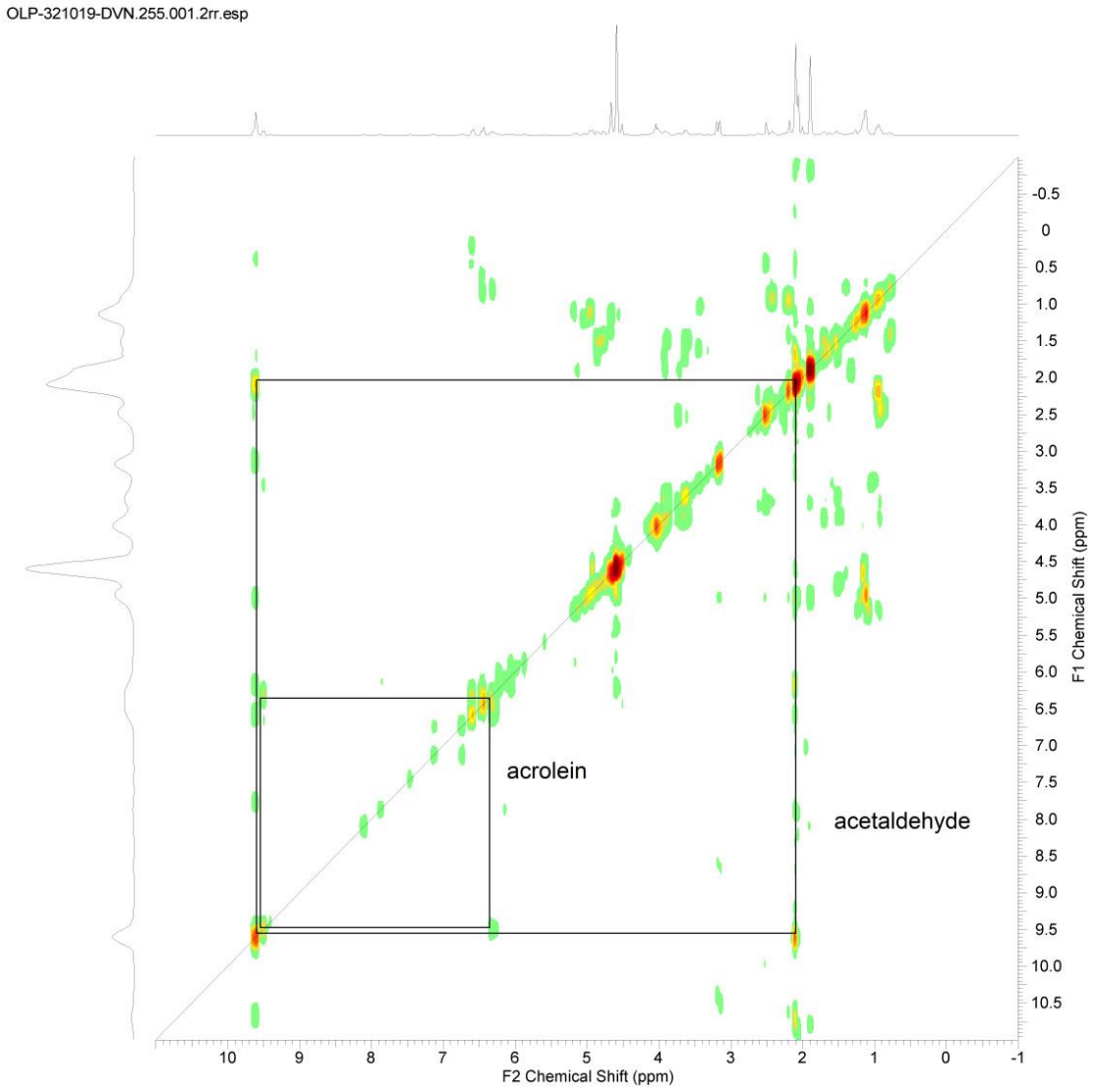

Figure 5.12: Qualitative analysis of acetaldehyde and acrolein at 470 °C temperature and C/O ratio of 5 on catalytic cracking of glycerol

CHAPTER 6

KINETIC MODLLING FOR CO-PROCESSING OF VGO WITH FPO

6.1 GENERAL

Kinetic study is a powerful tool for understating reaction and catalysis for any catalyzed chemical reaction. It helps in design of chemical reactors accurately and also provides the progress of the chemical reaction. During catalytic cracking of vacuum gas oil (VGO), the reaction occurs are complex and may take place in series and parallel, a number of reactions may occur simultaneously. Typically, VGO containing hundreds of components, which complicate the detail analysis as the number of reactions are taking place simultaneously and the reaction network is very complicated. In the analysis of catalytic cracking of VGO the feed is lumped into a small number of groups. The lump modelling approach has been extensively used, for the kinetic parameter estimation, in case where the feed lump is identical to the individual components present in it. Once the mathematical model is developed for various lumps, the kinetic parameters can be estimated using a non linear regression analysis.

So far many researchers estimated the kinetic parameters for the catalytic cracking of vacuum gas oil based on number of lumps due to the complex and multi components present in the feed gas oils as well as FCC products. These lumps may be classified on the basis of boiling range or molecular structure of hydrocarbons. Weekman et al. (1970) developed a kinetic scheme for catalytic cracking reaction modelling based on the concept proposed by Wei et al. (1963). The 3–lumps kinetic scheme was used for the estimation of kinetic parameter by assuming feedstock, gasoline and gases including coke as first, second and third lumps, respectively. The gas oil conversion and gasoline yield was predicted in fixed and fluidized bed reactors at isothermal condition. Further, this 3–lump kinetic scheme has been extended to 34 lumps in which the theoretical solution was provided up to 10 lumps. Mostly the 3–lump [Lee et al., 1989; Theologos et al., 1993], 4–lump [Yen et al., 1988; Larocca et al., 1990; Sertic-Bionda et al., 2010; Ancheyta et al., 1997, 1999, 2000; Bollas et al., 2007; Corella et al., 1991; Dupain

et al., 2003], 5–lump [Anchyeta et al., 1997, Ancheyta and Murillo, 2000], 6–lump [Coxon et al., 1987], 10– [Jacob et al., 1976], 11–lump [Mao et al., 1985], 12–lump [Oliviera et al., 1987], 13–lump [Sa et al., 1995], 19–lump [Pitault et al., 1994; Gupta et al., 2007] models have been extensively considered for the kinetic parameter estimation. During the optimization of kinetic parameters, several problems may occur, such as:

(i). rigorous convergence problems in cases where the number of parameters to be estimated are large.

(ii). initialization of the kinetic parameter values, that may converge to local minimum of the objective function usually given by the sum of square errors between experimental and predicted product yields.

Several approaches are available in the literature to overcome the above mentioned limitations. Oliveira and Biscaia (1989) first cracked the vacuum gas oil for the kinetic parameters estimation, and then separately cracked one of the product obtained after catalytic cracking of VGO, i.e. gasoline, for the estimation of other kinetic parameters. The approach was used to avoid the convergence problems in the kinetic parameter estimation during the catalytic cracking. Lappas et al. (1997) successfully applied the approach proposed by Oliveira and Viscaia (1989) for the kinetic parameters estimation. However, this approach has the several disadvantages, such as:

(i). large number of experiments have to be carried out for the kinetic parameter estimation.

(ii). large number of samples are required to carry out the experiments for understanding the cracking behaviour of some of the products. Though the samples are available, however they are not completely representative ones.

Hari et al. (1995) experimentally reported the gas oil conversion and product yields in a microactivity reactor at a constant catalyst–to–oil (C/O) ratio, reaction temperature and WHSVof 3.65, 528 ^{0}C and 10 h^{-1}, respectively. The kinetic parameters were estimated in the form of combined cracking and decay constants ($k_i\phi$) ,using a modified 3-lump kinetic model, where gas oil was considered as first lump; gasoline and middle distillates as second lump and; and combined coke and gas as third lump). First order reaction was assumed for the formation of gasoline and middle distillates and catalytic cracking while second order reaction was assumed

for gas oil to coke and gas cracking. The deviation between the experimental and predicted yields was obtained from 15 to 20%, which is quite high. The deactivation constant, to evaluate the kinetic parameters, was estimated using the approach proposed by Weekman et al. (1969).

Ancheyta et al. (1997) proposed a methodology for estimation of kinetic constants in catalytic cracking reactions. The newly proposed approach decreased the number of kinetic parameters to be estimated simultaneously, and therefore enhanced the accuracy of solution for the estimation of kinetic constants. They also carried out experiments at different reaction temperatures varying from 480–520 ^{0}C in a MAT unit. The 3–, 4–, and 5–lump kinetic models were used for estimation of kinetic parameters, and thus activation energies. They reported that the cracking reaction for gasoline can be neglected since the value of kinetic parameter is very less as compared to others.

Further, Ancheyta and Murillo (2000) proposed an approach for predicting product yields in a FCC process from experimental data obtained in a MAT unit. The predicted product yields were compared and validated with the experimental data of Wang et al. (1974). The kinetic constants were predicted using 4-lump kinetic model. The nonlinear regression analysis is not required for the estimation of kinetic parameter in the newly proposed model. The predicted and experimental yields were in good agreement with each other and the average deviations were less than 3%.

A sequential approach for estimation of kinetic constants, for cracking of gas oil, was proposed by Ancheyta and Sotelo (2000).The proposed scheme reduced the number of kinetic parameters to be estimated simultaneously, and hence reduce the convergence problems. A 5–lump model (VGO, LPG, dry gas, gasoline, and coke), derived from 3– and 4– lump kinetic models, and was used for kinetic parameter estimation. The cracking of gas oil was carried out in a MAT unit at different reaction temperatures and WHSV ranging from 480–500 °C and 6-48 h^{-1}. For the evaluation of kintic parameters using 5–lump kinetic model, from experimental data, three industrial feedstocks were used. A commercial equilibrium catalyst (E-CAT) was used for the evaluation of the kinetic parameters. A good agreement between the predicted and the experimental yields was obtained with average deviations < 2%.

In the present work, the approach proposed by Anchyeta et al. (1997) and Ancheyta and Murillo, 2000) has been used for the kinetic parameters estimation. A 5–lump model, derived from 3– and 4– lumps, was used to represent the experimental data. A set of new experiments

were carried out, catalytic cracking of VGO and coprocessing of FPO with VGO, for the kinetic parameters estimation by varying WHSV from 6–24 hr^{-1}, at a constant reaction temperature and C/O ratio of 530 $^{\circ}C$ and 5, respectively. The conditions were maintained to produce higher gasoline yields from vacuum gas oil by catalytic cracking over equilibrium FCC catalyst. The process parameters have been validated with the 4–lumped model proposed by Ancheyta et al. (2000) using Wang's (1970) experimental data. The theoretical approach for kinetic parameter estimation and validation with experimental data available in the literature has been discussed in the sections 6.2 and 6.3, respectively. The new experimental data and the kinetic parameters obtained with 4– and 5– lumps are discussed in sections 6.4 and 6.5, respectively.

6.2 STRATEGY FOR KINETIC PARAMETER ESTIMATION

The 5-lump kinetic model considered in the present study was adopted from the Ancheyta et al. (1997), as shown in Figure 6.1. In 5–lump kinetic model the refinery FCC products like dry gas (H_2, C1-C2 hydrocarbons), LPG (C3-C4 hydrocarbons), gasoline (C5-216 °C), coke and unconverted VGO, i.e. light cycle oil (216-370 °C) and heavy cycle oil (>370 °C) were considered as individual lumps. In a similar way, the model has nine kinetic constants, which includes one for catalyst deactivation.

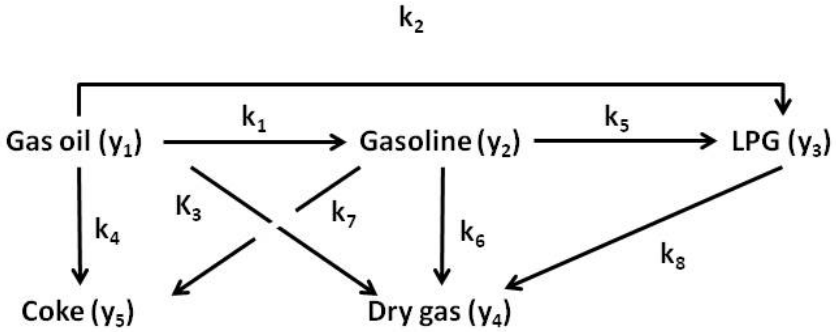

Figure 6.1: 5–lump kinetic model

Thus, the kinetic expression for rate of reaction (r_i) was put together as a function of kinetic constants (k_i), product yields (y_i) and deactivation function (φ). In which the catalytic cracking of vacuum gas oil was considered as second order reaction while LPG and gasoline were considered as first order reaction [Wang et al., 1970; Anchyeta et al., 1997; Ancheyta and Murillo, 2000; Ancheyta and Sotelo, 2000]. The overall rate of reaction for disappearance of gas oil and the rate of formation of gasoline, LPG, dry gas and coke are as follows:

$$\frac{dy_1}{dt} = -(k_1 + k_2 + k_3 + k_4)y_1^2\varphi \quad (6.1)$$

$$\frac{dy_2}{dt} = (k_1 y_1^2 - k_5 y_2 - k_6 y_2 - k_7 y_2)\varphi \quad (6.2)$$

$$\frac{dy_3}{dt} = (k_2 y_1^2 + k_5 y_2 - k_8 y_3)\varphi \quad (6.3)$$

$$\frac{dy_4}{dt} = (k_3 y_1^2 + k_6 y_2 + k_8 y_3)\varphi \quad (6.4)$$

$$\frac{dy_5}{dt} = (k_4 y_1^2 + k_7 y_2)\varphi \quad (6.5)$$

The catalyst decay function can be written as:

$$\varphi = e^{-k_d t_c} \quad (6.6)$$

It was assumed that the decay of catalyst follows the law of exponential; where t_c is time-on-stream. The catalyst deactivation coefficient (k_d) is the function of temperature and is given by Arrhenius-type equation. In the present work the kinetic parameters were estimated, for the 5-lump model, using a sequential method (Achentaya et al, 1997) in order to minimize the number of parameters to be estimated simultaneously.

6.2.1 Sequential Approach

In this approach few kinetic parameters were calculated from 3-lump model and then from 4-lump model. A few of them are in common with 5-lump model or can be easily calculated using 3– and 4– lump models. The sequential lumping is described in Figure 6.2. The 3-lump model basically involves cracking of gas oil or vacuum gas oil (y_1) into gasoline (y_2) and cluster of gas and coke (y_3) with gasoline subsequently cracking into the latter. The kinetic constant for VGO cracking into gasoline and cluster of gas and coke is common with 4-lump and 5-lump kinetic models. The rate equations for 3–lump model are mentioned below:

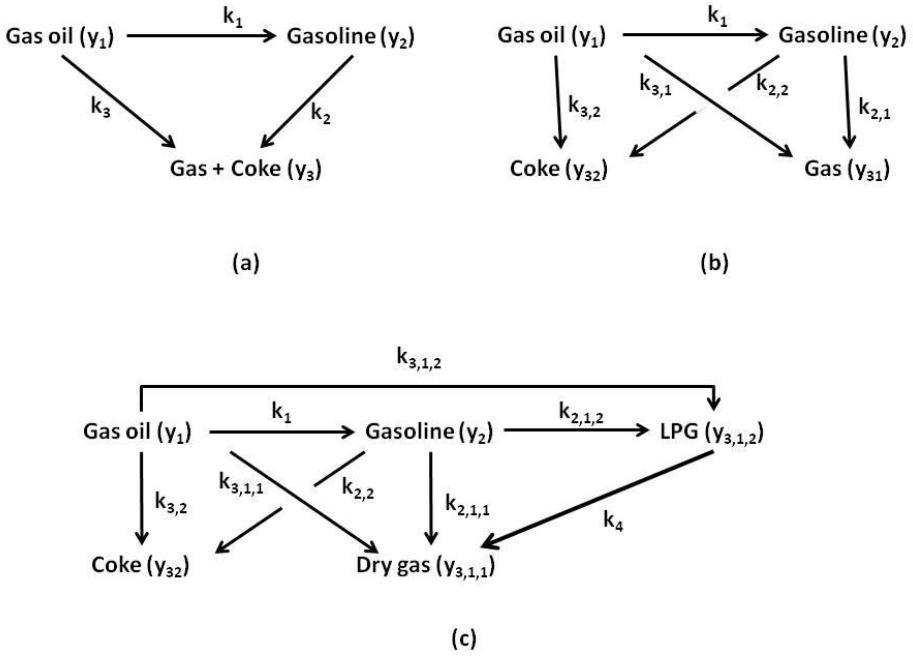

Figure 6.2: Sequential modelling approaches for 5–lump model

$$\frac{dy_1}{dt} = -(k_1 y_1^2 \emptyset + k_3 y_1^2 \emptyset) = -k_0 y_1^2 \emptyset; \quad k_0 = k_1 + k_3 \tag{6.7}$$

$$\frac{dy_2}{dt} = (k_1 y_1^2 - k_2 y_2)\emptyset \tag{6.8}$$

$$\frac{dy_3}{dt} = (k_3 y_1^2 + k_2 y_2)\emptyset \tag{6.9}$$

In 4-lump kinetic model the cluster of gas and coke is split into gas (y_{31}) and coke (y_{32}). The rate equations for gas and coke lumps are as follows:

$$\frac{dy_{31}}{dt} = (k_{31} y_1^2 + k_{21} y_2)\emptyset \tag{6.10}$$

$$\frac{dy_{32}}{dt} = (k_{32} y_1^2 + k_{22} y_2)\emptyset \tag{6.11}$$

In 5-lump kinetic model the cluster of gas is split into dry gas (y_{312}) and LPG (y_{311}). The rate equations for dry gas and LPG lumps are as follows:

$$\frac{dy_{311}}{dt} = (k_{311}y_1^2 + k_{211}y_2 + k_4 y_{312})\emptyset \tag{6.12}$$

$$\frac{dy_{312}}{dt} = (k_{312}y_1^2 + k_{212}y_2 - k_4 y_{312})\emptyset \tag{6.13}$$

The kinetic parameters were evaluated using a successive approach i.e. first by the 3–lump model, then by 4–lump model and then by the 5–lump model. In the 5–lump model there are 9 independent parameters to be determined, i.e. 8 kinetic constants and 1 deactivation constant. The number of independent parameters required to completely describe the 5–lump model are reported in Table 6.1.

Table 6.1 Lump models and the number of kinetic parameters associated with them

Sr. no.	Lump	No. of parameters
1	3 lump	4
2	4 lump	2
3	5 lump	3

In the present work the similar approach has been used for the estimation of kinetic parameters using lump modelling as suggested by Ancheyta and Murillo (2000) and Hari et al. (1995). According to the approach the equations were reformulated as follows (if *x* is conversion of gas oil then $x = 1–y_1$):

$$\frac{dy_1}{dx} = -1 \tag{6.14}$$

$$\frac{dy_2}{dx} = r_1 - r_2\frac{y_2}{y_1^2} \tag{6.15}$$

$$\frac{dy_3}{dx} = r_1 - r_3\frac{y_3}{y_1^2} \tag{6.16}$$

$$\frac{dy_{31}}{dx} = r_{31} + r_{21}\frac{y_2}{y_1^2} \tag{6.17}$$

$$\frac{dy_{32}}{dx} = r_{32} + r_{22}\frac{y_2}{y_1^2} \tag{6.18}$$

$$\frac{dy_{311}}{dx} = r_{311} + r_{211}\frac{y_2}{y_1^2} + r_4\frac{y_{312}}{y_1^2} \tag{6.19}$$

$$\frac{dy_{312}}{dx} = r_{312} + r_{212}\frac{y_2}{y_1^2} - r_4\frac{y_{312}}{y_1^2} \tag{6.20}$$

where

$$r_1 = \frac{k_1}{k_0}; \qquad r_2 = \frac{k_2}{k_0}; \qquad r_3 = \frac{k_3}{k_0}; \qquad r_4 = \frac{k_4}{k_0} \tag{6.21a}$$

$$r_{21} = \frac{k_{21}}{k_0}; \qquad r_{22} = \frac{k_{22}}{k_0}; \qquad r_{31} = \frac{k_{31}}{k_0}; \qquad r_{32} = \frac{k_{32}}{k_0} \tag{6.21b}$$

$$r_{211} = \frac{k_{211}}{k_0}; \qquad r_{212} = \frac{k_{212}}{k_0}; \qquad r_{311} = \frac{k_{311}}{k_0}; \qquad r_{312} = \frac{k_{312}}{k_0} \tag{6.21c}$$

The relation between different rates of reactions (r_i) are as follows:

$$r_1 + r_3 = 1; \quad r_3 = r_{31} + r_{32}; \qquad r_{31} = r_{311} + r_{312}; \qquad r_{21} = r_{211} + r_{212}; \qquad r_2 = r_{21} + r_{22} \tag{6.22}$$

Equations 6.14–6.16, 6.17–6.18 and 6.19–6.20 were derived from 3–, 4– and 5–lump models, respectively. These equations result into a total of 7 independent variables. The rest two independent variables were estimated from equations 6.7–6.12. For optimizing the required variables a non-linear regression analysis was carried out for the objective function:

$$S^2 = \sum_{i=1}^{i=N} \left(y_{exp} - y_{pred}\right)^2 / N \tag{6.23}$$

The values of 2 independent variables, i.e. r_1 and r_2, using equations 6.14–6.16, were obtained by nonlinear regression. Similarly, from 4–lump model, the values of r_{31} and r_{21} were estimated. Further, using 5–lump model, the values of r_{311}, r_{211} and r_4 were estimated. The values of k_0 and k_d were obtained from 5–lump model, where equations were used considering t as an independent variable. These two values combined with above obtained values of r's give other the independent values.

6.3 COMPARISON OF PRESENT PREDICTIONS WITH THE LITERATURE

The model developed was first validated with the work of Anchyeta and Morillo (2000), where the experimental data of Wang et al. (1974) were used. Anchyeta and Morillo (2000) used 4–lump modelling approach for the kinetic parameters estimation. The kinetic constant ratios and the kinetic parameters obtained from the present work have been compared with the predicted data of Anchyeta et al. (2000) and are shown in Tables 6.2 and 6.3, respectively. It can be seen from Tables 6.2 and 6.3, that there is approximately 5% deviation between the present predictions and Anchyeta et al (2000) work in kinetic constant ratios and kinetic parameters, which also validates the model used in the present work.

Table 6.2: Kinetic constant ratios obtained from present work and Anchyeta et al. (2000)

Kinetic constant ratio	r_1	r_2	r_{21}	r_{22}	r_{31}	r_{32}
Anchyeta et al. (2000)	0.7433	0.0458	0.0369	0.0088	0.1999	0.0568
Present work	0.7480	0.0436	0.0354	0.0082	0.1924	0.0596

Table 6.3: Rate of reactions and catalyst decay function obtained from present work and Anchyeta et al. (2000)

(Rate of reaction × Catalyst decay function)	$k_1\phi$	$k_2\phi$	$k_3\phi$	$k_{21}\phi$	$k_{22}\phi$	$k_{31}\phi$	$k_{32}\phi$	k_0
Anchyeta et al. (2000)	0.7116	0.0438	0.2458	0.0354	0.0084	0.1914	0.0544	0.9574
Present work	0.7302	0.0426	0.2460	0.0346	0.008	0.1878	0.0582	0.9762

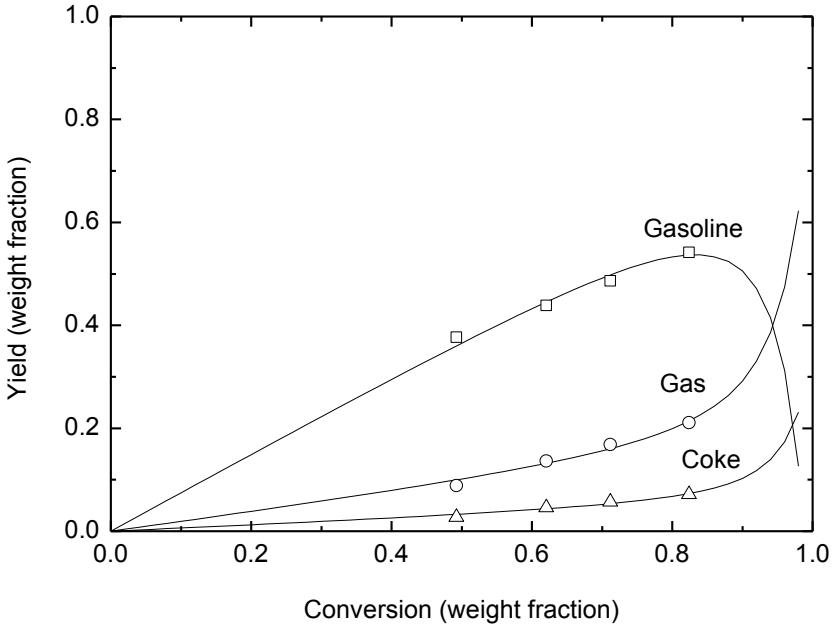

Figure 6.3 Comparison of product yields between the present predictions (lines) and experimental (symbols) data data reported in the literature (Wang et al. 1970).

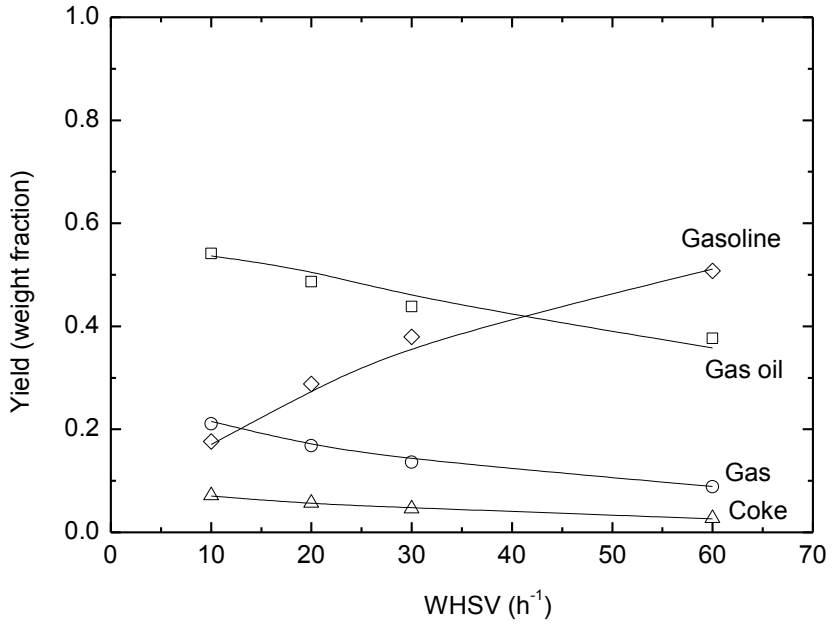

Figure 6.4 Comparison of gasoline, gas, and coke yields (weight fraction) with experimental (symbols) data reported in the literature (Wang, 1970).

Figures 6.3 and 6.4 show the comparison between the experimental data available in the literature and the present prediction for yields of gasoline, gas, and coke. The variation of products yields with conversion (weight fraction) and WHSV (hr^{-1}), can also be seen from Figure 6.3 and 6.4. The predicted products yields in the present work were found in good agreement with the values reported by Anchyeta and Murillo (2000). The average deviations in the products yields obtained from present and Anchyeta and Murillo (2000) work were less than 5%.

6.4 EXPERIMENTS FOR KINETIC PARAMETER ESTIMATION

The experiments were further performed, by varying the weight hourly space velocity (WHSV) from 6 to 24 h^{-1}, in order to finalize the process parameter towards the maximization of gasoline yield and collecting the process performance data for estimation of kinetic parameters. The experiments were carried out in an ACE-R unit; details are discussed in Chapter 3. The commercially available vacuum gas oil and an equilibrium fluid catalytic cracking catalysts was used for catalytic cracking experimental studies. To study the effect of WHSV on products yields, the WHSV was varied in the range of 6-24 h^{-1} by keeping constant C/O ratio (5) and reactor temperature (530 °C). The product distribution was quantified by their boiling point range as gas (H_2, C_1-C_5 hydrocarbons), dry gas (C_1-C_2 hydrocarbons), LPG (C_3-C_4 hydrocarbons), gasoline (IBP–216 °C), gas oil (> 216 °C) and coke, respectively. The product yields were calculated as weight percentage of the reactant. The Liquid products were analyzed by the chromatographic simulated procedure described by ASTM D-2887 method with an Agilent 6890 gas chromatograph, using a HP-1 methyl silicon column and a flame ionization detector. The product gases were analyzed with a Varian CP-3800 gas chromatograph equipped with three detectors, a flame ionization detector (FID) and two thermal conductivity detectors.

It was observed that the FCC conversion decreases linearly from 69 to 55 wt.% with an increase in space velocity from 6 to 24 h^{-1} (Table 6.4). It may be due to the steadily decrease in the yield of gasoline and gases (dry gas and LPG). The results indicated that the FCC conversion is function of space velocity on catalytic cracking of VGO over equilibrium FCC catalyst. Thus, lower space velocity lead to an increase in contact time of VGO over catalytic bed favors the FCC conversion. In a similar way the yield of coke also decreased from 6 to 4 wt.% with an

increase in space velocity. While the yield of LCO and HCO were increased from 18 to 24 wt.% and 11 to 19 wt.%, respectively, with increase in space velocity.

Table 6.4: Effect of WHSV on catalytic cracking of VGO products yields at 530 °C temperature and C/O ratio of 5

WHSV, hr^{-1}	**Dry gas, wt.%**	**LPG, wt.%**	**Gasoline, wt.%**	**LCO, wt.%**	**HCO, wt.%**	**Coke, wt.%**	**Con.%**	**VGO*, wt.%**
6	1.82	16.1	45.12	18.91	11.12	6.05	69.09	30.90
8	1.79	15.5	44.02	19.84	12.40	5.58	66.89	33.10
12	1.72	13.6	40.31	21.62	16.80	4.66	60.29	39.70
24	1.66	12.4	36.88	24.55	19.21	4.14	55.08	44.91

*i.e. unconverted or total yield of LCO and HCO

Further, it was observed that the FCC conversion decreases linearly from 77 to 63 wt.% with an increase in WHSV from 6 to 24 h^{-1} (Table 6.5) on co-processing of VGO with FPO at 5% blending ratio. The results indicated lower space velocity lead to an increase in contact time of FPO blended feed over catalytic bed, which favors the FCC conversion in similar to catalytic cracking of VGO. In a similar way, the yield of coke decreases from 5.9 to 4.8 wt.% with an increase in space velocity. While the yields of LCO and HCO were increased from 12 to 22 wt.% and 8 to 12 wt.%, respectively, with an increase in space velocity. However, the yield of LPG on co-processing of FPO with VGO is higher than direct processing of VGO.

Table 6.5: Effect of WHSV on catalytic cracking of VGO+FPO products yields at 530 °C temperature and C/O ratio of 5

WHSV, hr^{-1}	**Dry gas, wt.%**	**LPG, wt.%**	**Gasoline, wt.%**	**LCO, wt.%**	**HCO, wt.%**	**Coke, wt.%**	**Con.%**	**VGO*, wt.%**
6	2.49	39.12	30.12	12.34	7.98	5.96	77.69	22.31
8	2.18	38.87	29.03	14.88	8.05	5.48	75.56	24.44
12	2.02	33.82	27.67	18.43	10.91	5.19	68.7	31.3
24	1.83	29.46	26.94	22.32	12.59	4.89	63.12	36.88

*i.e. unconverted or total yield of LCO and HCO

6.5 KINETIC PARAMETER ESTIMATIONS

The similar approach has been used, as discussed in sections 6.2 and 6.4, for the estimation of kinetic parameters. The kinetic parameters were obtained considering both 4– and 5– lumps modeling approaches. The kinetic constant ratios and kinetic parameters with catalyst decay constant are reported in Tables 6.6 and 6.7, respectively. It can be seen that the kinetic constants for gasoline cracking were smaller as compared to the cracking of VGO, which shows the over-cracking of gasoline but in smaller extent. Further the more amount of coke is generated from gasoline as compared to the VGO, as can be seen from the small values kinetic constants for gasoline to coke and VGO to coke. While the amount of coke is generated more from VGO as compared to the gasoline which can be seen from the small values of kinetic constants for gasoline to coke and VGO to coke on co-processing VGO and FPO at 5% blending ratio.

The comparison between predicted and experimental yields obtained in the present work for 4– and 5–lumps is shown in Figure 6.5 and 6.7, respectively for VGO catalytic cracking; whereas Figure 6.9 and 6.10, respectively for co-processing of VGO with FPO at 5% blending ratio. It can be seen that the experimental and predicted product yields are in good agreement. Therefore, it can be concluded that the methodology used in the present work sufficiently predicts well the FCC product yields for the cases of VGO and VGO: FPO catyalytic cracking. The products yields with WHSV for 4– and 5–lumps are shown in Figure 6.6 and 6.8, respectively for VGO catalytic cracking; whereas 5-lumps is shown in Figure 6.10 for co-processing of VGO with FPO at 5% blending ratio and were found in good agreement with the experimental yields. The deviation between the predicted and experimental yields was less than 2%.

It can be seen that the gasoline yield is decreasing with an increase in WHSV, which can also be seen from Figure 6.6 and Figure 6.10. Typically, in a refinery FCC process it is aimed to maximize the gasoline yield, therefore the catalytic cracking of gas oil is avoided beyond the gasoline overcracking region (Wallenstein and Alkemade, 1996; Lappas et al., 1997; Mota and Rawet, 1995; Anchyeta et al., 1997, 2000, 2003). Though, in the present work the experiments were carried out well below the gasoline overcracking reaction, however, the gasoline yields can be sufficiently maximized for a given conversion level using 4– or 5–lump models with the estimation of kinetic parameters using the above mentioned approach (Figures 6.5–6.8). From the present analysis and the experimental results it can be concluded that the product yields

depend on the level of conversion of gas oil. Therefore, the experimental data obtained in the present work can be used for the development of kinetic model and the kinetic parameters estimation of the cracking reaction, which can be considered while designing and optimization of FCC reactor–regenerator system. Obviously, the hydrodynamics, heat balances have not been included in the proposed mathematical model, which exist in the industrial FCC units.

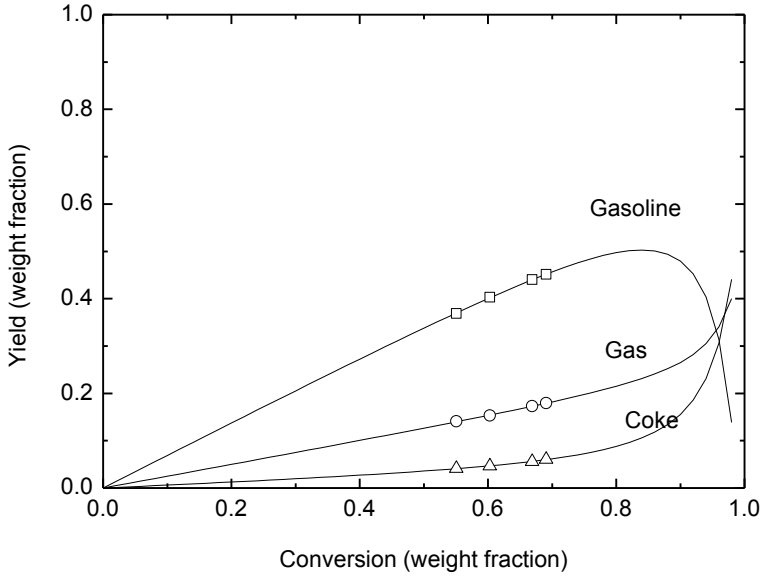

Figure 6.5 Variation of gasoline, gas, and coke yields with conversion and comparison with the experimental data at 530 °C temperature on catalytic cracking of VGO with 4-lump model

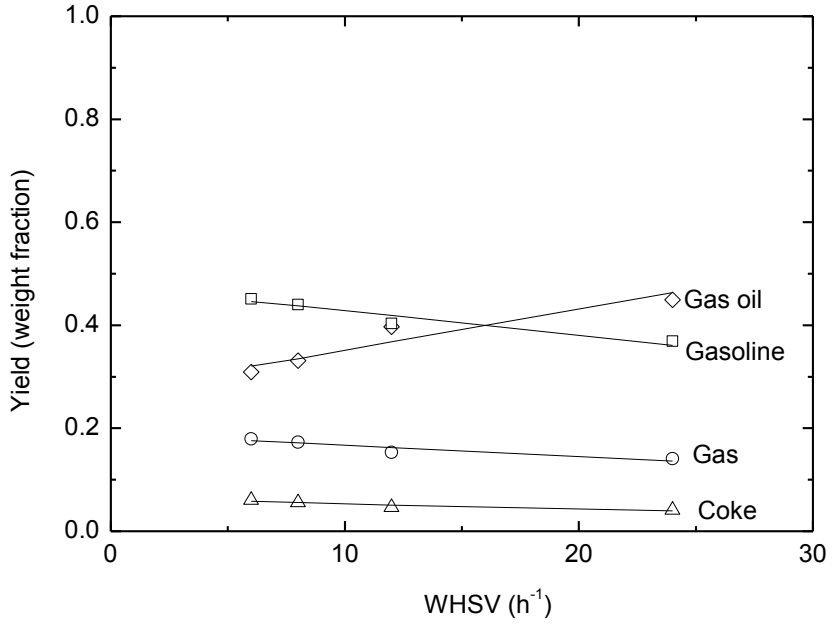

Figure 6.6: Variation of gasoline, gas, and coke yields with WHSV and comparison with the experimental data at 530 °C temperature on catalytic cracking of VGO with 4-lump model

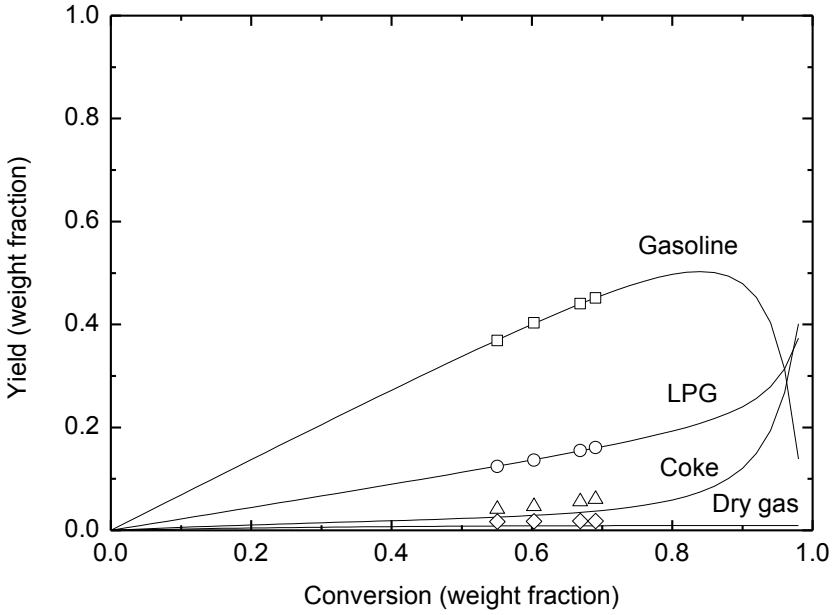

Figure 6.7: Variation of gasoline, gas, and coke yields with conversion and comparison with the experimental data at 530 °C temperature on catalytic cracking of VGO with 5-lump model

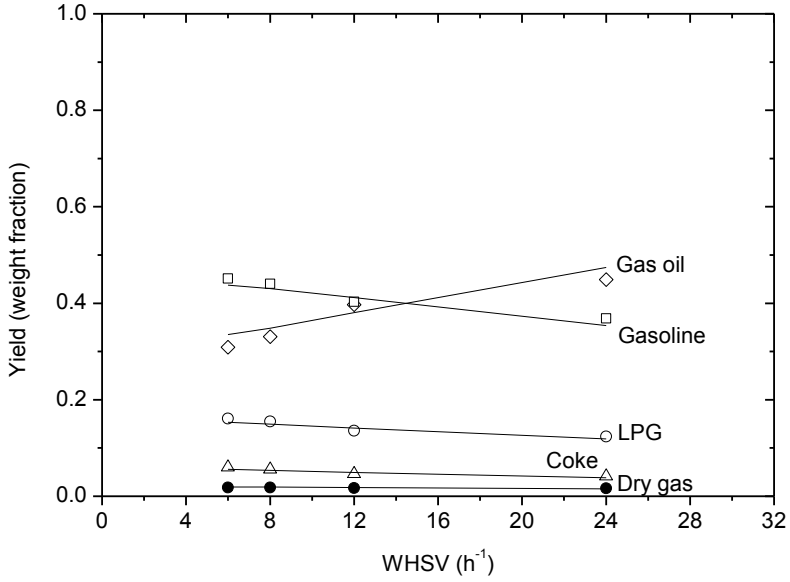

Figure 6.8: Variation of gasoline, gas, and coke yields with WHSV and comparison with the experimental data at 530 °C temperature on catalytic cracking of VGO with 5-lump model

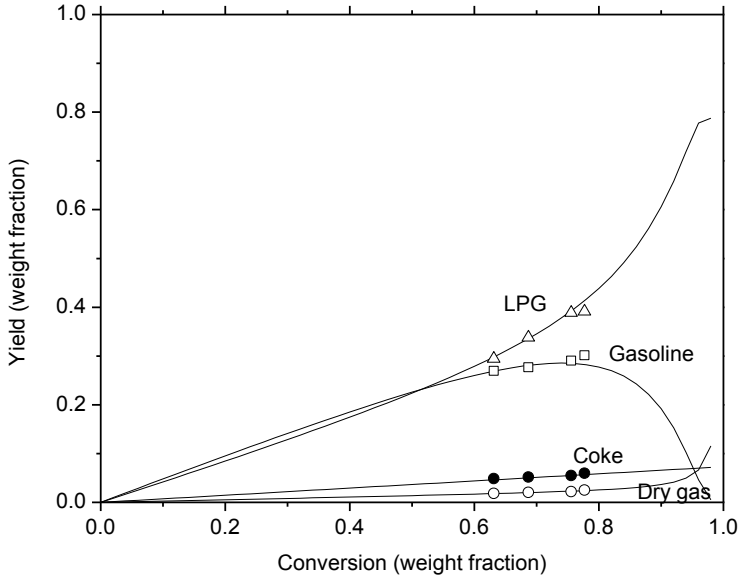

Figure 6.9: Variation of gasoline, LPG, dry gas and coke yields with conversion for catalytic cracking of VGO+FPO (95:5) and comparison with the experimental data at temperature and C/O ratio of 5 and 530 °C, respectively with 5-lump model.

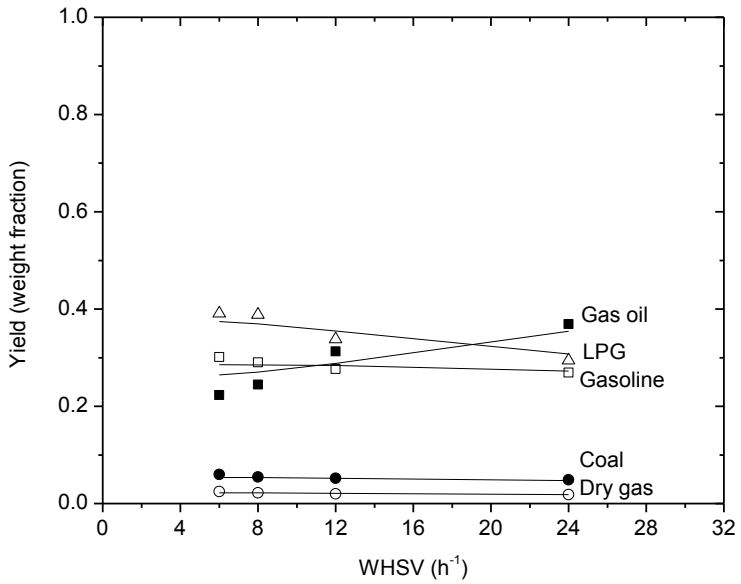

Figure 6.10: Variation of gasoline, LPG, dry gas and coke yields with WHSV (h^{-1}) for catalytic cracking of VGO+FPO (95:5) and comparison with the experimental data at temperature and C/O ratio of 5 and 530 °C 5, respectively with 5-lump model.

Table 6.6: Reaction rate ratio estimated for catalytic cracking of VGO and VGO with FPO at C/O ratio of 5 and 530 °C

Parameter	**4–lump model**	**5–lump model**	
	VGO	**VGO**	**VGO:FPO**
r_1	0.6898	0.6896	0.4838
r_2	0.0351	0.0349	0.1136
r_3			
r_{21}	0.0102		
r_{211}		0.0001	0.0015
r_{212}		0.004	0.1120
r_{22}	0.0248	0.0308	0.0001
r_{31}	0.2488		
r_{311}		0.0249	0.0265
r_{312}		0.229	0.4165
r_{32}	0.0613		
r_4		0.0063	0.0024

Table 6.7: Kinetic parameters estimated for catalytic cracking of VGO and VGO with FPO at C/O ratio of 5 and 530 °C

Parameter	**4–lump model**	**5–lump model**	
	VGO	**VGO**	**VGO:FPO**
k_1	0.4507	0.4536	0.56635
k_2	0.0229		
k_{21}	0.0067		
k_{211}		0.0001	0.0017
k_{212}		0.0026	0.1311
k_{22}	0.0162	0.0202	0.0001
k_3	0.2026		
k_{31}	0.1626		
k_{311}		0.164	0.0311
k_{312}		0.1506	0.4878
k_{32}	0.0401	0.0372	0.0856
k_4		0.0041	0.0029
k_d	0.2916	0.2864	0.4140

CHAPTER 7

CONCLUSIONS AND RECOMMENDATIONS

7.1 OBSERVATIONS

On the basis of studies carried out in this thesis for the co–processing of JCC–derived FPO with VGO in FCC unit to produce LPG and gasoline, following observations were made:

7.1.1 Catalytic Cracking of Vacuum Gas Oil (VGO)

- At first the process parameters, such as C/O ratio, reactor temperature, and weight hourly space velocity (WHSV), were optimized for maximum gasoline yield from catalytic cracking of vacuum gas oil (VGO) in advanced cracking evaluation FCC unit.
- The optimized process parameters for the maximum gasoline yield were as follows:
    - Catalyst-to-oil (C/O) ratio of 5,
    - Riser or reactor temperature of 530 °C
- The weight hourly space velocity (WHSV) of 8 h^{-1} and lower gives better FCC conversion.

7.1.2 Catalytic Cracking of VGO with Fast Pyrolysis Oil

- The heavy fraction of JCC-derived pyrolysis oil was highly oxygenated with 32 wt.% oxygen and contains char particles with the size of >200 nm, and hence, it cannot be directly processed in fluid catalytic cracking (FCC) process.
- However, on use of pretreatment techniques like membrane filtration helped in reducing the char particles in FPO to the size of 200 nm;
- On hydrodeoxygenation of FPO over Pd/Al_2O_3 helped in reducing the oxygen content to a value of 10 wt.% at the operating pressure of 80 bar and 300 °C.
- On co–processing of FPO with VGO, it was observed that the addition of FPO and HDO with VGO resulted into the total CH_3 carbon content remains same, and the amount of

long end chain CH_3 was lower in the case of co-processing of FPO (at 5:95 ratio) as compared to the co-processing of HDO (at 5:95 ratio).

- This finding was also reflected from the higher value of branchiness index (BI) in oil (at 5:95), which indicated that the product of FPO, co-processing with VGO, contains more iso-paraffinic CH_3 substructure, and the product of HDO, co-processing with VGO, contains more paraffinic CH_3 substructure.
- The coke yield was found to be within the limit (<6 wt.%), and in fact, lower than the pure VGO processing over the same equilibrium FCC catalyst.
- Further, it was envisaged that the HDO may be coprocessed instead of FPO with VGO at a lower blending ratio of up to 5:95 in the FCC unit without major modifications in the process configuration and catalyst if the demand for LPG is more, as is the case in India. In the feeds, H/C_{eff} was found to vary from 1.47 to 1.725.
- The aromatic protons varied from 15.5 to 21.69, with higher di-aromatic and polyaromatic protons in products for the blending ratios of 5: 95 and 10: 90.
- This indicated that the product of HDO, co-processing with VGO, contains more paraffinic CH_3 substructure, and the product of FPO, co-processing with VGO, contains more iso-paraffinic CH_3 substructure.

7.1.3 Catalytic Cracking of VGO with Pyrolysis Oil Model Compounds

7.1.3.1 Catalytic cracking of VGO with C2-C3 carbonyls

- It was observed that the acetol can be co–processed with VGO up to a blending ratio of 5:95 without major changes in the original FCC product slate; beyond that, the liquefied petroleum gas (LPG) range products were increased.
- It was observed that there is a limit for the co–processing of glycolaldehyde with VGO refinery fluid catalytic cracking unit, because of the increase in polyaromatics formation.
- It is required to improve the ability of FCC catalyst toward higher hydrogen transfer reactions (by adding more rare earths) to stop the over-cracking of liquid products if the blending is carried out beyond 5%.
- In another way, there is great scope to improve the yield of LPG by co–processing of acetol with VGO. Furthermore, to co-process the FPO with VGO in refinery FCC units to obtain better yields of LPGs the acetol can be separated from FPO.

7.1.3.2 Catalytic cracking of VGO with acetic acid and guaiacol

- An increase in coke and aromatics was observed, with an increase in C/O ratio, in the following order of guaiacol + VGO > acetic acid +VGO > VGO.
- Higher yields of light olefins, CO and CO_2 were observed while catalytic cracking of acetic acid +VGO with equilibrium FCC catalyst, subsequently light olefins were reduced in case of guaiacol + VGO as compared to other feeds.
- Therefore, it was recommended to separate the aromatic oxygenated compounds from pyrolysis oil before co-processing it with VGO in refinery FCC unit by keeping in mind the limitations of total aromatics and the benzene percentages in gasoline.
- Accordingly, a scheme was proposed for the co-processing of FPO in refinery FCC units. Thus, it was reported that the aliphatic oxygenates are easily crackable in the FCC process at lower blending ratios, whereas the aromatic hydrocarbons were not easily cracked.
- Further, it was proposed to first separate the aliphatic and aromatic oxygenates from the pyrolysis oil, either by solvent extraction or other techniques.
- This type of approach may help petroleum refineries to integrate it with fast pyrolysis process to increase the yield of LPG and, also, the valuable and most demanded petrochemical feedstock (i.e., propylene).

7.1.4 Catalytic Cracking of VGO with Glycerol

- In addition to pyrolysis oil, a second generation biofuel, a byproduct of first generation biofuels, i.e. glycerol, was catalytically cracked in direct processing and co-processing modes.
- On direct catalytic cracking of biomass-derived oxygenate, over equilibrium FCC catalyst, the conversion was 100 w/w% for the temperatures ranging from 470-550 °C in fluid catalytic cracking (FCC) unit.
- However, at lower temperatures, i.e. 350 and 390 °C, unconverted glycerol was found, which resulted into the decrease in the conversion at lower temperatures.
- The coke yield was increased from 7.7 to 10.4 wt.% with a decrease in temperature from 550 to 350 °C.

- The products like acetaldehyde, acrolein, 1, 2-propanediol, and unconverted glycerol were observed in the liquid products, while carbon dioxide, methane, ethane, ethylene, propane and propylene were found in the gas products.
- Further, the acetaldehyde yield increased from 18 to 53 wt.%, at a constant C/O ratio of 5 wt.%, with an increase in temperature from 350 to 550 °C; whereas maximum yield of acrolein, i.e. 7.6%, was obtained at lower temperature, i.e. 430 °C
- At higher temperatures, 100% glycerol conversion and more than 53% of acetaldehyde yield was achieved by operating a fluid catalytic cracking (FCC) process in block operation mode; whereas the maximum acrolein yield was observed at lower temperature, i.e. 430 °C.

7.1.5 Estimation of Kinetic Parameters for Catalytic Cracking of VGO

- A 5–lump kinetic model was used for kinetic parameters estimation for catalytic cracking of VGO with HDO by varying WHSV from 6–24 h^{-1}. The 5–lump modelling was carried out in sequential approach.
- The predicted product yields, obtained from 5–lump kinetic model, were in good agreement with the experimental yields. The deviation between the present experimental and predicted product yields was less than 2%.

7.2 CONCLUSIONS

On the basis of work carried out in this thesis for the co–processing of JCC–derived FPO with VGO in FCC unit, following conclusions were made:

- ❖ The char particles (leftover from cyclone) having size of > 200 nm can be separated from FPO by membrane filtration.
- ❖ The lignin-derived compounds like guaiacol, catechol and p-hydroxy phenyl groups were completely removed on hydrodeoxygenation of FPO over Pd/Al_2O_3 catalyst at 300 °C and 80 bar temperature and pressure, respectively.
- ❖ Due to incomplete cracking of lignin-derived monomers while co-processing FPO with VGO resulted to leftover of 8% more aromatics as compared to the co-processing of HDO (obtained at 300 °C) with VGO at 5:95 blending ratio.

- The gasoline yield obtained from co-processing of FPO with VGO is ~3% more than the value obtained from co-processing of HDO with VGO at constant blending ratio of 5.
- The LPG yield obtained from co-processing of FPO with VGO is ~10% more than the value obtained from co-processing of HDO with VGO at constant blending ratio of 5.
- The density of liquid obtained from co-processing of FPO with VGO is 0.932; whereas it is 0.925 on co-processing of HDO with VGO at constant blending ratio of 5.
- The total loss of carbon from biomass to final FCC hydrocarbons is on co-processing of HDO with VGO is 80.2%, i.e. the carbon leftover is 19.8%.
- The carboxylic acids (like acetic acid) can be completely cracked with VGO in FCC and its addition helps in increase in BI from 0.35 (100% VGO) to 0.38 (6% acetic acid).
- The aromatic compounds (like guaiacol) cannot be cracked in FCC; it produces benzene in the liquid distillate and decreases the BI value from 0.35 (100% VGO) to 0.32 (12.4% guaiacol).
- A decrease in fraction of aromaticity (f_a) can be seen from 0.54 to 0.46 with increase in blending ratio of acetol from 5 to 15% with VGO.

7.3 RECOMMENDATIONS

On the basis of the present study, the following recommendations can be made for the future study:

1. It is better to separate the pyrolysis oil into various fractions and then co–process the individual fractions with petroleum-derived fractions in refinery units like fluid catalytic cracking (FCC), steam reforming, and hydrocracking unit.
2. The FCC catalyst is able to crack straight chain hydrocarbons or oxygenates of pyrolysis oil. Therefore, it is recommended to co–process the aliphatic oxygenates with VGO in FCC process after separating the compounds of lignin-derived monomers.
3. The steam reforming unit of refineries is able to crack the aqueous fraction of pyrolysis oil and the produced hydrogen can be utilized for the refinery utilization and make it economical.
4. The lignin-derived monomers or aromatic fraction of pyrolysis oil can be cracked in hydrocracking unit along with petroleum-derived fractions.

5. It is very much essential to develop the specific catalysts for the co–processing in refinery units like FCC, steam reforming and hydrocracking unit.
6. Integrations of pyrolysis process with refinery units would give an opportunity in reducing the processing and transportation costs of biomass-derived oxygenates while co–processing.
7. It can be recommended that the co–processing of pyrolysis oil with petroleum-derived fraction is feasible by means of effective utilization of refinery's infrastructure without major modifications.

REFERENCES

Abdel-A, H.K.; Mohamed, A.; Fahim, M.A., Petroleum and Gas Field Processing Handbook. Marcel Dekker Inc., New York, Basel, 317-329, **2003**.

Adam, J.; Antonakou, E.; Lappas, A.; Stocker, M.; Nilsen, M.H.; Bouzga, A.; Hustad, J.E.; Oye, G., In situ catalytic upgrading of biomass derived fast pyrolysis vapours in a fixed bed reactor using mesoporous materials. *Microporous and Mesoporous Materials*, 96, 93–101, **2006**.

Adjaye, J.D.; Bakhshi, N.N., Production of hydrocarbons by catalytic upgrading of a fast pyrolysis bio-oil, Part II: comparative catalyst performance and reaction pathways. *Fuel Process. Technol.*, 45, 185–202, **1995a**.

Adjaye, J.D.; Bakhshi, N.N., Production of hydrocarbons by catalytic upgrading of a fast pyrolysis bio-oil. *Fuel Process. Technol.*, 45, 161–183, **1995b**.

Adjaye, J.D.; Katikaneni, S.P.R.; Bakhshi, N.N., Catalytic conversion of a biofuel to hydrocarbons: effect of mixtures of HZSM-5 and silica-alumina catalysts on product distribution. *Fuel Process. Technol.*, 48, 115–143, **1996**.

Agblevor, F.A.; Besler, S., Inorganic Compounds in Biomass Feedstocks, 1, Effect on the Quality of Fast Pyrolysis Oils. *Energy & Fuels*, 10, 2, 293-298, **1996**.

Aguado, R.; Olazar, M.; San Jose, M.J.; Aguirre, G.; Bilbao, J., Pyrolysis of sawdust in a conical spouted bed reactor: Yields and product composition. *Ind. Eng. Chem. Res.*, 39, 1925-1933, **2000**.

Ahmaruzzaman, M.; Sharma, D.K., Non-isothermal kinetic studies on co-processing of vacuum residue, plastics, coal and petrocrops. *J. Anal. Appl. Pyrol.*, 73, 263-275, **2005**.

Ahmaruzzaman, M.; Sharma, D.K., Co-processing of petroleum vacuum residue with plastics, coal and biomass and its synergistic effects. *Energy & Fuels*, 21, 2, 891-897, **2007a**.

Ahmaruzzaman, M.; Sharma, D.K., Kinetic studies on co-cracking of petroleum vacuum residue

with biomass (petrocrop). *Petro. Sci. Tech.*, 25, 925-936, **2007b**.

Ahmaruzzaman, M.; Sharma, D.K., Chemical reaction engineering studies on co-cracking of petroleum vacuum residue with coal, plastics and biomass (bagassse and petrocrop). *Petro. Sci. Tech.*, 25, 937-947, **2007c**.

Ahmaruzzaman, M.; Sharma, D.K., Characterisation of liquid products obtained from co-cracking of petroleum vacuum residue with coal and biomass. *J. Anal. Appl. Pyrol.*, 81, 1, 37-44, **2008**.

Ahmaruzzaman, M.; Sharma, D.K., TG-DTA studies on cracking of petroleum vacuum residue and co-cracking with plastics, coal and biomass. *Energy Sources, Part A*, 35, 17, 1670-1679, **2013**.

Alhajri, I.; Alper, E.; Is, G.; Fung, J.; Lo, J.; Yanez, K.; Elkamel, A., Optimization Model for the Integration of Biomass into a Conventional Oil Refinery. In Proceedings of International Conference on *Ind. Eng. Ope. Man*., Indonesia, January **2014**.

Altgelt ,K. H.; Boduszynski, M.M., Composition and Analysis of Heavy Petroleum

Fractions. Marcel Dekker, New York, 393-484, **1994**.

Ancheyta-Juarez, J., A strategy for kinetic parameter estimation in the fluid catalytic cracking process. *Ind .Eng. Chem. Res.*, 36, 12, 5170–5174, **1997**.

Ancheyta-Juarez, J.; Lopez-Isunza, F.; Anguilar-Rodriguez, E., 5-Lump kinetic model for gas oil catalytic cracking. *Appl. Catal. A: General*, 177, 227-235, **1999**.

Ancheyta-Juarez, J.; Murillo-Hernandez, J.A., A simple method for estimating gasoline, gas, and coke yields in FCC processes. *Energy & Fuel*, 14, 2, 373-379, **2000**.

Ancheyta-Juarez, J.; Sotelo-Boyas, R., Estimation of kinetic constants of a five-lump model for fluid catalytic cracking process using simpler sub-models. *Energy & Fuel*, 14, 6, 1226-1231, **2000**.

Anh., Simultaneous cracking of phenolic compounds and hydrocarbons over zeolites. PhD

Thesis, Norman, Oklahama, **2014.**

Arbogast, S.V., Preferred Paths for Commercializing Pyrolysis Oil at Conventional Refineries, Deliverable 1, Quality Considerations for the Transport and Processing of Pyrolysis Oil in Existing Petroleum Refineries. Global Energy Management Institute: Houston, TX, In press as an NREL report, **2008**.

Ardiyanti, A.R.; Ermakov, D.; Heeres, H.J.; Khromova, S.; Parmon, V.; Venderbosch, R.H., Process for the hydrotreatment of vegetal materials. Patent: WO 2012030215 A1, March **2012**.

Ardiyanti, A.R., Hydrotreatment of fast pyrolysis oils: Catalyst development and process-product relations. Ph.D Thesis, University of Groningen, Netherlands, **2013**.

Arenillas, A.; Pevida, C.; Rubiera, F.; Palacios, J.M.; Navarrete, R.; Denoyel, R.; Rouquerol, J.; Pis, J.J., Surface characterization of synthetic coal chars made from model compounds. *Carbon*, 42, 1345–1350, **2004**.

Azad, F.S.; Salehi, E.; Abedi, J.; Harding, T., Biomass to hydrogen via catalytic steam reforming of bio-oil over Ni-supported alumina catalysts. *Fuel Process. Technol.*, *92*, 563-569, **2011**.

Azeez, A.M.; Meier, D.; Odermatt, J.; Willner, T., Fast Pyrolysis of African and European Lignocellulosic Biomasses Using Py-GC/MS and Fluidized Bed Reactor. *Energy & Fuels*, 24, 2078–2085, **2010**.

Baldauf, W.; Balfanz, U.; Rupp, M., Upgrading of flash pyrolysis oil and utilization in refineries. *Biomass Bioenergy*, 7, 237–244, **1994**.

Behera, B.; Ray, S.S.; Singh, I.D., Structural characterization of FCC feeds from Indian refineries by NMR spectroscopy. *Fuel*, 87, 2322–2333, **2008**.

Behera, B.; Ray, S.S.; Singh, I.D., NMR studies of FCC feeds, catalysts and coke. Chapt.12, Fluid Catalytic Cracking VII: Materials, Methods and Process Innovations, Studies in Surface Science and Catalysis, Elsevier B.V. Publishers, 166, 163-200. **2007**.

Ben, H.; Ragauskas, A.J., One step thermal conversion of lignin to the gasoline range liquid

products by using zeolites as additives. *RSC Advances*, 2, 12892–12898, **2012**.

Bertero, M.; Puente, G.; Sedran, U., Effect of Pyrolysis Temperature and Thermal Conditioning on the Coke-Forming Potential of Bio-oils. *Energy & Fuels*, 25, 1267–1275, **2011**.

Blackadder, W.; Rensfelt, E.A., Pressurized thermo-balance fro pyrolysis and gasification studies of biomass, wood and peat. In Fundamentals of Thermochemical Biomass Conversion. Overend, R.P.; Milne, T.A.; Mudge, L.K., Eds.; Elsevier Applied Science Publishers, London, 747-759, **1985**.

Bollas, G.M.; Lappas, A.A.; Iatridis,D.K.; Vasalos, I.A., Five-lump kinetic model with selective catalyst deactivation for the prediction of the product selectivity in the fluid catalytic cracking process. *Catal. Today*, 127, 31–43, **2007**.

Borosiac, S.; Doczekalska, B., X-ray diffraction studies of pine wood treated with KOH. *Fibers & Textiles Eastern Europe*, 13, 87-89, **2005**.

Boucher, M.E.; Chaala, A.; Roy, C., Bio-oils obtained by vacuum pyrolysis of softwood bark as a liquid fuel for gas turbines, Part I: properties of bio-oil and its blends with methanol and a pyrolytic aqueous phase. *Biomass Bioenergy*, 5, 19, 337–350, **2000**.

Branca, C.; Giudicianni, P.; Blasi, C.D., GC/MS Characterization of Liquids Generated from Low-Temperature Pyrolysis of Wood. *Ind. Eng. Chem. Res.*, 42, 14, 3190–3202, **2003**.

Branca, C.; Blasi, C.D., Multistep Mechanism for the Devolatilization of Biomass Fast Pyrolysis Oils. *Ind. Eng. Chem. Res.*, 45, 5891-5899, **2006**.

Brem, G.; Bramer, E.A., PyRos: a new flash pyrolysis technology for the production of bio-oil from biomass residues. www.tno.nl/Full Paper Biomass Conference, Singapore, **2007**.

Brown, J.K.; Ladner, W.R., A study of the hydrogen distribution in coal like materials by high-resolution nuclear magnetic resonance spectroscopy II – a comparison with infrared measurement and the conversion to carbon structure. *Fuel*, 39, 87–96, **1960**.

Brown, J.N., Development of a lab-scale auger reactor for biomass fast pyrolysis and process optimization using response surface methodology. Graduate Thesis and Dissertations.

Paper 10996, **2009**.

Brown, R.C., Thermochemical Processing of Biomass: Conversion into Fuels, Chemicals and Power. John Wiley & Sons Publishers, March **2011a**.

Brown, R.C.; Smith, R., A systems approach to bio-oil stabilization. Prepared by Iowa State University under the contract DG-FG36-08G018205, **2011b**.

Bulushev, D.A.; Ross, J.R.H., Catalysis for conversion of biomass to fuels via pyrolysis and gasification: A review. *Catalysis Today*, 171, 1– 13, **2011**.

Bustin, R.M.; Guo, Y., Abrupt changes (jumps) in reflectance values and chemical compositions of artificial charcoals and inertinite in coals. *Int. J. Coal Geol.*, 38, 237–260, **1999**.

Cantor, D.M., Nuclear magnetic resonance spectrometric determination of average molecular structure parameters for coal-derived liquids. *Anal. Chem.*, 50, 8, 1185–1187, **1978**.

Cantu, T.S.; Daugaard, D.E.; Gong, K.; Platon, A., Integrated fcc biomass pyrolysis/upgrading. Patent No. WO2012091815 A1, **2012**.

Carlson, T.R.; Vispute, T.P.; Huber, G.W., Green Gasoline by Catalytic Fast Pyrolysis of Solid Biomass Derived Compounds. *Chem. Sus. Chem.*, 1, 397 – 400, **2008**.

Carlson, T.R., Catalytic fast pyrolysis of biomass for the production of fuels and chemicals. Doctoral Dissertation, University of Massachusetts, **2010**.

Carlson, T.R.; Cheng, Y.T.; Jae, J.H.; Huber, G.W., Production of green aromatics and olefins by catalytic fast pyrolysis of wood saw dust. *Energy Environ. Sci.*, **4**, 145–161, **2011**.

Channiwala, S.A; Parikh, P.P., A unified correlation for estimating HHV of solid, liquid and gaseous fuels. *Fuel*, 81, 1051-1063, **2002**.

Chen, N.Y.; Degnan, J.T.F.; Koenig, L.R., Liquid Fuel from Carbohydrates. *Chem. Tech.*, 16, 506-511, **1986**.

Chen, N.Y.; Walsh, D.E.; Koenig, L.R., Fluidized-bed upgrading of wood pyrolysis liquids and related-compounds. In Pyrolysis Oils from Biomass; Soltes, J.; Milne, T.A.; Eds.;

American Chemical Society: Washington, DC, USA, 277–289, **1988**.

Chen, B.; Johnson, E.J.; Chefetz, B.; Zhu, L.; Xing, B., Sorption of polar and nonpolar aromatic organic contaminants by plant cuticular materials: the role of polarity and accessibility. *Environ. Sci. Technol.*, 39, 6138–6146, **2005**.

Chen, T.; Wu, C.; Liu,R.; Fei,W.; Liu, S., Effect of hot vapor filtration on the characterization of bio-oil from rice husks with fast pyrolysis in a fluidized-bed reactor. *Bioresource Technol.*, 102, 6178–6185, **2011**.

Chen, T.; Wu, C.; Liu, R., Steam reforming of bio-oil from rice husks fast pyrolysis for hydrogen production. *Bioresource Technol.*, 102, 9236-9240, **2011**.

Chun, Y.; Sheng, G.Y.; Chiou, C.T.; Xing, B.S., Compositions and sorptive properties of crop residue-derived chars. *Environ. Sci. Technol.*, 38, 4649–4655, **2004**.

Churin, E.; Grange, P.; Delmon, B., Quality Improvement of Pyrolysis Oils. Final report on contract no. EN3B-0097-B for the Directorate-General Science, Research and Development, Commission of the European Communities, **1989**.

Clutter, D.R.; Petrakis, L.Z.; Stenger, R.L.; Jensen, R.K., Carbon-13 and proton nuclear magnetic resonance characterizations in terms of average molecule parameters. *Anal. Chem.* 44, 8, 1395–1405, **1972**.

Corella, J.; Frances, E., Analysis of the Riser Reactor of a Fluid Cracking Unit Model Based on Kinetics of Cracking and Deactivation from Laboratory Tests. Fluid Catalytic Cracking II: *ACS Symposium Series*, Chapter 10, 452, 165–182, **1991**.

Corma, A.; Martinez, C.; Ketley, G.; Blair, G.; On the mechanism of sulfur removal during catalytic cracking. *Appl. Catal. A*, 208, 135-152, **2001**.

Corma, A.; Huber, G.W.; Sauvanaud, L.; Connor, P.O., Processing biomass-derived oxygenates in the oil refinery: Catalytic cracking (FCC) reaction pathways and role of catalyst**.** *J. Catal.*, 247, 307–327, **2007**.

Corma, A.; Huber, G.W.; Sauvanaud, L.; Connor, P.O., Biomass to chemicals: Catalytic

conversion of glycerol/water mixtures into acrolein, reaction network. *J. Cat.*, 257, 163–171, **2008**.

Coxon, P.G.; Bischoff, K.B., Lumping strategy: Introduction techniques, and application of cluster analysis. *Ind. Eng. Chem. Res.*, 26, 1239-1248, **1987**.

Das, A.K.; Bhattacharyya, D.; Mandal, S.; Murthy, V.L.N.; Singh, S.; Rao, M.R.; Ghosh, S., Fluid catalytic cracking process, Patent US 6267873 B1, July **2001**.

Das, P.; Ganesh, A., Bio-oil from pyrolysis of cashew nut shell—a near fuel. *Biomass & Bioenergy*, 25, 1, 113-117, **2003**.

Das, P.; Ganesh, A.; Wangikar, P., Influence of pretreatment for deashing of sugarcane bagasse on pyrolysis products. *Biomass & Bioenergy*, 27, 5, 445-457, **2004a.**

Das, P.; Sreelatha, T.; Ganesh, A., Bio oil from pyrolysis of cashew nut shell-characterisation and related properties. *Biomass & Bioenergy*, 27, 3, 265-275, **2004b.**

Decroocq, D., Catalytic Cracking of Heavy Petroleum Fractions. Imprimerir Louis-Jean, Paris, **1984**.

Demirbas, A., Biorefineries: For biomass upgrading facilities. *Green Energy and Technol.*, 75-92, **2010**.

Dewachtere, N. V.; Santaella, F.; Froment, G. F., Application of a Single Event Kinetic Model in the Simulation of an Industrial Riser Reactor for the Catalytic Cracking of Vacuum Gas Oil. Chem. Eng. Sci., 54, 3653-3660, 1999.

Dickerson, T.; Soria, J., Catalytic Fast Pyrolysis: A Review. *Energies*, 6, 514-538, **2013**.

Diebold, J.P.; Chum, H.L.; Evans, R.J.; Milne, T.A.; Reed, T.B.; Scahill, J.W., Low pressure upgrading of primary pyrolysis oils from biomass and organic wastes. In: Klass, D.L., Eds., Energy from Biomass and Wastes, Elsevier Applied Sciences Publishers, London, 801-830, **1987**.

Diebold, J.P.; Scahill, J., Biomass to gasoline: upgrading pyrolysis vapors to aromatic gasoline with zeolites catalysis at atmospheric pressure. In: Soltes, E.J.; Milne, T.A., Eds., Pyrolysis Liquids from Biomass, ACS, Washington, DC, 264–276, **1988**.

Diebold, J.P.; Scahill, J.W.; Czernik, S.; Phillips, S.D.; Feik, C.J., Progress in the production

of hot gas filtered biocrude oil at NREL. Technical repot no. NREL/TP-431-7971, May **1995**.

Diebold, J. P., Czernik, S., Additives to Lower and Stabilize the Viscosity of Pyrolysis Oils during Storage. *Energy & Fuels*, 11, 1081-1091, **1997**.

Diebold, J.P., A review of the chemical and physical mechanisms of the storage stability of fast pyrolysis bio-oils. In Fast pyrolysis of biomass: A handbook, CPL Press: Newbury, UK, **2005**.

Dinda, S.; Chintala,P.K.; Gohel, A.; Yadav, A.; Mandal, S.; Ravichandran,G.; Das,A.K., Process and composition of catalyst/additive for reducing fuel gas yield in fluid catalytic cracking (FCC)process. Patent US 2014/0116923 A1, May 1, **2014**.

Doddrell, D.M.; Pegg, D.T.; Bendall, M.R., Distortionless Enhancement of NMR Signals by Polarization Transfer. *J. Magnetic resonance*, 48, 323-327, **1982**.

Dudley, B., BP Energy Outlook 2035. http://www.bp.com/content/dam/bp/pdf/ Energy-economics/Energy-Outlook/Energy Outlook 2035 booklet. pdf (accessed on 23rd May, 2014), January **2014**.

Dung, N.A.; Klaewkla, R.; Wongkasemjit, S.; Jitkarnka, S., Light olefins and light oil production from catalytic pyrolysis of waste tire. *J. Anal. Appl. Pyrolysis*, 86, 281–286, **2009**.

Dupain, X.; Gamas, E. D.; Madon, R.; Kelkar, C. P.; Makkee, M.; Moulijn, J. A., Aromatic gas oil cracking under realistic FCC conditions in a microriser reactor. *Fuel*, 82, 1559–1569, **2003**.

Efremova, S.V.; Korolev, Y.M.; Sukharnokov, Y.I., X-ray Diffraction Characterization of Silicon–Carbon Nanocomposites Produced from Rice Husk and Its Derivatives. *Doklady chemistry*, 419:77-80, **2008**.

Eissen, M.; Metzger, J.O.; Schmidt, E.; Schneidewind, U., 10 Years after Rio-Concepts on the Contribution of Chemistry to a Sustainable Development. *Angew. Chem.*, 114, 402−425, **2002**.

Elliott, D.C.; Baker, E.G., Upgrading biomass liquefaction products through hydrodeoxygenation. *Biotech. Bioeng. Symp.*, 14, 159–174, **1984**.

Elliott, D. C.; Schiefelbein, G. F., Liquidhydrocarbon fuels from biomass. Abstracts of papers of the American Chemical Society, 34, 1160–1166, **1989**.

Elliott, D.C.; Neuenschwander, G.G., Liquid fuels by low-severity hydrotreating of biocrude. In: Developments in Thermochemical Biomass Conversion, Bridgwater, A.V.; Boocock, D. G. B., eds., Blackie Academic & Professional, London, 1, 611-621, **1996**.

Elliott, D.C., Historical Developments in Hydroprocessing Bio-oils. *Energy & Fuels*, 21, 1792-1815, **2007**.

Elliott, D.C.; Hart, T.R.; Neuenschwander, G.G.; Rotness, L.J.; Zacher, A.H., Catalytic hydroprocessing of biomass fast pyrolysis bio-oil to produce hydrocarbon products. *Environ. Prog. Sus. Energy***,** 28, 3, 441–449, **2009**.

Elliott, D.C.; Lee, S.J.; Hart, T.R., Stabilization of Fast Pyrolysis Oil: Post Processing. PNNL Report No. 21549 prepared for US DOE under contract DE-AC05-76RL01830, March **2012a**.

Elliott, D.C.; Hart, T.R.; Neuenschwander, G.G.; Rotness, L.J.; Olarte, M.V.; Zacher, A.H.; Solantausta, Y., Catalytic hydroprocessing of fast pyrolysis bio-oil from pine sawdust. *Energy & Fuels*, 26, 6, 3891–3896, **2012b**.

Figueiredo, J.L.; Pereira, M.F.R.; Freitas, M.M.A.; Órfão, J.J.M., Modification of the surface chemistry. *Carbon*, 37: 1379–1389, **1999.**

Fogassy, G.; Thegarid, N.; Schuurman, Y.; Mirodatos, C., From biomass to bio-gasoline by FCC co-processing: effect of feed composition and catalyst structure on product quality. *Energy Environ. Sci*., 4, 5068-5076, **2011**.

Fogassy, G.; Thegarid, N.; Toussaint, G.; van Veen, A. C.; Schuurman, Y.; Mirodatos, C., Biomass derived feedstock co-processing with vacuum gas oil for second-generation fuel production in FCC units, *Appl. Catal., B*, 96, 476−485, **2010**.

French, R.; Czernik, S., Catalytic pyrolysis of biomass for biofuels production. *Fuel Process. Technol.*, 91, 25-32, **2010**.

French, R.J.; Stunkel, J.; Baldwin, R.M., Mild Hydrotreating of Bio-Oil: Effect of Reaction Severity and Fate of Oxygenated Species. *Energy & Fuels*, 25, 3266–3274, **2011**.

Fu, C.M.**;** Schaffer, A.M., Effect of nitrogen compounds on cracking catalysts. *Ind. Eng. Chem. Prod. Res. Dev.*, 1, 68-75, **1985**.

Fu, P.; Hu, S.; Xiang, J.; Sun, L.; Li, P.; Zhang, J.; Zheng, C., Pyrolysis of maize stalk on the characterization of chars formed under different devolatilization conditions. *Energy & Fuels*, 23, 4605-4611, **2009**.

Garcia-Perez, M.; Chen, S.; Zhou, S.; Wang, Z.; Lian, J.; Johnson, R.L.; Liaw, S.; Das, O., New bio-refinery concept to convert soft bark wood to transport fuels. Washington State University, Ecology Pyblication.09-07-061, **2009**.

Gayubo, A.G.; Aguayo, A.T.; Atutxa, A.; Aguado, R.; Bilbao, J., Transformation of oxygenate components of biomass pyrolysis oil on a HZSM-5 zeolite.I. Alcohols and phenols. *Ind. Eng. Chem. Res.*, 43, 2610–2618, **2004a**.

Gayubo, A.G.; Aguayo, A.T.; Atutxa, A.; Aguado, R.; Olazar, M.; Bilbao, J., Transformation of oxygenate components of biomass pyrolysis oil on a HZSM-5 zeolite. II. aldehydes, ketones, and acids. *Ind. Eng. Chem. Res.*, 43, 2619–2626, **2004b**.

Gayubo, A.G.; Aguayo, A.T.; Atutxa, A.; Valle, B.; Bilbao, J.; Gayubo, A.G.; Aguayo, A.T.; Atutxa, A.; Valle, B.; Bilbao, J., Undesired components in the transformation of biomass pyrolysis-oil into hydrocarbons on a HZSM-5 zeolite. *J.Chem. Technol. Biotechnol.*, 80, 11, 1244-1251, **2005**.

Gomez-serrano, A.; Pastro-Villegas, J.; Perez-Florindo., A.; Duran-valle, C.; Valenzuela-calahorro, C., FT-IR study of rockrose and of char and activated carbon. *J. Anal. Appl. Pyrol.*, 36, 1, 71–80, **1996**.

Gopakumar, S.T.; Adhikari, S.; Gupta, R.B.; Tu, M.; Taylor, S., Production of hydrocarbon fuels

from biomass using catalytic pyrolysis under helium and hydrogen environments. *Bioresource Technol.*, 102, 6742–6749, **2011**.

Goyal, N.; Gupta, R.; Pant, K. K., Hydrogen production by steam reforming of model bio-oil using structured Ni/Al2O3 catalysts. *Inter. J. Hydrogen Energy*, 38, 921-933, **2013**.

Graca, I.; Comparot, J.D.; Laforge, S.; Magnoux, P.; Lopes, J.M.; Ribeiro, M.F.; Ribeiro, F.R., Influence of phenol addition on the H-ZSM-5 zeolite catalytic properties during methylcyclohexane transformation. *Energy & Fuels*, 23, 4224–4230, **2009a**.

Graca, I.; Comparot, J.D.; Laforge, S.; Magnoux, P.; Lopes, J.M.; Ribeiro, M.F.; Ribeiro, F.R., Effect of phenol addition on the performances of H-Y zeolite during methylcyclohexane transformation. *Appl. Catal. A,* 353, 123–129, **2009b**.

Graça, I.; Ribeiro, F.R.; Cerqueira, H.S.; Lam, Y.L.; de Almeida, M.B.B., Catalytic cracking of mixtures of model bio-oil compounds and gasoil. *Appl. Catal. B*, 90, 556–563, **2009c**.

Graça, I.; Lopes, J.M.; Ribeiro, M.F.; Ribeiro, F.R.; Cerqueira, H.S.; de Almeida, M.B.B., Catalytic cracking in the presence of guaiacol. *Appl. Catal., B,* 101, 613–621, **2011a**.

Graca, I.; Fernandes, A.; Lopes, J.M.; Ribeiro, M.F.; Laforge, S.; Magnoux, P.; Ribeiro, F.R., Bio-oils and FCC feed stocks co-processing: impact of phenolic molecules on FCC hydrocarbons transformation over MFI. *Fuel*, 90, 467–476, **2011b**.

Graeser, U.; Kretschmar, K.; Niemann, K., *Erdoel and Kohle-Erdgas-Petrochemie*, 8, 362–365, **1983**.

Graham, R.G.; Huffman, D.R., Commercial aspects of rapid thermal processing (RTP™). Proc. Power Production from Biomass II Conference, Espoo, Finland, VTT, April **1995**.

Grange, P.; Laurent, E.; Maggi, R.; Centeno, A.; Delmon, B., Hydrotreatment of pyrolysis oils from biomass: reactivity of the various categories of oxygenated compounds and preliminary techno-economical study. *Catal. Today*, 29, 297-301, **1996**.

Gronli, M.; Antal Jr M.J.; Varheghi, G., A round robin study of cellulose pyrolysis kinetics by

thermogravimetry. *Ind. Eng. Chem. Res.*, 38, 2238-2244, **1999**.

Guillen, M.D.; Diaz, C.; Blanco, C.G., Characterization of coal tar pitches with different softening points by ^{1}H NMR: role of the different kind of protons in thermal process. *Fuel Process. Technol.*, 58, 1–15, **1998**.

Guerrero, M.; Ruiz, M.P.; Millera, A.; Alzueta, M.U.; Bilbao, R., Characterization of biomass chars formed under different devolatilization conditions: differences between rice husk and eucalyptus. *Energy & Fuels*, 22, 1275–1284, **2008**.

Gupta, R.K.; Kumar, V.; Srivastava, V., A new generic approach for the modeling fluid catalytic cracking riser reactor. *Chem. Eng. Sci.*, 62, 17, 4510-4528, **2007**.

Gutierrez, A.; Domine, M.E.; Solantausta, Y., Co-processing of upgraded bio-liquids in standard refinery units fundamentals.15th European Biomass Conference & Exhibition, Berlin, May 7-11, **2007**.

Hari, C.; Balaraman, K. S.; Balakrishnan, A. R., Fluid catalytic cracking: Selectivity and product yield patterns. *Chem. Eng. Tech*., 18, 364-369 **1995**.

Hedley, G., FIDA Engineering solutions: Remote Bioenergy. Alternative Energy Solutions Report prepared for "Energy Efficiency and Conservation Authority, September **2007**.

Heo, H.S.; Park, H.J.; Yim, J.; Sohn, J.M.; Park,J.; Kim, S.; Ryu, C.; Jeon, J.; Park, Y., Influence of operation variables on fast pyrolysis of miscanthus sinensis var. Purpurascens. *Bioresource Technology*, 101, 3672–3677, **2010**.

Hew, K. L.; Tamidi, A. M.; Yusup, S.; Lee, K. T.; Ahmad, M. M., Catalytic cracking of bio-oil to organic liquid product (OLP). *Bioresource Technol.*, 101, 22, 8855−8858, **2010**.

Hogendoorn, J.A.; Kersten, S.R.A.; De Miguel Mecader, F., Process for the catalytic cracking of pyrolysis oils. Shell International Research, Netherland, EP 2325281 A1, **2011**.

Hollander, M.A.; Makkee, M.; Moulijn, J.A., Fluid catalytic cracking (FCC): activity in the (milli) seconds range in an entrained flow reactor. *Appl. Catal.*, 187, 3-12, **1999**.

Holmgren, J.; Nair, R. M. P.; Elliott, D.; Bain, R., Consider upgrading pyrolysis oils into

renewable fuels. *Hydrocarbon Proc*., 95–103, **2008**.

Horne, P.A.; Nugranad, N.; Williams, P.T., Catalytic co-processing of biomass-derived pyrolysis vapors and methanol. *J. Anal. Appl. Pyrol.*, 34, 87–108, **1995**.

Huber, G. W.; Iborra, S.; Corma, A., Synthesis of Transportation Fuels from Biomass: Chemistry, Catalysis, and Engineering. *Chem. Rev.*, 106, 9, 4044−4098, **2006**.

Huber, G.W.; Corma, A., Synergies between Bio- and Oil Refineries for the Production of Fuels from Biomass, *Angew. Chem. Int. Ed.*, 46, 7184–7201, **2007**.

Ibsen, K., Equipment design and cost estimation for small modular biomass systems, synthesis, gas cleanup, and oxygen separation equipment. Contract report NREL/SR-510-39943, NREL Technical Monitor, May **2006**.

Ingram, L.; Mohan, D.; Bricka, M.; Steele, P.; Strobel, D.; Crocker, D.; Mitchell, B.; Mohammad, J.; Cantrell, K.; Pittman, C.U., Pyrolysis of Wood and Bark in an Auger Reactor: Physical Properties and Chemical Analysis of the Produced Bio-oils. *Energy & Fuels***,** *22,* 614–625, **2008**.

Jacob, S.M.; Gross, B.; Voltz, S.E.; Weekman, V.W. Jr., A lumping and reaction scheme for catalytic cracking. *AIChE J.*, 22, 701-713, **1976**.

Javaid, A.; Ryan, T.; Berg, G.; Pan, X.; Vispute, T.; Bhatia, S.R.; Huber, G.W.; Ford, D.M., Removal of char particles from fast pyrolysis bio-oil by microfiltration. *J. Mem. Sci.*, 363,120-127, **2010**.

John, C.; Paul, H. ; Beamon, J. A.; Naolitano, S.; Schaal, A. M.; Turnure, J. T. Westfall, L., International Energy Outlook, 2013, Report number: DOE/EIA-0484 **2013**.

Jones, S.B.; Holladay, J.E.; Valkenburg, C.; Stevens, D.J.; Walton, C.W.; Kinchin, C.; Elliott, D.C.; Czernik, S., Production of Gasoline and Diesel from Biomass via Fast Pyrolysis, Hydrotreating and Hydrocracking: A Design Case, PNNL Report No-18284, US Department of Energy, February **2009**.

Jung, S.H.; Kang, B.S.; Kim, J.S., Production of bio-oil from rice straw and bamboo sawdust

under various reaction conditions in a fast pyrolysis plant equipped with a fluidized bed and a char separation system. *J. Anal. Appl. Pyrol.*, 82, 240–247, **2008**.

Kang, B.S.; Lee, K.H.; Park, H.J.; Park, Y.K.; Kim, J.S., Fast pyrolysis of 182adiate pine in a bench scale plant with a fluidized bed: influence of a char separation system and reaction conditions on the production of bio-oil. *J. Anal. Appl. Pyrolysis*, 76, 32–37, **2006**.

Kristi, A.F.; Tiepan, S.; Constantino, B.; Terry, S.C.; Milena, V.; Ruben, V.D.; Marty, P.; Leen, G., Deep deoxygenation of biocrudes utilizing fluidized catalytic cracking co-processing with hydrocarbon feedstocks. Albemarle Corporation, USA, US 0316176 A1, **2014**.

Lappas, A. A.; Patiaka, D. T.; Dimitriadis, B. D.; Vasalos, I. A., Separation, characterization and catalytic cracking kinetics of aromatic fractions obtained from FCC feedstocks. *Appl. Catal. A: Gen.*, 152, 7–26, **1997**.

Lappas, A.A.; Bezergianni, S.; Vasalos, I.A., Production of biofuels via co-processing in conventional refining processes, *Catal. Today*, 145, 55–62, **2009**.

Larocca, M.; Ng, S.; de Lasa, H., Catalytic cracking of heavy gas oils: Modeling coke deactivation. *Ind. Eng. Chem. Res.*, 29, 2, 171-180, **1990**.

Lee, L.S., Four lump kinetic model for FCC process. *Can. J. Chem. Eng.*, 67, 615–619, **1989**.

Lee, S.W.; Glavincevski, B., NMR method for determination of aromatics in middle distillate oils. *Fuel Process. Technol.* 60, 1, 81–86, **1999**.

Lehto, J.; Oasmaa, A.; Solantausta, Y.; Power, M.; Chiaramonti, D., Fuel oil quality and combustion of fast pyrolysis bio-oils. VTT Technology 87, Espoo **2013**.

Lu, Q.; Zhang, Y.; Tang, Z.; Li, W.Z.; Zhu, X.F., Catalytic upgrading of biomass fast pyrolysis vapors with titania and zirconia/titania based catalysts. *Fuel*, 89, 2096-2103, **2010a**.

Lu, Q.; Zhang, Z.F.; Dong, C.Q.; Zhu, X.F., Catalytic Upgrading of Biomass Fast Pyrolysis Vapors with Nano Metal Oxides: An Analytical Py-GC/MS Study. *Energies*, 3, 1805-1820, **2010b**.

Luo, Z.; Wang, S.; Liao, Y.; Zhou, J.; Gu, Y.; Cen, K., Research on Biomass Fast Pyrolysis for Liquid Fuel. *Biomass Bioenergy*, *26*, 455-462, **2004**.

Mandal, S.; Das, A.K.; Yadav, A.; Yadav, M., A fluid catalytic cracking (fcc) process for manufacturing propylene and ethylene in increased yield. Patent EP2364343 A2, **2011**.

Magee, J.S.; Mitchell, M.M., Studies in Surface Science and Catalysis. Fluid Catalytic Cracking: Science & Technology. Vol. 76. Elsevier, London, **1993**.

Mao, X.; Weng, H.; Zhu, Z.; Wang, S.; Zhu, K., Investigation of the lumped kinetic model for catalytic cracking: analyzing light oil feed and products and measurement of kinetic constants. Acta. Pet. Sin. (Pet. Process Sect.), 1, 11, **1985**.

Marker, T.L.; Petri, J.A., Gasoline and diesel production from pyrolytic lignin produced from pyrolysis of cellulosic waste. Patent WO 2008/027699, **2008**.

Marker, T.; Czernik, S.; Elliot, D.; Shonnard, D., Opportunities for biorenewables in oil refineries. Technical report, US DOE award no.DE-FG36-05GO15085, **2005**.

Melero, J. A.; Iglesias, J.; Garcia, A., Biomass as renewable feedstock in standard refinery units. Feasibility, opportunities and challenges. *Energy Environ. Sci.* 5, 7393, **2012**.

Mercader, F.M., Pyrolysis oil upgrading for co-processing in standard refinery units. Ph.D. Thesis, University of Twente, Netherlands, **2010a**.

Mercader, F.M.; Groeneveld, M.J.; Kersten, S.R.A.; Way, N.W.J.; Schaverien, C.J.; Hogendoorn, J.A., Production of advanced biofuels: Co -processing of upgraded pyrolysis oil in standard refinery units. *Appl. Catal., B*, 96, 57-66, **2010b**.

Mercader, F.M.; Groeneveld, M.J.; Kersten, S.R.A.; Venderbosch, R.H.; Hogendoorn, J.A., Pyrolysis oil upgrading by high pressure thermal treatment. *Fuel*, 89, 2829–2837, **2010c**.

Mercader, F. M.; Groeneveld, M. J.; Kersten, S. R. A.; Geantet, C.; Toussaint, G.; Way, N. W. J.; Schaverien, C. J.; Hogendoorn, K. J. A., Hydrodeoxygenation of pyrolysis oil fractions: process understanding and quality assessment through co-processing in refinery units.

Energy Environ. Sci., 4, 985–997, **2011**.

Mohammed, A.H.A.K.; Esgair, K.K., Fluid catalytic cracking of petroleum fraction (vacuum gas oil) to produce gasoline. *Iraqi J. Chem. Petro. Eng.*, 11, 4, 33- 45, **2010**.

Mohan, D.; Pittman, Jr. C. U.; Steele, P. H., Pyrolysis of Wood/Biomass for Bio-oil: A Critical Review. *Energy & Fuels*, 20, 848-889, **2006**.

Mohanty, P.; Pant, K. K.; Das, S. K.; Vasudevan, P., Fuel production from biomass: Indian perspective for pyrolysis oil. *J. Scientific and Ind. Res.*, 70, 8, 668-674, **2012**.

Mortensen, P.M.; Grunwaldt, J.D.; Jensen, P.A.; Knudsen, K.G.; Jensen, A.D.; A review of catalytic upgrading of bio-oil to engine fuels. *Appl. Catal. A: Gen.*, 407, 2, 1–19, **2011**.

Moreira, J.R.; Nogueira, L.A.H.; Parente, V., Biofuels for transport, development and climate change: lessons from brazil. In: Bradley, R.; Baumert, K.A. (eds), Growing in the greenhouse: Protecting the climate by putting development first, World Research Institute, Washington, DC, **2005**.

Mota, C.J.A.; Rawet, R., Mechanism of aromatic hydrocarbon formation in FCC naphtha. *Ind. Eng. Chem. Res.*, 34, 12, 4326-4332, **1995**.

Naik, D.V; Kumar, V.; Prasad, B.; Behera, B.; Atheya, N.; Singh, K.K.; Adhikari, D. K.; Garg, M. O., Catalytic cracking of pyrolysis oil oxygenates (aliphatic and aromatic) with vacuum gas oil and their characterization, *Chem. Eng. Res. Des.*, 92, 1579-1590, **2014a**.

Naik, D.V; Kumar, V.; Prasad, B.; Behera, B.; Atheya, N.; Adhikari, D. K.; Nigam, K.D.P.; Garg, M. O., Catalytic cracking of C2-C3 carbonyls with vacuum gas oil, *Ind. Eng. Chem. Res.*, 53, 49, 18816-18823, **2014b**.

Naik, D.V; Kumar, V.; Prasad, B.; Behera, B.; Singh, K.K.; Bangwal, D.P.; Atheya, N.; Garg, M. O., Catalytic Cracking of Glycerol to Fine Chemicals over Equilibrium Fluid Catalytic Cracking Catalyst, *Energy Procedia*, 54, 593-598, **2014c**.

Netzel, D.A., Quantitation of carbon types using DEPT/QUAT NMR pulse sequences:

application to fossil-fuel-derived oils. *Anal. Chem.*, 59, 1775–1779, **1987**.

Ng, S.H.; Nakajima, N.; Fairbridge, C.; Kuehler, C., Production of light olefins through gas oil cracking. http://www.nt.ntnu.no/users/skoge/prost/proceedings/aiche-2006/data/papers/P61373.pdf, **2006**.

Niccum, P.K., Diesel creation in the FCC centered refinery. Coking & Cat Cracking Conference, Galveston, TX, May 8–10, **2013**.

Nogueira, L.A.H.; Capaz, R.S., Biofuels in Brazil: Evolution, achievements and perspectives on food security. *Global Food Security*, 2, 2, 117-125, **2013a**.

Nogueira, L.A.H.; Moreira, J.R.; Schuchardt, U., The rationality of biofuels. *Energy Policy*, 61, 2013, 595–598, **2013b**.

Oasmaa, A.; Leppamaki, E.; Levander, P.K.J.; Tapola, E., Physical characterization of biomass-based pyrolysis liquids application of standard fuel oil analyses. VTT PUBLICATIONS 306, **1997**.

Oasmaa, A.; Kuoppala, E.; Solantausta, Y., Fast pyrolysis of forestry residue: Physicochemical composition of product liquid, *Energy & Fuels*, 17, 2, 433-443, **2003**.

Oasmaa, A.; Kuoppala, E.; Selin, J.; Gust, S.; Solantausta, Y., Fast Pyrolysis of Forestry Residue and Pine: Improvement of the Product Quality by Solvent Addition. *Energy & Fuels*, 18, 1578-1583, **2004**.

Oasmaa, A., Norms and Standards for Pyrolysis Liquids: End-User Requirements and Specifications. *Energy & Fuels*, 19, 2155-2163, **2005**.

Oasmaa, A.; Kuoppala, E.; Ardiyanti, A.; Venderbosch, R. H.; Heeres, H. J., Characterization of Hydrotreated Fast Pyrolysis Liquids. *Energy & Fuels*, 24, 5264−5272, **2010a**.

Oasmaa, A.; Elliott, D.C.; Korhonen, J., Acidity of Biomass Fast Pyrolysis Bio-oils. *Energy & Fuels*, 24, 6548–6554, **2010b**.

Oasmaa, A.; Peacocke, C., Properties and fuel use of biomass-derived fast pyrolysis liquids: A

guide. VTT Publications 731, Espoo **2010c**.

Oasmaa, A.; van de Beld, B.; Saari, P.; Elliot, D.C.; Solantausta, Y., Norms, standards, and legislation for fast pyrolysis bio-oils from lignocellulosic biomass. *Energy & Fuels*, 29, 4, 2471-2484, **2015**.

Oliviera, L.L., Estimação de Parâmetros e Avaliação de Modelos de Craqueamento Catalítico, tese de mestrado, COPPE/UFRJ, Rio de Janeiro, Brazil, **1987**.

Oliveira, L.L.; Biscaia, Jr. E.C., Catalytic cracking kinetic models. Parameter estimation and model evaluation. *Ind. Eng. Chem. Res.*, 28, 264–271, **1989**.

Osmont, A.; Catoire,L.; Gökalp,I.; Swihart, M.T., Thermochemistry of C-C and C-H bond breaking in fatty acid methyl esters. *Energy & Fuels*, 21, 4, 2027–2032, **2007**.

Ozbay, N., Putun, A.E., Putun, E., Structural analysis bio-oils from pyrolysis and steam pyrolysis of cottonseed cake. *J. Anal. Appl. Pyrol.*, 60, 1, 89–101, **2001**.

Pant, K. K.; Mohanty, P.; Agarwal, S.; Dalai, A. K., Steam reforming of acetic acid for hydrogen production over bifunctional Ni–Co catalysts. *Catalysts Today*, 207, 36-43, **2013**.

Pattiya, A.; Suttibak, S., Production of bio-oil via fast pyrolysis of agricultural residues from cassava plantations in a fluidised-bed reactor with a hot vapour filtration unit. *J. Anal.Appl. Pyrol.*, 95, 227–235, **2012**.

Patwardhan, P.R.; Dalluge, D.L.; Shanks, B.H.; Brown, R.C., Distinguishing primary and secondary reactions of cellulose pyrolysis. *Bioresource Technol.*, 102, 5265–5269, **2011**.

Peng, J.; Chen, P.; Lou, H.; Zheng, X. M., Upgrading of bio-oil over aluminum silicate in supercritical ethanol. *Energy & Fuels*, 22, 5, 3489–3492, **2008**.

Peters, W.; von Steinkohlen, S., In: Habilitation thesis. RWTH Aachen University, **1963**.

Petrakis, L.; Allen, D., NMR for liquid fossil fuels. Elsevier, Amsterdam, **1987**.

Pitault, I.; Nevicato, D.; Forissier, M.; Bernard, J.R., Kinetic model on a molecular description

for catalytic cracking of vacuum gas oil. *Chem. Eng. Sci.*, 49, 4249-4262, **1994**.

Pu, Y.; Cao, S.; Ragauskas, A.J., Application of quantitative 31P NMR in biomass lignin and biofuel precursors Characterization. *Energy Environ. Sci.*, 4, 3154–3166, **2011**.

Putun, A.E.; Ozean, A.; Putun, E., Pyrolysis of hazelnut shells in a fixed-bed tubular reactor: yields and structural analysis of bio-oil. *J. Anal. Appl. Pyrol.* 52, 1, 33–49, **1999**.

Qiang, L.; Xu-lai, Y.; Xi-feng, Z., Analysis on chemical and physical properties of bio-oil pyrolyzed from rice husk. *J. Anal. Appl. Pyrolysis*, 82, 191–198, **2008**.

Radlein, D.; Bridgwater, A.V. (Ed.), Fast pyrolysis of biomass. A handbook, CLP Press, Newbury, Berkshire, 164-185, **1999**.

Raveendran, K.; Ganesh, A.; Kartic, C. K., Influence of mineral matter on biomass pyrolysis characteristics. *Fuel*, 12, 1812–1822, **1995**.

Ray, J. C. ; You, K.S.; Ahn, J.W.; Ahn, W.S., Mesoporous alumina(I): comparison of synthesis schemes using anionic, cationic, and non-ionic surfactants, *Microporous Mesoporous Mater.*, 100, 183–190, **2007**.

Ringer, M.; Putsche, V.; Scahill, J., Large-Scale Pyrolysis Oil Production: A Technology Assessment and Economic Analysis. National Renewable Energy Laboratory Technical Report, NREL/TP-510–37779, November **2006**.

Sa, Y.; Liang, X.; Chen, X.; Liu, J., Study of the 13 lump kinetic model for residual catalytic cracking. Selective papers in memorial of 30th anniversary of FCC process in China, Luoyan, Petrochemical Corporation, Luoyang, China, 145, **1995**.

Sadeghbeigi, R., Fluid Catalytic Cracking Handbook: Design, Operation, and Troubleshooting of FCC Facilities, 2nd ed. Gulf Professional Publishing, Houston, **2000**.

Sadhukhan, A.K.; Gupta, P.; Saha, R.K., Modeling and Experimental Studies on Pyrolysis of Biomass Particles, *J. Anal. App. Pyrol.*, 81, 2, 183-192, **2008a**.

Sadhukhan, A.K.; Gupta, P.; Goyal, T.; Saha, R.K., Modelling of pyrolysis of coal-biomass

blends using thermogravimetric analysis, *Bioresource Technol.*, 99, 17, 8022-8026, **2008b**.

Sadhukhan, A.K.; Gupta, P.; Saha, R.K., Modelling of pyrolysis of large wood particles, *Bioresource Technol.*, 100, 2, 3134-3139, **2009**.

Samolada, M.C.; Baldauf, W.; Vasalos, I.A., Production of a bio-gasoline by upgrading biomass flash pyrolysis liquids via hydrogen processing and catalytic cracking, *Fuel*, 77, 1667–1675, **1998**.

Samolada, M.C.; Papafotica, A.; Vasalos, I.A., Catalyst evaluation for catalytic biomass pyrolysis. *Energy & Fuels*, 14, 1161–1167, **2000**.

Satou, M.; Nemoto, H.; Yokoyama, S.; Sanada, Y., Determination of atomic groups of hydrocarbons in coal-derived liquids by high performance liquid chromatography and nuclear magnetic resonance. *Energy & Fuels*, 5, 632–637, **2010**.

Scherzer, J.; McArthur, D.P., Tests show effects of nitrogen compounds on commercial fluid cat cracking catalysts. *Oil & Gas J.*, 27, 76-82, **1986**.

Scherzer, J., Process for the catalytic cracking of feedstock containing high levels of nitrogen, Patent US4810369, May 7, **1987**.

Scherzer, J.; McArthur, D.P., Catalytic cracking of high-nitrogen petroleum feed stocks: Effect of catalyst composition and properties. *Ind. Eng. Chem. Res.*, 27, 9, 1571-1576, **1988**.

Scherzer, J., Octane-enhancing zeolitic FCC catalysts: Scientific and Technical Aspects. CRC Press, **1990**.

Sedran, U.A., Laboratory testing of FCC catalysts and hydrogen transfer properties evaluation. *Catal. Rev. Sci. Eng.*, 36, 3, 405–431, **1994**.

Sertic-Bionda, K.; Gomzi, Z.; Muzic, M., Modeling of gas oil catalytic cracking in a fixed bed reactor using a five-lump kinetic model. *Chem. Eng. Comm.*, 197, 275–288, **2010**.

Sharma, R.K.; Bakhshi, N.N., Catalytic upgrading of pyrolysis oil. *Energy & Fuels*, 7, 306–314, **1993**.

Sharma, R.K.; Hajaligol, M.R.; Smith, P.A.M.; Wooten, J.B.; Baliga, V., Characterization char from pyrolysis of chlorogenic acid. *Energy & Fuels*, 14, 1083–1093, **2000**.

Srinivas, S.T.; Dalai, A.K.; Bakhshi, N.N., Thermal and catalytic upgrading of biomass-derived oil in a dual reaction system. *Can. J. Chem. Eng.*, 78, 2, 343–354, **2000**.

Stournas, S.; Lois, E.; Polyssis, P., Performance assessment of novel substitute gasoline components. *ACS Fuel Chem. Prep.*, 35, **1990**.

Stratiev, D.; Dinkov, R., Evaluation of FCC process variables impact on yield distribution and product quality. Petroleum & Coal, 49, 3, 71-77, **2007**.

Thegarid, N.; Fogassy, G.; Schuurman, Y.; Mirodatos, C.; Stefanidis, S.; Iliopoulou, E.F.; Kalogiannis, K.; Lappas, A.A., Second-generation biofuels by co-processing catalytic pyrolysis oil in FCC units. *Appl. Catal., B*, 145, 161-166, **2013**.

Theologos, K.N.; Marcatos, N.C., Advanced modeling of fluid catalytic cracking riser type-reactors. *AIChE J.*, 39, 1007-1017, **1993**.

Talmadge, M.S.; Baldwin, R.M.; Biddy, M.J.; McCormick, R.L.; Beckham, G.T.; Ferguson, G.A.; Czernik, S.; Magrini-Bair, K.A.; Foust, T.D.; Metelski, P.D.; Hetrick, C.; Nimlos, M.R., A perspective on oxygenated species in the refinery integration of pyrolysis oil, *Green Chem.*, 16, 407-453, **2014**.

Tiplady, I.R.; Peacocke, G.V.C.; Bridgwater, A.V., Physical Properties of Fast Pyrolysis liquids from the Union Fenosa pilot plant. Bio-oil Production & Utilization. In: Ed., Bridgwater, A.V.; Grassi, G., Elsevier Applied Science, London, 164-174, **1991**.

Tremblay, G.; Vastola, F.J.; Walker, P.L., Thermal desorption analysis of oxygen surface complexes on carbon. *Carbon,* **16,** 35–39, **1978**.

Underwood, G., Commercialization of fast pyrolysis products. In: 'Biomass thermal processing', Hogan, E.; Robert, J.; Grassi, G.; Bridgwater, A.V., CPL press, 226-228, **1992**.

Vamvuka, D., Bio-oil, solid and gaseous biofuels from biomass pyrolysis processes: An

overview. *Int. J. Energy Res.*, 35, 835-862, **2011**.

Van Krevelen, D.W., Graphical-statistical method for the study of structure and reaction processes of coal, *Fuel*, 29, 269-283, **1950**.

Venderbosch R.H.; Heeres H.J., Pyrolysis Oil Stabilisation by Catalytic Hydrotreatment, Biofuel's Engineering Process Technology, Dr. Marco Aurelio Dos Santos Bernardes (Ed.), ISBN: 978-953-307-480-1, In Tech, Available from: http://www.intechopen.com/books/biofuel-s-engineering-process-technology/pyrolysisoil-stabilisation-by-catalytic-hydrotreatment (accessed on November, 2014), **2011**.

Venderbosch, R.H.; Ardiyanti, A.R.; Wildschut, J.; Oasmaa, A.; Heeres, H.J., Stabilization of biomass-derived pyrolysis oils. http://onlinelibrary.wiley.com/doi/10.1002/jctb.2354/ pdf, (accessed on 23rd May, 2014), **2010a**.

Venderbosch, R.H.; Prins, W., Review: Fast pyrolysis technology development. *Biofuels Bioprod. Bioref.*, 4, 2, 178–208, **2010b**.

Venkatakrishnan, V.K.; Degenstein, J, C.; Smeltz, A.D.; Delgass, W.N.; Agrawal. R.; Ribeiro, F.H., High-pressure fast-pyrolysis, fast-hydropyrolysis and catalytic hydrodeoxygenation of cellulose: production of liquid fuel from biomass. *Green Chem.*, 16, 792-802, **2014**.

Venkatakrishnan, V.K.; Delgass, W.N.; Ribeiro, F.H.; Agrawal. R., Oxygen removal from intact biomass to produce liquid fuel range hydrocarbons via fasthydropyrolysis and vapor-phase catalytic hydrodeoxygenation. *Green Chem.*, 17, 178-183, **2015**.

Venuto, P.B.; Hamilton, L.A.; Landis, P.S., Organic reactions catalyzed by crystalline aluminosilicates. II. Alkylation reactions: mechanistic and aging considerations. *J. Catal.*, 5, 484–493, **1966**.

Wagenaar, B.M., The rotating cone reactor for rapid thermal solids processing. Ph.D. Thesis, University of Twente, Netherlands, **1994**.

Wallenstein, D.; Alkemade, U., Modeling of selectivity data obtained from microactivity testing of FCC catalysts. *App. Catal. A*, 137, 1, 37-54, **1996**.

Wang, I., High temperature catalytic cracking. Ph D Dissertation, Fuels and Engineering Department, University of Utah, Salt Lake City, Utah, **1974**.

Wang, X.; Kersten, S.R.A.; Prins, W.; Swaaij, P.M., Biomass Pyrolysis in a Fluidized Bed Reactor, Part 2: Experimental Validation of Model Results. *Ind. Eng. Chem. Res.*, 44, 8786-8795, **2005**.

Wang, C.; Du, Z.; Pan, J.; Li, J.; Yang, Z., Direct conversion of biomass to bio-petroleum at low temperature. *J. Anal. Appl. Pyrol.* 78, 438–444, **2007**.

Way, N.; Meesala, L.; Moppi, A.; Fogassy, G.; Toussaint, G.; Schuurman, Y.; Geantet, C.; Mirodatos, C., Co-processing of upgraded pyrolysis oils in lab scale standard refinery units. NWBC 2011 Conference Proceedings, NWBC 2011, Stockholm, March 22-24, **2011**.

Weekman, V.W., Kinetics and dynamics of catalytic cracking selectivity in fixed-bed reactor. *Ind. Eng. Chem. Proc. Res. Dev.* 8, 3, 385–391, **1969**.

Weekman, V.W.; Nace, D.M., kinetics of catalytic cracking selectivity in fixed, moving and fluid-bed reactors. *AICHE J.*, 16, 397-404, **1970**.

Wei, J.; Prater, C.D., A new approach for first-order chemical reaction system. *AICHE J.*, **1963**.

Wenzel, F., Residual Upgrading and Waste Processing in the VCC Demonstration Plant. NPRA Annual Meeting, New Orleans, USA, 22–24 March **1992**.

Westerhof, R.J.M.; Brilman, D.W.F.; Swaaij, P.M.; Kersten, S.R.A., Effect of Temperature in Fluidized Bed Fast Pyrolysis of Biomass: Oil QualityAssessment in Test Units. *Ind. Eng. Chem. Res.*, 49, 1160–1168, **2010**.

Whitmore, F.C., Mechanism of the polymerization of olefins by acid catalysts. *Ind. Eng. Chem.*, 26, 94–95, **1934**.

Wildschut, J.; Mahfud, F.H.; Venderbosch, R.H.; Heeres, H.J., Hydrotreatment of Fast Pyrolysis Oil Using Heterogeneous Noble-Metal Catalysts. *Ind. Eng. Chem. Res.*, 48, 10324–10334, **2009**.

Williams, R.B., Characterization of hydrocarbons in petroleum by nuclear magnetic resonance spectrometry. *ASTM Spectrosc. Technol. Publ.* 224, 168–194, **1958**.

Xiong, W. M.; Zhu, M. Z.; Deng, L.; Fu, Y.; Guo, Q. X., Esterification of Organic Acid in Bio-Oil using Acidic Ionic Liquid Catalysts. *Energy & Fuels*, 23, 2278–2283, **2009**.

Yang, Y., Liu, B., Xi, H., Sun, X., Zhang, T., Study on relationship between the concentration of hydrocarbon groups in heavy oils and their structural parameter from 1H NMR spectra. *Fuel*, 82, 721–727, **2003**.

Yen, L.C.; Wrench, R.E.; Ong, A.S., Reaction kinetic correlation equation predicts fluid catalytic cracking coke yields. *Oil & Gas J.*, 86, 67-70, **1988**.

Yingxian, Z.; Fen, W.; Ying, Y., Inhibition of coke formation in cracking of 2-methylpentane on USHY by addition of steam. *Chin. J. Chem. Eng.*, 16, 5, 726–732, **2008**.

Zacher, A.H.; Olarte, M.V.; Santosa,D.M.; Elliott, D.C.; Jones, S.B., A review and perspective of recent bio-oil hydrotreating research, *Green Chem.*, 16, 491-515, **2014**.

Zapata, P.A.; Faria, J.; Ruiz, M.P.; Resasco, D.E., Condensation/Hydrogenation of Biomass-Derived Oxygenates in Water/Oil Emulsions Stabilized by Nanohybrid Catalysts. *Top. Catal.*, 55, 38–52, **2012**.

Zeman F. S.; Keith, D. W., Carbon neutral hydrocarbons. *Philos. Trans. R. Soc.* Lond. A, 366, 3901–3918, **2008**.

Zhang, Q.; Chang, J.; Wang, T. J.; Xu, Y., Upgrading bio-oil over different solid catalysts. *Energy & Fuels*, 20, 6, 2717–2720, **2006**.

Zhang, H., Cheng, Y., Vispute, T.P., Xiao, R., Huber, G.W., Catalytic conversion of biomass-derived feedstocks into olefins and aromatics with ZSM-5: the hydrogen to carbon effective ratio. *Energy Environ. Sci.*, 4, 2297–2307, **2011**.

Zhang, H.; Torren R. Carlson, Rui Xiao and George W. Huber. Catalytic fast pyrolysis of wood and alcohol mixtures in a fluidized bed Reactor. *Green Chem.*, 14, 98-110, **2012**.

Zhang, J.; Toghiani, H.; Mohan , D.; Pittman, Jr., C.U.; Toghiani, R.K., Product Analysis and

Thermodynamic Simulations from the Pyrolysis of Several Biomass Feedstocks, *Energy & Fuels*, 21, 4, 2373–2385, **2007**.

Zhao, H.; Zhou, C.H.; Wu, L.M.; Lou, J.Y.; Li, N.; Yang, H.M.; Tong, D.S.; Yu, W.H., Catalytic dehydration of glycerol to acrolein over sulphuric acid activated montmorillonite catalysts. *Appl. Clay Sci.*, 74, 154−162, **2012**.

WEB LINKS

www.ogj.com , Worldwide look at reserves and production, *Oil & Gas J.*, **110**, 28-31, **2012**.

http://www.pytecsite.de/pytec_eng/ (accessed November 2014).

http://www.dynamotive.com/industrialfuels/biooilplus (accessed November 2011).

http://www.btg-btl.com (accessed November 2011)

http://petrofed.winwinhosting.net/upload/25-28May10/S_Bose.pdf (28th October 2012).

http://www.btg-btl.com/index.php?r=faq (22nd November 2012).

http://petrofed.winwinhosting.net/upload/25-28May10/S_Bose.pdf (28th October 2012).

http://www.kbr.com/Technologies/Refining/Veba-Combi-Cracking/Process/Default.aspx (Viewed on 24th March 2013).

www.netl.doe.gov/publications/proceedings/02/.../2.04paper.pdf (accessed November 2011)

http://petroleum.nic.in/ refinery.pdf

ASTM Standard D1552–08(2014)e1, Standard test method for sulphur in petroleum products (High-temperature method), ASTM International, DOI: 10.1520/D1552-08R14E01, Available from: http://www.astm.org (Accessed on November, 2014).

ASTM Standard D7579–09 (2013), Standard test method for pyrolysis solids content in pyrolysis liquids by filtration of solids in methanol, ASTM International, DOI: 10.1520/D7579, Available from: http://www.astm.org (Accessed on December, 2014).

BIO-DATA

Name: Desavath Viswanatha Naik

Educational qualification:

B. Tech, Chemical Eng., JNTU Hyderabad, INDIA (1997-2001)

M. Tech, Chemical Eng., IIT Kharagpur, INDIA (2001-2003)

Professional Experience:

Jr. Eng., Rashtriya Chemicals & Fertilizers Ltd., Mumbai, INDIA (2004-06)

Scientist, CSIR-Indian Institute of Petroleum, Dehradun, INDIA (2006 onwards)

PUBLICATIONS

International Journals

1) Naik, D.V; Kumar, V.; Prasad, B.; Behera, B.; Poddar, M.K.; Bal, R.; Khatri, O.P.; Adhikari, D.K.; Garg, M.O., Catalytic cracking of jatropha-derived fast pyrolysis oil with VGO and their NMR characterization, *RSC Adv.* 5, 398-409, **2015**.
2) Naik, D.V; Kumar, V.; Prasad, B.; Garg, M.O., Hydrodeoxygenationof fast pyrolysis oilover Pd/Al_2O_3 catalyst, *Asia Pacific J. Chem. Eng.* (communicated) **2015**.
3) Naik, D.V; Kumar, V.; Prasad, B.; Behera, B.; Atheya, N.; Singh, K.K.; Adhikari, D. K.; Garg, M. O., Catalytic cracking of pyrolysis oil oxygenates (aliphatic and aromatic) with vacuum gas oil and their characterization, *Chem. Eng. Res. Des.*, 92, 1579-1590, **2014a**.
4) Naik, D.V; Kumar, V.; Prasad, B.; Behera, B.; Atheya, N.; Adhikari, D. K.; Nigam, K.D.P.; Garg, M. O., Catalytic cracking of C2-C3 carbonyls with vacuum gas oil, *Ind. Eng. Chem. Res.*, 53, 49, 18816-18823, **2014b**.
5) Naik, D.V; Kumar, V.; Prasad, B.; Behera, B.; Singh, K.K.; Bangwal, D.P.; Atheya, N.; Garg, M. O., Catalytic Cracking of Glycerol to Fine Chemicals over Equilibrium Fluid Catalytic Cracking Catalyst, *Energy Procedia*, 54, 593-598, **2014c**.

Research Articles Under Preparation

6) Naik, D.V; Kumar, V.; Prasad, B.; Garg, M.O., Kinetic modeling: coprocessing of vacuum gas oil with fast pyrolysis oil. *Chem. Eng. Sci.*

International Conferences

1. Naik, D.V; Kumar, V.; Prasad, B.; Garg, M.O., Hydrodeoxygenation of fast pyrolysis oil over Pd/Al_2O_3 catalyst**. Lovraj Kumar Memorial Trust lecture**, R&D Meet, 2015, Delhi, India, July 22, 2015.
2. Naik, D.V; Kumar, V.; Prasad, B.; Kumar, R., A perspective of fast pyrolysis oil processing in refinery. *4th International Conference on Sustainable Development*, ***SUSCON-2015***, IIM Shillong, India, March 11-13, 2015.
3. Naik, D.V; Kumar, V.; Prasad, B.; Poddar, M.K.; Atheya, N.; Singh, K.K.; Adhikari, D.K.; Garg, M.O., Processing of fast pyrolysis oil-derived tar fraction in fluid catalytic cracking unit. ***21st World Petroleum Congress***, Moscow, Russia, 15-19 June, 2014.
4. Naik, D.V; Kumar, V.; Prasad, B.; Behera, B.; Singh, K.K.; Bangwal, D.P.; Atheya, N.; Gupta, P.; Adhikari, D. K.; Garg, M. O., Catalytic cracking of biomass-derived glycerol to fine chemicals in a refinery FCC unit. *4th International conference on advances in energy research* (**ICAER-2013**), 10-12 December, 2013b.
5. Naik, D.V; Kumar, V.; Prasad, B.; Behera, B.; Bal, R.; Poddar, M.K.; Atheya, N.; Singh, K.K.; Adhikari, D.K.; Garg, M.O., Co-processing of upgraded fast pyrolysis oil in fluid catalytic cracking unit. *18th Refinery Technology Meet* (**RTM-2013**), 11-13 November, 2013a.
6. Naik, D.V; Kumar, V.; Prasad, B.; Behera, B.; Atheya, N.; Singh, K.K.; Adhikari, D.K.; Garg, M.O., Catalytic cracking of pyrolysis oil pyrolytic oil model compound with gas oil: a case study of acetic acid. **CHEMCON 2012**, 27-30 December, 2012.

Awards: Best paper award for the paper listed at S.No. 1 and entitled "A perspective of fast pyrolysis oil processing in refinery FCC unit" presented at 4th International Conference on Sustainable Development, SUSCON-2015 held at IIM Shillong, India during March 11-13, 2015.